CALIX[4]PYRROLE-BASED RECEPTORS FOR BIOLOGICALLY RELEVANT POLAR MOLECULES: FROM ORGANIC TO AQUEOUS MEDIA

Daniel Hernández Alonso

UNIVERSITAT ROVIRA I VIRGILI
CALIX[4]PYRROLE-BASED RECEPTORS FOR BIOLOGICALLY RELEVANT POLAR MOLECULES: FROM ORGANIC TO AQUEOUS MEDIA
Daniel Hernández Alonso

UNIVERSITAT ROVIRA I VIRGILI
CALIX[4]PYRROLE-BASED RECEPTORS FOR BIOLOGICALLY RELEVANT POLAR MOLECULES: FROM ORGANIC TO AQUEOUS MEDIA
Daniel Hernández Alonso

DOCTORAL THESIS

Daniel Hernández Alonso

CALIX[4]PYRROLE-BASED RECEPTORS FOR BIOLOGICALLY RELEVANT POLAR MOLECULES: FROM ORGANIC TO AQUEOUS MEDIA

Supervised by Dr. Pablo Ballester Balaguer

Tarragona

2017

UNIVERSITAT ROVIRA I VIRGILI
CALIX[4]PYRROLE-BASED RECEPTORS FOR BIOLOGICALLY RELEVANT POLAR MOLECULES: FROM ORGANIC TO AQUEOUS MEDIA
Daniel Hernández Alonso

ICIQ
Institut Català d'Investigació Química
Av. Països Catalans,16
43007, Tarragona, Spain
Tel +34 977920200 (Ext. 316)
Fax +34 977920221

UNIVERSITAT ROVIRA I VIRGILI
DEPARTAMENT DE QUIMICA ANALITICA I QUIMICA ORGANICA
C/ Marcel·lí Domingo s/n
Campus Sescelades
43007 Tarragona
Tel. 34 977 55 97 69
Fax 34 977 55 84 46
e-mail: secqaqo@urv.net

I STATE that the present study, entitled "Calix[4]pyrrole-Based Receptors for Biologically Relevant Polar Molecules: From Organic to Aqueous Media", presented by Daniel Hernández Alonso for the award of the degree of Doctor, has been carried out under my supervision in the Institute of Chemical Research of Catalonia (ICIQ).

Tarragona, 1, November 2017

Doctoral Thesis Supervisor/s

Dr. Pablo Ballester Balaguer

UNIVERSITAT ROVIRA I VIRGILI
CALIX[4]PYRROLE-BASED RECEPTORS FOR BIOLOGICALLY RELEVANT POLAR MOLECULES: FROM ORGANIC TO AQUEOUS MEDIA
Daniel Hernández Alonso

"Todo lo que no tiene un objetivo por alcanzar, un resultado por conquistar, un enigma por resolver, un misterio por penetrar, no me interesa"

Pablo Picasso

UNIVERSITAT ROVIRA I VIRGILI
CALIX[4]PYRROLE-BASED RECEPTORS FOR BIOLOGICALLY RELEVANT POLAR MOLECULES: FROM ORGANIC TO AQUEOUS MEDIA
Daniel Hernández Alonso

Acknowledgements

Finally, after an incredible amount of coffees, cigarettes, headaches, stress, paracetamol and of course good and bad moments this stage has ended. But the work presented in this thesis would certainly not have been possible without the help, support and advices of many peoples.

Primero de todo me gustaría agradecer a mi director de tesis **Prof. Pau Ballester**. Gracias Pau por todo lo que me has enseñado de química supramolecular, pero sobre todo por haberlo hecho de forma tan paciente. Gracias por haberme animado a ir siempre un paso más allá, a no conformarme con cualquier cosa y ser mucho más crítico (sobre todo con mi trabajo), a prestar atención a los detalles y hacer las cosas de la forma más profesional posible, aunque se tratase de una simple figura. Gracias también por confiar en mí y darme la oportunidad de poder enseñar a otras personas que han llegado al grupo lo que he aprendido. Gracias por esas charlas de termodinámica (a veces horas) delante del ITC. En definitiva, gracias por haberme permitido trabajar en tu grupo todos estos años.

Secondly, I would like to thank two post-doc that remarkably contributed to the work presented in this thesis but also made me a better chemist and person. Thank to **Dr. Louis Adriaenssens** for teaching me how to deal with organic chemistry from the most basic level. Without your lessons and tricks for running reactions, this thesis would have been impossible. Thanks for your patience, for encourage me in those moments in which nothing works and for your friendship. I will never forget that chemistry is always knocking at your door!!!. También me gustaría darle las gracias a la **Dr. Gemma Aragay** por todos esos momentos que tenía para resolverme dudas por el comunicador, por los escasos *bon dia* los casi inexistentes *fins demà* y los siempre puntuales *a dinaaaaaaaar*. Gracias por encargarte de que el laboratorio funcionase (nunca entenderé como haces para decirle a la gente que haga las cosas ¡¡y que las hagan!!). Pero sobre todo gracias Gemma por estar siempre dispuesta a ayudarme y aconsejarme, por sacarnos una sonrisa a cualquiera en los momentos de desesperación, por las innumerables correcciones y saber quitarle importancia a los problemas haciendo que todo parezca más sencillo. De lo que no te puedo dar las gracias son de esas charlas después de comer sobre embarazos, partos y olores que me daban arcadas hahaha.

También me gustaría agradecer a todos los miembros del grupo (pasados y presentes) con los que he compartido tantas horas en el laboratorio, razón por la cual en algún momento he

llegado a odiaros (igual que vosotros a mí), pero que han convertido el laboratorio en mi segundo hogar. En especial me gustaría darle las gracias a aquellos con los que he compartido más tiempo dentro y fuera del laboratorio:

Nelson Giménez por su amistad, por las discusiones de futbol y por luchar junto a mí por poner música de verdad. Gracias a **Albano Galán** por llenar de vida el laboratorio desde bien temprano con su *buenos diiiaaaas chicoooos*. Por ser el aliado perfecto para gastar bromas a los novatos, por acompañarme los fines de semana en el laboratorio y por tu insistencia para tomar *una cerveza y ya*. En resumen, gracias por hacer del laboratorio un lugar más agradable. Espero que algún día nos cuentes la verdad de tu brazo. Gracias a **Ramón Romero** por su ayuda, por su amistad, por preocuparte siempre de todos nosotros, y por hacer que el grupo fuese eso, un grupo. Gracias también por compartir conmigo los momentos de odio extremo hacia la química cuando nada funcionaba ni tenía sentido. Gracias a **Jordi Aguilera** por todo lo que me has enseñado de MOFs, nanoparticulas, copper paddle wheels, y un largo etc, por transmitirme que hay cosas mucho más importantes que la química, por los bocadillos de fuet, las canciones chorras, el caloret y las veinte maneras distintas que tenéis los valencianos de decir patata. Gracias Jordi por hacer del laboratorio un lugar más agradable. Thanks to **Sasa korom** for his funny stories, smelly reactions and helpfulness. Gracias a **Frank Arroyave** por compartir sus ideas y estar siempre dispuesto a dar consejos sobre química. Gracias a **Guillem Peñuelas** y **Giulia Moncelsi** por traer nuevos aires al laboratorio, por ayudar a que el laboratorio sea un lugar más agradable y por vuestras preguntas que a veces me hacían sudar, os deseo lo mejor en los años que os quedan en el laboratorio. Gracias a **Virginia Valderrey** y **Mónica Espelt** por sus consejos y su peculiar manera de ver las cosas. Gracias a Luis escobar y Alejandro Díaz por los proyectos que compartimos. Gracias a Beatriz Martín por su infinita paciencia y todos los *¿Bea tienes un segundo*? que me respondió amablemente (y fueron muchos). Gracias Bea por estar siempre pendiente de la ingente cantidad de papeles que nos piden, de las fechas para entregarlos y de todo lo que te pedimos a lo largo del día. Gracias Bea por facilitarnos tanto el trabajo.

También quiero agradecer a aquellas personas que sin ser del PB4 o del ICIQ han contribuido de una manera u otra a que esta etapa sea mas llevadera. Gracias a R. Martin Romero, J. M. M. Beloqui y Alba Matas por su impagable amistad y apoyo. Por las tardes de juegos de mesa (aunque seáis unos tramposos) y copas, por los días de south park y lacasitos!!! y por comeros todos los pistachos. Gracias por llenar esta etapa de anécdotas que nunca olvidaremos. Gracias

a Leticia Peña por su compañía, amistad y apoyo. Aunque no fueses miembro oficial del PB4 para todos fuiste como una más.

Thanks to the people from the ICIQ Research Support Units that have helped me during the thesis. En especial me gustaría agradecer a las personas de la unidad de difracción Marta Martínez, Eduardo Escudero por su inestimable ayuda y consejos a la hora de cristalizar. Gracias a la unidad de cromatografía Marta Serrano, Simona Curreli y María José Hueso por su amabilidad y dedicación siempre que he necesitado su ayuda. Gracias también a la unidad de RMN Grabriel González, Israel Macho, Germán Gómez por estar siempre dispuestos a ayudar con sus consejos y resolver mis innumerables preguntas. También me gustaría agradecer a Laia Pellejà y al ICIQ por darme la oportunidad de participar en los Bojos per la química. Gracias Laia por tener siempre una palabra amable y por enseñarme todo lo bueno de la divulgación científica.

I would like also thanks to T. Guinovart, P. Blondeau, F. X. Rius, and F. J. Andrade as well as R. Pinalli, G. Brancatelli, A. Pedrini, D. Menozzi, S. Geremia and E. Dalcanale for the successful collaborations.

También me gustaría darles las gracias a aquellas personas que aun estando lejos siempre han estado ahí. Gracias a mis padres por su apoyo incondicional en todas las decisiones que he tomado en mi vida. Por ayudarme y animarme a dar lo máximo de mí en todo. Por todo el cariño y dedicación que habéis empleado en mi educación. Sin vosotros todo esto hubiese sido imposible. Gracias a mi hermano por su cariño y apoyo en todo momento, gracias por compartir conmigo estos últimos años de mi estancia en Tarragona y hacerla aún mejor.

Por supuesto no me podía olvidar de Rocío, mi compañera en la vida. Gracias por tu increíble apoyo en todas las decisiones que he tomado durante todos estos años y por creer siempre en mí. Gracias por acompañarme cuando tomé la decisión de venir a Tarragona y soportar todos esos días de caras largas, estrés y apatía, si algún día lo pagué contigo no era mi intención. Gracias por soportar todos esos fines de semana que te he robado y por los días en los que estaba demasiado cansado para salir. Pero sobre todo gracias por tu cariño, por saber sacarme siempre una sonrisa y por hacerme sentir especial a tu lado.

The work contained in this thesis has been made possible thanks to the financial support of Ministerio de economía industria y competitividad, Genaralitat de Catalunya and ICIQ Foundation.

UNIVERSITAT ROVIRA I VIRGILI
CALIX[4]PYRROLE-BASED RECEPTORS FOR BIOLOGICALLY RELEVANT POLAR MOLECULES: FROM ORGANIC TO AQUEOUS MEDIA
Daniel Hernández Alonso

A mis padres,

UNIVERSITAT ROVIRA I VIRGILI
CALIX[4]PYRROLE-BASED RECEPTORS FOR BIOLOGICALLY RELEVANT POLAR MOLECULES: FROM ORGANIC TO AQUEOUS MEDIA
Daniel Hernández Alonso

Table of Contents

UNIVERSITAT ROVIRA I VIRGILI
CALIX[4]PYRROLE-BASED RECEPTORS FOR BIOLOGICALLY RELEVANT POLAR MOLECULES: FROM ORGANIC TO AQUEOUS MEDIA
Daniel Hernández Alonso

Chapter 1

Introduction

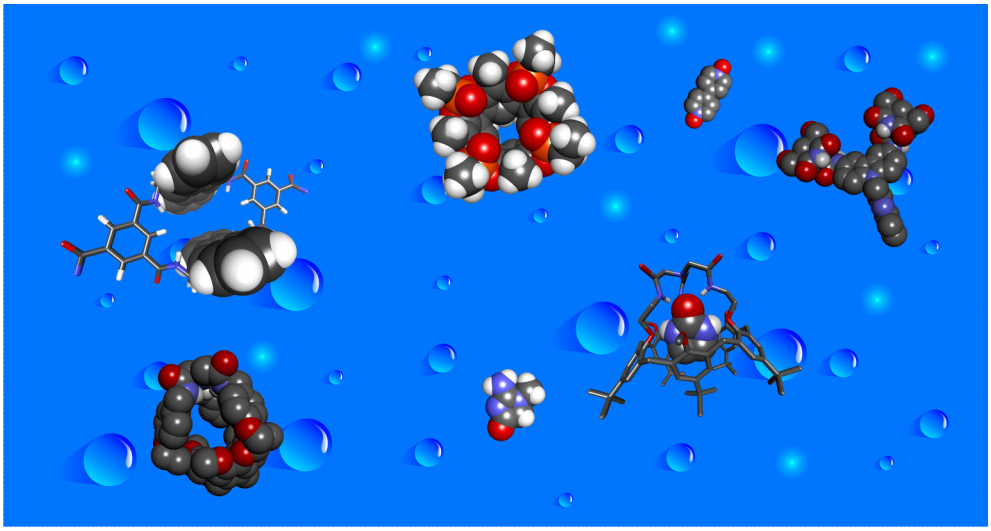

UNIVERSITAT ROVIRA I VIRGILI
CALIX[4]PYRROLE-BASED RECEPTORS FOR BIOLOGICALLY RELEVANT POLAR MOLECULES: FROM ORGANIC TO AQUEOUS MEDIA
Daniel Hernández Alonso

1.1 General introduction

1.1.1 Supramolecular binding in water

The design and synthesis of receptors able to bind substrates in water with high affinity and selectivity is still a challenging goal for supramolecular chemists. One of the reasons is the tedious synthetic pathways required for the construction of water-soluble receptors with a reduced tendency for self-aggregation. On the other hand, the highly competitive nature of water that results in a strong solvation of ions and polar molecules, either from the host or guest molecules, and consequently weakens the favorable electrostatic interactions in the host:guest complex.

In water, the release of solvation water molecules from either the guest or the host surface during the complexation process contribute to the free energy of binding. Studies using receptors based on non-polar cavities in aqueous solution have shown that enthalpy drives the binding event (nonclassical hydrophobic effect) in contrast with the classical explanation based on entropically driven processes due to the release of solvating water molecules to the bulk solution (classical hydrophobic effect). The most sensible explanation for this observation is the lower number hydrogen-bonding interactions of the water molecules that fill the non-polar cavities (high-energy water molecules) compared to the higher number of interactions of free water molecules in solution. The replacement of these high-energy water molecules from the cavity by a guest molecule highly contributes to the gain in enthalpy.[1]

The selectivity of water-soluble receptors with non-polar cavities such as cyclodextrines,[2,3] cyclophanes,[4,5] resorcinarenes,[6,7,8] or pillarenes[9,10,11,12,13] is mainly based on the complementary of size, shape and chemical surface in the host:guest complex. However, the hydrophobic effect is sometimes supported by other attractive non-covalent interactions such as π-stacking or dispersion, or by electrostatic interactions when polar or charged guests are included in the inner hydrophobic cavities of the receptors. For example, cucurbiturils[14] are able to combine the hydrophobic nature of their cavities with the establishment of additional charge-dipole interactions between charged groups of the guest and the carbonyl groups lining the entrance of the receptor's cavity. A binding constant as large as $K_a \approx 10^{17}$ M^{-1} has been described in aqueous solution for the complexation of cucurbit[7]uril and a diamantane derivative containing two trimethyl ammonium moieties in water.[15]

Unequivocally, the best option to accomplish a highly selective and strong binding of polar substrates in water media is mimicking natural systems. This means, the use of receptors with polar groups complementary to the guests that converge in an inner hydrophobic cavity of an adequate size.

Biological receptors such as enzymes show strong and selective complexation towards specific guests presenting polar functional groups. For example, avidine is able to complex biotin with a binding constant of Ka ≈ 10^{15} M^{-1}.[16] The binding site of avidine consists in a hydrophobic pocket formed by the aromatic residues of Trp and Phe that encloses polar functional groups of Asn, Ser, Tyr and Thr aminoacids that perfectly complement polar functional groups of biotine stablishing simultaneous hydrogen-bonding interactionsFigure 1. 1.[17]

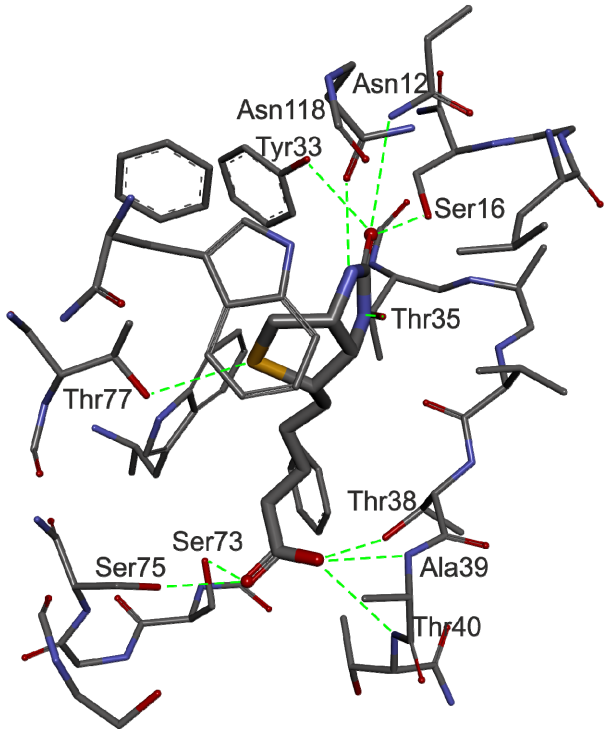

Figure 1. 1: X-ray structure of the binding site of avidine with a bound molecule of biotine. Hydrogen-bonding interactions have been highlighted in green.

Unfortunately, the amount of reported synthetic receptors featuring complementary hydrogen-bonding groups converging in a hydrophobic cavity resembling biological systems is limited.

For the sake of brevity and close relationship with the topic studied in the present thesis, the primary objective of this introduction is to review relevant examples of water-soluble synthetic receptors able to form thermodynamically stable complexes with neutral organic guests or the neutral part of an organic charged guest in aqueous media through the establishment of hydrogen-bonding interactions. The complexation of charged guests in aqueous media using synthetic receptors has been the topic of previous reviews and it is not included in the scope of this thesis.[18,19,20,21,22,23,24,25,26,27,28]

1.1.2 Acyclic receptors

One of the first examples reporting the formation of hydrogen-bonding interactions between a neutral guest and a synthetic receptor in water was reported in 1995 by Rebek et al.[29] The reported receptors (**1**, **2** and **3**) Figure 1. 2 were able to complex 9-ethyladenine (**4**) in water through the combination of π-stacking and hydrogen-bonding interactions. The authors determined the thermodynamic parameters of the complex formation by NMR titration experiments at different temperatures. Because both receptors **1** and **2** were constructed from a carbazole ring, the authors expected that both receptors had similar hydrophobic overlap with the bound **4**. Thus, the expected differences in binding were primarily due to the two extra hydrogen-bonding interactions formed in the **1**⊃**4** complex. The calculated association constants values derived from ^{1}H NMR titration experiments yielded an enthalpy difference $\Delta\Delta H$ of -1.6 kcal × mol^{-1} between the 1:1 complexes formed by **4** and the receptors **1** and **2**, respectively. This difference assigned an enthalpy gain of -0.8 kcal × mol^{-1} per hydrogen bond. The authors attributed the observed low energy gain to the exposed aqueous environment in which the receptors operate.

Against the classical hydrophobic effect, the entropic contribution for the complexes of both receptors (**1** and **2**) were negative ($\Delta S_{\mathbf{1}\supset\mathbf{4}}$ = -13 cal × mol^{-1} × K^{-1}; $\Delta S_{\mathbf{2}\supset\mathbf{4}}$ = -18 cal × mol^{-1} × K^{-1}) and the $\Delta\Delta S$ was -5 cal × mol^{-1} × K^{-1}. The favorable entropy gain expected from desolvation of **1** was opposed by the entropy loss attributed to the fixing of the amide rotors in one of the

two possible and equally probable positions, and to the inclusion of **4** in a more confined cleft, forming a tighter complex.

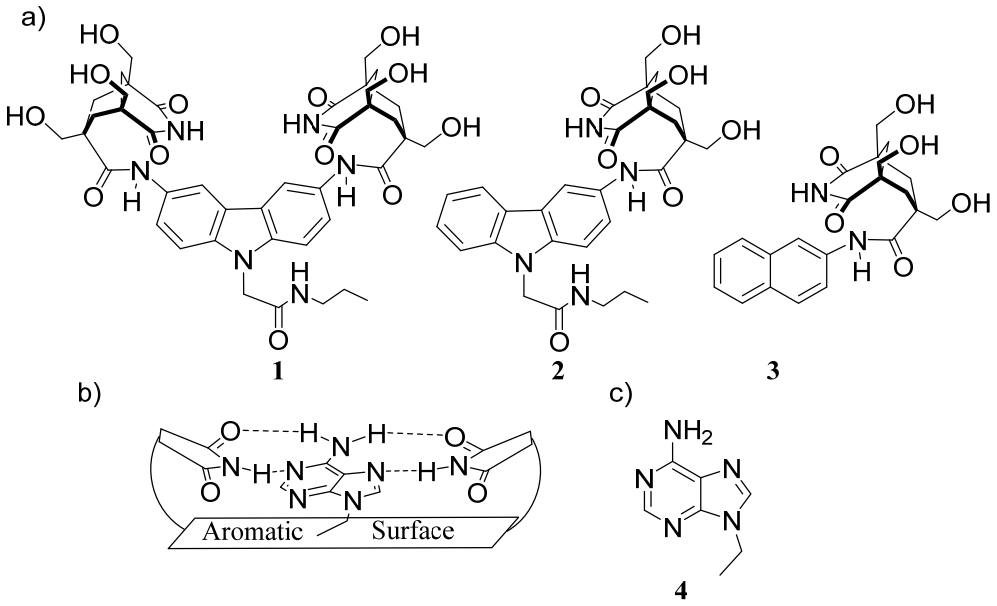

Figure 1. 2: a) Water-soluble receptors **1-3** reported by Rebek et al. b) Schematic view of the host-guest complementarity. c) Structure of 9-ethyladenine, guest **4**.

Similarly, by comparison of receptors **2** and **3**, the authors were able to study the influence of the hydrophobic surfaces on the binding of **4**. The binding enthalpy of **3** towards **4** was -3.4 kcal × mol^{-1} more favorable than for **2**. The authors attributed this observation to the more polarizable character of the naphthyl compared to carbazolyl surface. As in the previous case, the entropy term was negative ($\Delta S_{\mathbf{3}\supset\mathbf{4}}$ = -26 cal × mol^{-1} × K^{-1}), concretely -8 cal × mol^{-1} × K less favorable. Again, the authors attribute this observation to the formation of a tighter complex with receptor **3**.

Anslyn's group synthetized by a combinatorial approach an optical sensor based on a hexasubstituted 1,3,5-triethylbenzene able to selectively sense ATP in water.[30] The receptor (Figure 1. 3) incorporates two peptide side arms based on Ser-Tyr-Ser containing the fluorophores and a third arm that was used to link the host to a resin.

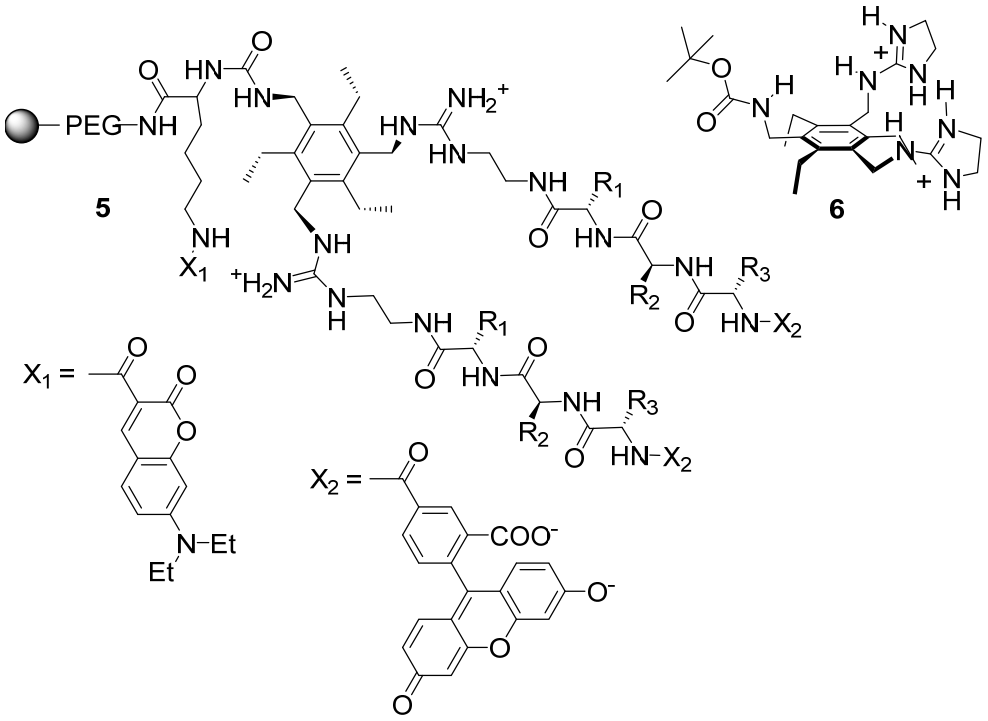

Figure 1. 3: Molecular structure of the ATP receptor **5** reported by Anslyn et al. and a simpler structural analogue **6**.

Receptor **5** was observed to complex ATP with a binding constant of 3.4×10^3 M^{-1} in HEPES buffer. Remarkably, binding was not observed with structurally similar and potentially competitors AMP and GTP. As a comparison for the study, the authors found that the much simpler receptor **6** was able to complex ATP in water with a binding constant of 3.5×10^2 M^{-1}, however, no selectivity was described for the nucleoside base (adenine). The authors attributed the high binding constant and the selectivity observed to several factors: first the electrostatic interactions of the triphosphate moiety and guanidinium groups of receptor **5**, and secondly, to the specific interactions between the nucleobase and the side chains present in receptor **5**. Specifically, the nucleobase discrimination was attributed to a combination of π-stacking interactions between the phenol of tyrosine and adenine and hydrogen-bonding interactions between the serine OH and/or the ribose or adenine. This example remarks the importance that hydrogen-bonding interactions in combination with hydrophobic surfaces may have in the selective recognition of structurally similar guests in aqueous media.

1.1.3 Cyclic receptors

Receptors able to bind selectively carbohydrates by non-covalent interactions in aqueous solution are a good example of the synergistically use of hydrogen-bonding and non-polar interactions to produce the complexation of the target guest.[31] The structural and physical properties of carbohydrates makes them challenging targets for complexation. They are uncharged molecules at neutral pH and comprise a high number of stereogenic centers, thus, there are a large number of isomeric structures and linkage points. Despite the necessity to compensate the energy cost for the desolvation of the host and the guest during complex formation, carbohydrates can form intramolecular hydrogen-bonding interactions between their OH groups which results in a weakening of the intermolecular hydrogen bonds in the expected host:guest complex.[32]

In 2012 Masahiko Inouye, Hajime Abe and coworkers reported their binding studies performed in non-polar and polar media with receptor **7** (Figure 1. 4) and different saccharides.[33] Macrocyclic receptor **7** possess an open cavity exposed to the bulk solution, that is functionalized with an array of pyridines and 4-pyrrolidones units that can act as hydrogen bond acceptor and donor groups complementing the saccharides OH groups. In DCM solution, a non-competitive media in which hydrogen-bonding interactions predominate, receptor **7** shows a binding constant for β-maltoside (Figure 1. 4) of 1.4×10^6 M^{-1}. Moving to a more polar, but non-protic solvent, like acetonitrile the binding constant decreased down to 1.8×10^3 M^{-1}. Unfortunately, when the binding experiments were performed in pure water, the authors did not observe complexation with any of the assayed saccharides using CD spectroscopy to monitor the complex formation. The dramatic attenuation in the binding strength observed for the complexation of saccharides by receptor **7** in aqueous solution exemplify the strong competitive nature of water molecules.

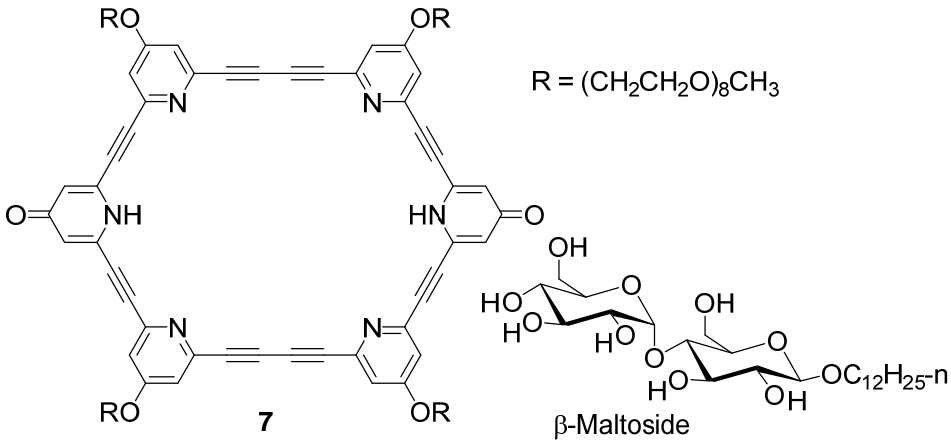

Figure 1. 4: Molecular structure of the macrocyclic receptor **7** reported by Masahiko Inouye, Hajime Abe et al and the guest used in their studies.

In 2005, A. P. Davis group reported a synthetic receptor **8** able to bind saccharides in aqueous solution.[34] The tricyclic cage was formed by two hydrophobic surfaces facing one to another (biphenyl) that are connected by four polar linkers forming an array of hydrogen-bonding groups (isophthalamides) Figure 1. 5. The biphenyl moieties perfectly complemented the two non-polar faces of glucose that are defined by the axially oriented CH groups while the isophthalamides units can establish hydrogen bond interactions with the equatorial OHs of the guest. Remarkably, ^{1}H NMR titration experiments performed with a freshly prepared solution of glucose in D_2O (anomeric ratio α/β 72:28) yielded a binding constant of 4.6 M^{-1}. However, the measured binding with a glucose D_2O solution that was equilibrated overnight (anomeric ratio α/β 40:60) yielded a binding constant of 9.2 M^{-1}. These results pointed out that the tricyclic cage can bind carbohydrates in the saccharides' natural environment (water) retaining the shown preference for β-glucosyl (OHs groups equatorially positioned) previously demonstrated in organic solvents.

In 2009, the same group reported a series of receptors **9**, (Figure 1. 5) featuring the same binding core than the tricyclic cage **8**, but incorporating apolar side chains in two of the four open entrances of the cavity.[35] The binding constants determined by ^{1}H NMR titration experiments in D_2O for receptor **9a-d** showed important effects of their structure with respect to the binding affinities towards different carbohydrates. For example, the stability constant determined for **9a**⊃glucose complex was 35 M^{-1} which is ≈ 4 times larger than the previously described for receptor **8** ($Ka_{\mathbf{8}\supset glucose}$ 9 M^{-1}) using the same technique. The incorporation of

larger hydrophobic groups produced an enhancement in the binding constant ($Ka_{\mathbf{9b}\supset glucose}$ = 41 M^{-1}; $Ka_{\mathbf{9c}\supset glucose}$ = 60 M^{-1}; $Ka_{\mathbf{9d}\supset glucose}$ = 47 M^{-1}). The increase in the binding affinity was attributed to a combination of different factors: modification of the solvation of the free receptor, the establishment of non-polar contacts between the CH carbohydrate moieties and the alkyl chains or the stabilization of the proper carbohydrate conformation. The decrease in the binding affinity of **9d** for glucose compared to **9c** was attributed to the presence of steric clashes between the bound glucose and the side butyl chains.

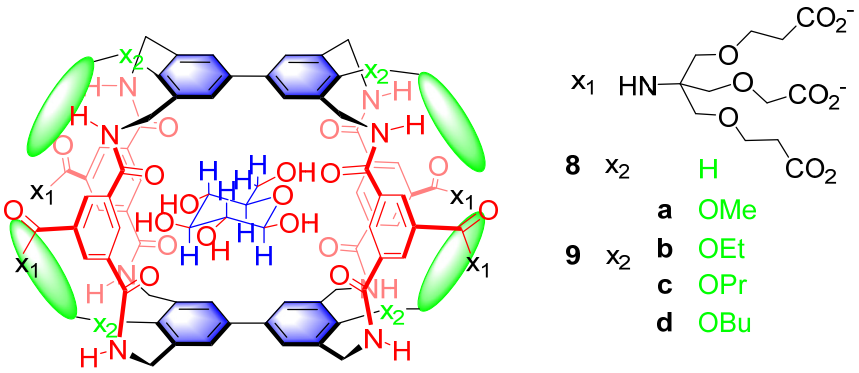

Figure 1. 5: Structure for receptors **8** and $\mathbf{9}_{\mathbf{a-d}}$ reported by A.P. Davis and coworkers enclosing a glucose molecule (β anomer). Complementary non-polar groups are shown in blue, hydrogen bonding groups in red.

Further studies regarding the role that hydrophobic interactions have in the recognition of monosaccharides in water were possible using receptor **10** (Figure 1. 6).[36] The biphenyl system present in receptor **9c** was substituted by anthracenes and the number of isophthalamides was reduced from four to two. The biphenyl units tend to twist due to the steric clashes between the hydrogen atoms *ortho* to the bond that connects the two aryl rings. This is translated into less effective CH-π interactions between the CH groups of the included saccharide and the aromatic surfaces. However, the incorporation of the anthracene units offers a more suitable platform for the establishment of CH-π interactions with the guest. In addition, the more accessible cavity of **10** allows the guest to freely slide on the surface reducing in this manner the loss of free energy due to rotational restrictions compared to receptor **9c**. The binding constant determined by ^{1}H NMR titration of **10** yielded a $Ka_{\mathbf{10}\supset glucose}$ of 56 M^{-1}. The Ka was only slightly smaller than the one determined for **9c** (60 M^{-1}), however, the selectivity against other monosaccharides was improved. Supported by ITC experiments,

the authors claimed that the presence of the extra polar spacers in **9c** made the receptor more dependent on polar interactions and thus, less reliant to the release of high energy water molecules. Experiments in a less competitive media like $CDCl_3$ (where hydrogen-bonding interactions dominate) also supported this idea. In $CDCl_3$, they observed that the binding constant for the organic soluble version of receptor **9c** against octyl β-D-glucoside was 100 times larger than the binding constant for the organic soluble version of receptor **10**. Additional improvement on binding constants were also observed by changing the water solubilizing groups for dendritic side chains.[37] For example the change of substituents X on **10** (6 negative charges) (Figure 1. 6) by the dendrimer shown in Figure 1. 8 (18 negative charges) produced an increase in the binding constant for glucose up to ≈ 90 M^{-1}. These receptors were developed to increase the binding affinity towards positively charged guest such as glucosamine. However, the increase in binding affinity towards neutral guests despite the absence of electrostatic interactions may needs to be studied in more detail.

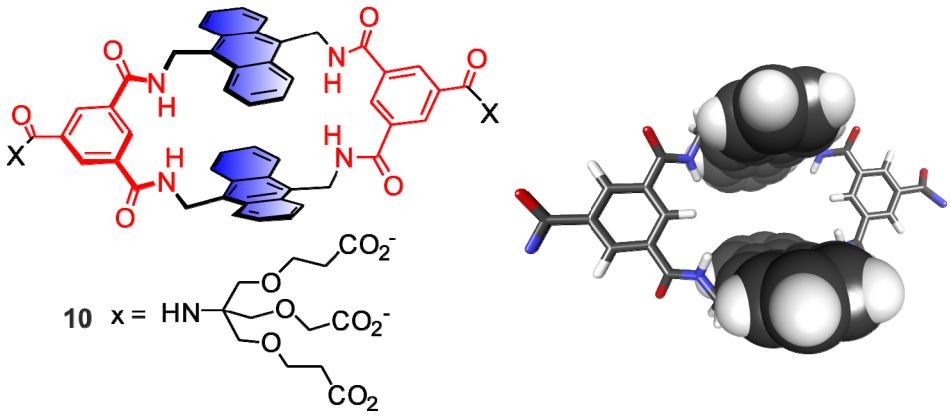

Figure 1. 6: Molecular structure of receptor **10** reported by A.P. Davis and coworker. Complementary non-polar groups are shown in blue, hydrogen bonding groups in red

The replacement of the biphenyl units in receptor **8** and **9a** by triphenyl units yielded macrocyclic receptors **11** (Figure 1. 7).[38] These receptors possessed larger cavities and aromatic surfaces compared to the biphenyl analogous. The authors studied the ability of these new receptors to bind disaccharides in their larger cavity. Table 1. 1 lists some of the binding constants measured for disaccharides (entries 1 to 6) and glucose monosaccharide (entry 7).

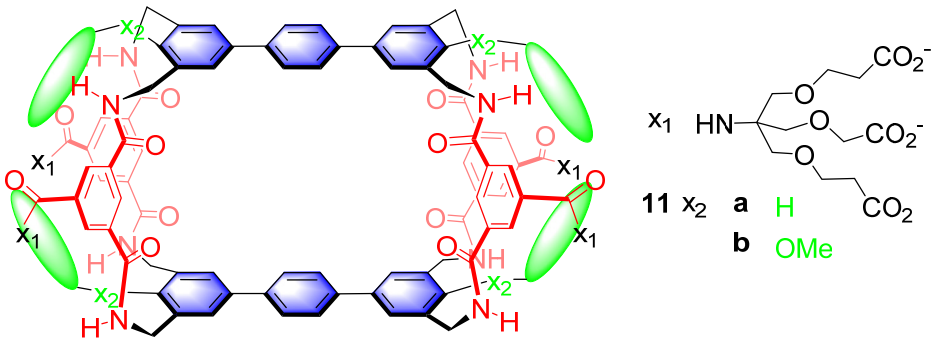

Figure 1. 7: Molecular structure of extended receptors **11a** and **11b** reported by A.P. Davis and coworkers. Complementary non-polar groups are shown in blue, hydrogen bonding groups in red.

The results showed that receptors **11a** and **11b** featured larger association constants for disaccharides, in particular for the disaccharides methyl β-D-cellobiose and D-cellobiose (constituted by units of glucose) > 10^3 M^{-1} than for simple glucose. This supposed an increase of ≈ 200 folds compared to the smaller and structurally analogue receptor **8**. The results obtained with other disaccharides also shows how minor changes in their structures can cause a dramatic attenuation on the binding constants. For example, while comparing the binding of D-lactose, that has only one OH group in axial position and the rest in equatorial, with D-cellobiose that possess all the OH equatorially positioned, to receptors **11a** or **11b**, the determined binding constant for the later was ≈ 10 folds higher than for the former one (Table 1. 1 entries 2 and 5). At the same time the binding constant for the monosaccharide glucose is reduced to almost cero in receptors **11**.

Table 1. 1: Association constants (Ka) for 1:1 complexes of receptors **8**, **11a** and **11b** with carbohydrate substrates in water, as determined by [a] ^{1}H NMR and [b] fluorescence titrations.

	Carbohydrate	Ka (M^{-1})		
Entry		**8**[a]	**11a**[b]	**11b**[b]
1	methyl β-D-cellobioside	-	-	4500
2	D-cellobiose	17	3140	3340
3	D-xylobiose	-	-	210
4	N,N'-diacetyl-D-chitobiose	Too small	-	910
5	D-lactose	Too small	230	270
6	D-maltose	Too small	67	72
7	D-glucose	9	-	2

Very recently, the same group reported the chiral water-soluble receptor **12** (Figure 1. 8) that combines different structural features from their previous works: i) flat aromatic surface (pyrene), ii) easy access to the cavity iii) dendrimers as water-solubilizing groups.[39] The chirality was imparted by the incorporation of a hexasubstituted 1, 3, 5-triethylbenzene ring as aromatic complementary surface to pyrene (Figure 1. 8). The reaction between a C_3-symmetric unit and a tetrasubstituted pyrene leaves an unreacted spacer unit of the pyrene moiety giving rise to a pair of enantiomeric products. Although the authors were not able to separate the two enantiomers of **12**, they could measure the binding constants by ^{1}H NMR titration experiments for at least one of the two expected diasteroisomeric complexes on the racemate. One of the enantiomers of receptor **12** showed a binding constant for glucose of Ka $\approx$ 250 M^{-1}. Unfortunately, they were not able to calculate the binding constant for the other enantiomer due to broadening of the signals (most likely due to intermediate chemical exchange). However, they observed early movement of the proton signals during the titration for this latter diasteromeric complex suggesting that the binding constant may be higher. The enantioselectivity of the receptor could be demonstrated using N-Acetyl-D-glucosamine. For this guest the authors were able to follow the chemical shift changes experienced by the receptor protons during the titration. Remarkably, the binding constant values determined for the two diasteromeric complexes were 1280 M^{-1} and 81 M^{-1}, respectively (enantioselectivity 16:1).

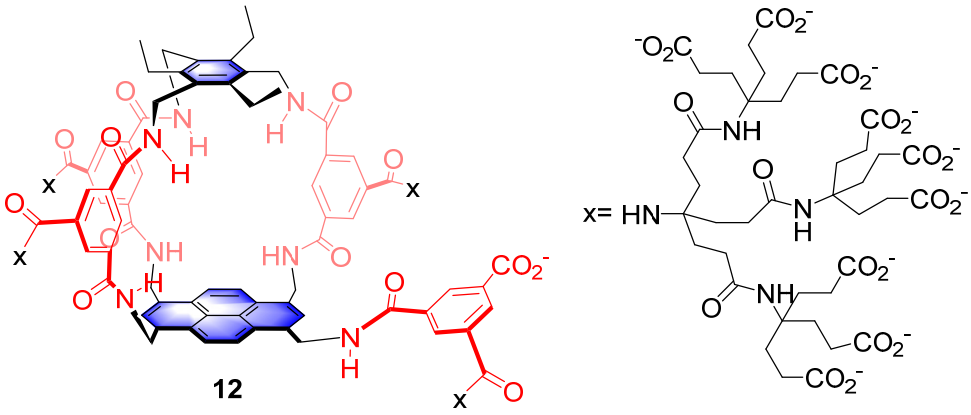

Figure 1. 8: Molecular structure of receptor **12** reported by A.P. Davis and coworkers. Complementary non-polar groups are shown in blue, hydrogen bonding groups in red.

1.1.4 Bowl-shape cyclic receptors

Water-soluble receptors containing bowl-shape macrocyclic scaffolds (resorcinares, calixarenes, hemicryptophanes, calix[4]pyrroles, etc.) decorated with polar neutral functional groups in the interior or periphery of the hydrophobic cavity have been described to successfully form thermodynamically stable supramolecular complexes with polar small molecules.

I. Javin and coworkers described very recently a calix[6]cryptamide receptor **13** (Figure 1. 9) capable to complex cyclic ureas and γ-lactam, **15-17**.[40] The receptor was based on a resorcin[6]arene in which three alternate phenol groups were functionalized with polyethyleneglycol chains to impart solubility in aqueous media. The others three phenol groups were functionalized with alkyl substituents containing amide groups connected between them by a tertiary amine. Receptor **13** was soluble in organic and aqueous media, thus, allowing the authors to compare the binding ability of the receptor in $CDCl_3$ and D_2O/CD_3OD (1:2).

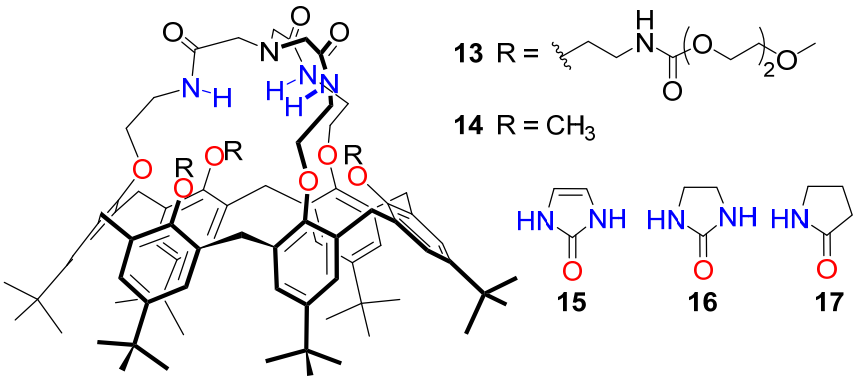

Figure 1. 9: Cryptamide receptor **13** and **14** and neutral guests (**15-17**). Complementary hydrogen bond donor and acceptor groups are shown in blue and red respectively.

As depicted in Figure 1. 10 the closely related **14⊃15** complex was stabilized by a DAAAD-ADDDA quintuple H-bonding array established between the carbonyl and the NH groups of the included guest, and the amide NH protons and the phenoxy groups of the host, as well as multiple CH–π interactions.

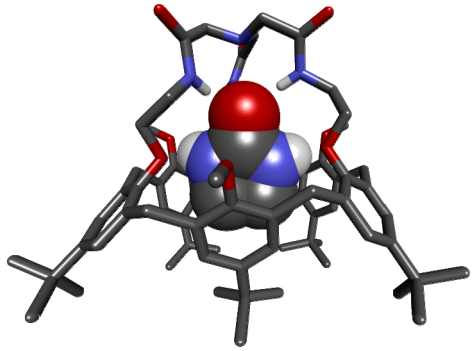

Figure 1. 10: X-ray structure of the **14⊃16** complex. Non-polar hydrogen atoms have been omitted for clarity. **16** is shown in CPK.

In organic as well as in aqueous solution, receptor **13** was able to complex guests **15-17** with a 1:1 stoichiometry. Interestingly, the CISs (complexation induced shifts) values observed in both solutions for each guest were comparable indicating a similar positioning of the bound guest independently of the solvent. The association constants (Table 1. 2) determined in organic solution increase notably from **17** < **16** < **15** in agreement with the number of hydrogen-bonding interactions involved in the complex and the acidity of the guest. However, in aqueous solution **15** resulted to form less stable complex. The authors attributed the observed difference to a larger hydration of the more polar and acidic molecules in aqueous solution.

Table 1. 2: Relative association constant values (Ka/**17**) of host **13** with neutral guests (**15-17**). The pKas of the guest are also reported.

	Ka relative to guest **17** in different media	
Guest(pKa)	$CDCl_3$	D_2O/CD_3OD (1:2)
15 (12.2)	1.1×10^2	0.46
16 (14.6)	19	3
17 (16.6)	1	1

Most of the examples of water-soluble cryptophanes and hemicryptophanes described in literature[41,42,43] reporting the complexation of neutral organic guests are purely based on hydrophobic interactions as the main driving force. Others describe the recognition of small ammonium cations by the establishment of cation-dipole interactions with the aromatic

macrocycle. Among them, there are few examples reporting the selective binding of biological relevant molecules driven by a synergistic combination of hydrogen-bonding, cation dipole, and hydrophobic interactions.

In 2011 J.P. Datusta and coworkers, reported the binding studies in aqueous solution of hemicryptophane **18** with zwitterionic guests (**19-27**) and cations (**28** and **29**).[44] The receptor was built from a cyclotriveratrylene (CTV) unit, able to bind an ammonium ion by cation–π interactions, and three amides groups capable to engage in hydrogen-bonding interactions with neutral and negatively charged complementary groups. The preorganization of the polar groups in receptor **18** favored the complexation of zwitterionic guests (**19**,**21**,**23**,**24**,**26**) in a mixture of acetonitrile/water (90:10) in a 1:1 stoichiometry. However, the presence of electron-rich aromatic panels connecting the triamide subunit and the CTV can yield to repulsive electrostatic interactions with the anionic group of the guest located in the cavity, and thus, destabilize the resulting host–guest complex.

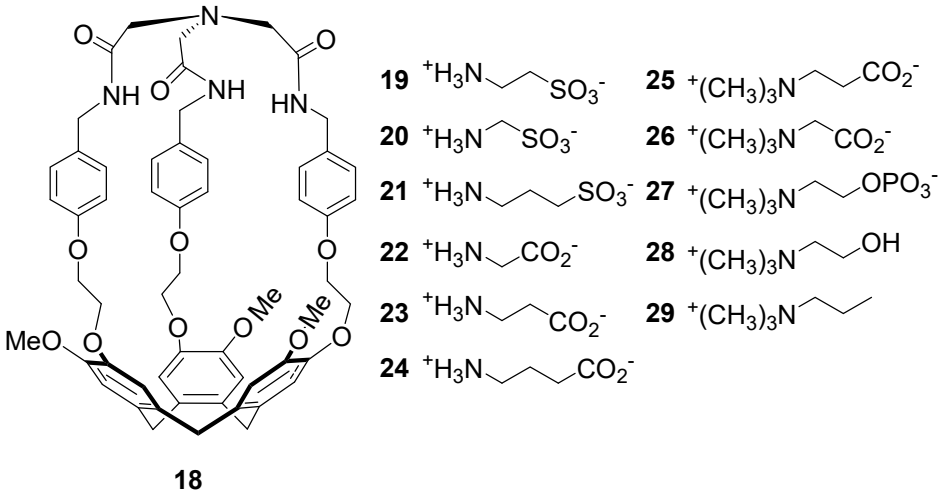

Figure 1. 11: Molecular structures of the hemicryptophane receptor **18** and the zwitterionic guests (**19-29**).

In order to overcome this problem, the same group reported in 2012 a new version of receptor **18**, the hemicryptophane **30** (Figure 1. 12). The three aromatic panels were removed and an electron-deficient phenyl spacer, which favored the guest's complexation by the establishment of anion-π interactions, was incorporated in a face-to-face orientation with respect to the CTV binding unit.[45] Additionally, three bis-amide linking groups were properly

located to stablish additional hydrogen-bonding interactions with the negatively charged groups of the included guests. The analysis of the chemical shift changes experienced by the guest protons when included in the host, allowed the mapping of the binding geometry for the formed complexes. As expected, the positively charged part of the guest was included in the aromatic cavity defined by the CTV unit, while the anionic head-group was oriented towards the electron-deficient aromatic spacer and hydrogen-bonded the amide groups of the receptor.

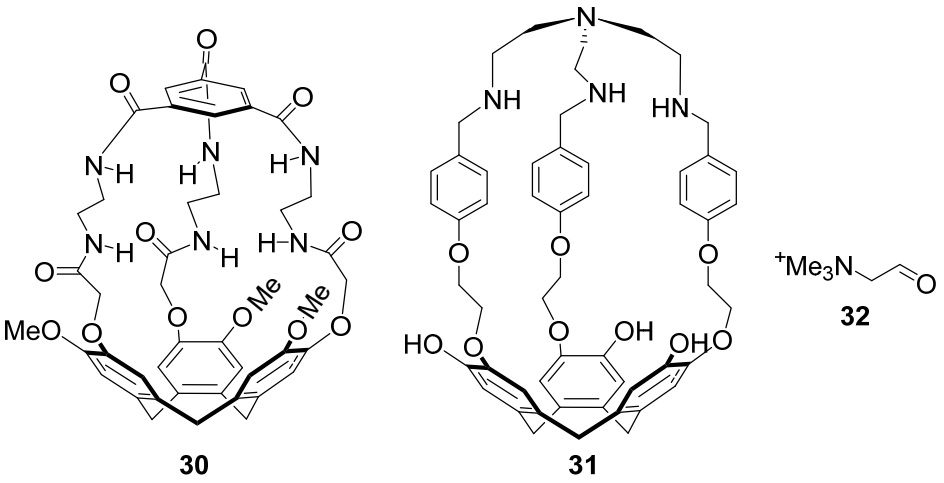

Figure 1. 12: Chemical structure of hemicryptophane receptors **30** and **31** and the guest **32**.

Even in more competitive media (acetonitrile/water 8:2), the structural modifications of receptor **30** compared to **18** produced a notable increase in the binding constant values for the studied guests (Table 1. 3). The observed increase of affinities was attributed to the existence of attractive anion-π interactions, as well as to the establishment of three additional hydrogen-bonding interactions in the complexes formed with receptor **30**.

The high affinities featured by the previous hemicryptophanes **18** and **30** in aqueous/organic mixtures were further investigated in pure aqueous solution using receptor **31** (Figure 1. 12).[46] Receptor **31** is structurally similar to receptor **18** in terms of functionalization. The water solubility of **31** was imparted by deprotonation of the phenol groups of the CTV unit in strong basic media (pH 12). Using ^{1}H NMR spectroscopy and ITC experiments the authors showed that the molecular receptor **31** efficiently included the ammonium neurotransmitter choline **28** within its polar aromatic cavity (Figure 1. 11). The resulting 1:1 complex had a binding constant value of 2.3×10^{3} M^{-1}. Moreover, hemicryptophane **31** resulted to be highly selective

for the binding of **28** in the presence of betaine aldehyde (**32**) and glycine betaine (**26**) (metabolites of **28**).

Table 1. 3: Association constants of hosts **18** and **30** with zwitterionic guests.

	Ka (M^{-1}) Receptor (D_2O:CD_3CN)	
Guest	**18** (1:9)	**30** (2:8)
23	8.5×10^3	1.5×10^4
19	1.4×10^4	5.0×10^5
24	5.1×10^2	2.3×10^5
21	5.3×10^2	1.1×10^5

Very recently, Wei Jiang and coworkers reported binding studies in water using the two isomers of the endo-functionalized molecular tubes **33** (**33a** and **33b**) with various hydrophilic small molecules (Figure 1. 13).[47] The hydrophobic cavities of the molecular tubes **33a** and **33b** are defined by four covalently connected naphthalene units, in which two amide NH groups converge. They found that receptors **33** were able to selective include one molecule of 1,4-dioxane in their inner cavity stablishing hydrogen-bonding interactions with the amide's NH protons. The binding constant values determined by ^{1}H NMR titration experiments were 1.35×10^4 M^{-1} for the **33a**⊃1,4-dioxane and 3.1×10^3 M^{-1} for the **33b**⊃1,4-dioxane counterpart. Other polar guests (DMF, MSO, acetone, 1,3-dioxane, THF, oxetane, oxepane) produced 1:1 inclusion complexes with binding constant values in the order of 10^2 M^{-1}. The enthalpic and entropic contributions of the binding events were determined using isothermal titration calorimetry (ITC) experiments. The ITC results revealed that the binding processes were mainly enthalpically driven with a minor contribution from the entropic term. The origin of the favorable enthalpic term was attributed to both the release of high-energy water molecules from the host's cavity and the establishment of hydrogen bond interactions in the host:guest complex. Interestingly, titration experiments conducted in $CDCl_3$ solution with the organic soluble analogues **34**, and 1,4-dioxane as guest produced lower association constant values for the complexes of both isomers. Specifically, 61 M^{-1} and 101 M^{-1} for **34a** and **34b** respectively. These results indicated that water and thus hydrophobic effects played an important role in the binding process.

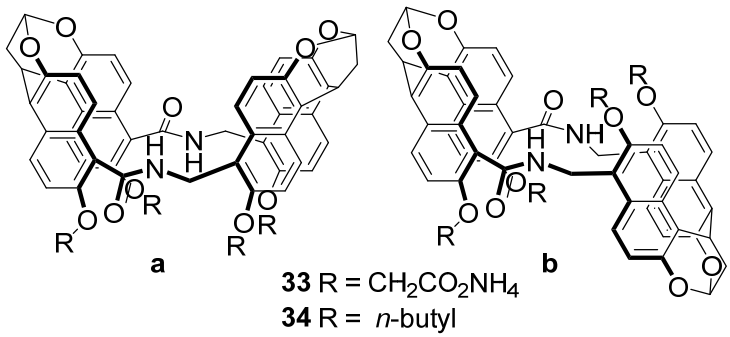

Figure 1. 13: Molecular structures of the isomeric tubes **33** and **34**.

In 2016, Dalcanale and coworkers reported a complete study related to the recognition of amino acids in aqueous and organic (methanol) media with the tetraphosphonate receptors **35** and **36** (Figure 1. 14).[48] These receptors comprise an array of hydrogen-bonding acceptor groups formed by the four inwardly directed oxygen atoms of the phosphonate bridging groups. As shown in the CPK model (Figure 1. 14 right) the polar phosphonates groups are surrounded by hydrophobic groups (Ar-Me and Et-P) which probably help to reduce their solvation by water molecules.

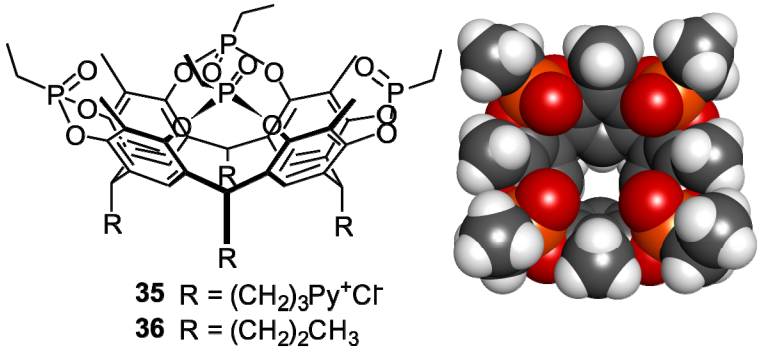

Figure 1. 14: Molecular structure of the water-soluble tetraphosphonate cavitand **35** and the organic soluble version **36** (left). Top view of the energy minimized structure (AM1 in water, SCIGRESS v 3.0.0, Fujitsu Ltd) of **35** represented as CPK model (right). The alkyl chains were modeled as methyl groups.

The binding processes of receptors **35** in water, and **36** in methanol, towards *N*-Me-GlyME·HCl and *Nε*-Me-Lys·HCl (Figure 1. 15) were studied by means of ^{1}H NMR spectroscopy and ITC experiments. The solid-state structures of the formed complexes were determined using X-ray diffraction of single crystals. In both solvents (water and methanol),

the receptors formed 1:1 thermodynamically stable complexes with *N*-MeGlyME·HCl through deep inclusion of the *N*-Me residue in their aromatic cavities. The driving force for the inclusion process was a combination of hydrophobic interactions, charge-dipole interactions and hydrogen bonding. ITC experiments revealed that in methanol the binding process was enthalpically and entropically driven while in water the entropic term opposed complex formation. This change in the sign of the entropic contribution was assigned to the formation of a tighter complex in aqueous solution, as well as to the formation of ordered structures of water molecules solvating it. Additionally, the X-ray structures of the receptors showed that the number of solvent molecules involved in solvating their cavities is larger in methanol than in water. This observation can help to explain the entropic gain observed in methanol for complex formation.

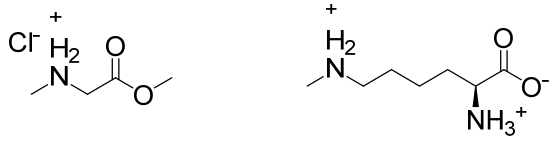

Figure 1. 15: Molecular structures of the aminoacids *N*-methylglycine methyl ester hydrochloride (***N*-MeGlyME·HCl**) and *Nε*-methyl-lysine hydrochloride (***Nε*-Me-lys HCl**).

Finally, it's worth mentioning that aryl-extended calix[4]pyrrole based receptors have also been shown to be efficient macrocyclic receptors for the recognition of polar neutral guest in aqueous solution. The binding of the polar guest by calix[4]pyrrole receptors is mainly based on the establishment of hydrogen-bonding and hydrophobic interactions. In the introductory sections of the following chapters we will review the use of calix[4]pyrrole derivatives as efficient receptors for molecular recognition studies in water and organic solvents.

1.1.5 Conclusions

Water soluble receptors purely based on non-polar interactions have been widely used for the complexation of non-polar guests in aqueous media, however the selectivity of these hosts is exclusively driven by size-shape complementarity between the host and the guest. Inspired by biological systems, the synthesis of receptors containing polar functional groups that converge in relatively non-polar environments have attracted great interest. This strategy aims to reduce

and protect the solvation of the polar groups with the bulk solvent. In this introduction, we have described selected examples of synthetic receptors able to bind small polar organic molecules in water. We have shown that high selectivities and affinities can be reached by combining polar and non-polar interactions for the binding event. However, the number of studies reported in literature using this type of receptors and performed in pure aqueous solution is still reduced. The relative contributions of polar and non-polar interactions in the formation and thermodynamic stabilization of supramolecular complexes in water is far from being completely understood. This is especially true when hydrogen bonding groups that can be solvated by water molecules are incorporated in the receptor's scaffold.

1.2 Aims of the thesis

The main objective of this thesis is the design and synthesis of water-soluble receptors able to selectively recognize biologically relevant small polar molecules in aqueous media. The designed receptors are based on aryl-extended calix[4]pyrrole scaffolds. The unique structure offered by aryl-extended calix[4]pyrroles makes them ideal candidates for our purpose. They possess four polar hydrogen bond donor groups buried in a sizeable hydrophobic cavity defined by four aryl rings that is closed at one end and open at the opposite one. The aromatic cavity protects the polar groups from solvation with the bulk solvent. In addition, the aryl rings are a perfect locations to introduce supplementary functional groups capable to establish additional interactions with the targeted guests increasing the selectivity and binding affinity of the receptors. However, to achieve this objective it was necessary to redesign the scaffolds of the already reported water soluble aryl-extended calix[4]pyrrole receptors in which the water solubilizing groups were introduced in the aryl rings that form the hydrophobic cavity.

Specifically, we pursued the following goals:

O.1.) **Preparation of water-soluble aryl-extended calix[4]pyrrole with unperturbed aromatic cavities**. Inspired by the known water-soluble resorcin[4]arene cavitands we envisioned that the preparation of water soluble aryl-extended calix[4]pyrroles in which the ionizable water solubilizing groups are placed opposite to the hydrophobic cavity (i.e. lower rim) will permit the future incorporation of additional functional groups close enough to the binding cavity to act as extra binding sites for the recognition of suitable guests. On the other hand, the water solubilizing groups will be far enough to avoid any interference with the deep

aromatic cavity that comprises the binding pocket. Within this objective, we also pursue the study of the binding ability of the new designed receptor towards polar neutral guests (i.e. pyridine *N*-oxides) in aqueous solution by means of NMR spectroscopy and ITC experiments.

O.2.) **Incorporation of additional polar functional groups in the upper rim of calix[4]pyrrole scaffolds and explore their binding ability towards biologically relevant small polar guests**.

Taking as inspiration the phosphonate receptors developed by Dalcanale and Dutasta groups, which are based on resorcin[4]arene scaffolds, our group described the synthesis of phosphonate calix[4]pyrrole receptors. We sought to further explore the incorporation of phosphonate and thiophosphonate groups at the upper rim of aryl-extended calix[4]pyrrole scaffolds aiming to develop unprecedented receptors soluble in organic solvents, as well as in water. The phoshonate and thiophosphonate groups will be used to connect covalently (bridge) two adjacent *meso*-3-hydroxy-phenyl -substituents of tetra-α isomers of aryl-extended calix[4]pyrroles and produce the corresponding cavitands. These polar (thio)phosphonate groups are known to function as efficient hydrogen bond acceptor units in molecular recognition processes. Moreover, we expect that the introduction of the polar bridging groups will increase the conformational rigidity of the receptor's cavity. We envisioned that the newly designed phosphonate cavitands could be used to recognize creatinine, an important biomarker for human health. Consequently, we plan to study the binding ability of the obtained receptors in organic solution for neutral creatinine and the creatininium cation. We are also interested in comparing the binding performance of the phosphonate cavitands in organic solution with their functioning in aqueous media. One final objective of this work is the incorporation of the prepared receptors in ion-selective electrodes for the quantification of creatinine in biological fluids such us urine and blood. This latter study will be carried out in collaboration with the group of Prof. Rius from the URV.

O.3.) **Synthesis of a fluorescent receptor for creatinine sensing**.

Our purpose is to synthesize a fluorescent chemosensor for sensing creatinine in organic media. We envisioned that the use of a calix[4]pyrrole cavitand combining a monophosphonate bridging unit and a fluorescent tag (e.g. dansyl group) could represent a good choice to achieve our plan. We expect that the use of a receptor featuring a deep aromatic cavity functionalized at its closed end and its upper rim would provide the necessary

selectivity and sensibility to the resulting chemosensor to compete with the previously described analogues used for creatinine sensing.

1.3 Outline of the thesis

This PhD thesis is divided in 5 different chapters including the present introduction (Chapter 1), 4 chapters of results and discussion (Chapters 2-5) and finally the general conclusions.

Following this short introduction, in chapter 2 we describe the synthesis and characterization of an unprecedented water-soluble aryl-extended calix[4]pyrrole macrocycle incorporating the water solubilizing groups at the lower rim, opposite to the binding site. We evaluate the binding ability of the receptor towards a series of pyridine *N*-oxides in aqueous solution.

Chapter 3 reports the synthesis of novel bis- and monophosphonate and tiophosphonate cavitands based on aryl-extended calix[4]pyrroles to serve as receptors for the biologically relevant target creatinine. The role of the phosphonate group in the recognition of creatinine was studied in detail in organic solvent. A short summary of the results obtained by incorporating of one of these receptors in ion selective electrodes for the quantitative detection of creatinine in bodily fluids is also described.

Chapter 4 deals with the design and synthesis of water-soluble bisphosphonate cavitands based on aryl-extended calix[4]pyrroles. The binding ability of these receptors towards creatinine and the role of the polar phosphonate groups in aqueous solution are discussed in this chapter. We also describe some complexation studies performed in water with other guests, such us diethyl nitrosamine.

In chapter 5 we describe the preparation of a fluorescent monophosphonate cavitand receptor incorporating a dansyl group as fluorophore. The receptor was used to develop a fluorescent chemosensor ensemble for the sensing of neutral creatinine in a non-polar organic solvent.

Finally, a summary of the more relevant conclusions drawn from the work performed in the thesis is provided at the end.

1.4 References and notes

[1] Biedermann, F.; Nau, W. M.; Schneider, H.-J. *Angew. Chem. Int. Ed.* **2014**, *53*, 11158-11171.
[2] Szejtli, J. *Chem. Rev.* **1998**, *98*, 1743-1754.
[3] Rekharsky, M. V.; Inoue, Y. *Chem. Rev.* **1998**, *98*, 1875-1918.
[4] Diederich, F.; Smithrud, D. B.; Sanford, E. M.; Wyman, T. B.; Ferguson, S. B.; Carcanague, D. R.; Chao, I.; Houk, K. N. *Acta Chem. Scand.* **1992**, *46*, 205-215.
[5] Diederich, F. In *Modern Cyclophane Chemistry*; Wiley-VCH Verlag GmbH & Co. KGaA: 2005, p 519-546.
[6] Biros, S. M.; Rebek, J. J. *Chem. Soc. Rev.* **2007**, *36*, 93-104.
[7] Jordan, J. H.; Gibb, B. C. *Chem. Soc. Rev.* **2015**, *44*, 547-585.
[8] Hooley, R. J.; Biros, S. M.; Rebek, J. J. *Chem. Commun.* **2006**, 509-510.
[9] Gomez-Gonzalez, B.; Francisco, V.; Montecinos, R.; Garcia-Rio, L. *Org. Biomol. Chem.* **2017**, *15*, 911-919.
[10] Dasgupta, S.; Mukherjee, P. S. *Org. Biomol. Chem.* **2017**, *15*, 762-772.
[11] Barbera, L.; Franco, D.; De Plano, L. M.; Gattuso, G.; Guglielmino, S. P. P.; Lentini, G.; Manganaro, N.; Marino, N.; Pappalardo, S.; Parisi, M. F.; Puntoriero, F.; Pisagatti, I.; Notti, A. *Org. Biomol. Chem.* **2017**, *15*, 3192-3195.
[12] Ogoshi, T.; Yamagishi, T.-a. *Eur. J. Org. Chem.* **2013**, *2013*, 2961-2975.
[13] Xue, M.; Yang, Y.; Chi, X.; Zhang, Z.; Huang, F. *Accounts Chem. Res.* **2012**, *45*, 1294-1308.
[14] Lagona, J.; Mukhopadhyay, P.; Chakrabarti, S.; Isaacs, L. *Angew. Chem. Int. Ed.* **2005**, *44*, 4844-4870.
[15] Cao, L.; Šekutor, M.; Zavalij, P. Y.; Mlinarić-Majerski, K.; Glaser, R.; Isaacs, L. *Angew. Chem. Int. Ed.* **2014**, *53*, 988-993.
[16] GREEN, N. *Biochem. J.* **1963**, *89*, 585-591.
[17] Livnah, O.; Bayer, E. A.; Wilchek, M.; Sussman, J. L. *Proc. Natl. Acad. Sci. U. S. A.* **1993**, *90*, 5076-5080.
[18] Snowden, T. S.; Anslyn, E. V. *Curr. Opin. Chem. Biol.* **1999**, *3*, 740-746.
[19] Kubik, S.; Reyheller, C.; Stüwe, S. *J. Incl. Phenom. Macrocycl. Chem.* **2005**, *52*, 137-187.
[20] García-España, E.; Díaz, P.; Llinares, J. M.; Bianchi, A. *Coord. Chem. Rev.* **2006**, *250*, 2952-2986.
[21] Kubik, S. *Chem. Soc. Rev.* **2010**, *39*, 3648-3663.
[22] Fabbrizzi, L.; Poggi, A. *Chem. Soc. Rev.* **2013**, *42*, 1681-1699.
[23] Alibrandi, G.; Amendola, V.; Bergamaschi, G.; Fabbrizzi, L.; Licchelli, M. *Org. Biomol. Chem.* **2015**, *13*, 3510-3524.
[24] Langton, M. J.; Serpell, C. J.; Beer, P. D. *Angew. Chem. Int. Ed.* **2016**, *55*, 1974-1987.
[25] Morshedi, M.; Thomas, M.; Tarzia, A.; Doonan, C. J.; White, N. G. *Chem. Sci.* **2017**, *8*, 3019-3025.
[26] Lochman, L.; Svec, J.; Roh, J.; Kirakci, K.; Lang, K.; Zimcik, P.; Novakova, V. *Chem. Eur. J.* **2016**, *22*, 2417-2426.
[27] Abraham, W. *J. Incl. Phenom. Macrocycl. Chem.* **2002**, *43*, 159-174.
[28] Kubik, S. *Chem. Soc. Rev.* **2009**, *38*, 585-605.
[29] Kato, Y.; Conn, M. M.; Rebek, J. *Proc. Natl. Acad. Sci. U. S. A.* **1995**, *92*, 1208-1212.
[30] Schneider, S. E.; O'Nei, S. N.; Anslyn, E. V. *J. Am. Chem. Soc.* **2000**, *122*, 542-543.
[31] Walker, D. B.; Joshi, G.; Davis, A. P. *Cell. Mol. Life Sci.* **2009**, *66*, 3177-3191.
[32] Deshmukh, M. M.; Bartolotti, L. J.; Gadre, S. R. *J. Phys. Chem. A* **2008**, *112*, 312-321.
[33] Abe, H.; Chida, Y.; Kurokawa, H.; Inouye, M. *J. Org. Chem.* **2011**, *76*, 3366-3371.
[34] Klein, E.; Crump, M. P.; Davis, A. P. *Angew. Chem. Int. Ed.* **2005**, *44*, 298-302.
[35] Barwell, N. P.; Crump, M. P.; Davis, A. P. *Angew. Chem. Int. Ed.* **2009**, *48*, 7673-7676.
[36] Ke, C.; Destecroix, H.; Crump, M. P.; Davis, A. P. *Nat. Chem.* **2012**, *4*, 718-723.
[37] Destecroix, H.; Renney, C. M.; Mooibroek, T. J.; Carter, T. S.; Stewart, P. F. N.; Crump, M. P.; Davis, A. P. *Angew. Chem. Int. Ed.* **2015**, *127*, 2085-2089.
[38] Sun, X.; James, T. D. *Chem. Rev.* **2015**, *115*, 8001-8037.
[39] Rios, P.; Mooibroek, T. J.; Carter, T. S.; Williams, C.; Wilson, M. R.; Crump, M. P.; Davis, A. P. *Chem. Sci.* **2017**, *8*, 4056-4061.

[40] Lascaux, A.; Leener, G. D.; Fusaro, L.; Topic, F.; Rissanen, K.; Luhmer, M.; Jabin, I. *Org. Biomol. Chem.* **2016**, *14*, 738-746.
[41] Brotin, T.; Martinez, A.; Dutasta, J.-P. In *Calixarenes and Beyond*; Neri, P., Sessler, J. L., Wang, M.-X., Eds.; Springer International Publishing: Cham, 2016, p 525-557.
[42] Brotin, T.; Dutasta, J.-P. *Chem. Rev.* **2009**, *109*, 88-130.
[43] Zhang, D.; Martinez, A.; Dutasta, J.-P. *Chem. Rev.* **2017**, *117*, 4900-4942.
[44] Perraud, O.; Robert, V.; Martinez, A.; Dutasta, J.-P. *Chem. Eur. J.* **2011**, *17*, 13405-13408.
[45] Perraud, O.; Robert, V.; Gornitzka, H.; Martinez, A.; Dutasta, J.-P. *Angew. Chem. Int. Ed.* **2012**, *51*, 504-508.
[46] Schmitt, A.; Robert, V.; Dutasta, J.-P.; Martinez, A. *Org. Lett.* **2014**, *16*, 2374-2377.
[47] Huang, G.-B.; Wang, S.-H.; Ke, H.; Yang, L.-P.; Jiang, W. *J. Am. Chem. Soc.* **2016**, *138*, 14550-14553.
[48] Pinalli, R.; Brancatelli, G.; Pedrini, A.; Menozzi, D.; Hernández, D.; Ballester, P.; Geremia, S.; Dalcanale, E. *J. Am. Chem. Soc.* **2016**, *138*, 8569-8580.

UNIVERSITAT ROVIRA I VIRGILI
CALIX[4]PYRROLE-BASED RECEPTORS FOR BIOLOGICALLY RELEVANT POLAR MOLECULES: FROM ORGANIC TO AQUEOUS MEDIA
Daniel Hernández Alonso

Chapter 2

Water-soluble aryl-extended calix[4]pyrroles with unperturbed aromatic cavities: synthesis and binding studies

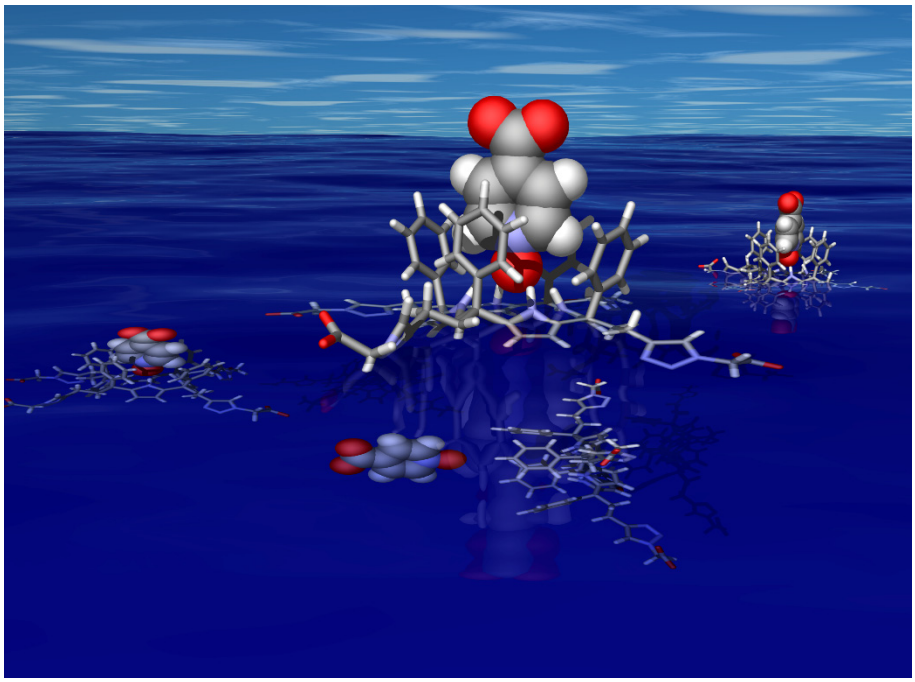

Part of this chapter has been published in:

Hernandez-Alonso, D.; Zankowski, S.; Adriaenssens, L.; Ballester, P. Org. Biomol. Chem. 2015, 13, 1022-1029.

UNIVERSITAT ROVIRA I VIRGILI
CALIX[4]PYRROLE-BASED RECEPTORS FOR BIOLOGICALLY RELEVANT POLAR MOLECULES: FROM ORGANIC TO AQUEOUS MEDIA
Daniel Hernández Alonso

2.1 Introduction

Calix[4]pyrroles are macrocyclic compounds constituted by four pyrrole rings linked through sp^3 carbon atoms also called *meso* carbons (Figure 2. 1).[1,2] It is known that calix[4]pyrroles can act as receptors for anions,[3] ion-pairs[4] and molecules containing electron rich groups.[5] When each *meso* carbon of the macrocycle is functionalized with a single aryl ring, they are called aryl-extended calix[4]pyrrole.[6,7] Depending on the relative orientation of the aryl ring, four different configurational isomers are possible. For example the *α, α, α, α* (tetra-α) isomer describes the one with the four aryl rings pointing in the same direction. They are also conformationally flexible, and depending on the media in which they are dissolved, they can exist in four different conformations.[8] For example in non-polar media the most favorable conformation is the 1,3-alternate, in which the pyrrole rings are alternatively oriented up and down with respect to the plane defined by the four *meso* carbons. Upon addition of a suitable hydrogen-bond acceptor (or when dissolved in certain polar solvents), the calix[4]pyrrole core adopts the cone conformation. In the cone conformation, all the NH's are pointing in the same direction and can simultaneously stablish hydrogen-bonding interactions with the included guest[9] (Figure 2. 1).

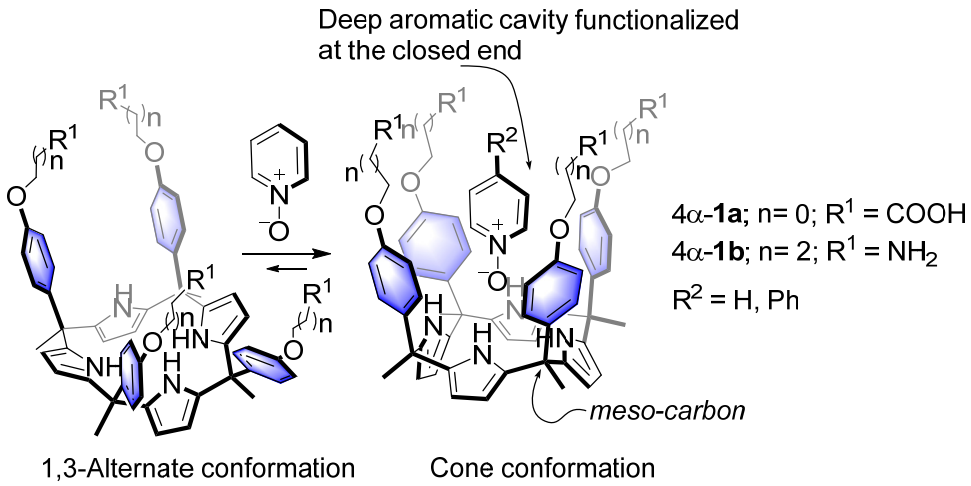

Figure 2. 1: The α,α,α,α-isomers of aryl-extended calix[4]pyrroles undergo a conformational change from the 1,3-alternate conformation to the cone conformation when binding guests capable of establishing H-bonding interactions.

More importantly, when the tetra-α isomer of an aryl-extended calix[4]pyrrole adopts the cone conformation, a deep aromatic cavity is formed. The aromatic cavity is closed at one end by the four converging pyrrole NHs, and open at the opposite end. The size of the cavity makes it suitable for the inclusion of a sizeable number of electron-rich neutral guests and anions. The intermolecular hydrogen bonds formed between the polar groups of the included guests and the polar NHs of the calix[4]pyrrole core result in a very specific relative orientation of the binding partners. Additional weak, non-covalent interactions such as CH–π and π–π stacking can also be established between the included guests and the aromatic walls of the receptor.

The polar aromatic cavity featured by aryl-extended calix[4]pyrrole receptors makes them very attractive for molecular recognition in aqueous media. In the cone conformation, the aromatic cavity shelter the convergent NHs groups from the bulk solvent. It is known that hydrogen-bonding interactions occurring in polar solvents with high dielectric constants (especially in water) are frequently much weaker than those that take place in non-polar solvents (low dielectric constant).[10,11] However, when the hydrogen bond partners are buried within an apolar cavity and are "sheltered" from the bulk water, the strength of their hydrogen bonding interactions becomes less solvent-dependent.[12,13,14,15] Taking advantage of this strategy, biological systems such as enzymes shelter the binding sites into hydrophobic pockets. This, ensure vital hydrogen-bonding interactions in the enzyme-substrate complexes, that would otherwise be suppressed by competition with molecules of water. While such interactions are ubiquitous in biological receptors, the synthesis of water-soluble receptors with polar functional groups included within a hydrophobic cavity is challenging.

The enormous synthetic possibilities offered by the polar and deep aromatic binding pocket of "four wall" aryl-extended calix[4]pyrroles have led to their extensive use as synthetic receptors[6,16,17] and binding units in supramolecular scaffolds such as catenanes,[18] non-covalent capsular assemblies,[19,20] covalent containers,[21] bola-type supra-amphiphiles,[22] metal-organic frameworks,[23,24] or rotaxanes.[25] Most of these studies have been carried out in organic media and the required functionality has been introduced at the open end of the cavity. From a supramolecular point of view, the understanding of molecular recognition processes in water, or in other words, the study of the magnitude of hydrophobic and in special hydrophilic interactions that govern the binding strength and selectivity, becomes more and more important.[26,27]

Excluding the present work, and to the best of our knowledge, only three examples of aryl-extended calix[4]pyrroles soluble in water have been reported in the literature.[28,29,30] From the previous examples, those reported from our group and Sessler's group, we learned the ability of aryl-extended calix[4]pyrrole to complex pyridine *N*-oxide group in water. The aryl-extended calix[4]pyrrole derivatives **1** (Figure 2. 1), which were employed in the above-mentioned studies, were rendered water soluble by covalently introducing four ionizable groups at the open end of their aromatic cavities, (in the *para* position of the *meso*-aryl rings), particularly amine and carboxylic groups. This synthetic strategy presented several design drawbacks. Firstly, the attachment of the solubilizing groups to the *meso*-aryl substituents alters the electronic nature of the pristine aromatic cavity. We have previously shown that the electronic properties of the cavity are tuned by the electron-withdrawing or electron-donating character of the substituents present in the meso-aryl groups. Secondly and even more importantly, the presence of the solubilizing groups at the upper rim impairs further elaboration of the aromatic cavity with other functional groups capable of interacting with the included guest, or with other molecules to provide higher order aggregates (i.e. dimeric capsules) or in the construction of more elaborate supramolecular systems.

In this chapter we describe the synthesis and preliminary binding studies of a new tetraphenyl water-soluble aryl-extended calix[4]pyrrole tetra-α-**2** (Scheme 2. 1). The new receptor was functionalized with "innocent" water-solubilizing groups located at the terminus of the *meso*-alkyl chains located at its lower rim. The solubilizing groups are sufficiently distant to avoid any interference with the pristine characteristics of the deep, hydrophobic and polar binding site. We envision that the described synthetic strategy will permit further elaboration of the aromatic cavity of water soluble aryl-extended calix[4]pyrroles through upper rim functionalization, eventually allowing access to higher order calix[4]pyrrole-based supramolecular structures in aqueous media.

2.2 Results and discussion

2.2.1 Synthesis and structural characterization

The novel water-soluble aryl-extended calix[4]pyrrole tetra-α-**2** was synthesized in five steps. Bearing in mind the expected low solubility in organic solvents of a tetraionic compound, the ionizable water-solubilizing groups are conveniently introduced in the final synthetic step. Thus, silica chromatography is an available purification technique in the synthesis of the tetra-

α-**3** calix[4]pyrrole precursor (Scheme 2. 1). This is an essential aspect due to the unavoidable need to remove the other configurational isomers and polymeric byproducts from the reaction mixture obtained in the condensation reaction of butynyl phenyl ketone **4** with pyrrole.

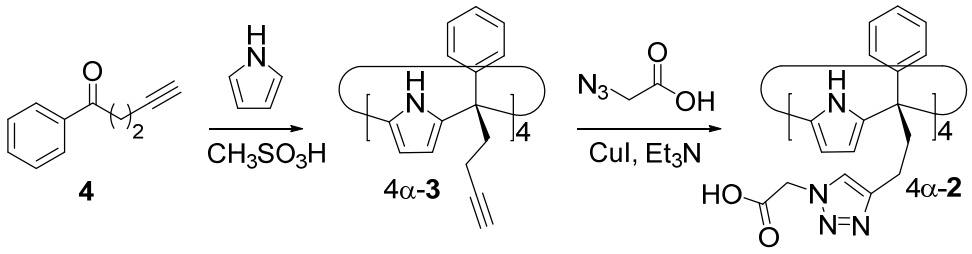

Scheme 2. 1: Synthetic scheme for the preparation of water soluble aryl-extended calix[4]pyrrole tetra-α-**2**.

The synthetic pathway to produce tetra-α-**2** requires the preliminary preparation of ketone **4** (Scheme 2. 2). Our first methodology started with the alkylation of the β-keto ester **5** with propargyl bromide using DBU as base. Then, the treatment of **6** with LiI produced the cleavage of the ester **6** and heat promoted decarboxylation of the corresponding β-keto acid (Scheme 2. 2, pathway a). Even though we were able to produce ketone **4** through this methodology, the decarboxylation step turned out to be capricious. A much better and reliable synthetic route for the preparation of the butynyl phenyl ketone **4** started from commercial acetophenone **7** and employed the methodology developed by Zaman et al. (Scheme 2. 2, pathway b).[31] Acetophenone **7** was converted in *N,N*-dimethyl hydrazone **8**, that after alkylation, followed by the hydrolysis of the hydrazone yielded ketone **4**. This robust synthetic pathway has the advantage of starting from simple and readily available acetophenones, meaning that water-soluble calix[4]pyrroles displaying *meso*-aryl rings with a wide variety of functionalization should be easily accessible.

The acid mediated cyclocondensation of ketone **4** with pyrrole to render tetra-α-**3** was very sluggish (Scheme 2. 1). After four days, the reaction crude consisted of a rich mixture of different products: Among them the desired tetra-α-isomer of the calix[4]pyrrole **3** was present, together with other configurational isomers (α, α, β, β and α, α, α, β), and higher order condensation products. After flash column chromatography purification of the reaction crude, followed by recrystallization in acetonitrile solution, we were able to isolate the tetra-α-isomer of calix[4]pyrrole **3** in low yield but with excellent purity.

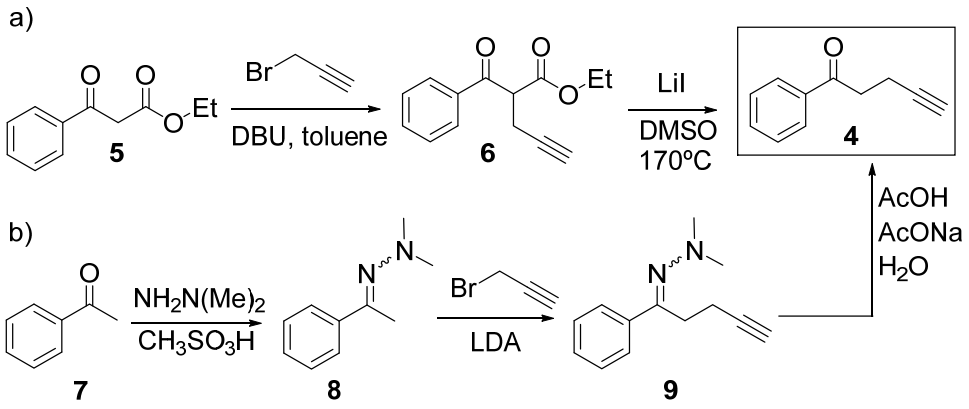

Scheme 2. 2: Alternative synthetic routes for the preparation of ketone **4**.

Luckily, single crystals of calix[4]pyrrole **3** suitable for X-ray analysis grew from acetonitrile solution. The solution of the diffraction data confirmed the configuration of the tetra-α-**3** isomer. As observed in Figure 2. 2, in the solid state, the tetra-α-**3** isomer adopts the cone conformation with a tilted molecule of acetonitrile included in its deep aromatic cavity. The nitrogen atom of the complexed acetonitrile is stablishing four simultaneous hydrogen bonding interactions with the four-pyrrole NHs, with an average N···N distance of 3.26 Å for the hydrogen bonds (Figure 2. 2).

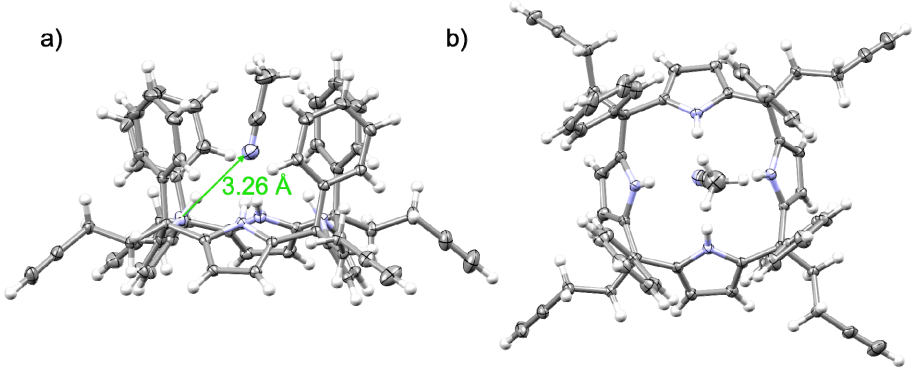

Figure 2. 2: Side a) and top b) view of the X-ray structure of the $CH_3CN\subset$tetra-α-**3** inclusion complex. In a) the hydrogen bond between tetra-α-**3** and bound acetonitrile has been highlighted. Thermal ellipsoids are set at 50% probability; H atoms are shown as spheres of 0.2 Å

Finally, we introduced the four ionizable groups to the tetra-α-**3** calix[4]pyrrole trough a click reaction. Thus, the reaction of tetra-alkyne tetra-α-**3** with azide **10** under standard copper (I)

catalyzed conditions, yielded the tetracarboxylic-functionalized receptor tetra-α-**2** in good yield (Scheme 2. 1). Gratifyingly, calix[4]pyrrole tetra-α-**2** was readily soluble in a variety of aqueous solutions such as diluted NaOH, and most notably, phosphate buffer saline (PBS) at pH 7.4, a solution often used to mimic biological media.

2.2.2 Binding studies

With the new water-soluble receptor tetra-α-**2** in hand, we explored its binding ability with three different pyridine *N*-oxide derivatives (PNO) in aqueous solutions. PNO are well known to be excellent guests for aryl-extended calix[4]pyrroles[19,32] and have previously been shown to form highly thermodynamically and kinetically stable complexes in aqueous solution.[30,33] Specifically, we analyzed the interaction of calix[4]pyrrole tetra-α-**2** with pyridine *N*-oxide **11**, 4-phenylpyridine *N*-oxide **12**, and isonicotinic acid *N*-oxide **13** (Figure 2. 3).

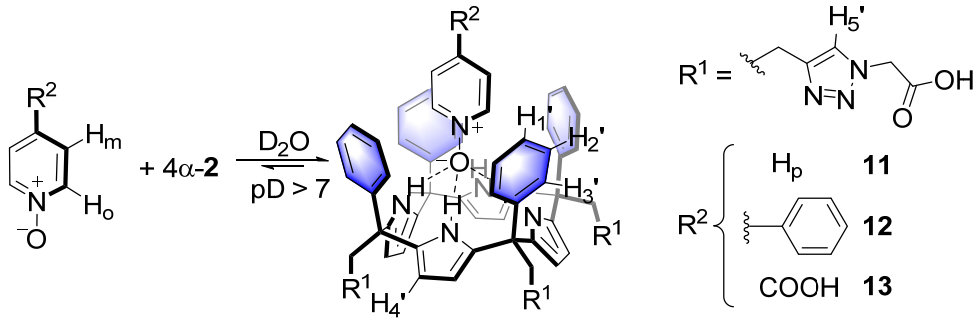

Figure 2. 3: Equilibrium involved in the formation of the inclusion complexes PNO⊂tetra-α-**2** and their proposed binding geometry.

Initially, we probed the complexation of the different PNO derivatives with receptor tetra-α-**2** using ^{1}H NMR titration experiments in slightly basic D_2O solutions (pD between 7.2 and 7.6 adjusted with NaOD). The ^{1}H NMR spectrum of tetra-α-**2** in D_2O showed sharp signals in agreement with an averaged C_{4v} symmetry (Figure 2. 4 a)). The ^{1}H NMR spectra acquired during the first stage of the titration experiment with PNO **11** to a ≈ 1 mM aqueous solutions of tetra-α-**2**, showed that the signals corresponding to the protons in the free receptor broadened and decreased in intensity. At the same time, we observed that a new set of broad signals appeared and grew at the expense of the signals of free tetra-α-**2** (Figure 2. 4b)). This new set of signals was assigned to the protons of the calix[4]pyrrole receptor in the inclusion

complex **11**⊂tetra-α-**2**. The signals corresponding to the *meta* and *para* pyridine *N*-oxide protons of the included **11** resonating at δ ≈ 6.5 (δ_{free} ≈ 7.5 ppm; Δδ = − 0.95 ppm) and 7.1 ppm (δ_{free} ≈ 7.6 ppm; Δδ = − 0.52 ppm), respectively, also became evident. The pyridine *N*-oxide protons *ortho* to the nitrogen atom of **11** (not shown in Figure 2. 4 due to the overlap with the broad water signal in this experiment, see Figure 2. 5) were the most affected by the magnetic anisotropy produced by the four *meso*-phenyl substituents. The *ortho* protons in the included PNO **11** experienced a very large upfield shift Δδ = − 4.0 ppm (δ_{free} ≈ 8.3 ppm). Taken together, these observations indicated the inclusion of the pyridyl *N*-oxide moiety of bound **11** at the bottom of the aromatic cavity of tetra-α-**2**. They also supported the proposed binding geometry for the **11**⊂tetra-α-**2** complex that is shown in Figure 2. 3. The *N*-oxide group of the PNO establishes four hydrogen-bonding interactions with the pyrrole NHs of tetra-α-**2**.[30] When slightly more than one equivalent of the PNO **11** was added to the solution, the proton signals corresponding to the free tetra-α-**2** disappeared completely (Figure 2. 4 c)). Only the proton signals assigned to the inclusion complex **11**⊂tetra-α-**2** were detected. The value of the integrals of the protons in tetra-α-**2** and **11** involved in the inclusion complex were in agreement with a 1:1 stoichiometry.

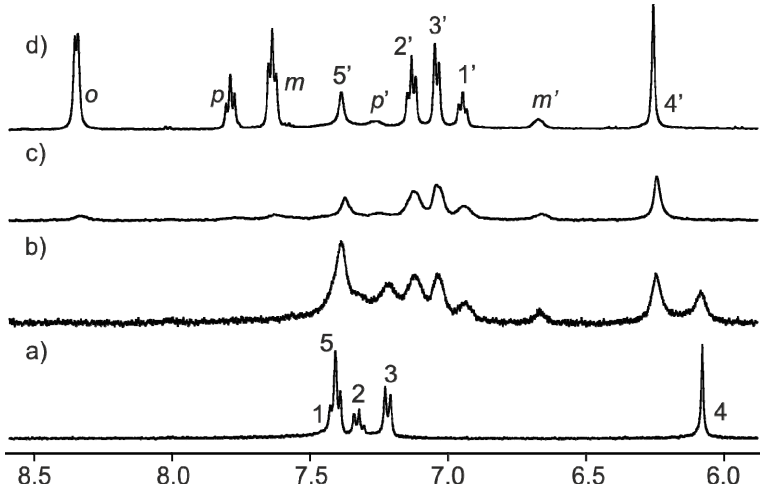

Figure 2. 4: Selected down field regions of the ^{1}H NMR spectra (400 MHz, D_2O pD ≈ 7.6, 298 K) acquired during the titration of calix[4]pyrrole tetra-α-**2** (1 mM) with incremental amounts of PNO **11**. (a) tetra-α-**2**; (b) tetra-α-**2** + 0.6 eq. **11**; (c) tetra-α-**2** + 1.1 eq. **11**; (d) tetra-α-**2** + 3.4 eq. **11**. Primed letters and numbers correspond to proton signals in the inclusion complex **11**⊂tetra-α-**2**. See Figure 2. 3 for proton assignment.

The addition of an excess of PNO **11** did not provoke changes in the chemical shifts or integrals of the signals corresponding to either tetra-α-**2** or **11** being involved in the **11**⊂tetra-α-**2** inclusion complex, however they experienced a notable sharpening. Simultaneously, a new set of proton signals corresponding to free PNO **11** emerged in the downfield region of the spectrum.

All together, these observations indicated that: a) the free species and their bound counterparts involved in the formation of the tetra-α-**2**⊃**11** inclusion complex were involved in a chemical exchange process that was slow on the ^{1}H NMR chemical shift time scale; b) the stability constant for the **11**⊂tetra-α-**2** complex can be estimated to be larger than 10^4 M^{-1}; and c) the hydrogen bonded pyridine *N*-oxide **11** must be rotating on its vertical axis when included in the deep aromatic binding pocket of tetra-α-**2** at a rate that at 298 K was fast on the chemical shift time-scale.

The geometry of the formed **11**⊂tetra-α-**2** complex and the kinetics of the binding process were also investigated by ROESY ^{1}H NMR experiments performed on the solution containing an excess of *N*-oxide **11** (Figure 2. 5).

The ROESY spectrum shows the existence of positive cross peaks between the signals assigned to the protons of PNO **11** in the free and bound states, **11**⊂tetra-α-**2** complex. This finding demonstrated that although the chemical exchange between the free and bound guest is slow on the chemical shift scale it is fast on the ROESY time scale (complex lifetime < 0.1 s). The observation of a cross peak between the signal of the protons *ortho* to the nitrogen atom in free **11** (H_o) and the highest upfield shifted signal belonging to the same protons in bound or included **11** confirms the deep inclusion of the *N*-oxide moiety into the cavity of the tetra-α-**2** receptor.

Completely analogous results were obtained for the titration of the tetra-α-**2** receptor with the *N*-oxide of 4-phenylpyridine **12** (Figure 2. 7 and Figure 2. 8).

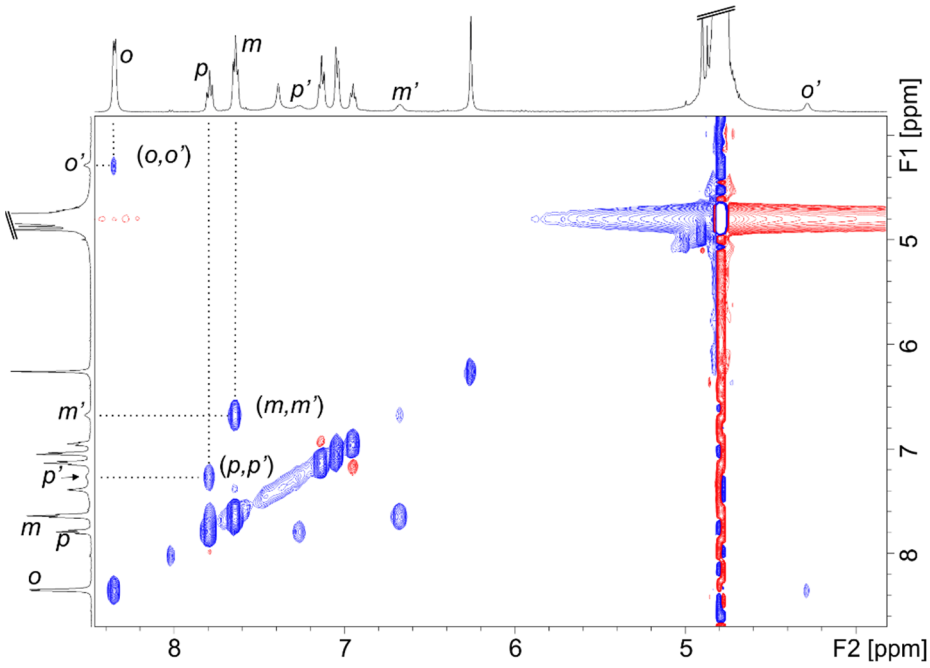

Figure 2. 5: Selected area of the ROESY ^{1}H NMR spectrum (500 MHz, D_2O, 298 K) of complex **11**⊂tetra-α-**2** in the presence of free **11** added in excess. The cross-peaks resulting from the chemical exchange process between protons of free and included **11** are indicated. Primed letters correspond to signals of the protons in the complex.

Isonicotinic acid **13**, in basic media, presents two polar groups able to stablish hydrogen-bonding interactions; the *N*-oxide and the carboxylate. Both groups have been reported to form thermodynamically stable complexes with calix[4]pyrroles.[34,35] The addition of incremental amounts of anionic **13**$^-$ to a solution of tetra-α-**2** in D_2O produced the appearance of a unique set of separated proton signals for the receptor, which were assigned to the receptor in the inclusion complex **13**⊂tetra-α-**2**. In close analogy to the results obtained with the PNO derivatives **11** and **12**, the inclusion complex **13**⊂tetra-α-**2** was formed quantitatively in the presence of 1 eq. of **13**. Two new signals corresponding to the protons of included **13** resonated at 6.9 and 4.3 ppm. The ROESY experiment recorded on a solution containing the inclusion complex **13**⊂tetra-α-**2** and free **13** added in excess showed that the highest upfield shifted proton appearing at 4.3 ppm were involved in a chemical exchange process with the signal for protons *ortho* to the nitrogen atom in free **13** (Figure 2. 10). Thus, the anionic form of isonicotinic **13**$^-$ was selectively included in the aromatic cavity of the tetra-α-**2** receptor through the *N*-oxide moiety. The carboxylate group of bound **13**$^-$ is exposed to the bulk solution and its negative charge seems to have a reduced effect in the binding strength

(estimated K_a (**13**$^-$⊂tetra-α-**2**) >10^4 M^{-1}) with the four-fold negatively charged receptor. Neutral *N*-oxides guests **11** and **12** produced inclusion complexes with similar kinetic and thermodynamic stabilities. In general, the ^{1}H NMR titration results reveal that the hydrophobic pocket of tetra-α-**2** is adequate to protect the pyrrole NHs from bulk water allowing the effective formation of hydrogen-bonding interaction with pyridine *N*-oxide guests. Although the establishment of hydrogen bonding interactions is the main factor responsible for the selectivity towards the *N*-oxide group (hydrophilic binding), the partial desolvation of the host and the guest required for the formation of the tight inclusion complexes (π–π and CH–π interactions) plays an important role in determining the binding strength (hydrophobic binding).

The results obtained from ^{1}H NMR titration experiments served to map-out the geometry of the inclusion complexes formed by the tetra-α-**2** receptor and the series of pyridine *N*-oxides, as well as determine their 1:1 stoichiometry. However, the stability constant values of the formed inclusion complexes are too high to be determined accurately by this technique (tetra-α-**2** receptor is fully complexed when one equivalent of *N*-oxide is added). For this reason, we determined the thermodynamic parameters in H_2O of the binding processes of tetra-α-**2** receptor with the series of PNOs using isothermal titration calorimetry (ITC) experiments.

All the ITC titrations performed with the PNO series **11-13** and the receptor tetra-α-**2** showed excellent fits to the theoretical binding isotherm that considers the exclusive formation of a complex with a 1:1 host:guest stoichiometry (Figure 2. 11). The fit of the titration data to the theoretical isotherms allowed the accurate determination of stability constant (K_a) and binding enthalpy (ΔH) values for the formation of the inclusion complexes. From these values, we could calculate the free energy of binding (ΔG) and the entropic ($T\Delta S$) component for each one of the binding processes. The obtained results are summarized in Table 2. 1.

Ratifying the results obtained using ^{1}H NMR titration experiments, the ITC results showed the formation of thermodynamically highly stable complexes with K_a values > 10^4 M^{-1}. In all cases, the binding processes were mainly enthalpically driven. Compared to the enthalpy components, the entropic terms are comparatively small and in the specific case of *N*-oxide **11** it also favored binding. These thermodynamic characteristics are in agreement with a tight fit of the interacting molecules in the inclusion complex and support the selective binding observed for the *N*-oxide group.[36]

Table 2. 1: Association constant values (K_a, M^{-1}), free energies of complexation (ΔG, kcal mol^{-1}) and corresponding enthalpic (ΔH, kcal mol^{-1}) and entropic components ($T\Delta S$, kcal mol^{-1}) measured in aqueous solution at 296 K for the inclusion complexes of the PNO series and aryl-extended calix[4]pyrrole tetra-α-**2**.

N-oxide	Medium/pH[b]	[a]K_a /10^4 (M^{-1})	ΔG	ΔH	$T\Delta S$
11	Water/7.2	4.3	-6.2	-4.5	1.7
12	Water/7.2	20.0	-7.2	-7.4	-0.2
13	Water/7.2	4.5	-6.3	-6.4	-0.1

[a]The reported values are the mean of those obtained from at least two ITC titration experiments. Errors (standard deviation) are determined to be less than 3%. [b]pH of the water solutions was adjusted with NaOH.

Our group reported previously the association constant values for the inclusion complexes of neutral PNOs **11** and **12** with the calix[4]pyrrole receptor tetra-α-**1a** (Figure 2. 1) in water. Receptor tetra-α-**1a** has four carboxylic groups at the upper rim close to the entrance of the cavity.[30] The reported values were measured using UV-vis titrations in H_2O solution (pH = 7.2) at concentrations that were similar to those used for the ITC experiments described here for the tetra-α-**2** receptor. The measured magnitudes in these two different studies compare well. The binding constant value determined for the **11**⊂tetra-α-**1a** complex was $K_a = 1.6 \pm 0.2 \times 10^4$ M^{-1}. This value is very close to the stability constant determined in this study for the **11**⊂tetra-α-**2** complex (Table 2. 1). Consequently, moving the water solubilizing anionic groups from the upper rim to the lower rim has a minimum impact on the binding of a small neutral molecules, like pyridine *N*-oxide **11**, with the calix[4]pyrrole core. We foresee that the change of location of the solubilizing groups should allow the functionalization of the upper rim of the calix[4]pyrrole receptor with groups that provide higher affinity and selectivity.

In contrast with the results obtained for PNO **11**, the previously reported binding constant for the **12**⊂tetra-α-**1a** ($K_a = 2.4 \pm 1.3 \times 10^3$ M^{-1}) was two orders of magnitude smaller than the one measured in this study for the related **12**⊂tetra-α-**2** complex. This result indicated that the location of the water solubilizing groups at the lower rim of a calix[4]pyrrole scaffold had a positive effect in the binding larger *N*-oxides like **12**. For this guest, the use of an alternative synthetic methodology for the placement of the water solubilizing groups at the lower rim without further modification of the upper rim was rewarding.

Remarkably, the binding constant values determined for the neural PNO **11** and the negatively charged counterpart **13**$^-$ with the tetra-α-**2** receptor are almost identical. This result surprised

us, because we were expecting that the negatively charged *N*-oxide **13**$^-$ would form a thermodynamically weaker complex with the also tetra-fold negatively charged calix[4]pyrrole tetra-α-**2** receptor. In water, the strong repulsive coulombic interactions that should be established between negatively charged species are highly attenuated, allowing the two molecules to form a tight complex. Water solvation is responsible of the screening of the negatively charged groups.

The stability constant calculated for the inclusion complex **12**⊂tetra-α-**2** is almost five-fold larger than that of the **11**⊂tetra-α-**2** counterpart. At first sight, this result can be attributed to the higher hydrophobicity of phenyl pyridine *N*-oxide **12** with respect to pyridine *N*-oxide **11**. One could expect that the larger apolar aromatic surfaces of **12** (higher hydrophobicity) will produce a stronger hydrophobic effect because of the favorable increase in desolvation entropy. However, as observed in Table 2. 1, the enhanced binding of **12** with respect to **11**, it is mostly due to an enthalpic gain. In addition, using simple molecular modelling studies the area of surface contacts for complexes **12**⊂tetra-α-**2** and **11**⊂tetra-α-**2** are predicted to be similar, as only the pyridyl *N*-oxide residue is included in the binding pocket (Figure 2. 6). The thermodynamic characteristics suggest a tighter geometry for the **12**⊂tetra-α-**2** complex that, as may be expected, is accompanied by a reduction in entropy gain, when compared to the looser complex formed by the same receptor with **11**. The effect exerted by the *p*-phenyl substituent in the thermodynamic stabilization of its complex with the receptor is far to be understood.

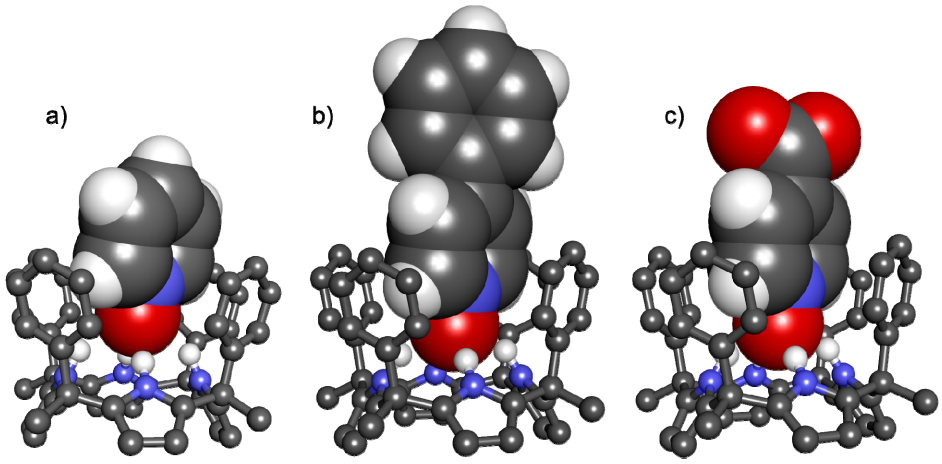

Figure 2. 6: Energy minimized (MO-G PM6 in water implemented in SCIGRESS Fujitsu Ltd. v 3.1.9) structures of the inclusion complexes of the *N*-oxides with tetra-α-**2**: (a) **11**⊂tetra-α-**2**; (b) **12**⊂tetra-α-**2**; and (c) **13**⊂tetra-α-**2**. The *meso*-alkyl chains of the receptor were modelled as methyl groups. For clarity, only NH hydrogen atoms of the receptor are shown and the included guests are represented as CPK models.

2.3 Conclusions

In conclusion, we described the synthesis of a novel water-soluble aryl-extended calix[4]pyrrole tetra-α-**2**. In contrast to previous examples, the carboxylic water-solubilizing groups in tetra-α-**2** are distal to the polar aromatic binding site. This leaves the aromatic binding site and the upper rim of the tetra-α-**2** calix[4]pyrrole pristine, making possible the future functionalization of the *meso*-aryl rings, thus, permitting the construction of more elaborated water soluble calix[4]pyrroles. The receptor tetra-α-**2** forms thermodynamically and kinetically stable complexes with a series of pyridine *N*-oxide guests in aqueous solution. The binding geometry of these complexes was probed using ^{1}H NMR titrations and their thermodynamic characteristics were determined using ITC experiments. The obtained results also demonstrated that in water the calix[4]pyrrole tetra-α-**2** preferentially engages in hydrogen bonding interactions of its four pyrrole NHs with a *N*-oxide moiety than with a carboxylate group. Nevertheless, the anionic tetra-α-**2** receptor binds negatively charged pyridine *N*-oxides with high affinity. Our results highlight the ability of the receptor's aromatic pocket to protect the pyrrole *N*-H groups and ensure selective hydrogen-bonding interactions even in water solution.

2.4 Experimental section

2.4.1 General information and instrumentation

Reagents were obtained from commercial suppliers and used without further purification. All solvents were commercially obtained and used without further purification except for pyrrole which was distilled (50 mbar, 58–59 °C) and then stored in the freezer for further use. Where indicated, solvents were degassed by 3 freeze–pump–thaw cycles. Routine ^{1}H NMR and ^{13}C NMR spectra were recorded on a Bruker Avance 300 (300 MHz for ^{1}H NMR), Bruker Avance 400 (400 MHz for ^{1}HNMR), Bruker Avance 500 (500 MHz for ^{1}H NMR) ultrashield spectrometer, or on a Bruker Avance III 500 (500 MHz for ^{1}HNMR) with a QNP cryoprobe. The deuterated solvents (Aldrich) used are indicated in the Experimental section; chemical shifts are given in ppm. The peaks were referenced relative to the solvent residual peak. All NMR *J* values are given in Hz. High resolution mass spectra were obtained on a MicroTOF II (Bruker Daltonics) ESI as ionization mode Mass Spectrometer or on a Bruker Ultraflex MALDI-TOF-TOF Mass spectrometer. Column chromatography was performed with silica gel, technical grade, pore size 60 Å, and 230–400 mesh particle size. Crystal structure determination was carried out using a Bruker-Nonius diffractometer equipped with an APEX2 4K CCD area detector, a FR591 rotating anode with MoKα radiation, Montel mirrors as the monochromator and a Kryoflex low temperature device (T = 100 K). Full sphere data collection was carried out by omega and phi scans. Programs used: data collection Apex2 V. 1.0–22 (Bruker-Nonius 2004), data reduction Saint + Version 6.22 (Bruker-Nonius 2001) and absorption correction SADABS V. 2.10 (2003). Crystal structure solution was achieved using direct methods as implemented in SHELXTL Version 6.10 (Sheldrick, Universität Göttingen (Germany), 2000) and visualized using the XP program. Missing atoms were subsequently located from difference Fourier synthesis and added to the atom list. Least-squares refinement on F2 using all measured intensities was carried out using the program SHELXTL Version 6.10 (Sheldrick, Universität Göttingen (Germany), 2000).

ITC titrations were carried out on a microcal VP-ITC microcalorimeter, at 298 K, in water adjusting the pH by addition of $NaOH_{(aq.)}$ solution until pH ≈ 11 and then adjusting with $HCl_{(aq.)}$ solution until pH ≈ 7.2. The association constants between receptor tetra-α-**2** and pyridine *N*-oxide **11**, **12**, and **13** were determined by monitoring the heat released by the system as incremental amounts of the *N*-oxide **11**, **12** or **13** were added. The values of the association constant K_a and the enthalpy of binding ΔH were calculated using Origin 7

software package. The values for the binding process were determined by averaging the values from two different titrations.

2.4.2 Synthetic procedures

Synthesis of ketone **4**. The synthesis of the ketone involves two steps:

Step 1, Hydrazone formation:[37] Benzene (38.5 mL) was added to acetophenone (7 mL, 59.4 mmol) contained in a 100 mL round bottom flask equipped with a Dean-Stark apparatus and under an argon atmosphere. Then 1,1-dimethylhydrazine (13.3 mL, 171 mmol) was added followed by methanesulfonic acid (0.19 mL, 2.93 mmol). After the addition of the acid, the mixture turned yellow. The reaction was refluxed overnight. The next day, the reaction mixture was concentrated under reduced pressure, affording the crude hydrazone **8** as a light yellow oil with a small amount of solid 10.5 g. This material was distilled at reduced pressure (13 mbar). The desired hydrazone **8** distilled in the range of 98–105 °C as a light yellow oil (8.5 g, 88%). The ^{1}H NMR spectrum is in agreement with that previously reported in the literature.[38]

Step 2 alkylation and hydrolysis of the hydrazone:[31] Lithium diisopropylamide (6.29 mL, 1.96 M, 12.33 mmol), freshly titrated using diphenylacetic acid as indicator, was added to a solution of hydrazone **8** (1 g, 6.16 mmol) in THF (15 mL, freshly distilled from sodium benzophenone) at -74 °C (achieved using a dry ice/acetone bath) under argon atmosphere. After 1 hour, 3-bromoprop-1-yne (80% solution in toluene, 0.69 mL, 6.16 mmol) was dropwise added. The reaction was stirred overnight while coming to rt. The next day, the reaction was quenched by adding 40 mL of saturated $NH_4Cl_{(aq)}$. The reaction mixture was extracted with diethylether (3 × 20 mL) and the organic extracts were combined, dried over Na_2SO_4, filtered and concentrated under vacuum to give a brown residue. Acetic acid 3 mL, sodiumacetate 1.45 g, water 0.5 mL and THF 3 mL were added to the resulting residue and the reaction was stirred under air for 7h (monitoring the hydrazone hydrolysis was done by ^{1}H NMR). The reaction mixture was quenched by adding $NaOH_{(aq)}$ (2 M) at 0 °C until the pH of the mixture was basic as judged by litmus paper. The mixture was stirred for 20 min and then 20 mL of diethyl ether were added. The two phases were separated and the aqueous layer was extracted with diethyl ether (2 × 20 mL). The organic extracts were combined, washed with 50 mL of water, and then with 50 mL of brine. Finally the organic extract was dried over Na_2SO_4, filtered and concentrated under vacuum, affording 0.82 g of the crude product as a

black solid. The solid was purified by column chromatography (40 g SiO_2 column, 1:1 DCM:hexane eluent, product RF = 0.5). The ketone **4** was obtained as light yellow crystals which were then sublimed in a bulb to bulb apparatus (0.1 mmHg, 80 °C), affording a white microcrystal-line powder (0.63 g, 65%). The ^{1}H NMR spectrum is in agreement with that previously reported in the literature.[39]

Synthesis of calixpyrrole tetra-α-**3**: Degassed methanol (10 mL) was added to pyrrole (0.44 mL, 6.34 mmol) and methanesulphonic acid (1.23 mL, 18.95 mmol, 3 eq.) contained in a 50 mL round bottom flask under argon atmosphere. Next, a methanolic solution of ketone **4** (17 mL, 0.37 M, 6.32 mmol) was added via syringe to the reaction mixture (heat is necessary to completely dissolve the ketone). After 4 days of stirring at room temperature, the reaction mixture was neutralized by adding 80 mL of saturated $NaHCO_3$(aq). The mixture was extracted with DCM (3 × 50 mL). The DCM extracts were combined, dried over Na_2SO_4 filtered, and concentrated under vacuum, affording 0.7 g of a dark colored residue. The crude was purified by column chromatography (20 g SiO_2, DCM:hexane 65 : 35, product Rf = 0.4). Two separate fractions containing the product were isolated: the first fraction (11.6 mg) contained the desired product and other configurational isomers. The second fraction (78 mg) contained the tetra-α-**3** isomer and an unidentified impurity with similar Rf = 0.4. Both fractions were separately dissolved in a minimum of hot acetonitrile. The solutions were cooled at 0 °C and the tetra-α-**3** isomer crystalized as small colorless cubes, 21.9 mg, 1-2 % yield. ^{1}H NMR (300 MHz, $CDCl_3$, 25 °C): δ(ppm) 7.25 (bs, 4H), 7.18–7.07 (m, 20H), 5.92 (d, J = 2.7 Hz, 8H), 2.56 (m, 8H), 2.09 (m, 8H), 1.95 (t, J = 2.6 Hz, 4H); ^{13}C{^{1}H}NMR (125 MHz, $CDCl_3$, 25 °C): δ(ppm) 135.1, 128.2, 128.1, 127.0, 106.4, 100.2, 84.5, 68.6, 48.6, 39.3, 15.0; HRMS (ESI-TOF) m/z: $[M + H]^+$ calcd for $C_{60}H_{53}N_4$ 829.4265; Found 829.4282; IR $\tilde{\nu}$ (cm^{-1}) 2116, 2961, 3301, 3370, 3404; m.p. 214–224 °C decomposition.

Synthesis of **10**:[40] Dry DMF (15 mL) was added to methyl bromoacetate (8 mL, 87 mmol) contained in a 100 mL round-bottom flask under argon atmosphere. The solution was stirred vigorously while sodium azide (6.21 g, 95 mmol) was added in several small portions. The reaction mixture was stirred for 2.5 additional hours followed by the addition of 50 mL of distilled water. The reaction mixture was extracted with diethyl ether (2 × 50 mL). Evaporation of the solvent afforded a light yellow oil. The oil was dissolved in 40 mL of THF and 40 mL of water. While stirring, 3 g of KOH were added to the solution in small portions. The mixture was stirred for 2.5 hours at 40 °C, cooled at r.t. and washed with ethyl acetate

(50 mL). The aqueous layer was acidified with HCl (1 M) until the pH of the solution was roughly 1 as judged by litmus paper. The aqueous layer was extracted with ethyl acetate (2 × 50 mL). Evaporation of the solvent afforded product **10** as a colorless oil (3.85 g, 44%). The ^{1}H NMR spectrum is in agreement with that previously reported in the literature.[40]

Synthesis of calixpyrrole tetra-α-**2** isomer: Degassed DMSO (0.9 mL) was added to tetra-α-calixpyrrole **3** (10 mg, 12 μmol) and 2-azidoacetic acid **10** (19 mg, 0.19 mmol) contained in a 2 mL flask under an argon atmosphere. Then, CuI (9.2 mg, 48 μmol) was added followed by Et_3N (7.9 mg, 77 μmol). A precipitate was immediately formed. The mixture was stirred vigorously and after 1 h the reaction was completed as judged by TLC. The reaction mixture was diluted with water (30 mL) and 10% $HCl_{(aq)}$ (10 mL) inducing the appearance of a solid that was isolated by filtration. The solid was washed with water (3 mL). Acetone was added to dissolve the filtered solid. The acetone solution was evaporated under vacuum to give 9.8 mg of the tetra-α-**2** isomer as a white powder, 66% yield. ^{1}H NMR (400 MHz, D_2O pD adjusted to 8 with NaOD, 25 °C): δ(ppm) 7.41 (m, 12H), 7.33 (m, 4H), 7.22 (d, J = 7.63 Hz, 8H), 6.08 (s, 8H), 4.89 (s, 8H), 2.82 (m, 8H), 2.48 (m, 8H); ^{13}C{^{1}H}NMR (125 MHz cryoprobe, D_2O pD adjusted to 8 with NaOD, 25 °C): δ (ppm) 174.7, 149.3, 145.7, 138.7, 129.9, 129.8, 128.5, 125.2, 106.9, 54.5, 49.9, 39.4, 22.4. HRMS (MALDI-TOF) m/z: $[M + Na]^+$ calcd for $C_{68}H_{64}N_{16}NaO_8$ 1255.4985; Found 1255.4998, IR $\tilde{\nu}$(cm^{-1}) 1728, 3332; m.p. 190 °C (decomposition)

2.4.3 Figures

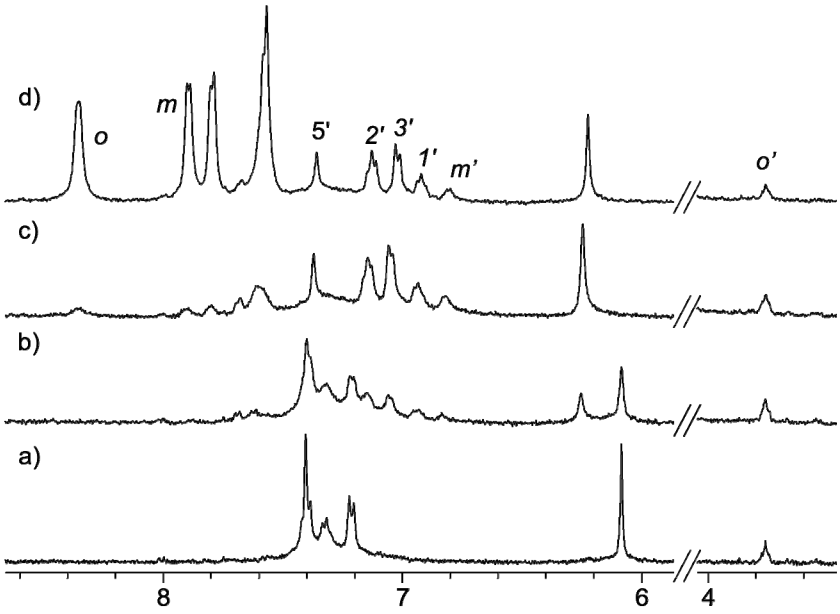

Figure 2. 7: Selected down field regions of the ^{1}H NMR spectra (400 MHz, D_2O adjusted to pD ≈ 7.6 with NaOD, 298 K) acquired during the titration of calix[4]pyrrole tetra-α-**2** (1 mM) with incremental amounts of **12**. (a) tetra-α-**2**; (b) tetra-α-**2** + 0.2 eq. **12**; (c) tetra-α-**2** + 1.1 eq. **12**; (d) tetra-α-**2** + 5.8 eq. **12**. Primed letters and numbers correspond to proton signals in the inclusion complex **12**⊂tetra-α-**2**. See Figure 2. 3 for proton assignment.

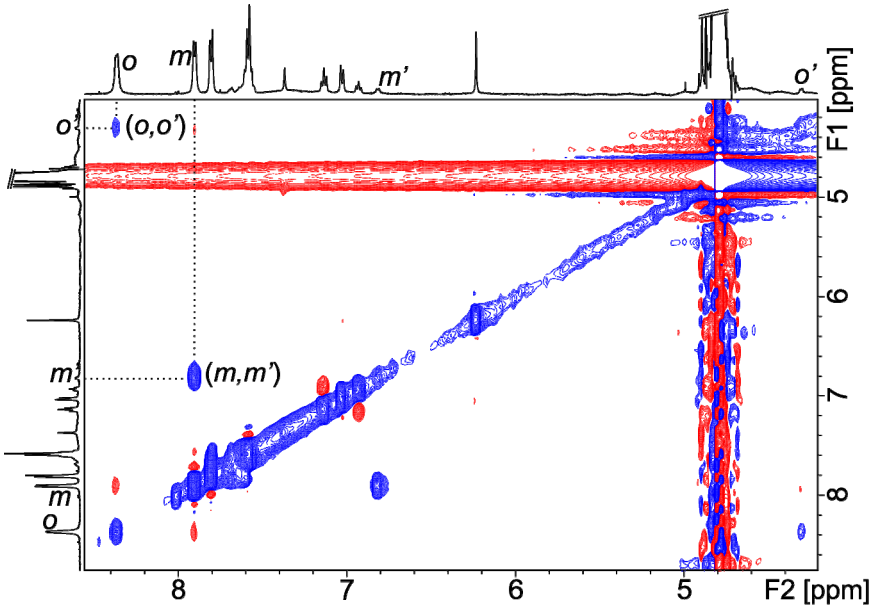

Figure 2. 8: Selected region of ROESY ^{1}H NMR (500 MHz, D_2O, 298 K) spectrum of complex **12**⊂tetra-α-**2** in the presence of free **12** in excess. The cross-peaks resulting from chemical exchange between protons of free and included **12** are indicated. Primed letters correspond to signals of the protons in the complex.

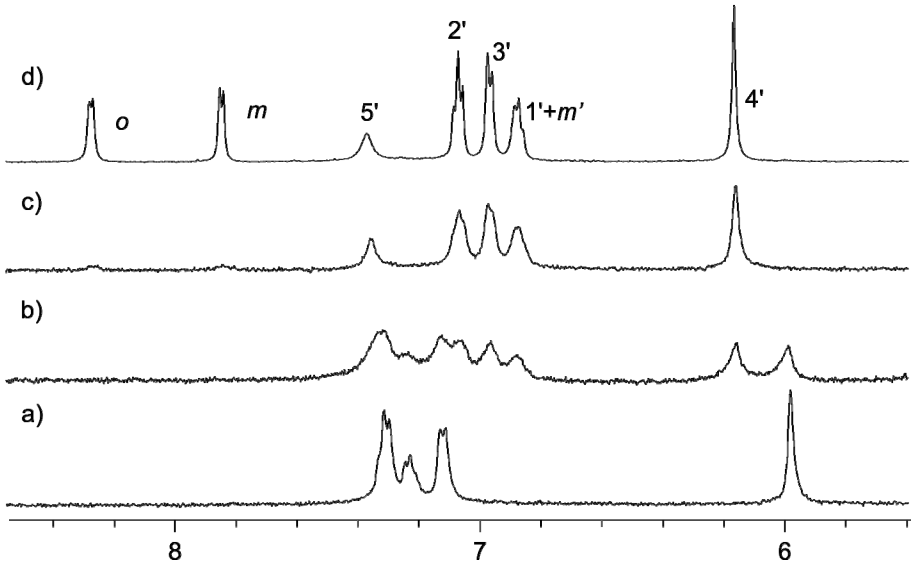

Figure 2. 9: Selected down field regions of the ^{1}H NMR spectra (400 MHz, D_2O adjusted to pD ≈ 7.2 with NaOD, 298 K) acquired during the titration of calix[4]pyrrole tetra-α-**2** (1 mM) with incremental amounts of **13**. (a) tetra-α-**2**; (b) tetra-α-**2** + 0.5 eq. **13**; (c) tetra-α-**2** + 1.1 eq. **13**; (d) tetra-α-**2** + 2.6 eq. **13**. Primed letters and numbers correspond to proton signals in the inclusion complex **13**⊂tetra-α-**2**. See Figure 2. 3 for proton assignment.

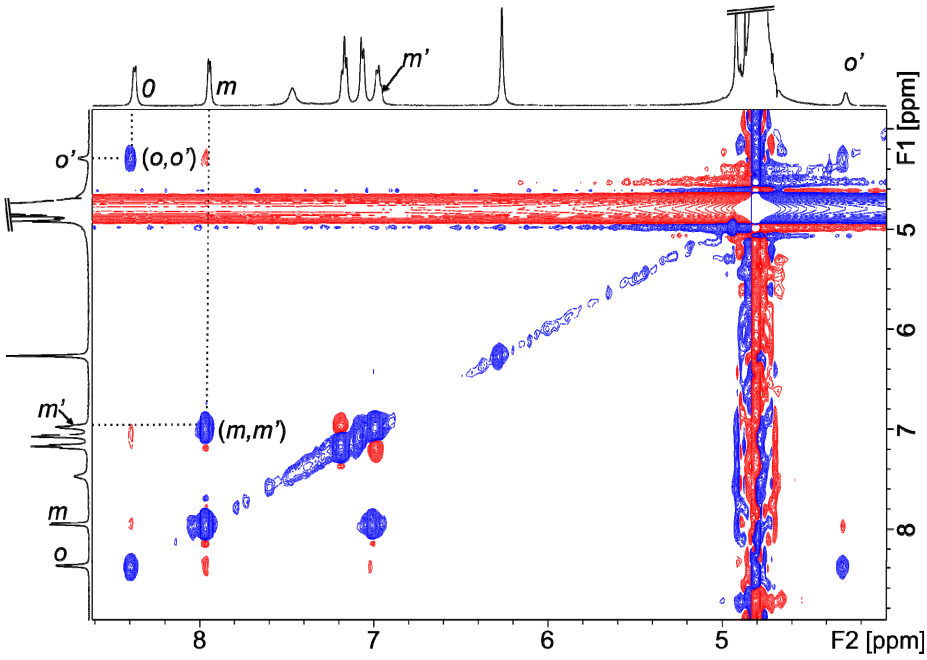

Figure 2. 10: Selected region of ROESY ^{1}H NMR spectrum spectra (500 MHz, D_2O, 298 K) of complex **13**⊂tetra-α-**2** in the presence of free **13** in excess. The cross-peaks resulting from chemical exchange between protons of free and included **13** are indicated. Primed letters correspond to signals of the protons in the complex.

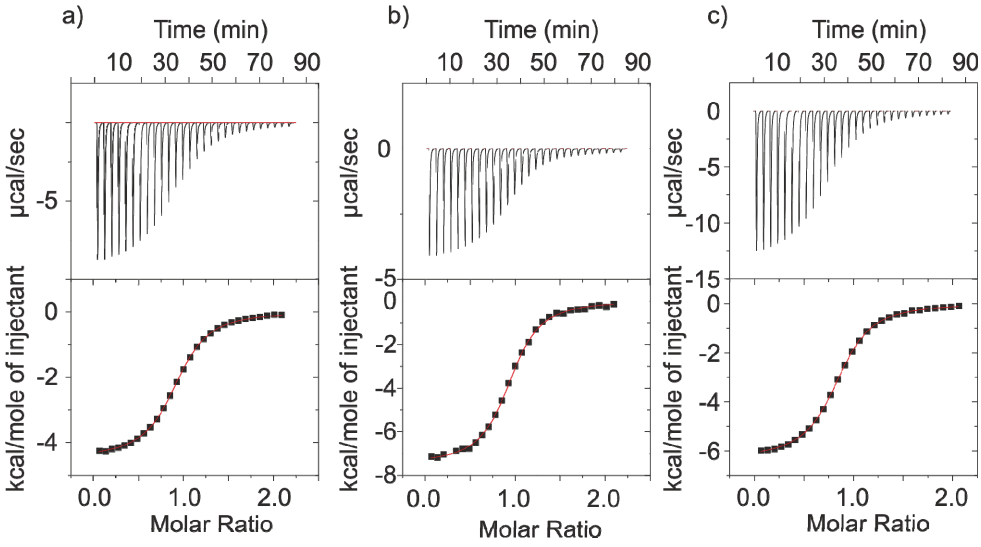

Figure 2. 11: ITC experiments; a) **11** added over [tetra-α-**2**;] = 0.62mM; b) **12** added over [tetra-α-**2**;] = 0.17mM; c) **13** added over [tetra-α-**2**;] = 0.63mM. Top trace: raw data for the ITC titration. Bottom trace: binding isotherm of the integrated calorimetric titration data.

2.5 References and notes

[1] Gale, P. A.; Sessler, J. L.; Kral, V. *Chem. Commun.* **1998**, 1-8.
[2] Gale, P.; Anzenbacher, P.; Sessler, J. *Coord. Chem. Rev.* **2001**, *222*, 57-102.
[3] Sessler, J. L.; Gross, D. E.; Cho, W. S.; Lynch, V. M.; Schmidtchen, F. P.; Bates, G. W.; Light, M. E.; Gale, P. A. *J. Am. Chem. Soc.* **2006**, *128*, 12281-12288.
[4] Kim, S. K.; Sessler, J. L. *Acc. Chem. Res.* **2014**, *47*, 2525-2536.
[5] Allen, W. E.; Gale, P. A.; Brown, C. T.; Lynch, V. M.; Sessler, J. L. *J. Am. Chem. Soc.* **1996**, *118*, 12471-12472.
[6] Anzenbacher, P.; Jursikova, K.; Lynch, V. M.; Gale, P. A.; Sessler, J. L. *J. Am. Chem. Soc.* **1999**, *121*, 11020-11021.
[7] Bonomo, L.; Solari, E.; Toraman, G.; Scopelliti, R.; Latronico, M.; Floriani, C. *Chem. Commun.* **1999**, 2413-2414.
[8] Blas, J. R.; López-Bes, J. M.; Márquez, M.; Sessler, J. L.; Luque, F. J.; Orozco, M. *Chem. Eur. J.* **2007**, *13*, 1108-1116.
[9] Wu, Y.-D.; Wang, D.-F.; Sessler, J. L. *J. Org. Chem.* **2001**, *66*, 3739-3746.
[10] Allott, C.; Adams, H.; A. Hunter, C.; A. Thomas, J.; L. Bernad Jr, P.; Rotger, C. *Chem. Commun.* **1998**, 2449-2450.
[11] Rotello, V. M.; Viani, E. A.; Deslongchamps, G.; Murray, B. A.; Rebek, J. *J. Am. Chem. Soc.* **1993**, *115*, 797-798.
[12] Sookcharoenpinyo, B.; Klein, E.; Ferrand, Y.; Walker, D. B.; Brotherhood, P. R.; Ke, C.; Crump, M. P.; Davis, A. P. *Angew. Chem. Int. Ed.* **2012**, *51*, 4586-4590.
[13] Torneiro, M.; Still, W. C. *J. Am. Chem. Soc.* **1995**, *117*, 5887-5888.
[14] Howgego, J. D.; Butts, C. P.; Crump, M. P.; Davis, A. P. *Chem. Commun.* **2013**, *49*, 3110-3112.
[15] Joshi, G.; Davis, A. P. *Org. Biomol. Chem.* **2012**, *10*, 5760-5763.
[16] Gil-Ramírez, G.; Escudero-Adán, E. C.; Benet-Buchholz, J.; Ballester, P. *Angew. Chem. Int. Ed.* **2008**, *47*, 4114-4118.
[17] Ciardi, M.; Galán, A.; Ballester, P. *J. Am. Chem. Soc.* **2015**, *137*, 2047-2055.
[18] Chas, M.; Ballester, P. *Chem. Sci.* **2012**, *3*, 186-191.
[19] Espelt, M.; Ballester, P. *Org. Lett.* **2012**, *14*, 5708-5711.
[20] Osorio-Planes, L.; Espelt, M.; Pericas, M. A.; Ballester, P. *Chem. Sci.* **2014**, *5*, 4260-4264.
[21] Galan, A.; Aragay, G.; Ballester, P. *Chem. Sci.* **2016**, *7*, 5976-5982.
[22] Chi, X.; Zhang, H.; Vargas-Zúñiga, G. I.; Peters, G. M.; Sessler, J. L. *J. Am. Chem. Soc.* **2016**, *138*, 5829-5832.
[23] Aguilera-Sigalat, J.; Sáenz de Pipaón, C.; Hernández-Alonso, D.; Escudero-Adán, E. C.; Galan-Mascarós, J. R.; Ballester, P. *Cryst. Growth Des.* **2017**, *17*, 1328-1338.
[24] Lee, J.; Waggoner, N. W.; Polanco, L.; You, G. R.; Lynch, V. M.; Kim, S. K.; Humphrey, S. M.; Sessler, J. L. *Chem. Commun.* **2016**, *52*, 8514-8517.
[25] Romero, J. R.; Aragay, G.; Ballester, P. *Chem. Sci.* **2017**, *8*, 491-498.
[26] Kataev, E. A.; Müller, C. *Tetrahedron* **2014**, *70*, 137-167.
[27] Oshovsky, G. V.; Reinhoudt, D. N.; Verboom, W. *Angew. Chem. Int. Ed.* **2007**, *46*, 2366-2393.
[28] Bhatt, K. D.; Vyas, D. J.; Makwana, B. A.; Darjee, S. M.; Jain, V. K. *Spectrochim Acta A Mol Biomol Spectrosc* **2014**, *121*, 94-100.
[29] Kongor, A.; Panchal, M.; Mehta, V.; Bhatt, K.; Bhagat, D.; Tipre, D.; Jain, V. K. *Arab. J. Chem* **2016**, https://doi.org/10.1016/j.arabjc.2016.1006.1019.
[30] Verdejo, B.; Gil-Ramírez, G.; Ballester, P. *J. Am. Chem. Soc.* **2009**, *131*, 3178-3179.
[31] Zaman, S.; Kitamura, M.; Abell, A. D. *Aust. J. Chem.* **2007**, *60*, 624-626.
[32] Adriaenssens, L.; Ballester, P. *Chem. Soc. Rev.* **2013**, *42*, 3261-3277.
[33] Adriaenssens, L.; Acero Sanchez, J. L.; Barril, X.; O'Sullivan, C. K.; Ballester, P. *Chem. Sci.* **2014**, *5*, 4210-4215.
[34] Gross, D. E.; Yoon, D.-W.; Lynch, V. M.; Lee, C.-H.; Sessler, J. L. *J. Inclusion Phenom. Macrocyclic Chem.* **2010**, *66*, 81-85.
[35] Kříž, J.; Dybal, J.; Makrlík, E.; Sedláková, Z.; Kašička, V. *Chem. Phys. Lett.* **2013**, *561*, 42-45.

[36] Highly selective substrate binding should be enthalpically driven see: F. Diederich, Cyclophanes, The Royal Society of Chemistry, Cambridge, 1991.
[37] Motiwala, H. F.; Gülgeze, B.; Aubé, J. *J. Org. Chem.* **2012**, *77*, 7005-7022.
[38] Sharma, S. D.; Pandhi, S. B. *J. Org. Chem.* **1990**, *55*, 2196-2200.
[39] Imagawa, H.; Kurisaki, T.; Nishizawa, M. *Org. Lett.* **2004**, *6*, 3679-3681.
[40] Chun, C. K. Y.; Payne, R. J. *Aust. J. Chem.* **2009**, *62*, 1339-1343.

Chapter 3

Recognition and Sensing of Creatinine

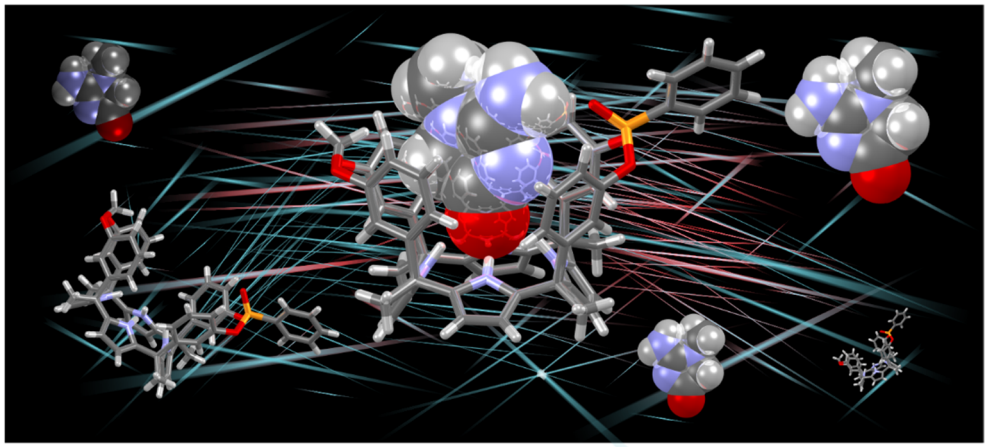

Part of this chapter has been published in:

Guinovart, T.; Hernández-Alonso, D.; Adriaenssens, L.; Blondeau, P.; Martínez-Belmonte, M.; Rius, F. X.; Andrade, F. J.; Ballester, P. *Angew. Chem. Int. Ed.* **2016**, *55*, 2435-2440.

UNIVERSITAT ROVIRA I VIRGILI
CALIX[4]PYRROLE-BASED RECEPTORS FOR BIOLOGICALLY RELEVANT POLAR MOLECULES: FROM ORGANIC TO AQUEOUS MEDIA
Daniel Hernández Alonso

3.1 Introduction

Determination of creatinine concentration in blood and urine is a physiological parameter that can be used to evaluate human health. Creatinine (**Cr**) is a metabolic product of creatine and phosphocreatine excreted through the urine. **Cr** concentration in urine and blood is used to calculate the glomerular filtration rate (GFR), a value that indicates the level of renal function.[1] Considering the importance that **Cr** levels have regarding human health, the current methods available for its quantification are suboptimal. The most widely used procedure for **Cr** quantification is the colorimetric determination of the complex formed by the reaction of **Cr** and picric acid under strong basic conditions known as Jaffe method.[2] However, this method suffers from several drawbacks: is complex, tedious, and sensible to interferences.[3] Enzyme-based methods for direct or indirect quantification of **Cr** levels with either colorimetric or electrochemical detection have overcome some of the drawbacks but still show analytical and practical weaknesses.[4,5] The use of isotope dilution gas chromatography yields very accurate results. Unfortunately, this methodology cannot be applied in a high-traffic routine laboratory due to the high cost.[6,7] In the mid 1990s, synthetic receptors able to form supramolecular complexes with **Cr** began to appear. The reported synthetic receptors are decorated with coplanar hydrogen-bonding acceptor and donor groups that converge complementing **Cr** functionalization Figure 3. 1.[8,9,10,11,12,13]

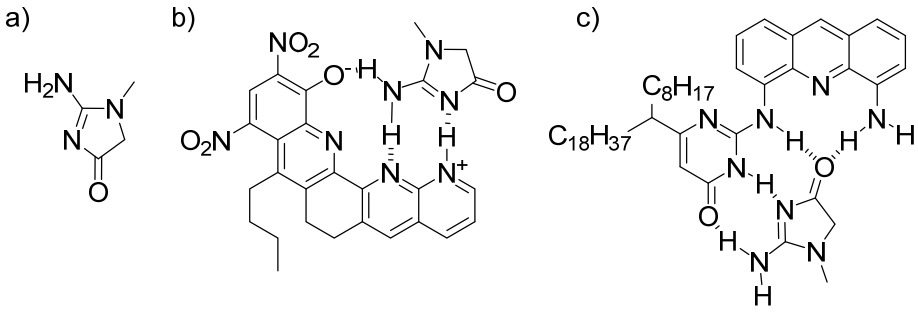

Figure 3. 1: Molecular structure of a) **Cr** and the supramolecular complexes reported by b) Bell[10] and c) Bühlmann[12].

Ion-selective electrodes (ISEs) are one of the simplest and most robust analytical methodologies to determine ion concentration and are already in use in routine clinical laboratories.[14] The major challenge in the development of ISEs for relatively complex

analytes, such as **Cr**, is the design of suitable synthetic receptors (ionophores) that preferentially bind the target ion especially in such complex matrix as urine or plasma.[15] Ionophores are responsible for an increase in ISE sensitivity and selectivity. However the reported examples of neutral synthetic ionophores for the potentiometric determination of **Cr** in solution did not satisfy the selectivities and detection limits required for the real sample analysis of biological samples.[16,17,18]

In this chapter, we describe the design, synthesis and binding studies of the calix[4]pyrrole receptor **1**, Scheme 3. 3, for the selective recognition of **Cr** and creatininium cation (**CrH**$^+$). In collaboration with the group of Dr. Francisco J. Andrade at the Universitat Rovira i Virgili, receptor **1** was tested as ionophore for the construction of ion selective electrodes for creatinine in bodily human fluids.

3.1.1 Ion selective electrodes (ISE)

An ISE is an electrochemical sensor that produce a potential (that is measured versus an outer reference electrode) for a given ion present in solution. The measured potential is a linear function of the logarithm of the ion activity according to Nernst equation. The key component of ISEs is the ion-selective membrane. The ISEs studied at the URV that contained the receptors presented in this chapter were based on polymeric membranes. These membranes were composed by PVC (polymeric matrix), *Ortho*-nitrophenyl octyl ether (plastizicer), potassium tetrakis[3,5-bis(trifluoromethyl)phenyl]borate (KBARF), and the ionophore.

The ionophore is the key component of the ion-selective membrane. The selectivity arise from the ability of the ionophore to bind preferentially the target ion against others present in the sample through the establishment of non-covalent interactions.

Considering the phase-boundary potential (E_{PB}) model,[19] the potential arise from an unequal distribution of the ion (I) across the interface. If there are not interferences from other ions present in the sample, a Nernstian response of the ISE is expected according to the following formula.

$$E_I = E_I^0 + \frac{RT}{z_I F} ln a_I$$

R, T and F refer to gas constant, temperature (in kelvin) and faraday constant respectively, a_I is the activity the ion (with charge z_I) in the aqueous sample and E^0_I is related with the activity of ion I in the organic membrane and the free energies of solvation in both phases.

3.2 Results and discussion

3.2.1 Design and synthesis

Our group reported the use of *α*, *α*, *α*, *α* -isomers of aryl-extended calix[4]pyrroles for the complexation of polar small guest in aqueous and organic solution.[20,21,22,23,24] In contrast to the previously reported flat receptors for **Cr**, aryl-extended calix[4]pyrroles possess a three-dimensional shape. Thus, they can include sizeable guests in its deep aromatic cavity in which four polar NH groups converge. The formed complexes are stabilized by a combination of hydrogen-bonding, CH–π, π–π, and hydrophobic interactions. We also reported the syntheses of bis- and tetra-phosphonate cavitands based on aryl-extended calix[4]pyrrole scaffolds featuring phosphonate bridging groups installed at their upper rim.[25,26] We observed that the relative orientation of the P=O groups with respect to the aromatic cavity, dictate the ion pair binding mode (close contact or host separated). In addition to the deep inclusion of the anion within the calix[4]pyrrole cavity, we detected intermolecular close-contact between the protons of the alkylammonium cation and those of the *meso*-phenyl substituents of the receptor when the upper-rim P=O groups were inwardly directed (i) with respect to its aromatic cavity. The alkylammonium cation that is located close to the upper rim of the receptor experienced charge-charge (coulombic) interactions with the bound anion and charge-dipole interactions with the P=O groups. On the other hand, when the P=O groups were outwardly directed (o) with respect to the receptor's aromatic cavity, the alkylammonium cation was preferentially located in the shallow cavity opposed to the included bound anion that is defined by the cone conformation of the calix[4]pyrrole core of the receptor. Bisphosphonate cavitands **2** (Scheme 3. 1) are readily accessible by simple reaction of the previously described tetra-phenoxy calix[4]pyrrole **3** and phenylphosphonic dichloride using Et_3N as base. The reaction yields a mixture of the three possible diastereoisomers that can be separated by flash column chromatography on SiO_2.

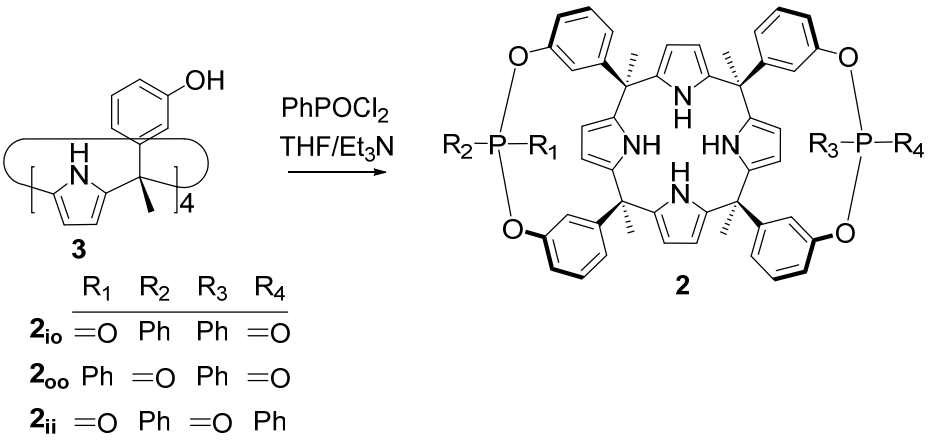

	R_1	R_2	R_3	R_4
$\mathbf{2_{io}}$	=O	Ph	Ph	=O
$\mathbf{2_{oo}}$	Ph	=O	Ph	=O
$\mathbf{2_{ii}}$	=O	Ph	=O	Ph

Scheme 3. 1: Synthetic scheme for the preparation of bisphosphonate cavitands **2**.

Simple molecular-modelling studies showed that the neutral **Cr** would be a perfect fit in terms of size and hydrogen-bonding complementarity to the polar aromatic cavity offered by the bisphosphonate-bridged cavitands $\mathbf{2_{ii}}$ and $\mathbf{2_{io}}$. As depicted in Figure 3. 2, the energy minimized structure of the **Cr**⊂$\mathbf{2_{io}}$ complex features the neutral **Cr** deeply included into the aromatic cavity of the receptor. Moreover, the bound **Cr** stablishes multiple intermolecular interactions with the polar groups and the aromatic rings of the receptor's scaffold.

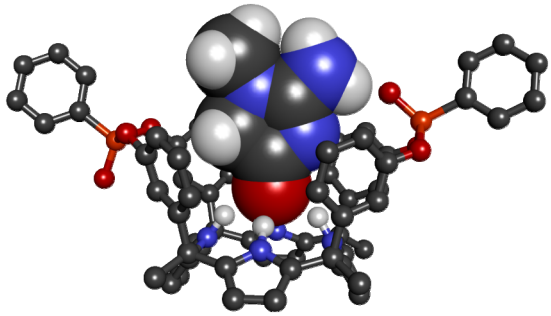

Figure 3. 2: Energy minimized structures (MM3) of the inclusion complex **Cr**⊂$\mathbf{2_{io}}$.

Preliminary studies using ISEs incorporating the three different diastereomeric bisphosphonates cavitands **2** into their respective membranes showed important interferences with Na^+ and K^+ cations. These cations are present in high concentrations in bodily fluids i.e. urine and plasma. These preliminary results prompted us to explore other calix[4]pyrrole

cavitand receptors as ionophores in the development of ISEs for creatinine quantification. We expanded the library of mono and doubly bridged cavitand receptors by changing the upper-rim functionalization of the parent tetra-hydroxyl calix[4]pyrrole **3**. We synthetized seven new cavitand receptors as possible candidates for selective ionophores for **Cr** quantification using ISEs Scheme 3. 2. The structural characterization of the seven newly prepared receptors can be found in the experimental section of this chapter.

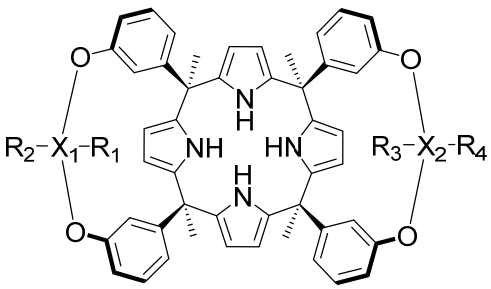

	X_1	X_2	R_1	R_2	R_3	R_4
PS_{io}	P	P	=S	Ph	Ph	=S
PS_{oo}	P	P	Ph	=S	Ph	=S
PS_{ii}	P	P	=S	Ph	=S	Ph
PO_iPS_o	P	P	Ph	=S	=O	Ph
PO_iPS_i	P	P	=S	Ph	=O	Ph
4_i	P	-	=O	Ph	-	-
1	P	C	=O	Ph	H	H

Scheme 3. 2: Molecular structures of the synthesized cavitands receptors. All receptors were evaluated as ionophores in the construction of ISEs for creatinine quantification in human bodily fluids.

A fast screening of the performance of the seven receptors incorporated in the membranes of ISE's, revealed that receptor **1** produced the ISE with the best response (selectivity and sensitivity) for the quantification of **Cr** in urine and plasma. Based on this result, we focused our binding studies in solution to the molecular recognition of **Cr** exerted by receptor **1**. The synthesis of **1** was achieved in three synthetic steps starting from the previously described calix[4]pyrrole **3**. Calix[4]pyrrole **3** was reacted with phenylphosphonic dichloride using the conditions reported for the synthesis of the bisphosphonates **2**. In complete agreement with the reported procedure the reaction yielded a mixture of the three possible diastereoisomers (ii, io and oo). Next, we applied the methodology reported by Tunstad et al.[27] for the cleavage of one of the four phosphonate groups installed at the upper rim of resorcin[4]arene derived cavitands, to the reaction crude that contained the mixture of the three diastereomeric bis-phosphonate cavitands **2**. Thus, the treatment of the mixture of diastereomeric bis-phosphonate cavitands **2** with catechol (1 eq.) under basic conditions produced the preferential excision of one of the two phosphonate bridging groups. After column chromatography purification of the obtained reaction crude, the pure monophosphonate **4_i** was isolated as a white solid in 18% yield. Finally, a methylene bridging group was incorporated at the upper

rim of **4i** by reacting it with $CH_2Br_2Cl_2$ using K_2CO_3 as base. The reaction yielded the mono-phosphonate-methylene bridged cavitand **1** as a white powder in 35% yield after column chromatography purification.

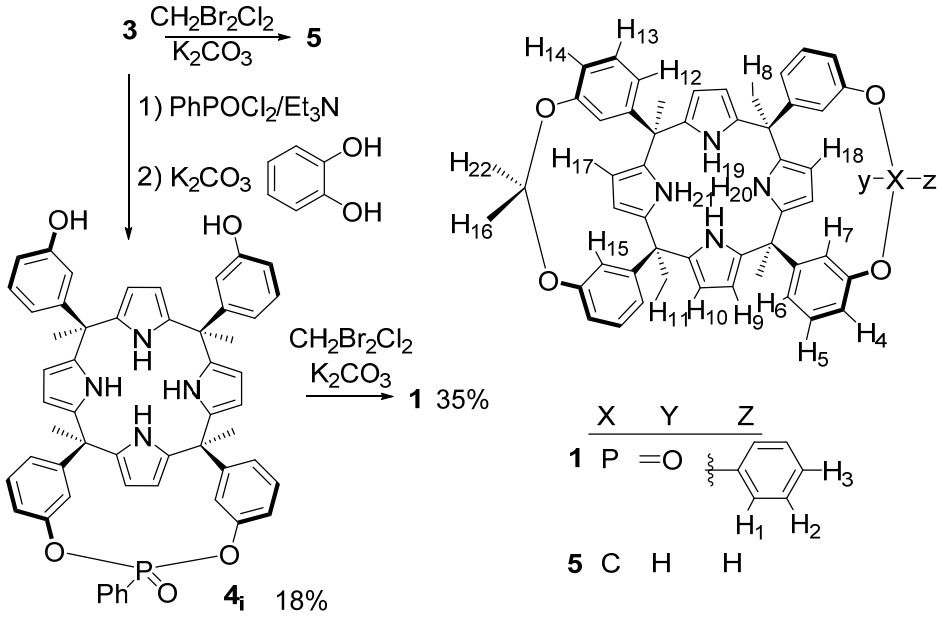

Scheme 3. 3: Synthetic scheme for the preparation of receptor cavitands **1** and **5**.

3.2.2 Binding studies of receptor **1** towards **Cr**

The ^{1}H NMR spectrum of **1** in CD_2Cl_2 solution showed sharp and well-defined proton signals. The number of signals and their integrals were in agreement with the expected C_s symmetry for **1** (Figure 3. 3 a)). Bearing in mind the well-known low solubility of neutral **Cr** in organic solvents,[28] we decided to perform solid–liquid extraction experiments. An excess of solid neutral **Cr** was added to a 1 mM solution of **1** in CD_2Cl_2. The resulting suspension was hand-shaken for several minutes and filtered. The filtered solution was analyzed using ^{1}H and ^{31}P $\{^1H\}$[29] NMR spectroscopy. The recorded ^{1}H NMR spectrum showed a single set of signals for the hydrogen atoms in **1**. Remarkably, the observed proton signals experienced significant changes in their chemical shift values compared to those of free **1** in CD_2Cl_2 solution. The ^{1}H and $^{31}P\{^1H\}$ NMR spectra of **1** registered before the extraction experiment was used as reference (Figure 3. 3 a) & c)).

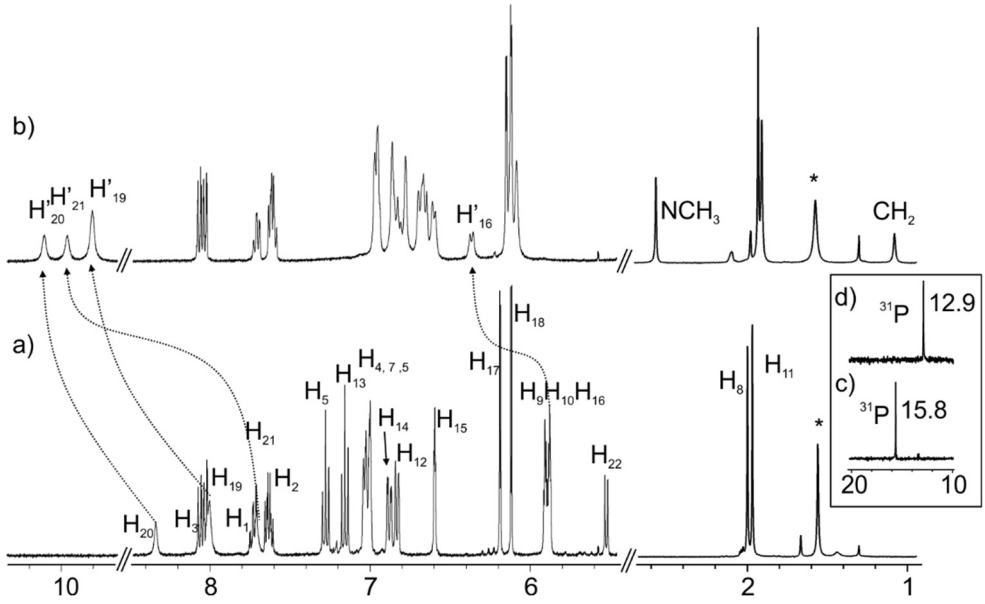

Figure 3. 3: Selected regions of the ^{1}HNMR spectra of monophosphonate cavitand **1** in CD_2Cl_2 a) and the corresponding filtered solution obtained after a solid–liquid extraction experiment with **Cr** (b). The corresponding ^{31}P {^{1}H} NMR spectra are shown as insets in (c) and (d). * refers to impurities. Proton assignment is shown in Scheme 3. 3.

After the extraction experiment, the three signals assigned to the NH pyrrole protons (with an integral ratio of 1:1:2) of receptor **1** experienced the most relevant and intense chemical shift changes. These three signals moved downfield ($\Delta\delta \approx 1.7–2.0$ ppm), suggesting their involvement in hydrogen-bonding interactions with the bound **Cr** guest. Two new singlets assigned to the methyl (NCH_3) and methylene protons (CH_2) of complexed **Cr** appeared at δ = 2.59 ppm (NCH_3) and 1.06 ppm (CH_2) (Figure 3. 3 b)). When compared to the chemical shift values of neutral **Cr** in [D6]DMSO solution Figure 3. 10, the proton signals for the bound **Cr** resonated significantly upfield shifted (δ_{free} = 2.9 ppm for NCH_3, $\Delta\delta \approx$ - 0.36 ppm and δ_{free} = 3.6 ppm for CH_2, $\Delta\delta \approx$ - 2.54 ppm). The upfield shift experienced by the methylene group of bound **Cr** was significantly larger than for methyl signal in the NCH_3 unit. Taken together, these observations strongly suggested a deep inclusion of the **Cr** in the aromatic cavity of **1** mainly driven by the hydrogen-bonding interactions established between the oxygen atom of the carbonyl group of **Cr** and the pyrrole NHs of **1**. The ratio of integral values for the proton signals assigned to **1** and **Cr** indicated that one equivalent of **Cr** had been extracted. A DOSY NMR experiment performed after the extraction of **Cr** provided an identical diffusion coefficient value of $9.3 \pm 0.3 \times 10^{-10}$ m^2/s (r = 5.7 Å) to the proton signals assigned to the

receptor **1** and the bound **Cr** Figure 3. 11 indicating their involvement in a unique complex. The intermolecular cross peak patterns observed for protons of bound receptor **1** and complexed **Cr** in 2D ROESY (Figure 3. 4) and NOESY (Figure 3. 13 and Figure 3. 14) experiments further confirmed the proposed binding geometry. All together, these results demonstrate that neutral **Cr** forms a thermodynamically highly stable inclusion complex with receptor **1**. The oxygen atom of neutral **Cr** established four hydrogen bonds with the four pyrrole NH groups of the calix[4]pyrrole core; one additional hydrogen bond was formed between the acyclic NH group of **Cr** and the oxygen atom of the P=O group. The **Cr** methylene hydrogen atoms were involved in CH–π interactions with two of the aryl substituents at the *meso* positions. The significant coverage offered by the aromatic cavity of **1** around the **Cr** surface in the inclusion complex **Cr⊂1** represents a breakthrough with respect to the previously described flat receptors for this analyte.

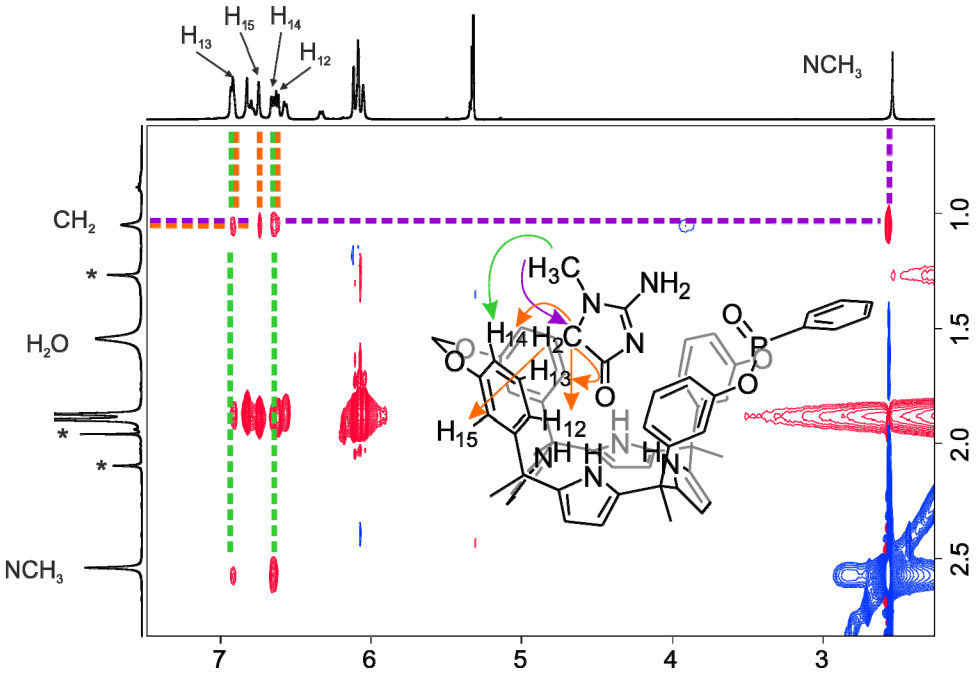

Figure 3. 4: Selected area of the ROESY ^{1}H-NMR spectrum (Figure 3. 12) acquired after extraction of solid neutral **Cr** with a 5.95 mM solution of receptor **1** in CD_2Cl_2. The inserted figure highlights the observed patterns of cross peaks between proton signals in bound **1** and **Cr** due to intermolecular close contacts (dipole coupling).

Assuming that the solubility of neutral **Cr** in CD_2Cl_2 is lower than 1×10^{-4} M and that after solid-liquid extraction only a 1:1 inclusion complex is formed, we could estimate the lower limit of the stability constant $K_{(\mathbf{Cr}\subset\mathbf{1})}$ to be 1×10^7 M^{-1} (complex/free host ratio > 100). Luckily, slow evaporation of a mM filtered solution of **1** after solid-liquid extraction with excess of solid **Cr** in DCM yielded single crystals that were suitable for X-ray diffraction analysis. The structure returned from the solution of the diffraction data (Figure 3. 5) shows the inclusion complex **Cr⊂1** in the solid state. The structure of the inclusion complex is in complete agreement with the results obtained in solution (NMR) and molecular modeling studies in the gas phase.

With the aim to assess the importance of the bridging phosphonate group in **1** for the thermodynamic stabilization of the complex, we performed extraction experiments with **Cr** and the previously described doubly methylene-bridged receptor **5**,[26] having a closely related structure and conformational flexibility to cavitand **1**, lacking the phosphonate group (Scheme 3. 1). We performed a solid-liquid extraction experiment using a CD_2Cl_2 solution containing receptor **5** and excess of the insoluble neutral **Cr**. Unfortunately, the ^{1}H NMR spectrum of the filtered solution did not show the presence of the free receptor or any complex in solution. Most likely, an insoluble aggregate is formed upon interaction of **5** and **Cr**. Remarkably, in acetone solution, receptor **1** was able to extract 0.40 eq. of **Cr** (Figure 3. 15), whereas **Cr** proton signals were not detected in control extraction experiments with reference receptor **5** or in the absence of any receptor. This result clearly supported the importance of the hydrogen bonding between the guest NH moiety of **Cr** and the inwardly directed PO group of receptor **1** in increasing its binding affinity towards **Cr**.

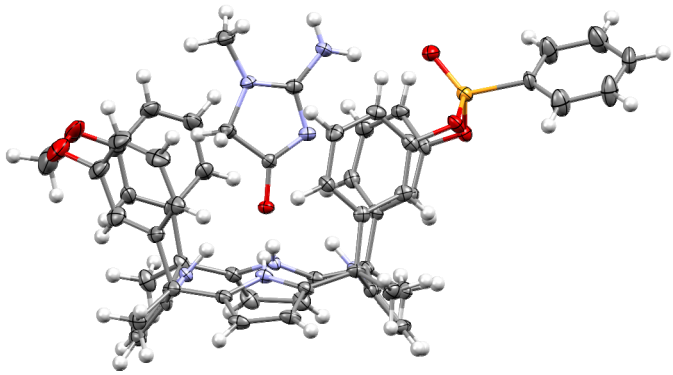

Figure 3. 5: Side view of the X-ray structure of the inclusion complex **Cr⊂1**. Thermal ellipsoids set at 50% probability. The H atoms are shown as spheres of 0.2 Å.

Due to the lack of solubility of **Cr** in DCM and especially because of the formation of insoluble aggregates when receptor **5** is treated with excess of solid **Cr**, we were not able to quantitatively determine the energetic contribution of the extra hydrogen bond established between the NH of **Cr** and the PO group of **1**. In order to increase the solubility of the **Cr** guest in DCM, we synthetized a lipophilic creatinine derivative (**CrHx**) by replacing the NCH_3 group with a *n*-hexyl alkyl chain (Figure 3. 16). This creatinine derivative was soluble in DCM solutions in concentrations up to 0.8 mM. The energy minimized structure of the inclusion complex **CrHx⊂1** (Figure 3. 16) shows that the *n*-hexyl chain can be located outside of the aromatic cavity of **1** without interfering with complex formation. Thus, we consider that the stability constant values for the complexes of **1** or **5** with **CrHx** are similar to those produced with **Cr**. Firstly, using NMR titration experiments, we verified that the formed complexes with **CrHx** were structurally related to those obtained with **Cr**. Due to solubility limitations, we performed reverse titrations (adding the receptor over **CrHx**). As observed in Figure 3. 6, the addition of 0.5 eq. of receptor **1** to a mM solution of **CrHx** in DCM produced the appearance of a new set of proton signals for **CrHx**. This new set of signals was assigned to the protons of bound **CrHx**. This observation of separate signals for free and bound **CrHx** indicated that the rate of exchange between them was slow on the chemical shift time scale. The signals of the two proton signals in bound **CrHx** CH_2 and NCH_2, (the latter analogous to the NCH_3 in **Cr**) resonate upfield shifted (δ_{free} = 3.3 ppm, $\delta_{complex}$ = 2.9 ppm, $\Delta\delta \approx$ - 0.41 ppm for NCH_2 and δ_{free} = 3.82 ppm, $\delta_{complex}$ = 1.1 ppm, $\Delta\delta \approx$ - 2.68 ppm for CH_2) in comparison to the chemical shift values in **CrHx** free in solution. These chemical shift changes are in

complete agreement with those observed for the bound natural **Cr**. Addition of more than one eq. of **1** did not produce additional changes on the proton signals assigned to bound **CrHx**. However, a new set of proton signals corresponding to free **1** became visible. The signal for the phosphorous atom in free **1** was also observed in the ^{31}P NMR spectrum of the mixture.

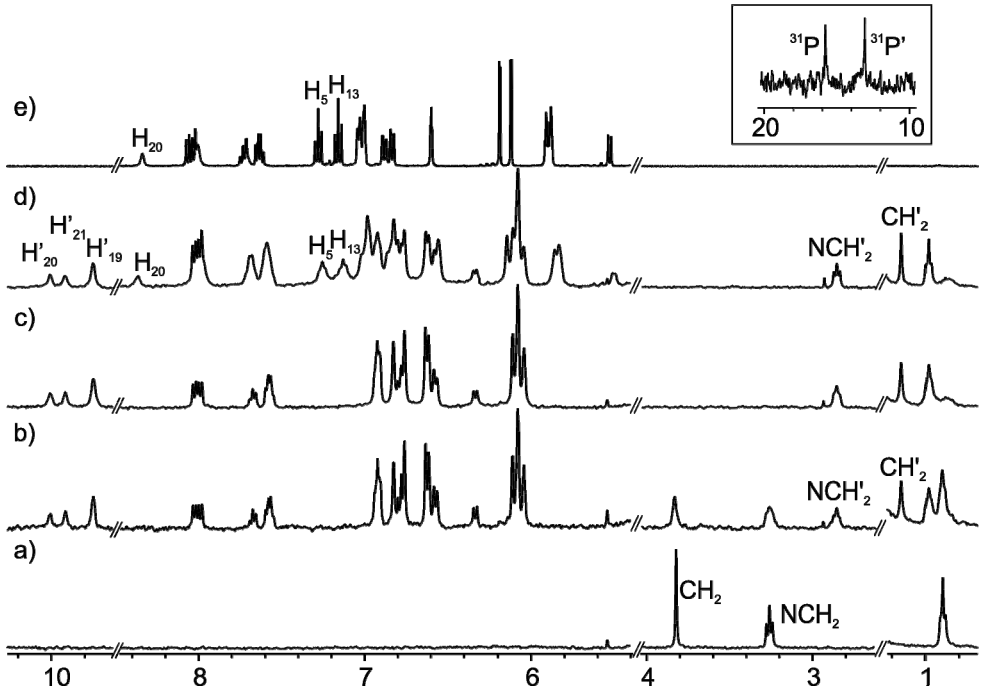

Figure 3. 6: Selected regions of the ^{1}H NMR spectra acquired during the titration of a 0.8 mM solution of **CrHx** in CD_2Cl_2 with incremental amounts of **1**. a) 0 eq. b) 0.5 eq. c) 1.0 eq. d) 2.4 eq. e) Free **1**. The $^{31}P\{^{1}H\}$NMR spectrum corresponding to d) is shown as inset.

All together, these results indicated that the formation of the 1:1 complex **CrHx⊂1** was completely analogous in terms of binding geometry, complex stoichiometry and thermodynamic stability (*K*a larger than 10^4 M^{-1}) to the one obtained with the natural **Cr**.

Following the same methodology, we titrated a solution of **CrHx** with incremental amounts of **5** (Figure 3. 17). Similar to the results obtained with receptor **1**, the addition of **5** to a **CrHx** DCM solution produced the appearance of new set of proton signals that was assigned to bound **CrHx**. The observed chemical shifts changes experienced by the protons of bound **CrHx** were comparable to those measured after the addition of equal quantities of receptor **1** (δ_{free} = 3.3 ppm, $\delta_{complex}$ = 2.9 ppm, $\Delta\delta \approx$ - 0.41 ppm for NCH_2 and δ_{free} = 3.82 ppm, $\delta_{complex}$ =

1.3 ppm, $\Delta\delta \approx$ - 2.53 ppm for CH_2). We also observed that the pyrrole NHs of the bound receptor resonated highly downfield shifted indicating their involvement in hydrogen-bonding interactions. The addition of one equivalent of **5** induced the complete disappearance of the proton signals corresponding to free **CrHx**. The incremental addition of more than one equivalent of **5** produced the appearance and increase of a separate set of proton signals that corresponded to free **5**. All together, these observations indicate that receptor **5** also forms a 1:1 inclusion complex with **CrHx**. The binding geometries for the complexes **CrHx⊂1** and **CrHx⊂5** are similar. Moreover, we can estimate that the binding constants for both complexes are larger than 10^4 M^{-1} because the quantitative formation of the complexes is reached by addition of just one equivalent of the receptor.

The thermodynamic parameters of the two binding processes were assessed using isothermal titration calorimetry (ITC) experiments. Owing to solubility problems, the titrations were performed by incremental injection of a DCM solution of the receptor (**1** or **5**) to a DCM solution of **CrHx** place in the cell. For both titrations, the fit of the normalized integration heat to a theoretical binding model that consider the exclusive formation of a complex with 1:1 stoichiometry was excellent (Figure 3. 18). The values of the binding constant (*K*a), enthalpy (ΔH), free energy of binding (ΔG) and entropy ($T\Delta S$) returned from the fits are summarized in Table 3. 1. In complete agreement with the NMR results, the ITC experiments revealed the formation of highly thermodynamically stable complexes (*K*a > 10^5 M^{-1}. The binding constant value determined for the **CrHx⊂1** complex is ≈ 20 times larger than for the **CrHx⊂5** counterpart. For the two receptors, the complex formation is mainly enthalpically driven. The entropic contribution is small but also favors the formation of the complex. The favorable entropic term suggested that desolvation of the binding partners and subsequent complex formation induced the release of solvent molecules to the bulk solution. The larger affinity featured by receptor **1** is mostly due to a gain in enthalpy (≈ -1 kcal × mol^{-1}), which agrees well with the formation of an extra hydrogen-bond between the PO group of **1** and the NH of the included **CrHx**.

Table 3. 1: Association constant values (Ka, M^{-1}), free energies of complexation (ΔG, kcal×mol^{-1}) and corresponding enthalpic (ΔH, kcal×mol^{-1}) and entropic components ($T\Delta S$, kcal×mol^{-1}) measured in DCM solution at 288 K for the inclusion complexes of **CrHx** and receptors **1** and **5**.

Receptor	Ka × 10^5	ΔG	ΔH	$T\Delta S$
1	19 ± 7	-8.2 ± 0.2	-7.49 ± 0.07	0.7 ± 0.2
5	1.1 ± 0.1	-6.60 ± 0.06	-6.5 ± 0.1	0.1 ± 0.1

In order to function as ionophore in ISEs, the receptor must be able to bind the protonated form of creatinine, the creatininium cation **CrH$^+$**, which is responsible of the change in electric current measured by the device. For this reason, we evaluated the ability of receptor **1** to bind **CrH$^+$**. We also used the bis(methylene)-bridged receptor **5** as a reference compound to study the importance of the PO group in the stabilization of the complex/es formed with the creatininium cation. In view of the well known ability of calix[4]pyrroles to bind anions and ion pairs,[30] and the previously mentioned low solubility of **Cr** in organic solvents, we selected tetrakis(3,5-bis(tri-fluoromethyl)phenyl)borate (BARF; Figure 3. 19) as solubilizing and non-competitive counterion for the **CrH$^+$** cation. The prepared, **CrH$^+$·BARF** salt, was readily soluble in DCM. We performed NMR titration experiments with receptors **1** and **5** in separate CD_2Cl_2 solutions by adding incremental amounts of **CrH$^+$·BARF**.

The addition of **CrH$^+$·BARF** produced the downfield shifting of the pyrrole NH signals in both receptors Figure 3. 7 and Figure 3. 21. However, the extent of the chemical shift change were significantly reduced, especially for **5**, when compared to the observed changes for the NH signals when both receptors were titrated with neutral **Cr** or its lipophilic version **CrHx** ($\Delta\delta_{NH} \approx$ 2ppm). According to literature precedents,[31] and to our own X-ray structure of **CrH$^+$·BARF** (Figure 3. 19), protonation of creatinine occurs at the cyclic nitrogen atom alpha to the carbonyl group. Protonation at this position is likely to substantially reduce the hydrogen-bonding-accepting properties of the carbonyl oxygen atom and might account for the reduced downfield shift experienced by the NH protons of the two receptors upon binding of **CrH$^+$** cation. In addition, during the ^{1}H NMR titration experiment of **1** with incremental amounts of **CrH$^+$·BARF**, we observed that the β-protons of the pyrrole rings not included in the 14-membered macrocycles (H_9 and H_{10}, Scheme 3. 3) experienced a non-monotonic change in chemical shift (Figure 3. 7). This titration behavior is typically observed when complexes with a stoichiometry that deviates from a simple 1:1 ratio are formed. In addition, only the methyl signal of the NCH_3 unit in the guest is clearly visible in the ^{1}H NMR spectra

acquired during the titration experiment of **1**. The methyl group resonates slightly upfield shifted. A broad singlet is also detected at ≈ 4 ppm (not shown in Figure 3. 20 it can be observed in Figure 3. 22). We assigned this signal to the methylene protons (CH_2) of the **CrH**$^+$.

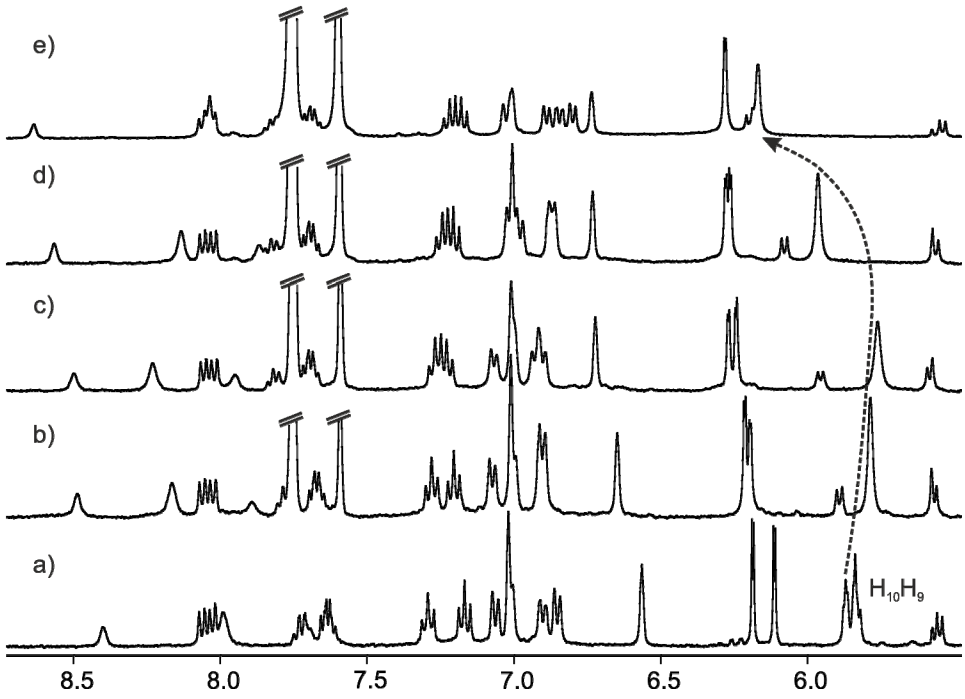

Figure 3. 7: Downfield region of the ^{1}HNMR spectra acquired during the titration of a 2.4 mM solution of **1** in CD_2Cl_2 with incremental amounts of **CrH**$^+$**·BARF**. a) 0 eq. b) 0.49 eq. c) 0.95 eq. d) 1.87 eq. e) 3.64 eq. Upfield region Figure 3. 20. Assignment shown in Scheme 3. 3.

Variable temperature ^{1}H NMR experiments were performed using a CD_2Cl_2 solution of receptor **1** (2.97 mM) and **CrH**$^+$**·BARF** (10.2 mM) Figure 3. 22. The ^{1}H NMR spectrum recorded at 213 K shows two sets of signals for the hydrogen atoms in the **CrH**$^+$ cation. A 2D ROESY experiment registered at the same temperature reveals intense intermolecular crosspeaks between one of these sets and the β-pyrrole protons ($H_{9,10,17,18}$) of **1** while the other set shows more intense intermolecular crosspeaks with the meso-aryl protons Figure 3. 23. These results suggested the formation of a complex with a stoichiometry different from the simple 1:1. The chemical shift changes observed for H_9 and H_{10} during the titration of **1** with **CrH**$^+$ were analyzed using HypMNR2008 software and a theoretical binding model that assumed the formation of two complexes with 1:1 and 2:1 (**CrH**$^+$:**1**) stoichiometries.[32] The fit

of the data was good, and the calculated binding constants for the two complexes are $K((\mathbf{CrH}^+)\subset\mathbf{1}) = 1.6 \times 10^4$ M^{-1} and $K((\mathbf{CrH}^+)_2\subset\mathbf{1}) = 0.8 \times 10^3$ M^{-1} Figure 3. 25. We propose that in the 1:1 complex, the **CrH**$^+$ cation is located in the deep and polar aromatic cavity of **1**, resulting in a binding geometry that is similar to the one observed for the inclusion complex of neutral **Cr** or **CrHx**. The interaction of the **CrH**$^+$ cation with the PO group of **1** was also supported by the chemical shift changes observed in the $^{31}P\{^1H\}$ NMR spectra acquired during the titration experiment Figure 3. 26. Upon increasing the concentration of **CrH**$^+$, the initially formed 1:1 complex bound an additional **CrH**$^+$ in the shallow and electron-rich cavity defined by the pyrrole rings opposite to the functionalized cavity producing a 2:1 complex. In short, **CrH**$^+$, showed a reduced binding affinity towards receptor **1** compared to its neutral counterpart and a dual binding mode.

The titration of the reference receptor, bis(methylene)-bridged derivative **5**, with **CrH**$^+$**·BARF** was indicative of the exclusive formation of a 1:1 complex (K(**CrH**+⊂**5**) = 1.0 × 10^3 M^{-1}). The complexation induced chemical-shift changes for the methyl and methylene protons of the **CrH**$^+$ suggested that the creatininium cation was not included in the deep and polar aromatic cavity of **5**. Instead, the **CrH**$^+$ cation was located in the shallower and electron-rich cavity defined by the pyrrole rings. A 2D ROESY experiment also supported the hypothesis that the cation is located in this cavity ("exo") (Figure 3. 28). Clearly, the lack of the upper-rim PO group was responsible for the selective inclusion of **CrH**$^+$ in the shallow cavity of **5** and the exclusive formation of an exo 1:1 complex, **CrH**$^+$⊂**5**, with reduced thermodynamic stability compared to the endo **CrH**$^+$⊂**1** complex.

3.2.3 ISE response

As introduced at the beginning of this chapter, the incorporation of ionophores in ion-selective membranes increases the selectivity and sensitivity to the corresponding Ion-Selective Electrode (ISE). In order to test the potential of the receptors described in this chapter in ISEs membranes, calix[4]pyrrole **1** and **5** were transferred to the group of Dr. Francisco J. Andrade at the URV. The group of Dr. Francisco J. Andrade, prepared three distinct electrodes with identical polymeric membrane compositions. Whereas the "blank" sensor did not contain any embedded ionophore, the two other sensors contained ionophores **5** and **1**. As a summary of the results obtained by the URV group, Figure 3. 8 shows the selectivity values obtained for

each electrode compared to the "required selectivity coefficients" over the most severe interferences present in biological samples, K^+ and Na^+ ions.

As observed, the presence of receptor **5** in the polymeric membrane increased the selectivity towards **CrH**$^+$ against Na^+ and K^+ ions when compared to the "blank" sensor (ISE without ionophore). However, the required levels for the quantification of **Cr** in blood were only satisfactory achieved by the incorporation of receptor **1** in the membrane.

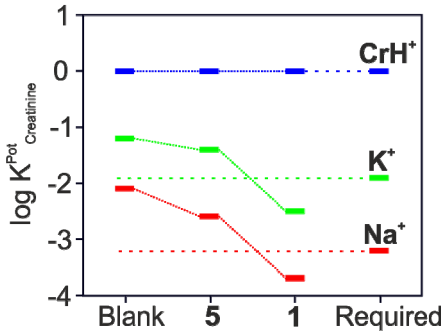

Figure 3. 8: Representation of the selectivity coefficients in logarithmic scale for the ISEs containing: no ionophore "Blank", receptor **5**, and receptor **1** as well as the required selectivity coefficients for Na^+ and K^+ for the sensing of creatinine in blood.

The larger performance of the ISE membrane embedding receptor **1** was already evident from the calibration curves with **Cr** (Figure 3. 9). ISE containing **1** showed a linear response in the range of 1 µM to 10 mM, while the sensor containing receptor **5** and the "blank" sensor showed Nernstian response in the range of 10 µM to 10 mM and 100 µM to 10 mM, respectively (Figure 3. 30).

The obtained results were in clear agreement with the results obtained by NMR spectroscopy and highlights once more the importance of the bridging phosphonate group in the recognition of creatinine.

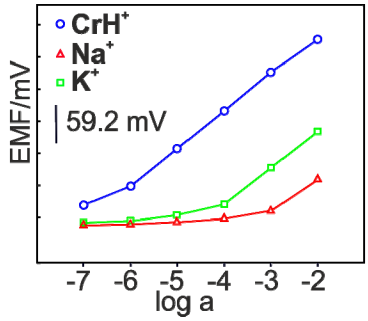

Figure 3. 9: Calibration curves for **CrH**$^+$ obtained with the ISE incorporating receptor **1**.

3.3 Conclusions

In conclusion, we have synthesized an unprecedented receptor (**1**) capable of establishing a three-dimensional array of intermolecular interactions with neutral creatinine (**Cr**) and the creatininium cation (**CrH**$^+$). Receptor **1** forms thermodynamically stable inclusion complexes with a 1:1 stoichiometry in the case of neutral **Cr**. On the other hand, the titration of **1** with **CrH**$^+$ showed the formation of two different aggregates having 1:1 and 2:1 stoichiometry. The binding processes of receptor **1** towards **Cr** and **CrH**$^+$ were studied and analyzed in detail using different techniques. The use of the reference receptor, bis(methylene)-bridged derivative **5** allowed us to assess the importance and the magnitude of the additional hydrogen-bonding interaction that is stablished between the inwardly directed polar PO group of **1** and the NH_2 unit of the included guest.

3.4 Experimental section

3.4.1 General information and instrumentation

All solvents and reagents used in the synthesis of the described compounds were obtained from commercial sources and were used without further purification except where noted. Pyrrole was distilled (50 mbar, 58–59 °C) and stored in the freezer (-20ºC) for further use. THF was distilled from sodium/benzophenone under argon atmosphere. Dried N,N-Dimethylformamide was obtained from a solvent purification system MBraun SPS-800. Catechol was recrystallized from toluene. Anhydrous DMSO was purchased from Acros Organics. Bromochloromethane was dried and stored over 4Å molecular sieves. Pyridine and

Et_3N were dried from CaH_2 and distilled. Flash column chromatography was performed with silica gel, technical grade, pore size 60 Å, and 230–400 mesh particle size.

Microwave experiments were carried out in a Biotage initiator Classic.

Routine ^1H NMR and $^{13}C\{^1H\}$NMR spectra were recorded on a Bruker Avance 400 (400 MHz for ^1H NMR), Bruker Avance 500 (500 MHz for ^1H NMR) ultrashield spectrometer, or on a Bruker Avance III 500 (500 MHz for ^1H NMR) with a QNP cryoprobe. Deuterated solvents were purchase from Aldrich. Chemical shifts are given in ppm. NMR spectra were referenced relative to the solvent residual peak. All NMR J values are given in Hz. High resolution mass spectra were obtained on a MicroTOF II (Bruker Daltonics) ESI as ionization mode Mass Spectrometer or on a MaXis Impact (Bruker Daltonics): UHPLC-ESI-QqTOF. X-Ray diffraction data were collected at 100K on a Rigaku XtaLab P200 Mo Kα rotating anode equipped with a Pilatus 200K hybrid pixel detector and an Oxford Cryostream 700 plus low temperature device or on an Apex Duo diffractometer equipped with an ApexII CCD area detector, a Microsource with Mo Kα radiation and a low temperature device (T = 100K). Full-sphere data collection was used with ω and ϕ scans.

NMR titrations were performed at room temperature. The NMR tube was filled with 0.5 mL of a solution containing the receptor (**1** or **5**). The titrant solution was prepared by dissolving the guest (10 times more concentrated than the receptor) in the above solution thus, the concentration of the receptor remain constant during the titration. Portions of the titrant (2-100 μL) were added by syringe to the NMR tube. After shaking the tube for few seconds the NMR spectra were recorded.

3.4.2 Synthetic procedures

Synthesis of **3**: To a 2 L round-bottomed flask equipped with a magnetic stir bar, was added 3'-Hydroxyacetophenone (14 g, 103 mmol), ethyl acetate (1 L) and pyrrole (7.5 mL, 108 mmol). HCl 36 % aq. (88 mL, 1.03 mol) was then slowly added (dropwise) via syringe under stirring. The flask was then capped and the reaction mixture was stirred at ambient temperature for 3 hours. To quench the reaction water (150 mL) was added. Solid KOH was added until the reaction crude reached pH 6, and then further neutralized with solid K_2CO_3 until pH 7. The organic phase was separated, washed two times with water, dried over Na_2SO_4, filtered and concentrated under reduced pressure. The residue was dissolved in Et_2O (400 mL)

and after filtration of insoluble impurities, the filtrate was concentrated under reduced pressure to afford 17g of crude material. The crude was dissolved in DCM (250 mL), and the solution was left overnight at room temperature. A white precipitate was collected and recrystallized from boiling acetonitrile, to yield colorless crystals of title product (5.6g, 29%). ^{1}H NMR spectrum of this compound was in agreement with that reported in the literature.[26] (Higher yields were obtained (38%) when the reaction was performed starting from 6g of 3'-Hydroxyacetophenone)

Synthesis of monophosphonate **4**: The synthesis was achieved in two steps starting from the mixture of three bisphosphonate stereoisomers **2** (in-in, out-out, and in-out) obtained following a previously described di-phosphonation of tetrol calix[4]pyrrole **3**.[26] Using chemistry applied by Dalcanale et al.[33] to the corresponding resorcinarine phosphonate analogues reaction of the mixture of three stereoisomers with 1,2-dihydroxybenzene excised one or two phosphonate groups giving monophosphonate diol **4** with several other products.

Step a) Synthesis of bisphosphonate calix[4]pyrroles was made following the synthetic procedure previously reported in the literature starting from **3** (0.8 g, 1.08 mmol) which yield 1.05 g of a crude containing the three isomers.[26]

Step b) To a two-necked 250 mL round-bottomed flask equipped with a magnetic stir bar, was added K_2CO_3 (1.47 g, 10.66 mmol) and the crude of the reaction obtained in the previous step. The flask was purged three timed with cycles of vacuum/argon. Dry DMF (89 mL) was added under argon. The reaction mixture was heated to 70 ºC, and recrystallized catechol (2.5 mL, 0.405 M in DMF, 0.97 mmol) was slowly added over a period of 1 h 40 min. The mixture was stirred overnight at 70ºC. The reaction was quenched with 10 % HCl_{aq} (50 mL). The aqueous phase was extracted with EtOAc (3 × 60 mL). The organic extracts were combined and washed with water (2 × 50 mL), dried (Na_2SO_4), filtered, and concentrated under reduced pressure. The reaction crude was absorbed onto silica gel and purified by flash chromatography on a silica gel column (40 g, gradient from 15 % to 50% EtOAc/DCM). Six fractions were collected. Fraction 1 (16mg) contained a mixture of bisphosphonate isomers. Fraction 2 (30 mg) contained a mixture of $\mathbf{2_{io}}$ and $\mathbf{4_o}$ isomers. Fraction 3 (135 mg, 14%) contained pure $\mathbf{4_o}$ isomer. Fraction 4 contained calixpyrrole **3** (75 mg). Fraction 5 (25 mg) contained a mixture of calixpyrrole **3** and $\mathbf{4_i}$. Fraction 6 contained $\mathbf{4_i}$ which was recrystallized from boiling acetone (0.17g, 18 % calculated from calixpyrrole **3**). Analytical TLC on silica gel: Rf: 0.32 (15/85 EtOAc/DCM) $\mathbf{4_i}$ could also be obtained from the reaction of

calix[4]pyrrole **3** with an equimolar amount of phenylphosphonic dichloride using the same reaction conditions described for the synthesis of bisphosphonate calixpyrrole.[26] These conditions produced higher amounts of $\mathbf{4_o}$ isomer, which complicates the purification step.

$\mathbf{4_i}$ ^{1}H NMR (500 MHz, Acetone-d6, 25 °C): δ(ppm) 8.93 (bs, 2H), 8.75 (bs, 1H), 8.70 (bs, 1H), 8.19 (s, 2H), 8.09-8.02 (m, 2H), 7.74 (bt, *J* = 7.6 Hz, 1H), 7.67-7.62 (m, 2H), 7.21 (t, *J* = 8.0 Hz, 2H), 7.07 (t, *J* = 8 Hz, 2H), 6.99 (d, *J* = 8.12 Hz, 2H), 6.96 (d, *J* = 8.12 Hz, 2H), 6.79 (bs, 2H), 6.60 (dd, *J* = 8.0, 2.3 Hz, 2H), 6.45 (d, *J* = 7.88 Hz, 2H), 6.42 (bs, 2H), 6.13-6.09 (m, 4H), 6.05 (t, *J* = 3.0 Hz, 2H), 5.95 (d, *J* = 2.4 Hz, 2H), 1.91 (s, 6H), 1.86 (s, 6H); ^{13}C{^{1}H}NMR (100 MHz, THF-d8, 25 °C):δ(ppm) 157.2, 152.3, 151.0, 150.0 (d, $^2J_{PC}$ = 10 Hz), 138.2, 137.9, 137.4, 136.4, 132.7 (d, $^4J_{PC}$ = 3.2 Hz), 131.0 (d, $^2J_{PC}$ = 10.3 Hz), 128.9, 128.5 (d, $^3J_{PC}$ = 15.8 Hz), 128.2, 124.5, 120.7 (d, $^3J_{PC}$ = 3.2 Hz), 120.0 (d, $^3J_{PC}$ = 3.2 Hz), 118.5, 114.9, 112.8, 105.5, 105.3, 104.9, 104.8, 44.6, 44.5, 29.1, 29.0 (C ipso to P was not observed). ^{31}P{^{1}H}NMR (161.98 MHz, Acetone-d6, 25 °C): δ(ppm) 14.15; HRMS (ESITOF) m/z: calcd for $C_{54}H_{48}N_4O_5P$ $[M + H]^+$ =863.3357; Found 863.3340

Synthesis of **1**: To a 5 mL microwave tube equipped with a magnetic stir bar, were added $\mathbf{4_i}$ (45 mg, 52 μmol) and K_2CO_3 (58 mg, 0.42 mmol). The tube was left under high vacuum for 3 h. Then, anhydrous DMSO (5.1 mL) was added under argon. The mixture was dissolved as best as possible and bromochloromethane (17.5 μL, 0.26 mmol) was added in one portion. The tube was sealed and heated in a microwave at 90ºC for 30 minutes. The reaction mixture was then cooled at rt, quenched with 20 mL 10% $HCl_{aqueous}$ and extracted with DCM (3 × 20 mL). The DCM extracts were combined, washed with water (3 × 20 mL), dried (Na_2SO_4), filtered, and concentrated under reduced pressure. The crude was purified by flash chromatography on a silica gel column (12 g, 0.5% IPA/DCM). The product was then recrystallized from boiling acetonitrile to yield title compound as colorless crystals. (16 mg, 35%). Analytical TLC on silica gel: Rf: 0.23 (DCM).

^{1}H NMR (500 MHz, CD_2Cl_2, 25 °C): δ(ppm) 8.33 (bs, 1H), 8.05 – 7.98 (m, 2H), 7.97 (bs, 2H), 7.72 – 7.66 (m, 2H), 7.63 – 7.57 (m, 2H), 7.25 (t, *J* = 7.8 Hz, 2H), 7.13 (t, *J* = 7.8 Hz, 2H), 7.02 – 6.95 (m, 6H), 6.84 (d, *J* = 7.8 Hz, 2H), 6.80 (d, *J* = 7.8 Hz, 2H), 6.57 (s, 2H), 6.14 (d, *J* = 2.6 Hz, 2H), 6.08 (d, *J* = 2.6 Hz, 2H), 5.90 – 5.83 (m, 5H), 5.49 (d, J_{gem} = 7.2 Hz, 1H), 1.96 (s, 6H), 1.93 (s, 6H); ^{13}C{^{1}H}NMR (125 MHz, CD_2Cl_2, 25 °C): δ(ppm) 156.5, 151.5, 150.8, 150.4 (d, $^2J_{PC}$ = 9.6 Hz), 138.4, 137.8, 137.6, 137.5, 133.7 (d, $^4J_{PC}$ = 2.9 Hz), 131.6 (d, $^2J_{PC}$ = 10.2 Hz), 129.4, 129.3, 129.2 (d, $^3J_{PC}$ = 16.1 Hz), 128.1 (d, $^1J_{PC}$ = 205.2 Hz), 124.3,

121.9, 121.1 (d, $^{3}J_{PC}$ = 3.0 Hz), 120.1, 118.3, 117.5, 106.6, 106.5, 106.1, 105.9, 92.0, 45.1, 45.0, 29.0, 29.37; $^{31}P\{^{1}H\}$NMR (161.98 MHz, CD_2Cl_2, 25 °C): δ(ppm) 15.96; HRMS(ESI-TOF)m/z: $[M + H]^+$ calcd for $C_{55}H_{48}N_4O_5P$ = 875.3357; Found = 875.3335.

Synthesis of **5** was prepared according to a slightly modified published procedure.[26] To an Ace pressure tube equipped with a magnetic stir bar and plunger valve, were added **3** (120 mg, 0.16mmol), and K_2CO_3 (179mg, 1.3 mmol). The system was dried under high vacuum overnight. The vacuum was satisfied with Ar and anhydrous DMSO (16 mL) was added. The mixture was dissolved as best as possible and bromochloromethane (52.6 µL, 0.81 mmol) was added in one portion. The flask was sealed and heated at 100ºC for 1 h in an oil bath. The reaction mixture was then cooled at RT and poured into 10% $HCl_{aqueous}$. The resulting suspension was extracted twice with DCM. The organic extracts were combined, washed with water, dried (Na_2SO_4), filtered and evaporated under reduced pressure, yielding a pale yellow powder. The crude material was purified by flash chromatography on a silica gel column (10g, DCM) to yielding pure product as a white powder (71.5 mg of 58% yield).

^{1}H NMR (400 MHz, $CDCl_3$, 25 °C): δ(ppm) 7.58 (bs, 2H), 7.39 (bs, 2H), 7.12 (t, *J* = 7.9 Hz, 4H), 6.86 (d, *J* = 7.9 Hz, 4H), 6.82 (d, *J* = 7.9 Hz, 4H), 6.58 (s, 1H), 6.09 (d, *J* = 2.6 Hz, 4H), 5.86-5.81 (m, 6H), 5.55 (d, J_{gem} = 7.1 Hz, 2H), 1.95 (s, 12H); $^{13}C\{^{1}H\}$NMR (100 MHz, $CDCl_3$, 25 °C): δ(ppm) 156.6, 150.2, 137.5, 136.5, 129.1, 121.6, 118.7, 117.6, 106.5, 106.4, 92.9, 44.9, 28.6; HRMS(ESI-TOF)m/z: calcd for $C_{50}H_{45}N_4O_4$ $[M + H]^+$ = 765.3435, found = 765.3426.

Synthesis of **CrH^+·BARF**: NaBArF (80 mg 90 µmol) was dissolved in 8.4 mL of water at 95-98 ºC. A solution of creatinine·HCl (421 mg, 2.82 mmol) dissolved in 4.2 mL of water at 95–98 ºC was slowly added to the NaBArF solution under stirring. During the course of the addition, a white precipitated appeared. The mixture was cooled at RT overnight without stirring. The solid was filtered, washed with water and dried under vacuum to afford pure product as a white powder (66 mg, 75%). If further purification is required, the product can be recrystallized in hot xylene. ^{1}H NMR (400 MHz, CD_2Cl_2, 25 °C): δ(ppm) 7.72 (bs, 8H), 7.57 (bs, 4H), 4.27 (s, 2H), 3.19 (s, 3H); $^{13}C\{^{1}H\}$NMR (100 MHz, CD_2Cl_2, 25 °C): δ(ppm) 166.1, 162.2 (q, J_{CB} = 49.8 Hz), 157.3, 135.2, 129.3 (q, *J* = 30 Hz), 125.0 (q, *J* = 272.6 Hz), 117.9 (bs), 32.3. CH_2 carbon of creatininium is not observed. $^{19}F\{^{1}H\}$ NMR (376.5 MHz, CD_2Cl_2, 25 °C): δ(ppm) -62.55; $^{11}B\{^{1}H\}$ NMR (128.4 MHz, CD_2Cl2, 25 °C): δ(ppm) -6.62.

Synthesis of **PS** cavitands: To a solution of calix[4]pyrrole **3** (0.5 g, 0.68 mmol) dissolved in pyridine (52 mL) and under Ar atmosphere, P,P-dichlorophenylphosphine (188 µL, 1.38 mmol) was added (the reaction mixture turned to yellow). After 1h a white precipitated was formed. 90 minutes after the addition the reaction crude was warmed up to 70 ºC and stirred for 30 minutes. Then, S_8 (69.2 mg, 0.27 mmol) was added at the same temperature (the solid dissolved) and the reaction was left at the same temperature overnight under stirring. Next day, the pyridine was removed under reduced pressure, and the resulting material dissolved in 20 mL of DCM. The DCM solution was treated with 10% $HCl_{aqueous}$ (10 mL) (The color of the crude changed from light yellow to colorless) the organic phase was separated and the aqueous phase was extracted with DCM 3 × 20 mL. Then, the DCM extracts were combined and washed with 10% $HCl_{aqueous}$ 3 × 20mL to remove the remaining pyridine. The DCM solution was dried (Na_2SO_4), filtered and concentrated under vacuum yielding 0.7 g of crude material. The crude was purified by column chromatography on SiO_2 (20 g) and DCM:Hx 6:4 as eluent mixture. (Fraction 1) **PS$_{ii}$** 118 mg 17%, (fraction 2) **PS$_{io}$** 160 mg 23%, (Fraction 3) **PS$_{oo}$** 90 mg 13%.

PS$_{ii}$: ^{1}H NMR (400 MHz, $CDCl_3$, 25 °C): δ(ppm) 8.09-8.00 (m, 6H), 7.98 (bs, 2H), 7.63-7.57 (m, 2H), 7.56-7.49 (m, 4H), 7.15 (t, *J* = 7.9 Hz, 4H), 6.89 (d, *J* = 7.9 Hz, 4H), 6.81 (d, *J* = 7.9 Hz, 4H), 6.68 (s, 4H), 4.14 (d, *J* = 2.3 Hz, 4H), 6.00 (d, *J* = 1.9 Hz, 4H), 1.96 (s, 12H); ^{31}P{^{1}H}NMR (161.98 MHz, $CDCl_3$, 25 °C): δ(ppm) 85.68; HRMS(ESI-TOF)m/z: calcd for $C_{60}H_{50}N_4NaO_4P_2S_2$ $[M + Na]^+$ = 1039.2641, found = 1039.2667.

PS$_{io}$: ^{1}H NMR (400 MHz, $CDCl_3$, 25 °C): δ(ppm) 8.10-8.01 (m, 4H), 7.87 (bs, 2H), 7.63-7.58 (m, 2H), 7.57-7.50 (m, 4H), 7.37 (bs, 2H), 7.28 (d, *J* = 7.9 Hz, 4H), 7.20 (t, *J* = 7.9 Hz, 4H), 7.05 (bs, 4H), 6.75 (d, *J* = 7.9 Hz, 4H), 6.22 (d, *J* = 2.7 Hz, 4H), 5.27 (d, *J* = 2.7 Hz, 4H), 2.06 (s, 12H); ^{31}P{^{1}H}NMR (161.98 MHz, $CDCl_3$, 25 °C): δ(ppm) 78.93; HRMS(ESI-TOF)m/z: calcd for $C_{60}H_{51}N_4O_4P_2S_2$ $[M + H]^+$ = 1017.2821, found = 1017.2838.

PS$_{oo}$: ^{1}H NMR (400 MHz, $CDCl_3$, 25 °C): δ(ppm) 8.29 (bs, 1H), 8.20 (bs, 2H), 8.13-8.05 (m, 4H), 7.98 (bs, 1H), 7.65-7.51 (m, 6H), 7.20-7.15 (m, 4H), 7.12 (d, *J* = 7.8 Hz, 2H), 7.06 (d, *J* = 8.1 Hz, 2H), 6.89 (d, *J* = 7.8 Hz, 2H), 6.81 (s, 2H), 6.75 (d, *J* = 7.8, 2H), 6.20 (d, *J* = 2.4 Hz, 2H), 6.15 (d, *J* = 2.4 Hz, 2H), 5.65 (bs, 2H), 5.61 (bs, 2H), 2.04 (s, 6H), 2.03 (s, 6H); ^{31}P{^{1}H}NMR (161.98 MHz, $CDCl_3$, 25 °C): δ(ppm) 84.70, 78.92; HRMS(ESI-TOF)m/z: calcd for $C_{60}H_{51}N_4O_4P_2S_2$ $[M + H]^+$ = 1017.2821, found = 1017.2872.

Synthesis of **PO$_i$PS**: To a solution of calix[4]pyrrole **4$_i$** (100 mg, 116 µmol) dissolved in pyridine (9 mL) and under Ar atmosphere, P,P-dichlorophenylphosphine (17.3 µL, 127 µmol) was slowly added. After the addition the reaction crude was warmed up to 70 ºC and stirred for 2 h (a precipitated was formed). Then, S_8 (6.0 mg, 23 µmol) was added and the reaction was left at the same temperature overnight under stirring. Next day, the pyridine was removed under reduced pressure, and the resulting material dissolved in 10 mL of DCM. The DCM solution was treated with 10% $HCl_{aqueous}$ (5 mL) (The color of the crude changed from light yellow to colorless) the organic phase was separated and the aqueous phase was extracted with DCM 2 × 20 mL. Then, the DCM extracts were combined and washed with 10% $HCl_{aqueous}$ 3 × 20 mL to remove the remaining pyridine. The DCM solution was dried (Na_2SO_4), filtered and concentrated under vacuum. The crude was purified by column chromatography on SiO_2 (10 g) and using a gradient of 3:7 Hx:DCM to 100% DCM until the second spot starts to come out, at this point a mixture of 5:95 EtOAc:DCM was used. (Fraction 1) **PO$_i$PS$_o$** 22.5 mg 19%, (Fraction 2) **PO$_i$PS$_i$** 36.2 mg 31%.

PO$_i$PS$_o$: ^{1}H NMR (400 MHz, $CDCl_3$, 25 °C): δ(ppm) 8.54 (bs, 1H), 8.16-8.08 (m, 4H), 8.06-7.98 (m, 2H), 7.96 (bs, 1H), 7.72-7.66 (m, 1H), 7.66-7.55 (m, 5H), 7.24 (t, *J* = 7.9 Hz, 2H), 7.20-7.13 (m, 6H), 7.09 (d, *J* = 7.9 Hz, 2H), 6.99 (bs, 2H), 6.93 (d, *J* = 7.9 Hz, 2H), 6.76 (d, *J* = 7.9 Hz, 2H), 6.16 (d, *J* = 2.7 Hz, 2H), 6.15 (d, *J* = 2.7 Hz, 2H), 5.74 (bt, *J* = 2.9 Hz, 2H), 5.63 (bt, *J* = 2.7 Hz, 2H), 2.03 (s, 6H), 2.02 (s, 6H); ^{31}P{^{1}H}NMR (161.98 MHz, $CDCl_3$, 25 °C): δ(ppm) 78.70, 15.54.

PO$_i$PS$_i$: ^{1}H NMR (400 MHz, $CDCl_3$, 25 °C): δ(ppm) 8.16-8.06 (m, 2H), 8.06-7.98 (m, 2H), 7.89 (bs, 2H), 7.70 (bs, 1H), 7.68-7.60 (m, 3H), 7.21 (app t, 4H), 7.13-7.06 (m, 4H), 7.00-6.93 (m, 4H), 6.74 (bs, 2H), 6.71 (bs, 2H), 6.19 (d, *J* = 2.6 Hz, 2H), 6.18 (d, *J* = 2.6 Hz, 2H), 5.79 (bt, 2H), 5.74 (bt, 2H), 2.02 (bs, 12H); ^{31}P{^{1}H}NMR (161.98 MHz, $CDCl_3$, 25 °C): δ(ppm) 84.43, 15.11.

Synthesis of **HxCr**: The synthetic procedure was adapted from the methodology described by Kumar et all.[34]

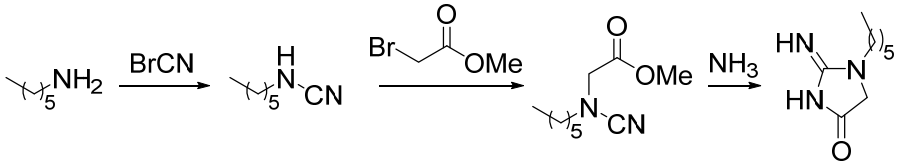

Step 1: cyanogen bromide (3.14g, 29.6 mmol) dissolved in a 1:1 mixture of anhydrous THF:Et_2O and under Ar, was added dropwise via cannula at 0 ºC to a previously dried 250 mL round bottom flask containing a solution of 1-hexylamine (5.0 g, 49.4 mmol) in anhydrous 1:1 THF:Et_2O (50 mL) under Ar. (0.6 eq.) (CAUTION: cyanogen bromide is highly toxic. The chemical should be weight in the fumehood and the reaction should be carried out in the fumehood). During the addition a white solid precipitated. After the addition, the mixture was stirred for 3.5 h at the same temperature. The solid was filtrated, and the solution was washed with water (2 × 100 mL). The organic phase was separated and dried (Na_2SO_4), filtered and concentrated under reduced pressure yielding pure cyanamide as a yellow oil 3g 80%. ^{1}H NMR (400 MHz, $CDCl_3$, 25 °C): δ(ppm) 3.82 (bs, 1H), 3.05 (dt, *J* = 7.0 Hz, 5.5 Hz, 2H), 1.59 (quin, *J* = 7.4 Hz, 2H), 1.39-1.24 (m, 6H), 0.88 (t, *J* = 6.9 Hz, 3H); ^{13}C{^{1}H}NMR (100 MHz, $CDCl_3$, 25 °C): δ(ppm) 116.5, 46.4, 31.4, 29.8, 26.0, 22.6, 14.0; HRMS(ESI-TOF)m/z: calcd for $C_7H_{14}N_2Na$ $[M + Na]^+$ = 149.1049, found = 149.1050.

Step 2: To a solution of the cyanamide synthetized in step 1 (2.0 g, 15.85 mmol) in anhydrous THF (50 mL), was added NaH (60 % oil suspension, 0.7g, 17.5 mmol) in three portions at 0 °C under Ar atmosphere and the reaction was stirred for 1h and 20 minutes. During that time a precipitated was formed. Then, a solution of Methyl 2-bromoacetate (1.5 mL, 15.85 mmol) in anhydrous THF (10 mL) was added at 0 °C, and the mixture was stirred overnight. Next day, the reaction mixture was filtered. The filtrate was evaporated to one-half of its total volume and dichloromethane (50 mL) was added. The combined organic layer was washed with water (2 × 50 mL), dried (Na_2SO_4) and filtered. The solvent was evaporated under reduced pressure to give the desired product as a yellow oil 3.08g (98%). Grease coming from the NaH was observed in the NMR. ^{1}H NMR (400 MHz, $CDCl_3$, 25 °C): δ(ppm) 3.80 (s, 3H), 3.78 (s, 2H), 3.08 (t, *J* = 7.27 Hz, 2H), 1.67 (quin, *J* = 7.2 Hz, 2H), 1.39-1.24 (m, 6H), 0.88 (m, 3H); ^{13}C{^{1}H}NMR (100 MHz, $CDCl_3$, 25 °C): δ(ppm) 168.4, 116.9, 52.6, 52.4, 52.2, 31.3, 27.5, 26.1, 22.5, 14.0; HRMS(ESI-TOF)m/z: calcd for $C_{10}H_{18}N_2NaO_2$ $[M + Na]^+$ = 221.1260, found = 221.1256.

Step 3: The product obtained in step 2 (1 g, 5.04 mmol) was treated with aqueous ammonia (30%, 50 mL, 693 mmol) and was vigorously stirred at rt for 30 minutes. The resulting solid was filtered and washed with water and methanol yielding pure product as a white solid 0.4g 43%. ^{1}H NMR (400 MHz, D_2O, 25 °C): δ(ppm) 4.08 (s, 2H), 3.41 (t, *J* = 7.1 Hz, 2H), 1.64 (quin, *J* = 7.4, 2H), 1.36-1.28 (m, 6H), 0.88 (t, *J* = 7.4 Hz, 3H). X-ray on Figure 3. 29.

4.4.3 Figures

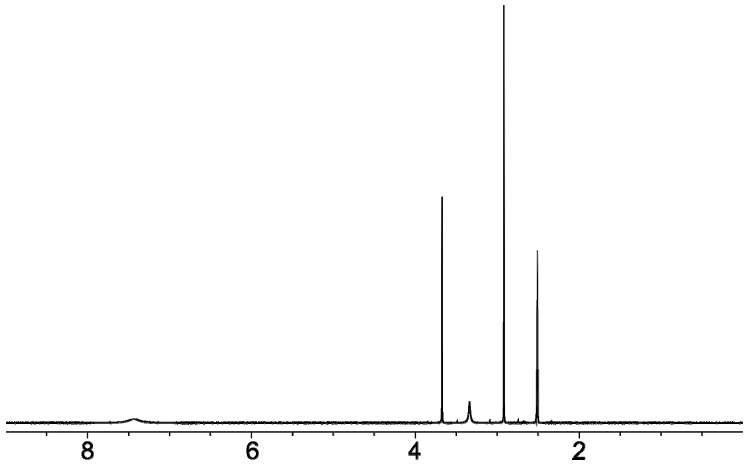

Figure 3. 10: ^{1}H NMR spectrum (400 MHz) of a **Cr** solution in [D6]DMSO at 298 K.

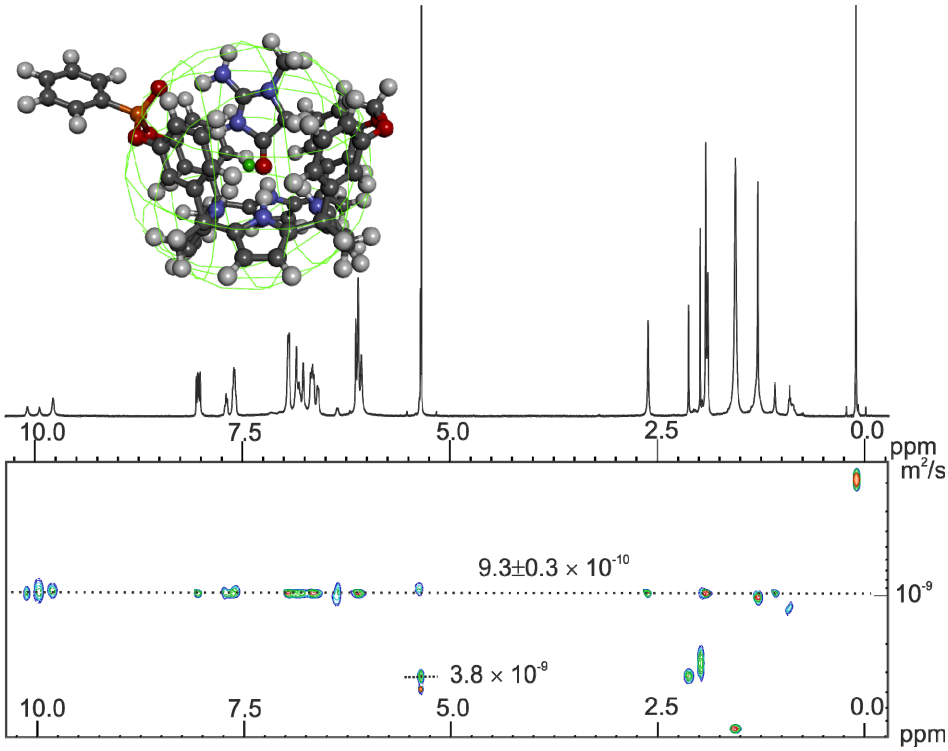

Figure 3. 11: ^{1}H pseudo-2D DOSY plot of a CD_2Cl_2 solution of **1** after solid-liquid extraction with neutral **Cr** and X-ray structure of the **Cr⊂1** complex enclosed within a sphere of 5.7 Å radius from the centroid (green ball)

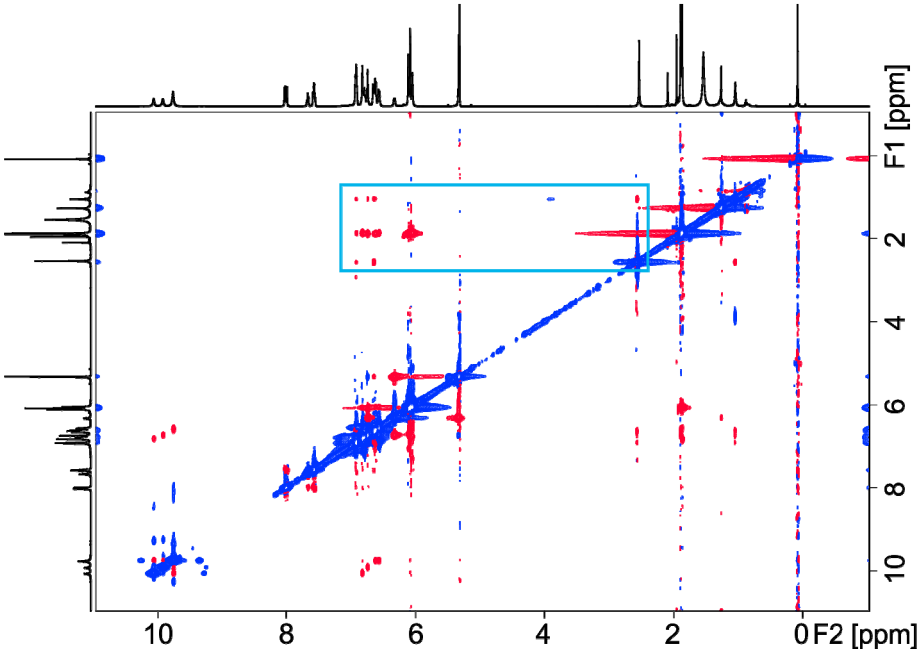

Figure 3. 12: ROESY ^{1}H NMR spectrum acquired after extraction of solid neutral **Cr** with a 5.95 mM solution of **1** in CD_2Cl_2. The blue box indicates the region of the spectrum showed in Figure 3. 4.

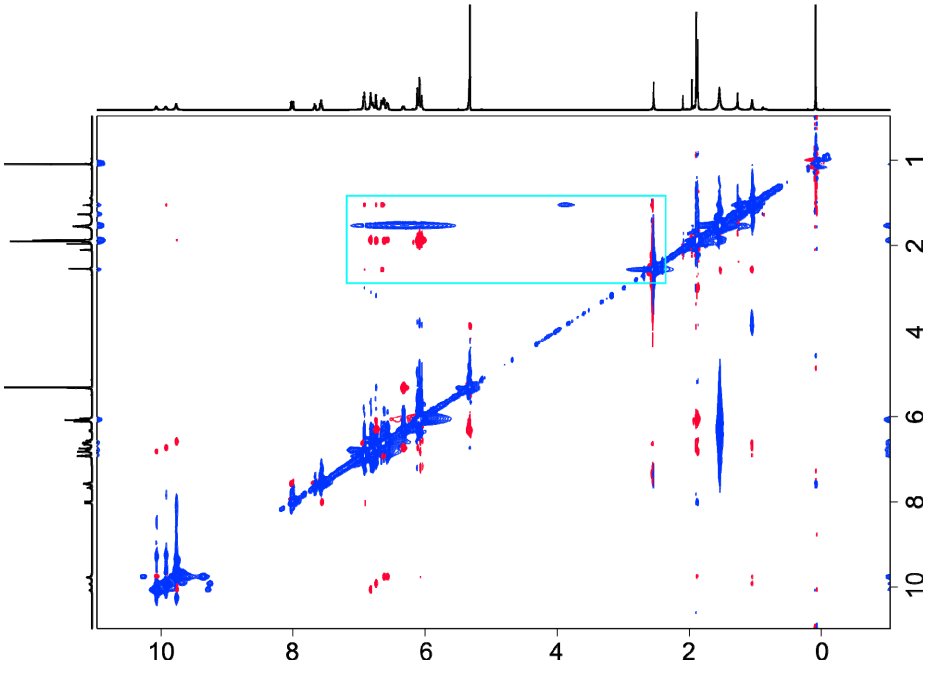

Figure 3. 13: NOESY ^{1}HNMR spectrum acquired after extraction of solid neutral **Cr** with a 5.95 mM solution of **1** in CD_2Cl_2. The blue box indicates the region of the spectrum showed in

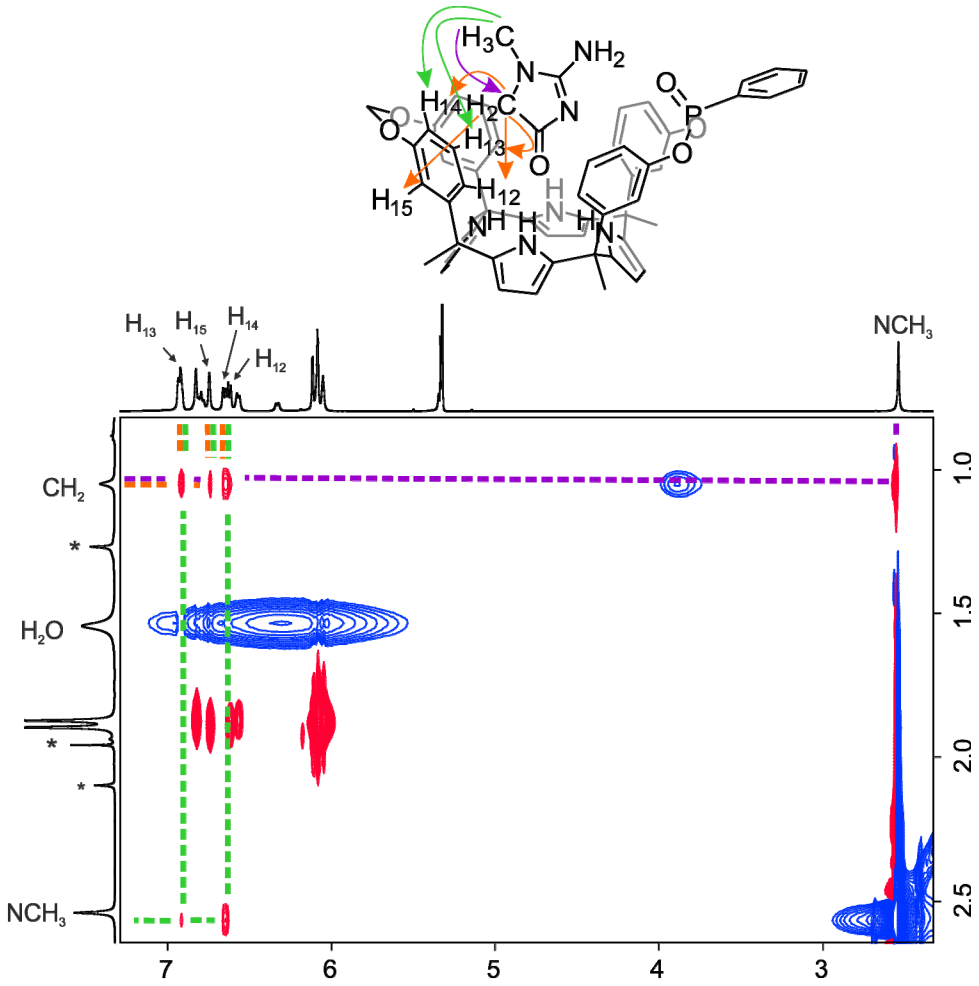

Figure 3. 14: Blowup of the portion of the NOESY ^{1}HNMR spectrum Figure 3. 13 contained within the blue box highlighting the intermolecular coupling patterns between **1** and **Cr**.

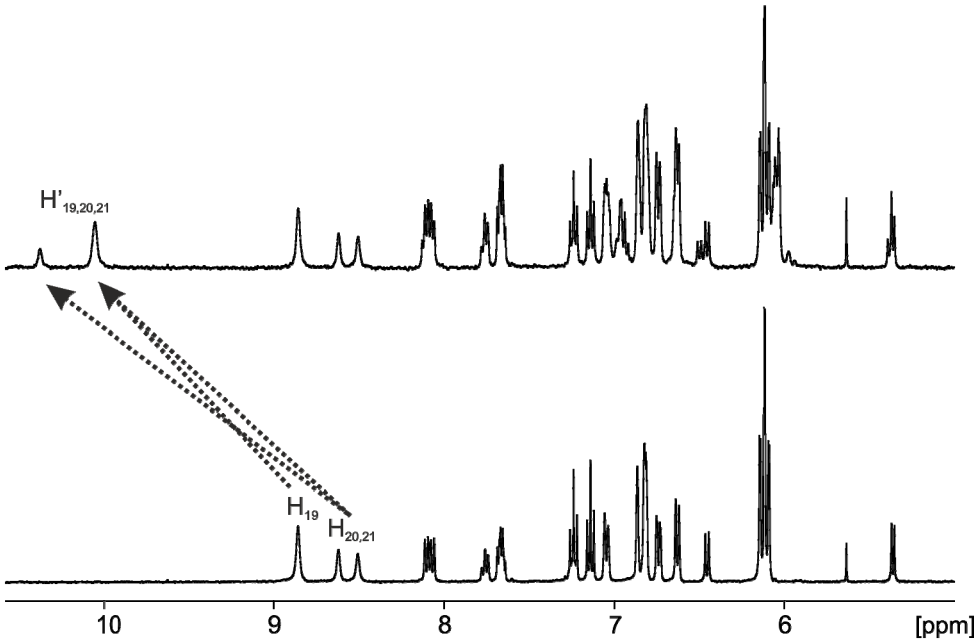

Figure 3. 15: Selected downfield regions of the ^{1}HNMR spectrum of a 2.23 mM solution of **1** in Acetone-d6 (bottom) and the corresponding filtered solution obtained after a solid-liquid extraction experiment with solid neutral **Cr** (top).

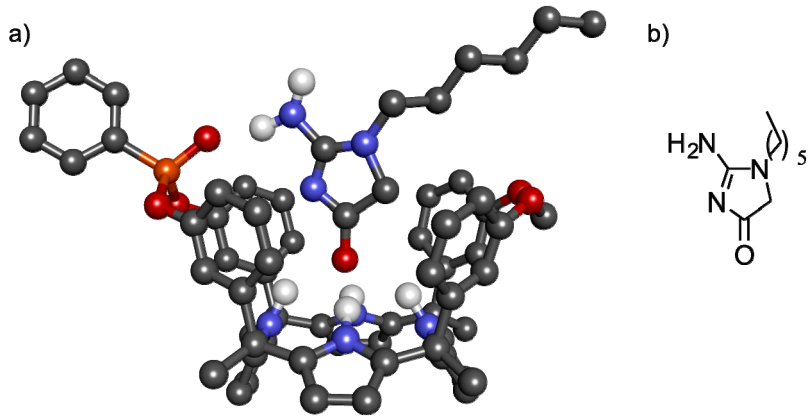

Figure 3. 16: a) Energy minimized structures (MM3) of the inclusion complex **CrHx⊂1**; Non-polar hydrogen atoms were removed for clarity; b) Structure of **CrHx**.

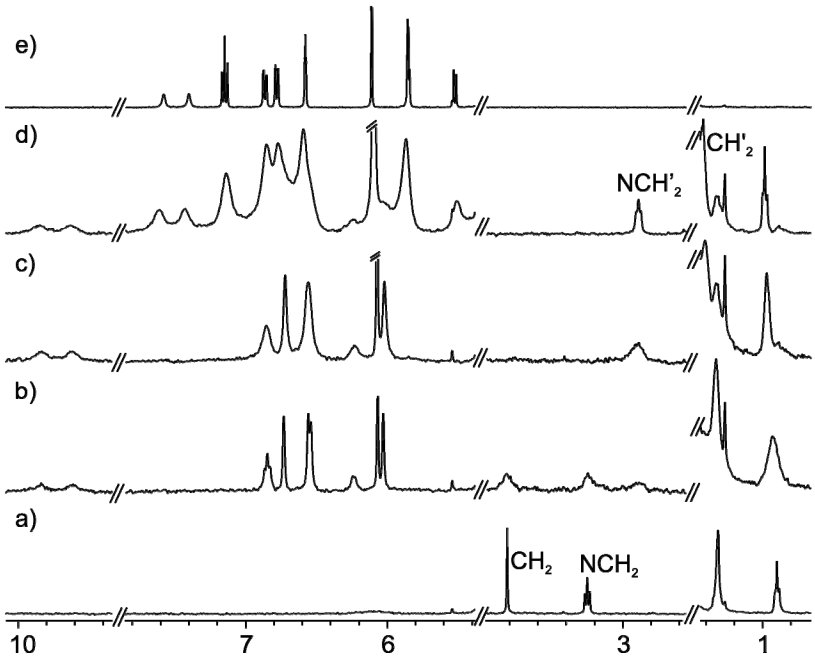

Figure 3. 17: Selected regions of the ^{1}HNMR spectra acquired during the titration of a 0.8 mM solution of **CrHx** in CD_2Cl_2 with incremental amounts of **5**. a) 0 eq. b) 0.5 eq. c) 1.0 eq. d) 3.0 eq. e) Free **5**.

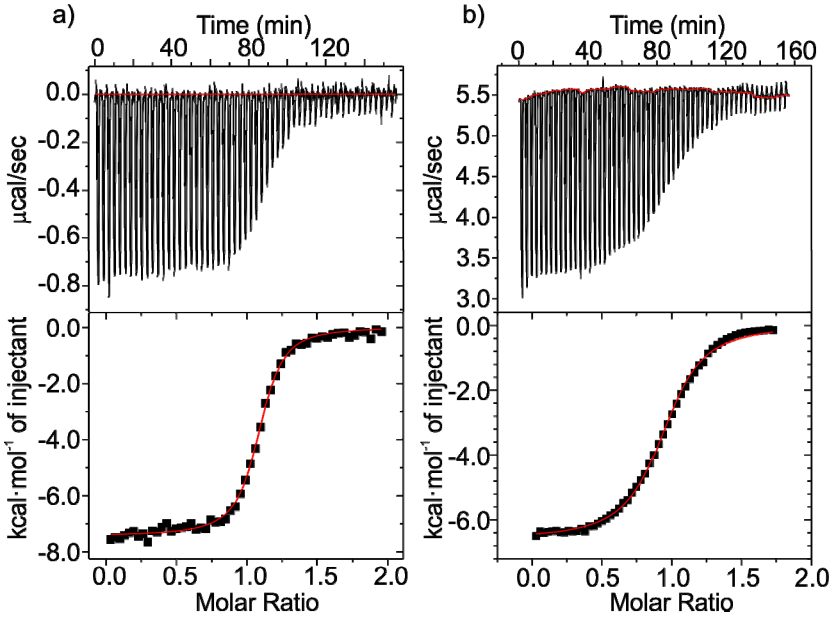

Figure 3. 18: Top: Raw data for the ITC titration of **Cr** with receptor a) **1** and b) **5**. Bottom: Binding isotherm of the integrated calorimetric titration data. Receptors were added over **CrHx**.

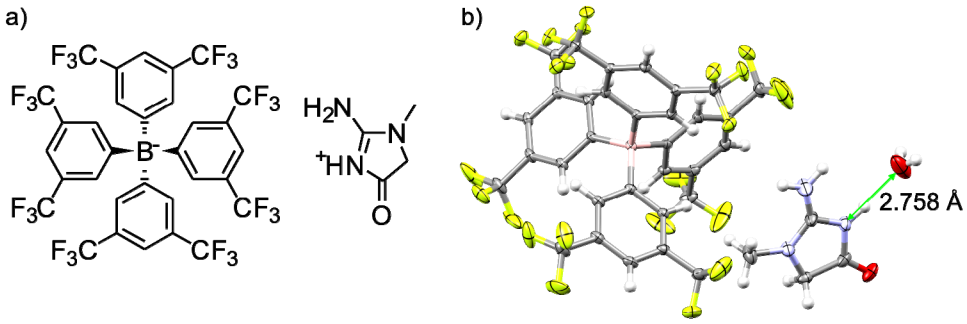

Figure 3. 19: a) Molecular structure of **CrH$^+$·BARF**; b) X-ray structure of **CrH$^+$·BARF** highlighting hydrogen bond of **CrH$^+$** with a molecule of water. This observation supports the idea that the protonation of **Cr** occurs at the nitrogen atom of the five-membered heterocycle. The thermal ellipsoids are set at 50% probability level and the H atoms as spheres of 0.2 Å.

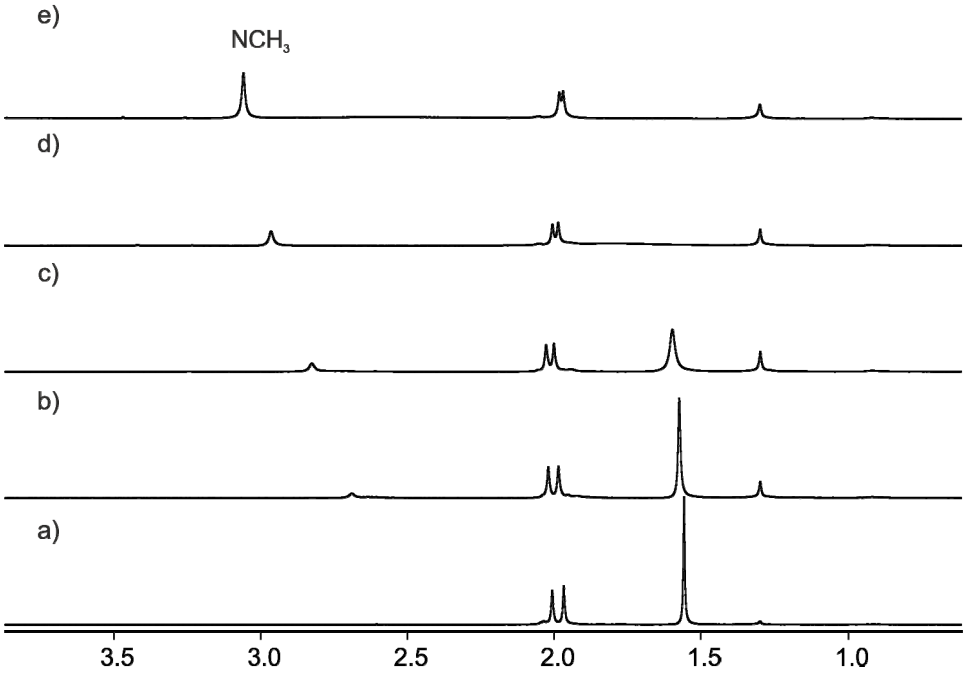

Figure 3. 20: Upfield region of the ^{1}H NMR spectra acquired during the titration of a 2.4 mM solution of **1** in CD_2Cl_2 with incremental amounts of **CrH$^+$·BARF**. a) 0 eq. b) 0.49 eq. c) 0.95 eq. d) 1.87 eq. e) 3.64 eq.

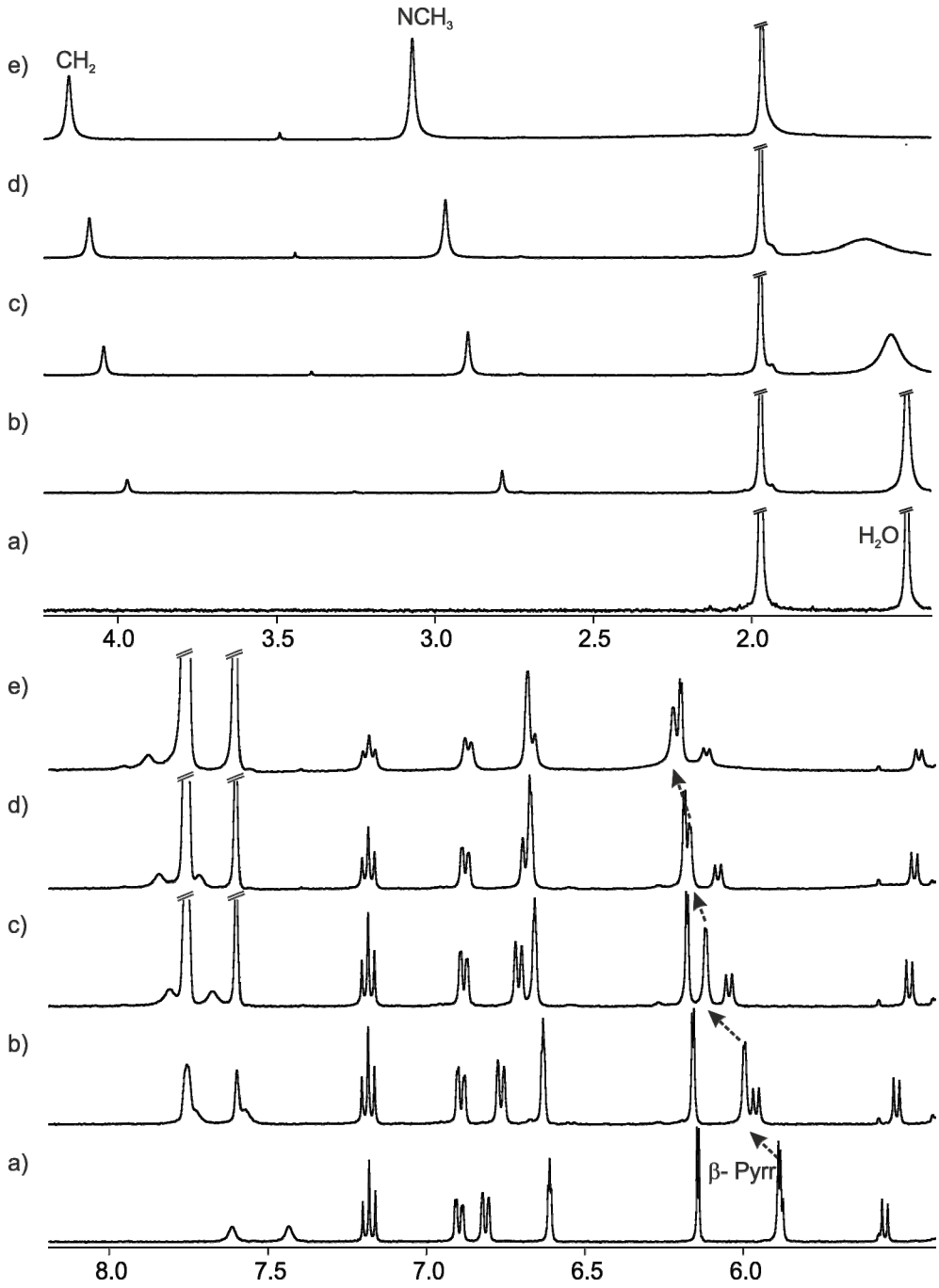

Figure 3. 21: Upfield (top) and downfield (bottom) region of ^{1}H NMR spectra obtained during the titration of **5** (2.72 mM) with **CrH$^+$·BARF** in CD_2Cl_2. a) 0 eq. b) 0.44 eq. c) 1.13eq. d) 1.70 eq. e) 3.42 eq.

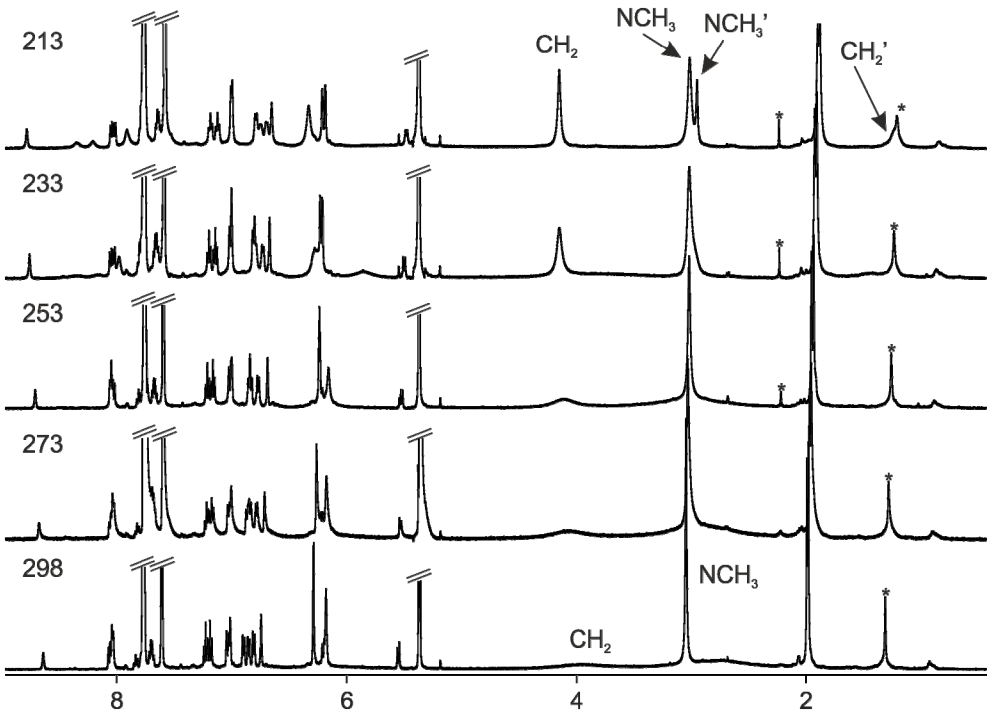

Figure 3. 22: ^{1}H NMR spectra of a CD_2Cl_2 solution of receptor **1** (2.97mM) and **CrH^{+}·BARF** (10.2 mM), at different temperatures expressed in K.

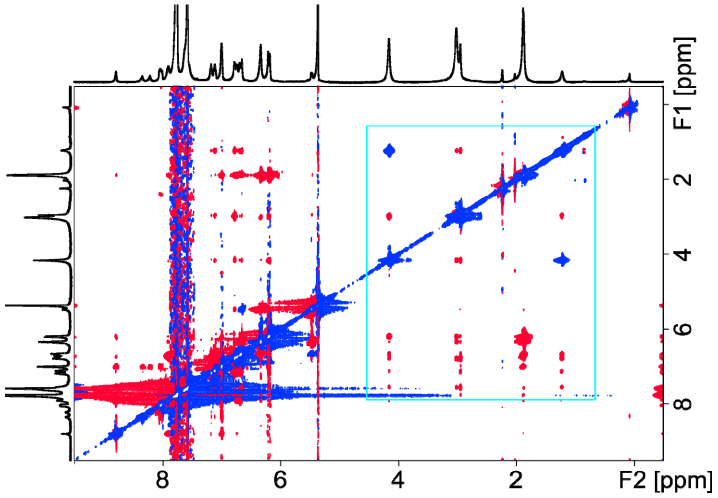

Figure 3. 23: ROESY ^{1}H NMR spectrum (213K) of a CD_2Cl_2 solution of receptor **1** (5.42 mM) and **CrH^{+}·BARF** (19 mM). The blue box indicates the region of the spectrum showed in Figure 3. 24.

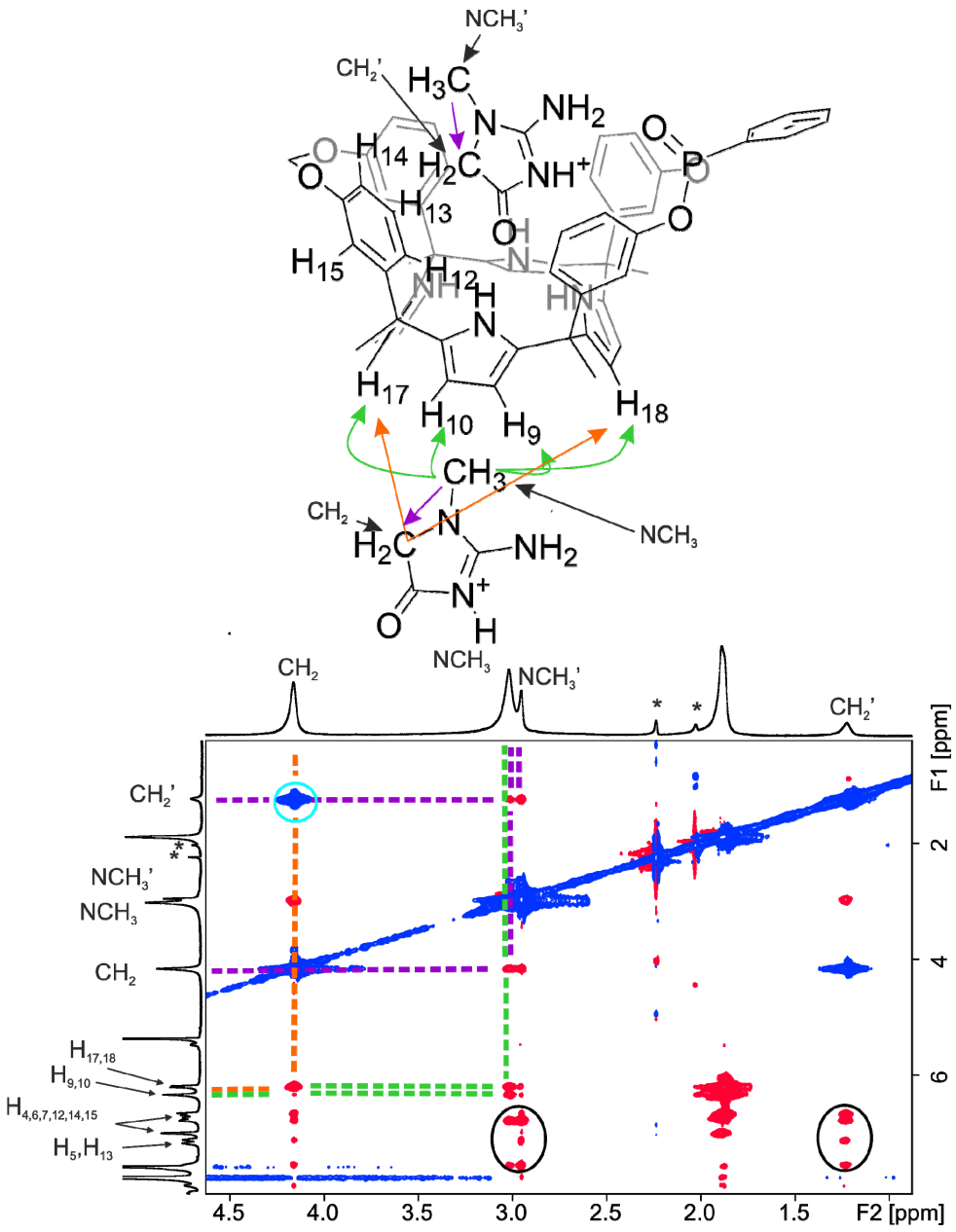

Figure 3. 24: Blowup of the portion of the ROESY **1**H NMR spectrum Figure 3. 23 contained within the blue box highlighting the intermolecular coupling patterns between **1** and **CrH**$^+$. NCH_3' and CH_2' correspond to **CrH**$^+$ cation deeply included into the polar aromatic cavity. Blue circle highlights a chemical exchange signal between CH_2' and CH_2. Black circles highlight intermolecular nOEs between the NCH_3' and CH_2' moieties of **CrH**$^+$ cation with the receptor's aryl protons. Note the lack of nOEs between CH_2' and the β-pyrrol protons $H_{9,10,17,18}$.

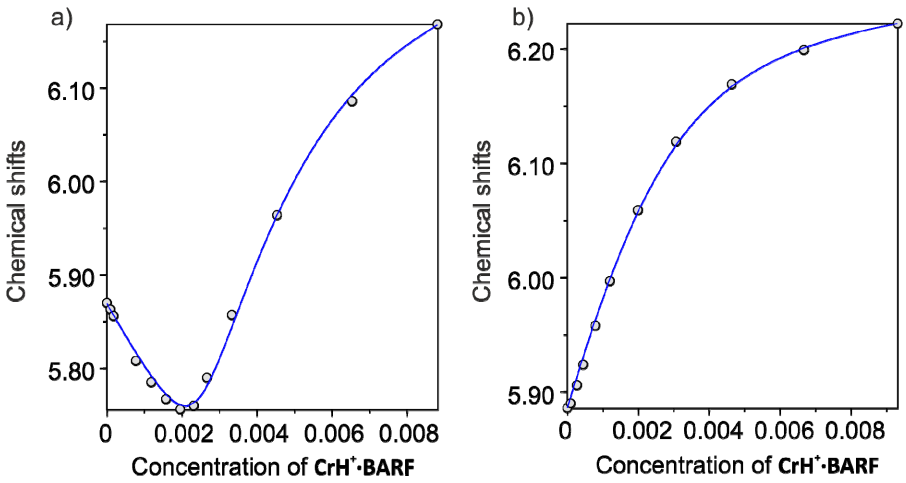

Figure 3. 25: Fitting of ^{1}H NMR titration data of a) receptor **1** and b) receptor **5** with **CrH^{+}·BARF** in CD_2Cl_2 (HypNMR Software) using chemical shift changes observed for β-pyrrol protons highlighted in Figure 3. 7 and Figure 3. 21.

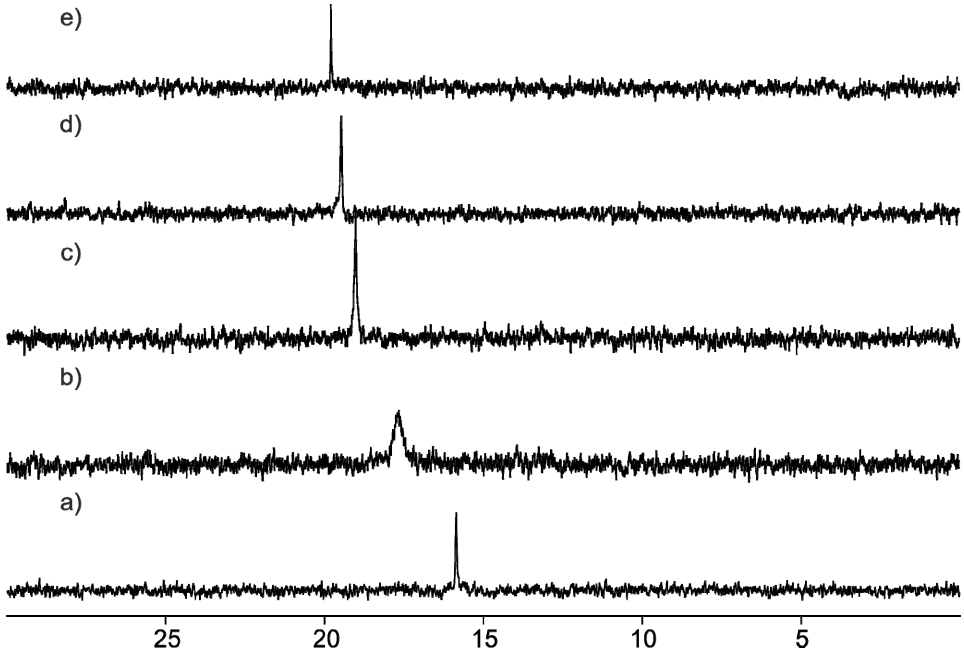

Figure 3. 26: ^{31}P{^{1}H} NMR spectra obtained during the titration of **1** (2.42 mM) with **CrH^{+}·BARF** in CD_2Cl_2. a) 0 eq. b) 0.49 eq. c) 0.95 eq. d) 1.87 eq. e) 3.64 eq.

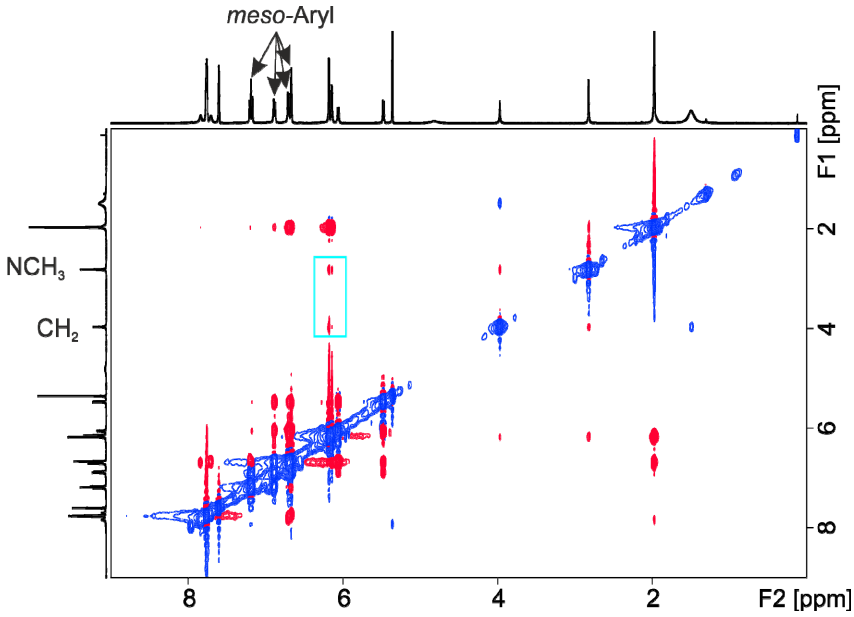

Figure 3. 27: ROESY ^{1}H NMR spectrum of a CD_2Cl_2 solution of receptor **5** (6.50 mM) and **CrH$^+$·BARF** in a 1:1 molar ratio. The blue box indicates the region of the spectrum showed in Figure S16. Note the lack of nOEs between CH_2 and the aryl protons.

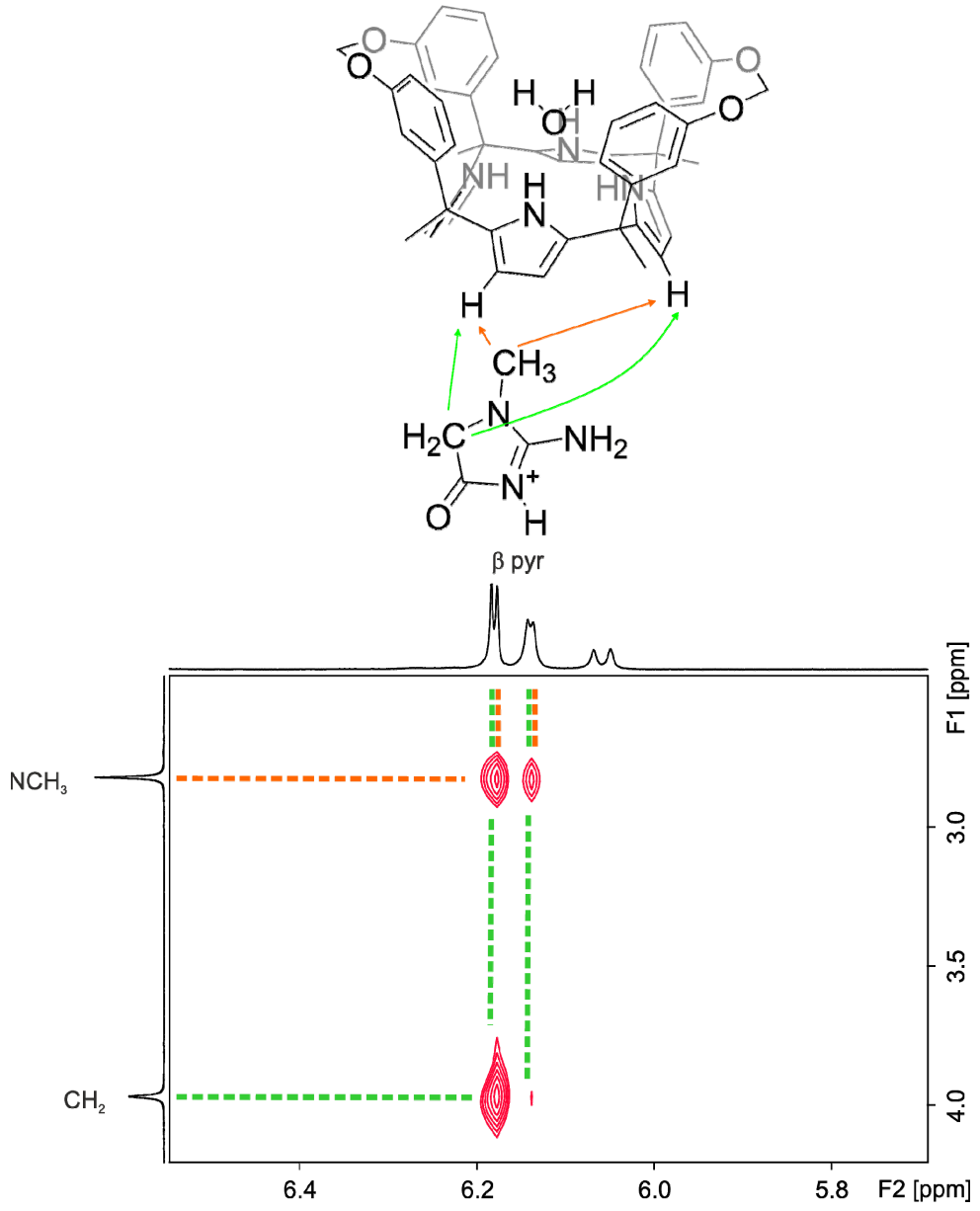

Figure 3. 28: Blowup of the portion of the ROESY ^{1}H NMR spectrum Figure 3. 27 contained within the blue box highlighting the intermolecular coupling patterns between **5** and **CrH**$^{+}$

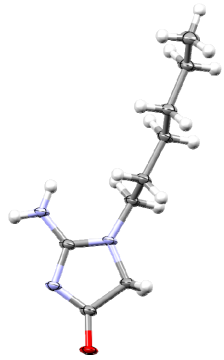

Figure 3. 29: X-ray structure of **CrHx**.

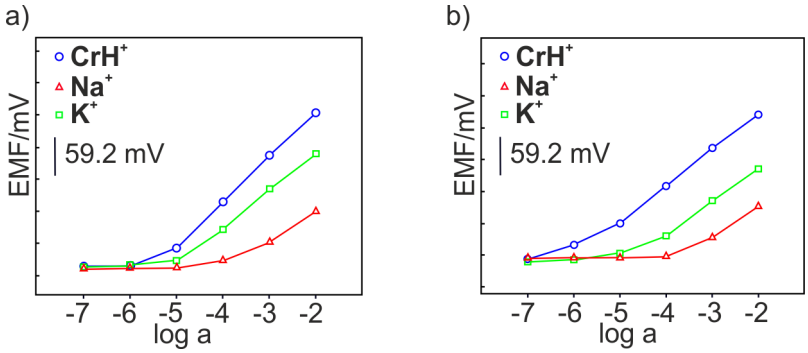

Figure 3. 30: Calibration curves for **CrH**$^+$ obtained with blank electrode a) and the ISE incorporating receptor **5** b).

3.5 References and notes

[1] Taal, M. W.; Brenner, B. M.; Rector, F. C. *Brenner & Rector's the kidney*; 9th ed.; Elsevier/Saunders: Philadelphia, PA, 2012.
[2] Delanghe, J. R.; Speeckaert, M. M. *NDT plus* **2011**, *4*, 83-86.
[3] Lolekha, P. H.; Jaruthunyaluck, S.; Srisawasdi, P. *J. Clin. Lab. Anal.* **2001**, *15*, 116-121.
[4] Lad, U.; Khokhar, S.; Kale, G. M. *Anal. Chem.* **2008**, *80*, 7910-7917.
[5] Jacobs, R. M.; Lumsden, J. H.; Taylor, J. A.; Grift, E. *Can. J. Vet. Res.* **1991**, *55*, 150-154.
[6] Stockl, D.; Reinauer, H. *Clin. Chem.* **1993**, *39*, 993-1000.
[7] Thienpont, L. M.; Deleenheer, A. P.; Stockl, D.; Reinauer, H. *Clin. Chem.* **1993**, *39*, 1001-1006.
[8] Bell, T. W.; Hext, N. M.; Khasanov, A. B. *Pure Appl. Chem.* **1998**, *70*, 2371-2377.
[9] Bell, T. W.; Firestone, A.; Liu, J.; Ludwig, R.; Rothenberger, S. D. In *Inclusion Phenomena and Molecular Recognition*; Atwood, J. L., Ed.; Springer US: Boston, MA, 1990, p 49-56.
[10] Bell, T. W.; Hou, Z.; Luo, Y.; Drew, M. G. B.; Chapoteau, E.; Czech, B. P.; Kumar, A. *Science* **1995**, *269*, 671-674.
[11] Beckles, D. L.; Maioriello, J.; Santora, V. J.; Bell, T. W.; Chapoteau, E.; Czech, B. P.; Kumar, A. *Tetrahedron* **1995**, *51*, 363-376.
[12] Buhlmann, P.; Simon, W. *Tetrahedron* **1993**, *49*, 7627-7636.
[13] Buhlmann, P.; Badertscher, M.; Simon, W. *Tetrahedron* **1993**, *49*, 595-598.
[14] Buhlmann, P.; Pretsch, E.; Bakker, E. *Chem. Rev. (Washington, DC, U. S.)* **1998**, *98*, 1593-1687.
[15] Bühlmann, P.; Chen, L. D. In *Supramol. Chem.*; John Wiley & Sons, Ltd: 2012.
[16] Elmosallamy, M. A. F. *Anal. Chim. Acta* **2006**, *564*, 253-257.
[17] Kelly, P. M.; Kataky, R.; Parker, D.; Patti, A. F. *J. Chem. Soc., Perkin Trans. 2* **1995**, 1955-1963.
[18] Buhlmann; Philippe, B. P. G. 2008; Vol. PCT/US2006/020366
[19] Bakker, E.; Bühlmann, P.; Pretsch, E. *Talanta* **2004**, *63*, 3-20.
[20] Hernandez-Alonso, D.; Zankowski, S.; Adriaenssens, L.; Ballester, P. *Org. Biomol. Chem.* **2015**, *13*, 1022-1029.
[21] Verdejo, B.; Gil-Ramirez, G.; Ballester, P. *J. Am. Chem. Soc.* **2009**, *131*, 3178-3179.
[22] Aragay, G.; Hernández, D.; Verdejo, B.; Escudero-Adán, E.; Martínez, M.; Ballester, P. *Molecules* **2015**, *20*, 16672.
[23] Espelt, M.; Aragay, G.; Ballester, P. *Chimia* **2015**, *69*, 652-658.
[24] Escobar, L.; Aragay, G.; Ballester, P. *Chem. Eur. J.* **2016**, *22*, 13682-13689.
[25] Ciardi, M.; Galan, A.; Ballester, P. *J. Am. Chem. Soc.* **2015**, *137*, 2047-2055.
[26] Ciardi, M.; Tancini, F.; Gil-Ramirez, G.; Escudero-Adan, E. C.; Massera, C.; Dalcanale, E.; Ballester, P. *J. Am. Chem. Soc.* **2012**, *134*, 13121-13132.
[27] Castro, P. P.; Zhao, G.; Masangkay, G. A.; Hernandez, C.; Gutierrez-Tunstad, L. M. *Org. Lett.* **2004**, *6*, 333-336.
[28] Beckles, D. L.; Maioriello, J.; Santora, V. J.; Bell, T. W.; Chapoteau, E.; Czech, B. P.; Kumar, A. *Tetrahedron* **1995**, *51*, 363-376.
[29]
[30] Kim, S. K.; Sessler, J. L. *Acc. Chem. Res.* **2014**, *47*, 2525-2536.
[31] Gao, J.; Hu, Y.; Li, S.; Zhang, Y.; Chen, X. *Chem. Phys.* **2013**, *410*, 81-89.
[32] Gans, P.; Sabatini, A.; Vacca, A. *HypNmr 2008 Version 4.0.66*.
[33] Cantadori, B.; Betti, P.; Boccini, F.; Massera, C.; Dalcanale, E. *Supramol. Chem.* **2008**, *20*, 29-34.
[34] Kumar, V.; Rana, H.; Kaushik, M. P. *Tetrahedron Lett.* **2012**, *53*, 6423-6425.

Chapter 4

Synthesis and preliminary binding studies of a new series of water soluble bisphosphonate calix[4]pyrrole biscavitands

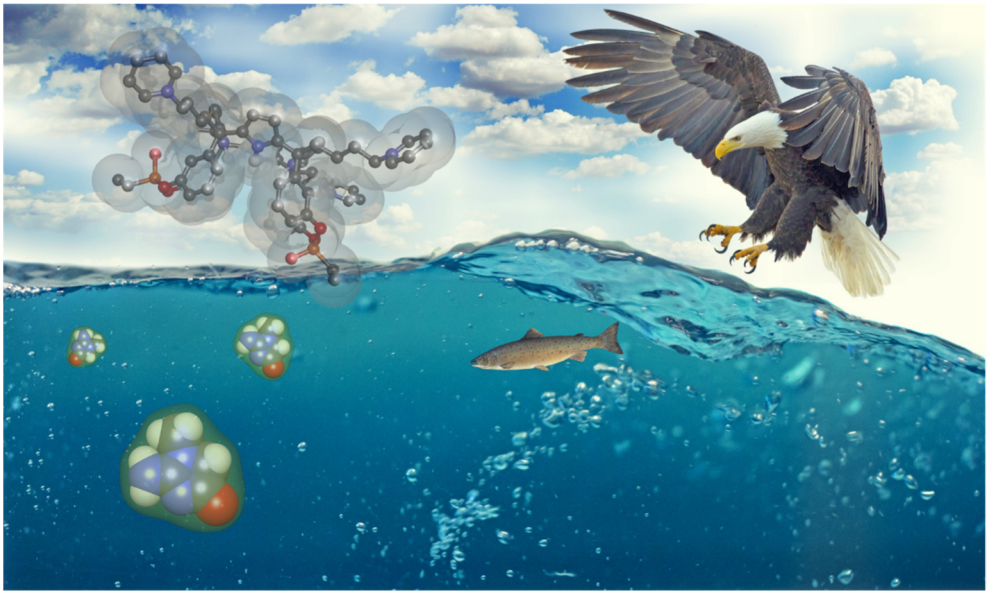

Unpublished results

UNIVERSITAT ROVIRA I VIRGILI
CALIX[4]PYRROLE-BASED RECEPTORS FOR BIOLOGICALLY RELEVANT POLAR MOLECULES: FROM ORGANIC TO AQUEOUS MEDIA
Daniel Hernández Alonso

4.1 Introduction

In cone confirmation, the tetra-α isomers of aryl-extended calix[4]pyrroles possess a deep aromatic cavity delimited by the four aryl rings covalently linked to the *meso* carbons of its calix[4]pyrrole core. The aromatic cavity protects the four polar NH groups from solvation when they are dissolved in solvents with high dielectric constants (such as water) by forming a hydrophobic environment around them. This special feature is what makes aryl-extended calix[4]pyrroles an ideal class of macrocyclic receptors for the recognition of polar substrates in water. In addition, the presence of four polar NHs able to stablish intermolecular hydrogen bonding interaction makes them even more attractive for the study of selective binding of polar substrates in water. The superior binding ability of cavitands and deep cavity cavitands in aqueous solution has been extensively studied in the case of resorcin[4]arene and calix[4]arene derivatives. They provide conformationally more rigid concave cavities that result in larger kinetic stabilities of the formed complex.[1] Cavitands based on a resorcin[4]arene scaffolds are structurally similar to those deriving from aryl-extended calix[4]pyrroles. The former have been used in a wide range of different applications such as supramolecular catalysis,[2,3,4] stabilization of reactive species,[5,6,7] photochemistry,[8,9,10,11,12,13] electrochemistry,[14] or binding studies[15,16,17,18,19,20,21,22,23] among others. In 2012, we reported the synthesis of three diastereomeric bisphosphonate calix[4]pyrrole cavitands by slightly modifying the reactions conditions developed by Dalcanale's group for the preparation of phosphonate cavitands derived from resorcin[4]arenes. We demonstrated the ability of bisphosphonate calix[4]pyrrole cavitands to act as a multitopic receptors for alkylammonium salts in organic solution. The diastereoisomers featuring one or two phosphonate bridging groups inwardly directed with respect to the cavity were able to complex the ion pairs in a close contact binding mode. On the contrary, the diastereoisomer with the two phosphonate groups outwardly directed with respect to the cavity preferred to exhibit a host-separated binding mode of the ion-pair. We attributed the origin of this dissimilar behavior, to the capability of the polar phosphonate groups installed at the upper rim of the receptor in establishing additional interactions with the co-bound cation.[24,25] Few years later, we exploited the capability of the inwardly directed phosphonate bridging groups to act as hydrogen-bond acceptor in the selective binding of neutral creatinine (**Cr**) and the creatininium cation in organic solution. We demonstrated the key role played by the inwardly oriented phosphonate group in the thermodynamic stabilization of the resulting inclusion

complexes.[26] Taking advantage of our previous experience on the syntheses of phosphonate cavitands based on aryl-extended calix[4]pyrrole in combination with the synthetic introduction of water solubilizing groups, either at the upper[27] or lower rims,[28] we decided to undertake the synthesis of a new series of bisphosphonate water-soluble calix[4]pyrrole cavitands. Herein, we describe the synthetic routes developed for their successful preparation, as well as our preliminary results of the binding studies of the prepared receptors towards biologically relevant molecules in aqueous solution.

4.2 Results and discussion

4.2.1 Design and synthesis

In chapter 2 we described the introduction of ionizable groups at the lower and upper rims of aryl-extended calix[4]pyrroles with the aim to gain water solubility. The introduction of water solubilizing groups at the lower rim of the receptor avoids the over-functionalization of the open end of the cavity. The latter approach imposed a significant effect in the binding properties of the pristine receptor's cavity. The presence of ionizable groups decorating the upper rim of the receptor's cavity may induce strong solvation effects in the binding process. The polar functionalization of the cavity's entrance might decrease the receptor's binding affinity owing to the energetic cost involved in the desolvation of the polar groups, which is required prior to the inclusion of the guest. In addition, the establishment of electrostatic interactions (attractive and repulsive) between ionizable groups installed at the upper rim of the cavity of resorcin[4]arene cavitands and the included guest are known.[29,30] We expected that the installation of the water solubilizing groups at the lower rim of the aryl extended calix[4]pyrrole receptors will minimize possible interferences in the inclusion processes of neutral and charged substrates. Nevertheless, this synthetic strategy presents two main limitations: a) the lack of suitable commercially available alkyl-phenyl ketones, which makes the synthetic route longer and tedious, and b) specially, the low yields obtained in the syntheses of tetra-α- isomers of aryl extended calix[4]pyrroles functionalized at their lower rims with substituents different from the simple methyl group. Similarly to the previous water-soluble receptors described in chapter 2, we considered the possibility to install four terminal carboxylic moieties as ionizable groups in the alkyl-substituents of the *meso*-carbons of the calix[4]pyrrole core. This simple methodology imparted mM water solubility to lower-rim decorated aryl-extended calix[4]pyrrole scaffolds. The synthetic approach described in

chapter 2 involved a final CuAAc reaction to covalently attach the carboxylic groups to the calix[4]pyrrole scaffold. The new proposed strategy is based on the synthesis of a lower-rim functionalized tetraester calix[4]pyrrole that derives from the direct condensation reaction of a suitably prepared arylalkyl ketone with pyrrole. We envisaged that hydrolysis of the terminal tetraester functions of the calix[4]pyrrole derivative should give access to the tetra acid counterpart. The synthetic route consisted on 6 synthetic steps (Scheme 4. 1). The first synthetic step involved the reaction of commercially available 3-methoxyphenylmagnesium bromide with glutaric anhydride that produced 5-(3-methoxyphenyl)-5-oxopentanoic acid (**1**) in good yields. After demethylation reaction by heating **1** in a 1:1 mixture (volume) of $48\%_{aq}$ HBr and glacial acetic acid,[31] followed by simple esterification reaction in ethanol, we were able to isolate the desired starting ketone **2a** in good yields. With ketone **2a** in our hands, we tested the acid-catalyzed cyclocondensation reaction of **2a** with pyrrole. First, we applied the same reaction conditions used for the previously described *meso* tetramethyl analogues.[26] Unfortunately, we were not able to isolate the desired (tetra-α) **3a** calix[4]pyrrole. The analysis of the reaction mixture revealed the presence of acyclic oligomeric products. The screening of several acids or reaction solvents did not produce significant improvement in the formation of the tetra-α isomer of **3a**. Remarkably, when ethanol and methanesulfonic acid were used, the ^{1}H NMR analysis of the crude reaction mixture showed the presence of the α, α, β, β isomer of **3a** as the major component.

Owing to the unsuccessful results obtained by applying typical reaction conditions for the preparation of aryl-extended calix[4]pyrroles, we decided to investigate the use of additives to improve the formation of the tetra-α isomer. We were pleased to find that the use of aliquat 336, an inexpensive mixture of C_8-C_{10} methyltrialkyl ammonium chloride salt enriched in C_8, was able to produce the tetra-α isomer of **3a** in a remarkably 20 to 23 % of yield. Due to the difficulty of removing the template salt from the crude reaction mixture, we decided to substitute aliquat 336 salt by methyltributyl ammonium chloride, which can be easily removed by simply washing the crude reaction mixture with water. It is worth mentioning here that we were able to successfully apply this template methodology to other aryl-extended calix[4]pyrrole presenting different functionalities at their lower and upper rims.[32] With calix[4]pyrrole **3a** in our hands, the phosphonate bridging groups were incorporated using similar reaction conditions than those employed in the synthesis of the methyl *meso*-substituted analogues (chapter 3). However, we decided to change the phenylphosphonic dichloride by ethylphosphonic dichloride in order to reduce the lipophilic nature of the

resulting phosphonate cavitands. In doing so, we expect to minimize possible aggregation problems and increase water solubility. After column chromatography purification of the crude reaction mixture, we isolated the three possible diastereisomers of **4a** (ii, io and oo) in 4%, 17% and 17% yield, respectively.

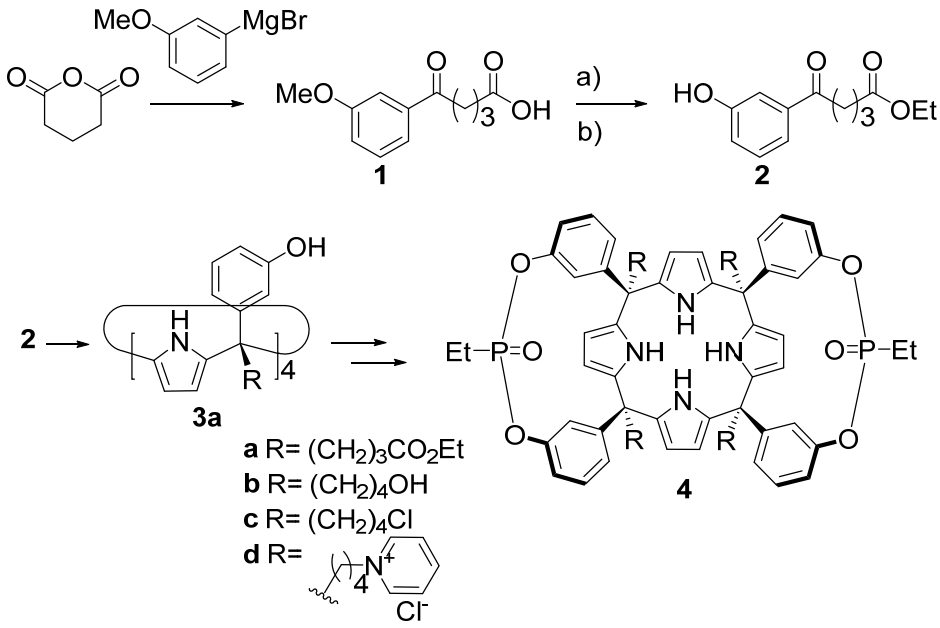

Scheme 4. 1: Synthetic scheme for the preparation of bisphosphonate cavitand **4**. a) CH_3COOH:HBr 1:1, reflux 6h; b) H_2SO_4, EtOH, reflux 90 min. For more details, see experimental part.

The last step of the proposed synthetic route was the hydrolysis of the ester groups to the corresponding carboxylic acids. Unluckily, we were not able to find suitable reaction condition affording the corresponding tetracarboxylic acid calix[4]pyrroles without affecting the bridging phosphonate groups. Figure 4. 7 shows the ^{1}H NMR spectra obtained after the treatment of **4a$_{oo}$** with NaOH in a 1:1:2 solvents' mixture of THF:water:EtOH. The lack of proton signals resonating close to 4 ppm confirmed the complete hydrolysis of the esters groups. However, the number of proton signals observed in the aromatic region of the spectrum together with the data of the HPLC-MS analysis of the crude reaction mixture (Figure 4. 8), confirmed the formation of more than one product during the hydrolysis step. The hydrolysis of the bridging phosphonate groups to the corresponding phosphonic acids when phosphonate cavitands derived from resorcin[4]arene scaffolds are exposed to aqueous

basic conditions was reported in literature.[33,34] The m/z values for some ions present in the mass spectra recorded during the HPLC-MS analysis of the crude reaction mixture indicated the hydrolysis of the phosphonate bridging groups under the basic reaction conditions (Figure 4. 9). Attempts to selectively hydrolyze the ester groups of **4a$_{oo}$** using acidic conditions were also unsuccessful.

Our unsuccessful attempts to selectively hydrolyze the ester groups forced us to change our strategy for the incorporation of ionizable groups in the lower rim of calix[4]pyrrole scaffolds. Accordingly, we considered the possibility to introduce pyridinium groups instead as water solubilizing groups. These groups have been satisfactorily used in resorcin[4]arene cavitands to impart water solubility over a wide range of pHs at concentrations up to 25 mM.[35,36] To achieve the synthesis of the new targeted receptors, we firstly reduced the ester groups of calix[4]pyrrole **3a** to hydroxyl groups using $LiAlH_4$ as reducing agent to produce the octa-hydroxy calix[4]pyrrole **3b**. The treatment of **3b** with *N*-chlorosuccinimide and triphenylphosphine, selectively converted the primary hydroxyl groups into the corresponding chloride derivatives, yielding **3c** in good yields. The reaction of **3c** with ethylphosphonic dichloride produced bis-phosphonate **4c** as a mixture of the three possible diastereoisomers, which were conveniently separated using column chromatography. Finally, treatment of **4c$_{io}$** or **4c$_{oo}$**, in separate reaction flask, with pyridine at 110 ºC produced the precipitation of the corresponding tetracationic derivatives **4d** in good yields and excellent purities. As expected, cavitands **4d** were soluble in water at mM concentrations. Due to the low yield obtained for the **4c$_{ii}$** isomer we were not able to form the corresponding pyridonium derivative **4d$_{ii}$**.

Once we confirmed the water solubility of the pyridinium derivatives **4d**, we undertook the synthesis of the alkylaryl ketone **6** featuring a terminal chloro substituent (Scheme 4. 2), with the aim to simplify the synthetic route of the former. Ketone **6** was synthetized by the addition of freshly prepared 4-chlorobutylmagnessium bromide to a solution of 3-methoxybenzoyl chloride to afford the methyl protected ketone derivative **5**. The demethylation reaction was performed using the same conditions applied in the synthesis of the ketone ester **2**. However, the demethylated compound was produced as the bromo- derivative. Treatment of the obtained mixture with substoichiometric amounts of methyltributyl ammonium chloride in 1,2-dichloroethane yielded the chloro-ketone **6** as the exclusive product. The acid catalyzed condensation reaction of **6** with pyrrole using methyltributyl ammonium chloride as additive,

allowed the isolation calix[4]pyrrole **3c** in 14% yield after column chromatography purification of the crude reaction mixture.

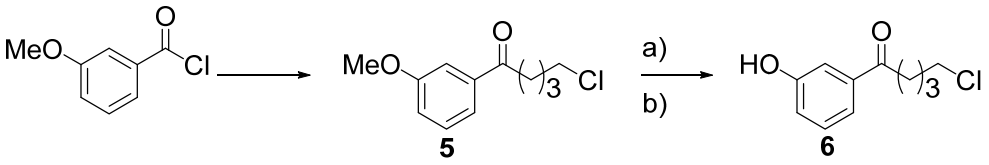

Scheme 4. 2: Synthetic scheme for the preparation of ketone **6**. a) CH_3COOH:HBr 1:1, reflux 3h 30min; b) MTBACl, DCE, reflux overnight. For more details, see experimental part.

4.2.2 Binding studies

We investigated the use of water soluble calix[4]pyrrole tetracationic phosphonate cavitands **4d** in the complexation of a series of polar guests. Considering the good results obtained in the binding studies of the neutral analogous receptors in organic solvents (concretely the one with an inwardly directed phosphonate group, chapter 3) with creatinine **Cr**, we decided to evaluate the binding of cavitands $\mathbf{4d_{io}}$ and $\mathbf{4d_{oo}}$ in water solution using the same guest.

Not surprisingly, the energy minimized structures of both complexes $\mathbf{4d_{io}}\supset\mathbf{Cr}$ and $\mathbf{4d_{oo}}\supset\mathbf{Cr}$ (Figure 4. 1), did not differ from those obtained using the organic soluble versions.[26] Similarly to the previously reported results, the $\mathbf{4d_{io}}$ isomer is able to establish one additional hydrogen bond interaction in the inclusion complex $\mathbf{4d_{io}}\supset\mathbf{Cr}$, between the inwardly directed phosphonate group and the acyclic NH moiety of the included **Cr**, when compared with the $\mathbf{4d_{oo}}\supset\mathbf{Cr}$ complex. We used receptor $\mathbf{4d_{oo}}$ as reference, in order to assess the importance of this additional polar interaction in water solution.

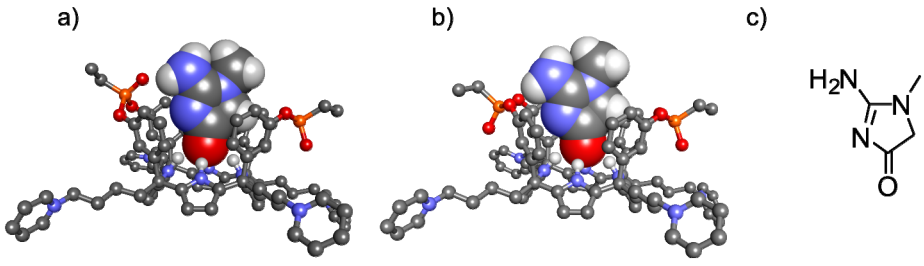

Figure 4. 1: Energy minimized (MM3) structure of a) $\mathbf{4d_{io}}\supset\mathbf{Cr}$ and b) $\mathbf{4d_{oo}}\supset\mathbf{Cr}$ complexes; c) molecular structure of **Cr**.

The binding of **Cr** to the two diastereomeric receptors was probed using ^{1}H NMR titration experiments in D_2O or D_2O:H_2O solutions. The experimentally determined pKa value of creatinine in water is 4.85. Consequently, in titration experiments performed at neutral pH, creatinine exists almost quantitatively in its neutral form.[37] Addition of incremental amounts of creatinine to a solution of **4d$_{io}$** in D_2O (or D_2O:H_2O) produced detectable changes in the chemical shift values of the receptor protons (Figure 4. 2). Especifically, the β-pyrrole protons up field shifted, in particular those that are not placed below the phosphonate bridging group. This observation was in complete agreement with the shift pattern observed in organic solution. Shifting of the aryl proton as well as the pyridinium proton signals are also clearly detectable. This observation clearly indicated that the binding process between **4d$_{io}$** receptor and **Cr** featured a chemical exchange process that was fast on the ^{1}H NMR time scale. Similar results were obtained for **4d$_{oo}$** receptor (Figure 4. 10).

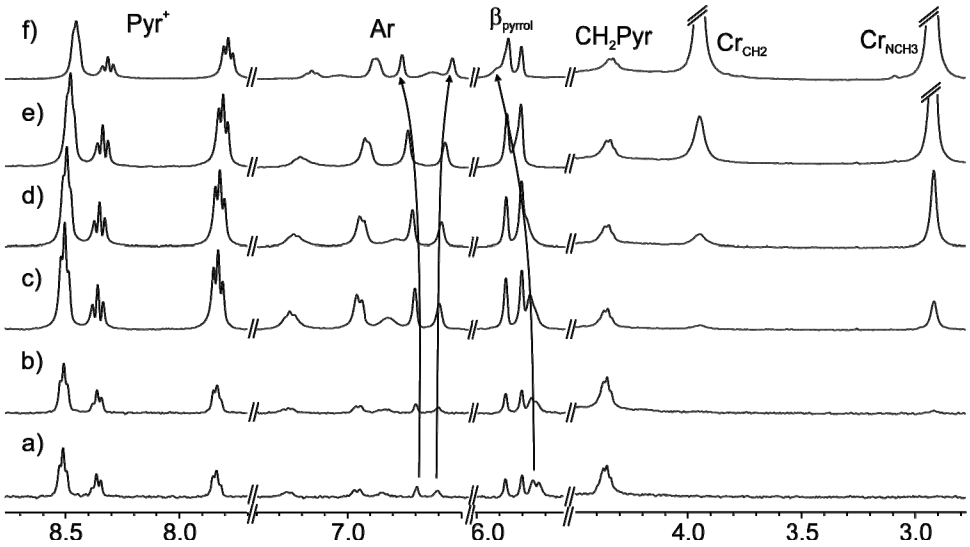

Figure 4. 2: Selected regions of the ^{1}H-NMR spectra recorded during the titration of **4d$_{io}$** in D_2O:H_2O 1:9 with incremental amounts of **Cr**. a) 0 eq.; b) 0.5 eq.; c) 1.0 eq.; d) 2.4 eq.; e) 5.9 eq.; f) 18.5 eq.

The obtained ^{1}H NMR titration data (chemical shift changes vs guest concentration) were fitted to a binding isotherm of a simple 1:1 binding model using the Hyp NMR2008 software. This fitting procedure allows the calculation of the value of the binding constant. In both cases, we obtained a good fit) of the experimental data (for at list two protons) to the theoretical model. (Figure 4. 11). The values of the binding constants returned from the fits were 1.3×10^2 M^{-1} for **4d$_{io}$** and 3.2×10^2 M^{-1} for **4d$_{oo}$**. The measured dramatic attenuation for

the thermodynamic stability of the complexes compared to the values obtained in organic solution (4 and 3 orders of magnitude, respectively) was not unexpected, owing to the large hydrogen-bonding competitive nature of water. However, the larger binding affinity for creatinine featured by the **4d$_{oo}$** diastereoisomer compared to the **4d$_{io}$** counterpart was indeed completely unexpected. As previously observed in organic solvents, we predicted a higher binding affinity of creatinine for the **4d$_{io}$** diastereoisomer due to the additional hydrogen bond interaction that can be stablished between the inwardly directed phosphonate group if compared to **4d$_{oo}$**. Considering the structural features of both receptors, we attributed the determined difference in binding constant values to the energetically more disfavored removal of water molecules located at the entrance of the aromatic cavity of the **4d$_{io}$** receptor that are strongly hydrogen bonded due to the inwardly directed PO group. The desolvation process that precedes **Cr** inclusion must be associated with an enthalpic penalty, which in turn translates into a decrease in free binding energy. To substantiate this hypothesis, we titrated both receptors with a lipophilic version of creatinine containing a *n*-hexyl chain (**HxCr**) instead of the methyl substituent. As observed in Figure 4. 3, the lipophilic alkyl chain of included **HxCr** resides outside of the cavity of the receptor demanding a larger desolvated area of its upper polar rim compared to the complex with the parent **Cr**. On the other hand, the face of the alkyl chain directly contacting with the desolvated receptor's upper rim area must release high-energy water molecules to the bulk solvent. The net result of these desolvation processes is expected to be both enthalpy and entropy favored and thus they should favor binding. Moreover, complex formation is expected to be reinforced by additional dispersion forces established between the two contacting organic surfaces. The ^{1}H NMR spectra recorded in separate titration of **4d$_{io}$** and **4d$_{oo}$** with incremental amounts of **HxCr** showed similar chemical shift changes than the observed for **Cr** (Figure 4. 12 and Figure 4. 13). The fit of the obtained ^{1}H NMR titration data to a 1:1 binding model was good (Figure 4. 14) and returned the following binding constants values:1.8×10^{3} M^{-1} for **4d$_{oo}$⊃HxCr** and 2.7×10^{2} M^{-1} for **4d$_{io}$⊃HxCr** complexes. In agreement with the predictions above, the measured binding constant values for **HxCr** were larger than those calculated for **Cr**. Concretely, the binding constant for **4d$_{io}$⊃HxCr** complex was approximately two-fold larger than the one obtained for **4d$_{io}$⊃Cr**. While the increase in binding affinity showed by receptor **4d$_{oo}$** is slightly larger than five-fold, in agreement with its C_2 symmetry. The bis-phosphonate receptor **4d$_{io}$**, having an inwardly directed PO group with respect to the aromatic cavity, can

be involved in an intermolecular NH···OP hydrogen bonding interaction with the included **HxCr** guest derivative. However, gives rise to thermodynamically less stable inclusion complexes than the **4d$_{oo}$** isomer. This result indicated that the above-mentioned intermolecular hydrogen bonding interaction does not compensate for the free energy cost associated with the desolvation of the polar groups, NH and PO.

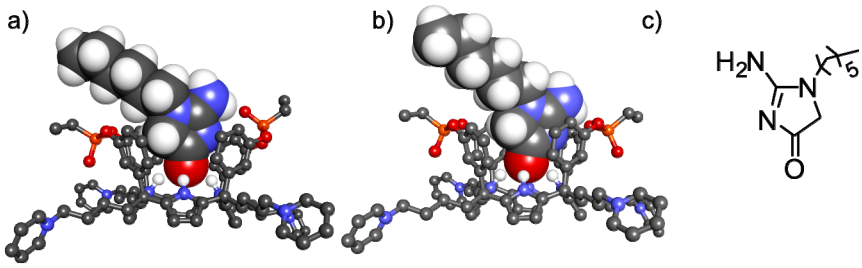

Figure 4. 3: Energy minimized (MM3) structures of a) **4d$_{io}$⊃HxCr** and b) **4d$_{oo}$⊃HxCr** complexes; c) molecular structure of **HxCr** in its zwitterionic resonant structure.

We performed preliminary ^{1}H NMR titration experiments with other polar guests in order to explore the potential application of the **4d$_{io}$** cavitand as selective receptor. The size of the selected guests was suitable to allow their inclusion in the aromatic polar cavity of **4d$_{io}$**. Moreover, they contained a hydrogen bond acceptor group that could bind to the four pyrrole NHs of the **4d$_{io}$** receptor and a hydrogen bond donor group adequately positioned to simultaneously interact with the in directed phosphonate group of the receptor. Some of selected guest are biologically relevant molecules i.e. biotin, cytosine and aminoacids like proline (Figure 4. 4). In all cases, the addition of these guests to millimolar aqueous solutions of the **4d$_{io}$** receptor produced noticeable chemical shift changes in the proton signals assigned to the free receptor. These observations were indicative of the formation of supramolecular complexes between the **4d$_{io}$** receptor and the investigated guests. Although, the obtained results were interesting we did not pursue the further characterization of the formed complexes owing to the large amounts of added guest necessary to reach saturation of chemical shift changes of the host.

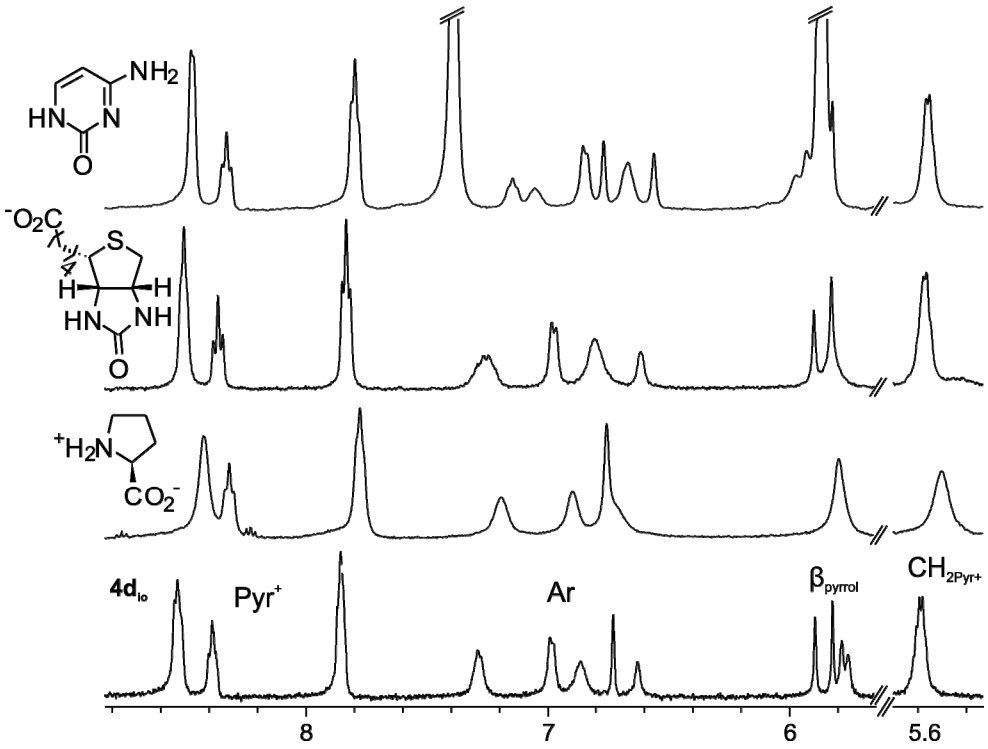

Figure 4. 4: Selected downfield regions of the ^{1}H NMR spectra of aqueous solutions containing 1mM **4d$_{io}$** and (from the bottom to the top): free **4d$_{io}$**, 15 eq. of proline, 1.4 eq. of biotine, 22 eq. of cytosine.

Nitrosamines are a class of compounds of special interest in healthcare owing to their high toxicity and carcinogenicity. After being activated in living organisms, they are converted in potent alkylating agents able to introduce alkyl chains in DNA, RNA and proteins.[38,39] Nitrosamines present in tobacco smoke are known as tobacco-specific *N*-nitrosamines (TSNAs). They include *N*-nitrosonornicotine (NNN), 4-(methylnitrosamino)-1-(3-pyridyl)-1-butanone (NNK) and 4-(methylnitrosamino)-1-(3-pyridyl)-1-butanal (NNAL).[40] Other carcinogenic nitrosamines have been also found in other commercial products such as smokeless tobacco, cosmetics, rubbers and food.[41,42] The addition of nitrite and/or nitrate salts, which are common additives used in food industry, represent one of most relevant sources involved in the formation of these compounds from the natural amine components.[43] Surprisingly and to the best of our knowledge, only one example of synthetic receptors able to bind the important family of nitrosamine molecules has been reported in literature.[44] Anzenbacher and co-workers described the use of cyclic and acyclic cucurbit[n]uril derivatives as receptors for nitrosamines. The authors claimed that the predominant forces

involved in the recognition of these compounds by cucurbit[n]util derivatives do not involve hydrogen-bond interactions, they were mainly hydrophobic and dipole-dipole interactions. In short, the recognition of the nitrosamines does not involve the binding of the nitroso group through the formation of hydrogen bonds.

N-nitrosodiethylamine (**NDEA**), Figure 4. 6, is a powerful carcinogenic compound that is currently classified in the group 2A as a possible carcinogen in humans. It is important to note that in every animal species tested and for every method of carcinogenesis bioassay employed, the exposure to **NDEA** produced different tumors. For example, after oral exposure to **NDEA**, mice developed liver, esophageal and forestomach tumors. **NDEA** has been found in mainstream and sidestream tobacco smoke, meet and whisky.[45]

Due to the biological relevance of nitrosamines and the lack of synthetic receptors able to interact predominantly with its nitroso group, we decided to study the ability of the water-soluble calix[4]pyrrole cavitands to bind **NDEA** in water. We decided to evaluate the binding properties of the $\mathbf{4d_{oo}}$ receptor for two main reasons: 1) weaker solvation of its cavity entrance compared to the io counterpart and 2) absence of polar groups in the **NDEA** molecular structure able to interact with an inwardly directed phosphonate group. The complexation ability of $\mathbf{4d_{oo}}$ host towards **NDEA** guest was probed using ^{1}H NMR spectroscopy. Addition of incremental amounts of **NDEA** to an aqueous solution of $\mathbf{4d_{oo}}$ (1 mM) produced significant changes in the chemical shifts of the receptor's protons. The observed changes were indicative of the establishment of intermolecular interactions between the receptor and the added guest. Moreover, the in the initial phases of the titration, the signals of the protons of NDEA were significantly up field shifted compared to those of free **NDEA** in solution. Taken together, these observations suggested the formation of a complex that involved the inclusion of **NDEA** in the cavity of the calix[4]pyrrole receptor. The fit of the titration data to a simple 1:1 binding model was good (Figure 4. 15) and the returned binding constant value was 1.8×10^2 M^{-1}.

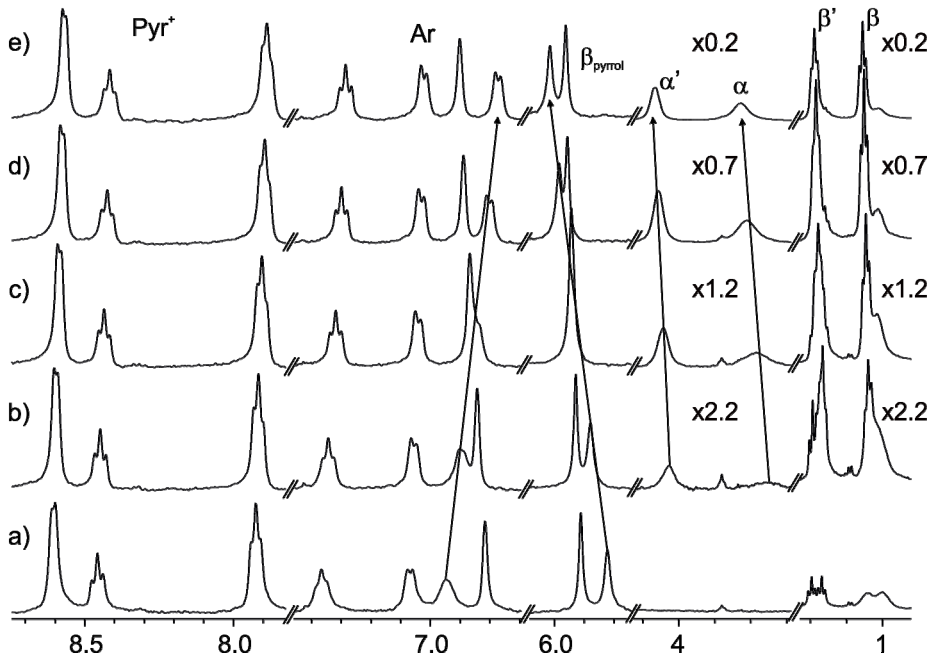

Figure 4. 5: Selected regions of the ^{1}H-NMR spectra recorded during the titration of **4d$_{oo}$** in D_2O with incremental amounts of **NDEA**. a) 0 eq.; b) 0.2 eq.; c) 5.4 eq.; d) 10.9 eq.; e) 19.9 eq.

Additionally, the fit of the titration data returned the estimated chemical shift values of the analyzed guest's protons in the **NDEA⊂4d$_{oo}$** inclusion complex. We used these values to calculate the complexation induce shift (CIS). CIS values are useful to gain some insight on the possible binding geometry of the formed complex. The calculated CIS values for the α and α' protons of diethyl nitrosamine were Δδ = -1.68 ppm and Δδ = -0.96 ppm, respectively, while for β and β' protons were Δδ= -0.51 ppm and Δδ = -0.39 ppm, respectively.[46] The larger complexation induced upfield shift calculated for the α and α' protons in comparison to the β and β' counterparts (Figure 4. 6) indicated the deeper inclusion of the former into the aromatic cavity of the receptor. This result supported that the inclusion of the nitrosamine in the receptor's cavity was driven by the establishment of hydrogen-bonding interactions between the oxygen atom of the nitrosamine group and the pyrrole NHs of the receptor. Interestingly α and β (protons in *cis* respect to the nitroso group) experimented a larger upfield shift compared to α' and β'. This observation indicated a deeper inclusion of these protons into the aromatic cavity due to the proper biding geometry of the complex (Figure 4. 6).

Our hypothesis is that to favor and effective interaction between the nitrosamine group and the calix[4]pyrrole core, the α protons have to be pointing to the inner cavity orienting the

βCH$_3$ to the outer part of the cavity minimizing steric clashes with the aromatic walls of the receptor ending with a larger shifting of the signals.

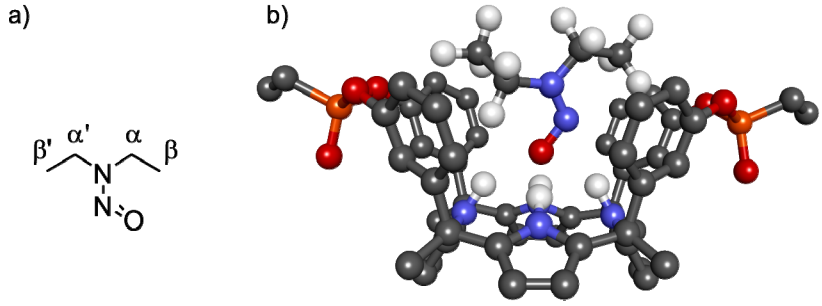

Figure 4. 6: a) Molecular structure of **NDEA**; b) Energy minimized (MM3) structure of **4d$_{oo}$⊃NDEA** complex, (*meso* functionalization with methyl groups was used for clarity).

4.3 Conclusions

In summary, we described the synthesis of two unprecedented diastereoisomeric water soluble bisphosphonate calix[4]pyrrole biscavitands **4d$_{oo}$** and **4d$_{io}$**. The water solubilizing groups were installed at the ends of the *meso*-alkyl substituents far away from the deep polar aromatic binding pocket. This approach aims to minimize possible perturbations of the binding site. During the optimization of the reaction conditions employed for the synthesis of the parent tetahydroxy calix[4]pyrrole **3d** we discovered a significant templating effect. Thus, the addition of methyltrialkyl ammonium chloride salts as reaction additive provoked a significant improvement in the isolated yield of the tetra-α isomer **3d** bearing functionalized alkyl chains at the *meso*-carbons. We assessed the binding constants of the two diastereoisomeric bis-phosphonate cavitands, **4d$_{io}$** and **4d$_{oo}$**, with natural creatinine (**Cr**) and with a lipophilic synthetic version (**HxCr**) in water. Both receptors formed thermodynamically stable complexes featuring 1:1 stoichiometry. Surprisingly to us, the **4d$_{oo}$** receptor displayed higher binding affinities towards both guests. Remarkably, the presence of a phosphonate group inwardly directed towards the aromatic cavity in the **4d$_{io}$** isomer that can be involved in an extra hydrogen bonding interaction with the included guest do not provide additional energetic stabilization to its complexes. We attributed this result to a more energetically demanding desolvation process for cavity entrance in the **4d$_{io}$** compared to the **4d$_{oo}$** counterpart. This difference is mainly dictated by the presence of the inwardly directed

PO group in the **4d$_{io}$** isomer. Finally, we reported that the **4d$_{oo}$** isomer is an effective receptor for **NDEA**, a potent carcinogenic agent, in water. The complexation process is mainly driven by hydrogen bonding interactions established between the oxygen atom of the *N*-nitroso moiety and the pyrrole NHs of the receptor. To the best of our knowledge, this finding represent the first report of a synthetic receptor for **NDEA**.

4.4 Experimental section

4.4.1 General information and instrumentation

All solvents and reagents used in the synthesis of the described compounds were obtained from commercial sources and were used without further purification except where noted. Pyrrole was distilled (50 mbar, 58–59 °C) and stored in the freezer (-20ºC) for further use. THF was distilled from sodium/benzophenone under argon atmosphere before use it. Triethyl amine was distilled from CaH_2 under argon atmosphere before use it. Methyltribuylammonium chloride (TBMACl) was purchased as aqueous solution, dried under vacuum and employed as a solid. Triphenyl phosphine was crystallized in boiling hexane. Pyridine was distilled from CaO under argon atmosphere. Flash columns chromatography were performed with silica gel, technical grade, pore size 60 Å, and 230–400 mesh particle size. The THF used for column chromatography was distilled before use it.

Routine ^{1}H-NMR and ^{13}C-NMR spectra were recorded on a Bruker Avance 400 (400 MHz for ^{1}H-NMR), Bruker Avance 500 (500 MHz for ^{1}H-NMR) ultrashield spectrometer, or on a Bruker Avance III 500 (500 MHz for ^{1}H-NMR) with a QNP cryoprobe. Chemical shifts are given in ppm. The peaks were referenced relative to the solvent residual peak. All NMR J values are given in Hz. High resolution mass spectra were obtained on a MicroTOF II (Bruker Daltonics) ESI as ionization mode Mass Spectrometer.

4.4.2 Synthetic procedures

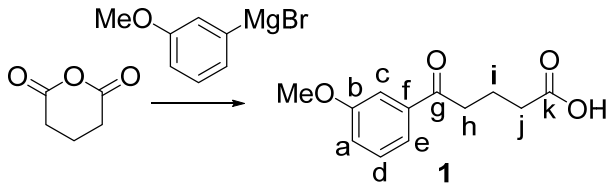

Synthesis of **1**: Glutaric anhydride (4 g, 35.1 mmol) was dissolved in 70 mL of anhydrous THF under Ar atmosphere at 0 ºC. 3-Methoxyphenylmagnesium bromide (1M solution in THF, 36.8 mL, 36.8 mmol, 1.05 eq.) was slowly added under vigorous stirring over 30 min. After addition, the reaction was left to slowly reach r.t. for 18 h. Next day, the reaction mixture was quenched with 50 mL of water and acidified until pH 1 with HCl (10% aq). The aqueous phase was extracted with EtOAc (3 x 50mL). The EtOAc extracts were combined, dried (Na_2SO_4), filtered and concentrated to dryness, yielding a yellow syrup. 20 mL of water were added and the mixture sonicated yielding a solid. The solid was filtered, washed with water (2 x 20 mL) and dried by passing air through it. Once the solid was dried, it was washed with hexane (2 x 20 mL) yielding desired product **1** as a white solid (5.4 g, 24.3 mmol, 69%). If necessary, the product was crystallized from boiling water. ^{1}H NMR (400 MHz, acetone-*d6*, 298 K): δ (ppm) = 10.59 (br s, 1H, COOH); 7.59 (ddd, 1H, $^3J_{He\text{-}Hd}$ = 7.6 Hz; $^4J_{He\text{-}Hc}$ = 1.5 Hz; $^4J_{He\text{-}Ha}$ = 1.0 Hz, He); 7.51 (dd, 1H, $^4J_{Hc\text{-}Ha}$ = 2.6 Hz, Hc); 7.42 (app t, 1H, app $^3J_{Hd\text{-}Ha}$ =$^3J_{Hd\text{-}He}$ = 7.9 Hz, Hd); 7.17 (ddd, 1H, $^3J_{Ha\text{-}Hd}$ = 8.2 Hz, Ha); 3.86 (s, 3H, OCH3); 3.11 (t, 2H, $^3J_{Hh\text{-}Hi}$ = 7.3 Hz, Hh), 2.43 (t, 2H, $^3J_{Hj\text{-}Hi}$ = 7.3 Hz, Hj), 1.98 (app quin, 2H, Hi). ^{13}C{^{1}H} NMR (100.6 MHz, acetone-*d6*, 298 K): δ (ppm) = 199.7 (Cg); 174.5 (Ck); 160.9 (Cb); 139.5 (Cf); 130.6 (Cd); 121.2 (Ce); 119.8 (Ca); 113.3 (Cc); 55.7 (OCH3); 38.2 (Ch); 33.3 (Cj); 20.3 (Ci). HRMS (ESI-TOF): m/z Calcd for $C_{12}H_{13}O_4$ $[M\text{-}H]^-$ = 221.0819; Found = 221.0820.

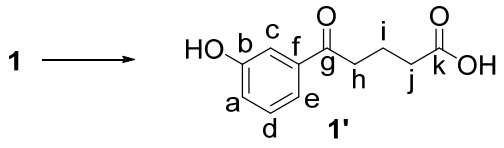

Syntheis of **1'**: **1** (13.28 g, 59.8 mmol) was dissolved in a mixture of 80 mL of acetic acid and 80 mL of HBr (48% aq solution). The mixture was refluxed for 6h. Then it was cooled down to r.t. and diluted with water (typically 100 mL). The crude was extracted with EtOAc (3 x 60 mL). The EtOAc extracts were combined, dried (Na_2SO_4), filtered and concentrated to dryness, yielding the desired product **1'** as a brown solid (10.4 g, 50.2 mmol, 84%). ^{1}H NMR (500 MHz, acetone-*d6*, 298 K): δ (ppm) = 10.57 (br s, 1H, COOH); 8.75 (br s, 1H, OH); 7.49 (ddd, 1H, $^3J_{He\text{-}Hd}$ = 7.7 Hz; ^{4}J$_{He\text{-}Hc}$ = 1.6 Hz; ^{4}J$_{He\text{-}Ha}$ = 1.0 Hz, He); 7.44 (dd, 1H, ^{4}J$_{Hc\text{-}Ha}$ = 2.5 Hz, Hc); 7.33 (app t, 1H, $^3J_{Hd\text{-}Ha}$ = $^3J_{Hd\text{-}He}$ = 7.9 Hz, Hd); 7.07 (ddd, 1H, $^3J_{Ha\text{-}Hd}$ = 8.1 Hz, Ha); 3.07 (t, 2H, $^3J_{Hh\text{-}Hi}$ = 7.3 Hz, Hh), 2.42 (t, 2H, $^3J_{Hj\text{-}Hi}$ = 7.3 Hz, Hj), 1.98 (app quin, $^3J_{Hi\text{-}Hj}$ = $^3J_{Hi\text{-}Hh}$ = 7.3 Hz 2H, Hi). ^{13}C{^{1}H} NMR (125.7 MHz, acetone-*d6*, 298 K): δ (ppm) = 199.7 (Cg); 174.6 (Ck); 158.6 (Cb); 139.5 (Cf); 130.6 (Cd); 120.8 (Ca); 120.1 (Ce); 115.1 (Cc); 38.2

(Ch); 33.3 (Cj); 20.3 (Ci). HRMS (ESI-TOF) m/z: Calcd for $C_{11}H_{11}O_4$ $[M-H]^-$ = 207.0663; Found = 207.0662.

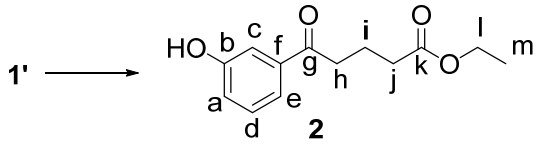

Synthesis of **2**: H_2SO_4 (1.1 mL, 96%, 20.4 mmol, 0.5 eq.) was added to a solution of **1'** (8.5 g, 40.8 mmol) in absolute EtOH (400 mL), and the mixture was refluxed for 1.5 h. The mixture was concentrated under reduced pressure. The crude was redissolved in CH_2Cl_2 (100 mL) and washed with $NaHCO_3$ (aq sat) until complete neutralization of the acid. The CH_2Cl_2 solution was dried (Na_2SO_4), filtered and concentrated to dryness. The product was purified by column chromatography on silica gel (CH_2Cl_2:EtOAc 95:5 to CH_2Cl_2:EtOAc 9:1). Ketone **2** was isolated as a white solid (8.2 g, 34.7 mmol, 85% yield). Rf = 0.39 (9:1 CH_2Cl_2:EtOAc). ^{1}H NMR (400 MHz, acetone-*d6*, 298 K): δ (ppm) = 8.63 (br s, 1H, OH); 7.49 (ddd, 1H, $^3J_{He-Hd}$ = 7.7 Hz; $^4J_{He-Hc}$ = 1.6 Hz; $^4J_{He-Ha}$ = 1.0 Hz, He); 7.43 (ddd, 1H, $^4J_{Hc-Ha}$ = 2.5 Hz, $^4J_{Hc-Hd}$ = 0.4 Hz, Hc); 7.34 (br app t, 1H, $^3J_{Hd-Ha}$ = $^3J_{Hd-He}$ = 7.9 Hz, Hd); 7.08 (ddd, 1H, $^3J_{Ha-Hd}$ = 8.1 Hz, Ha); 4.09 (q, 2H, $^3J_{Hl-Hm}$ = 7.1 Hz, Hl); 3.06 (t, 2H, $^3J_{Hh-Hi}$ = 7.2 Hz, Hh), 2.41 (t, 2H, $^3J_{Hj-Hi}$ = 7.4 Hz, Hj), 1.97 (app quin, 2H, $^3J_{Hi-Hh}$ = $^3J_{Hi-Hj}$ = 7.3 Hz, Hi); 1.21 (t, 3H, Hm). ^{13}C{^{1}H} NMR (125.7 MHz, acetone-*d6*, 298 S4 K): δ (ppm) = 199.6 (Cg); 173.5 (Ck); 158.5 (Cb); 139.5 (Cf); 130.6 (Cd); 120.8 (Ca); 120.2 (Ce); 115.1 (Cc); 60.6 (Cl); 38.1 (Ch); 33.8 (Cj); 20.3 (Ci); 14.6 (Cm). HRMS (ESI-TOF) m/z: Calcd for $C_{13}H_{15}O_4$ $[M-H]^-$ = 235.0976; Found = 235.0984. FTIR (ATR): ῡ (cm-1) = 3324, 2983, 2965, 2942, 2907, 1688, 1674, 1446, 1266, 1203, 1168. M.p.: 48-50 ºC.

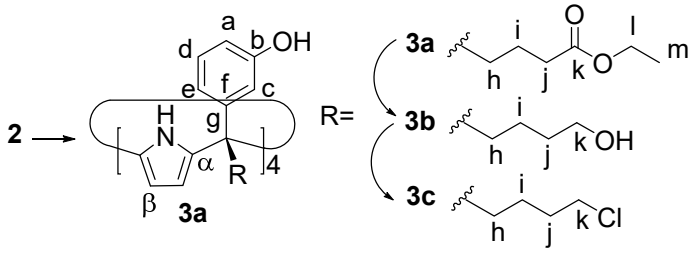

Synthesis of **3a**: Ketone **2** (2 g, 8.46 mmol), TBMACl (6g, 25.4 mmol) and pyrrole (0.59 ml, 8.46 mmol) were dissolved in 17 mL of CH_2Cl_2. Then, HCl (6.35 mL, 4M in dioxane, 25.4 mmol) was dropwise added to the reaction mixture under vigorous stirring; the reaction was

capped and stirred at r.t. for 6h. Then, more CH_2Cl_2 (40 mL) was added and the mixture washed with $NaHCO_3$ (aq sat) (2 x 50 mL). The aqueous phase was extracted with CH_2Cl_2 (2 x 40 mL). The organic extracts were combined, dried (Na_2SO_4), filtered and concentrated under vacuum. The crude was passed through a short column of silica (CH_2Cl_2:EtOAc 7:3). Then, it was further purified by column chromatography on silica gel (CH_2Cl_2:Acetone 9:1). The fraction containing the target compound was concentrated and recrystallized from CH_2Cl_2:Hexane yielding pure **3a** as a light yellow solid. α,α,α,α isomer: (0.55 g, 0.49 mmol, 23%). Rf = 0.3 (7:1 CH_2Cl_2:EtOAc). ^{1}H NMR (400 MHz, acetone-*d6*, 298 K): δ (ppm) = 8.58 (br t, 4H, NH); 8.16 (br s, 4H, OH); 7.09 (app t, 4H, $^3J_{Hd\text{-}Ha} = {}^3J_{Hd\text{-}He}$ = 7.9 Hz, Hd); 6.59 (ddd, 4H, $^3J_{Ha\text{-}Hd}$ = 8.1 Hz; $^4J_{Ha\text{-}Hc}$ = 2.5 Hz; $^4J_{Ha\text{-}He}$ = 1.0 Hz, Ha); 6.52 (ddd, 4H, $^3J_{He\text{-}Hd}$ = 7.7 Hz; $^4J_{He\text{-}Hc}$ = 1.7 Hz, He); 6.48 (dd, 4H, Hc); 6.01 (d, 8H, $^4J_{Hβ\text{-}NH}$ = 2.7 Hz, Hβ); 4.05 (q, 8H, $^3J_{Hl\text{-}Hm}$ = 7.1 Hz, Hl); 2.35 (m, 8H, Hh); 2.23 (t, 8H, $^3J_{Hj\text{-}Hi}$ = 7.3 Hz, Hj); 1.40 (m, 8H, Hi); 1.19 (t, 12H, Hm). ^{13}C{^{1}H}NMR (100.6 MHz, acetone-*d6*, 298 K): δ (ppm) = 173.7 (Ck); 157.5 (Cb); 148.7 (Cf); 137.9 (Cα); 129.9 (Cd); 121.6 (Ce); 116.9 (Cc); 114.5 (Ca); 105.7 (Cβ); 60.4 (Cl); 49.1 (Cg); 40.7 (Ch); 34.7 (Cj); 21.6 (Ci); 14.6 (Cm). HRMS (ESI-TOF): m/z Calcd for $C_{68}H_{75}N_4O_{12}$ $[M\text{-}H]^-$ = 1139.5387; Found = 1139.5364. FTIR (ATR): ῡ (cm-1) = 3409, 2974; 1701; 1596, 1582; 1445; 1196; 769. M.p.: >110 ºC (decompose)

Synthesis of **3b**: To a dried 100 mL round bottom flask charged with a solution of **3a** (0.84g, 0.74 mmol) in 36.8 mL of anhydrous THF and under an atmosphere of Ar, $LiAlH_4$ (3 mL, 2M in THF, 6 mmol) was slowly added at r.t. with stirring (release of H_2 and precipitation of aluminates is observed) and left under the same conditions for 2h and 30 minutes. Then, EtOAc was slowly added (quenching the excess of $LiAlH_4$) until release of H_2 stopped. Then, EtOAc (20 mL) and water (20 mL) were added and the mixture was acidify with 10% aqueous solution of HCl until all aluminates dissolved. The organic phase was separated and the aqueous phase was extracted 2 x 50mL with EtOAc. The EtOAc extracts were combined dried (Na_2SO_4), filtered and concentrated under vacuum. The product was purified by column chromatography on silica gel (DCM:THF 55:45). **3b** was isolated as a white light brown solid (0.64 g, 0.66 mmol, 90%). ^{1}H NMR (400 MHz, acetone-*d6*, 298 K): δ (ppm) = 8.57 (br s, 4H, NH); 8.09 (s, 4H, ArOH); 7.07 (app t, 4H, $^3J_{Hd\text{-}Ha} = {}^3J_{Hd\text{-}He}$ = 7.8 Hz, Hd); 6.56 (dd, 4H, $^3J_{Ha\text{-}Hd}$ = 7.8 Hz; $^4J_{Ha\text{-}Hc}$ = 1.8 Hz, Ha); 6.51 (d, 4H, $^3J_{He\text{-}Hd}$ = 7.8 Hz, He); 6.46 (br s, 4H, Hc); 5.96 (d, 8H, $^4J_{Hβ\text{-}NH}$ = 2.4 Hz, Hβ); 3.47 (app q, 8H, $^3J_{Hk\text{-}Hj} \approx {}^3J_{Hk\text{-}OH}$ = 5.8 Hz, Hk); 3.34 (t, 4H, $^3J_{Hk\text{-}OH}$ = 5.8 Hz, OH); 2.38-2.27 (m, 8H, Hh); 1.46 (app quin, 8H, $^3J_{Hj\text{-}Hk} \approx {}^3J_{Hj\text{-}Hi}$ = 6.8 Hz, Hj); 1.22-1.11 (m, 8H, Hi). ^{13}C{^{1}H}NMR (100.6 MHz, acetone-*d6*, 298 K): δ (ppm) = 157.4 (Cb);

149.1 (Cf); 138.1 (Cα); 129.8 (Cd); 121.7 (Ce); 117 (Cc); 114.4 (Ca); 105.6 (Cβ); 62.5 (Ck); 49.27 (Cg); 41.6 (Ch); 34.3 (Cj); 22.6 (Ci). HRMS (ESI-TOF): m/z Calcd for $C_{60}H_{67}N_4O_8$ $[M-H]^-$ = 971.4964; Found = 971.4969.

Synthesis of **3c**:

Method 1: A solution of triphenyl phosphine (1.75 g, 6.66 mmol) in 24 mL of anhydrous THF and under Ar atmosphere, was added to a stirred solution of N-chlorosuccinimide (0.88 g, 6.62 mmol) in 16 mL of anhydrous THF and under Ar atmosphere at r.t. forming a suspension which was stirred for 5 minutes at the same temperature. Then, a solution of **3b** (0.80, 0.82 mmol) in 26 mL of anhydrous THF under Ar was dropwise added over the suspension, and the reaction was stirred overnight. Next day, reaction mixture was poured into water and extracted with DCM (3 x 50 mL) (if a strong emulsion is formed addition of 10% HCl in water, helps to disperse it after shaking). The DCM extracts were combined, dried (Na_2SO_4), filtered and concentrated under vacuum. The product was purify by column chromatography on SiO_2 (DCM:EtOAc 8:2) (0.75g, 0.72 mmol, 87%). ^{1}H NMR (400 MHz, acetone-*d6*, 298 K): δ (ppm) = 8.59 (br s, 4H, NH); 8.15 (s, 4H, ArOH); 7.09 (app t, 4H, $^3J_{Hd\text{-}Ha} = {}^3J_{Hd\text{-}He}$ = 7.8 Hz, Hd); 6.59 (ddd, 4H, $^3J_{Ha\text{-}Hd}$ = 7.8 Hz; $^4J_{Ha\text{-}Hc}$ = 2.4 Hz; $^4J_{Ha\text{-}He}$ = 0.9 Hz, Ha); 6.52 (ddd, 4H, $^3J_{He\text{-}Hd}$ =7.8 Hz; $^4J_{He\text{-}Hc}$ = 1.6 Hz; $^4J_{He\text{-}Ha}$ = 0.9 Hz, He); 6.47 (dd, 4H, $^4J_{Hc\text{-}Ha}$ = 2.4 Hz; $^4J_{Hc\text{-}He}$ = 1.6 Hz, Hc); 5.98 (d, 8H, $^4J_{Hβ\text{-}NH}$ = 2.8 Hz, Hβ); 3.54 (t, 8H, $^3J_{Hk\text{-}Hj}$ = 6.6 Hz, Hk); 2.40-2.31 (m, 8H, Hh); 1.71 (app quin, 8H, $^3J_{Hj\text{-}Hk} \approx {}^3J_{Hj\text{-}Hi}$ = 6.9 Hz, Hj); 1.34-1.20 (m,8H, Hi). ^{13}C{^{1}H}NMR (100.6 MHz, acetone-*d6*, 298 K): δ (ppm) = 157.4 (Cb), 148.8 (Cf), 137.9 (Cα), 129.8 (Cd), 121.6 (Ce), 116.9 (Cc), 114.5 (Ca), 105.6 (Cβ), 49.1 (Cg), 45.7 (Ck), 40.7 (Ch), 33.9 (Cj), 23.3 (Ci). HRMS (ESI-TOF): m/z Calcd for $C_{60}H_{63}Cl_4N_4O_4$ $[M-H]^-$ = 1043.3609; found = 1043.3579.

Method 2: Ketone **6** (2 g, 9.40 mmol), TBMACl (6.65g, 28.2 mmol) and pyrrole (0.65 ml, 9.40 mmol) were dissolved in 18.8 mL of CH_2Cl_2. Then, HCl (7.05 mL, 4M in dioxane, 28.2 mmol) was dropwise added to the reaction mixture under vigorous stirring, the reaction was capped and stirred at r.t. for 7h. Then, more CH_2Cl_2 (40 mL) was added and the mixture washed with $NaHCO_3$ (aq sat) (2 x 50 mL). The aqueous phase was extracted with CH_2Cl_2 (2 x 40 mL). The organic extracts were combined, dried (Na_2SO_4), filtered and concentrated under vacuum yielding a black solid. The product was purified by column chromatography on silica gel (DCM 100% to DCM:EtOAc 85:15). The fraction containing the target

compound was concentrated and recrystallized from CH_2Cl_2:Hexane (0.35g, 0.334 mmol, 14%).

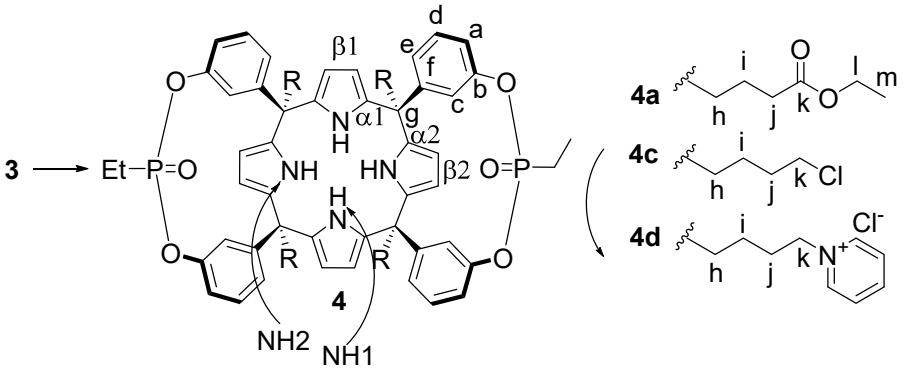

Synthesis of **4a**: Ethyl phosphonic dichloride (94 µL, 0.876 mmol) was slowly added to a stirred solution of **3a** (0.4g, 0.35 mmol) and anhydrous triethyl amine (980 µL, 7.03 mmol) in 20 mL of anhydrous THF at r.t. and under Ar atmosphere. The reaction mixture was left under the same conditions for 3h (a suspension is formed). Then, 20 mL of water and 10% aqueous HCl were added (until pH 1) and the organics were extracted (3 x 40 mL) with EtOAc. The EtOAc extracts were combined and washed (3 x 20 mL) with water. The EtOAc phase was separated, dried (Na_2SO_4), filtered and concentrated under reduced pressure. The three isomers were separated by column chromatography on SiO_2 (DCM:EtOAc 9:1 to 1:1) (to re cover the ii isomer pure EtOAc was passed through the column. **4a$_{oo}$** (79.2 mg, 17%), **4a$_{io}$** (76.8 mg, 17%), **4a$_{ii}$** (16.9 mg, < 4%).

4a$_{io}$: ^{1}H NMR (400 MHz, $CDCl_3$, 298 K): δ (ppm) = 8.46 (br s, 1H, NH2); 8.24 (br s, 2H, NH1); 7.72 (br s, 1H, NH2); 7.25 (app t, 2H, $^3J_{Hd\text{-}Ha} = {}^3J_{Hd\text{-}He}$ = 7.9 Hz, Hd); 7.17 (d, 2H, $^3J_{He\text{-}Hd}$ = 7.9 Hz, He); 7.13 (app t, 2H, $^3J_{Hd\text{-}Ha} = {}^3J_{Hd\text{-}He}$ = 7.9 Hz, Hd); 7.08 (d, 2H, $^3J_{He\text{-}Hd}$ = 7.9 Hz, He); 6.99 (br s, 2H, Hc); 6.96 (br s, 2H, Hc); 6.90 (d, 2H, $^3J_{Ha\text{-}Hd}$ = 7.9 Hz, Ha), 6.87 (d, 2H, $^3J_{Ha\text{-}Hd}$ = 7.9 Hz, Ha); 6.02 (d, 2H, $^4J_{H\beta\text{-}NH2}$ = 2.6 Hz, Hβ2); 6.00 (d, 2H, $^4J_{H\beta\text{-}NH2}$ = 2.6 Hz, Hβ2); 5.75 (app br t, 2H, $^3J_{H\beta\text{-}H\beta'} = {}^4J_{H\beta\text{-}NH1}$ = 2.7 Hz, Hβ1); 5.65 (app br t, 2H, $^3J_{H\beta\text{-}H\beta'} = {}^4J_{H\beta\text{-}NH1}$ = 2.7 Hz, Hβ1); 4.14-4.06 (m, 8H, Hl); 2.54-2.28 (m, 8H, Hh), 2.26 (app t, 8H, $^3J_{Hj\text{-}Hi}$ = 7.0 Hz, Hj); 2.20-2.04 (m, 4H, $POCH_2$); 1.66-1.47 (m, 8H, Hi); 1.46-1.32 (m, 6H, $POCH_3$), 1.23 (app t, 6H, $^3J_{Hm\text{-}Hl}$ = 7.1 Hz, Hm); 1.22 (app t, 6H, $^3J_{Hm\text{-}Hl}$ = 7.2 Hz, Hm); $^{13}C\{^1H\}$NMR (100.6 MHz, $CDCl_3$, 298 K): δ (ppm) = 173.50 (Ck); 173.48 (Ck); 150.77 (d, $^2J_{Cb\text{-}P}$ = 10.5 Hz, Cb); 149.84 (d, $^2J_{Cb\text{-}P}$ = 10.5 Hz, Cb); 147.65 (Cf); 147.39 (Cf); 136.62 (Cα); 136.24 (Cα);

136.08 (Cα); 135.47 (Cα); 128.91 (Cd); 128.4 (Cd); 124.82 (Ce); 124.08 (Ce); 121.33 (Cc); 121.01 (Cc); 118.93 (Ca); 118.16 (Ca); 107.67 (Cβ1); 107.37 (Cβ1); 105.49 (Cβ2); 105.33 (Cβ2); 60.24(Cl); 48.82 (Cg); 48.76 (Cg); 37.74 (Ch); 37.59 (Ch); 34.00 (Cj); 20.53 (d, $^{1}J_{CCH2PO-P}$ = 150.0 Hz, CCH2PO); 20.58 (d, $^{1}J_{CCH2PO-P}$ = 149.1 Hz, CCH2PO); 20.34 (Ci); 20.26 (Ci); 14.26 (Cm); 6.43 (CCH3PO); 6.36 (CCH3PO). $^{31}P\{^{1}H\}$NMR (162.0 MHz, $CDCl_3$, 298K): δ (ppm) = 31.1, 28.9. HRMS (ESI-TOF): m/z Calcd for $C_{72}H_{82}N_4NaO_{14}P_2$ $[M+Na]^+$ = 1311.5195; found = 1311.5175.

4a$_{oo}$: ^{1}H NMR (400 MHz, $CDCl_3$, 298 K): δ (ppm) = 8.41 (br s, 2H, NH1); 7.31 (br d, 4H, $^{3}J_{He-Hd}$ = 7.9 Hz, He); 7.15 (app t, 4H, $^{3}J_{Hd-Ha}$ = $^{3}J_{Hd-He}$ = 7.9 Hz, Hd); 7.09 (br s, 6H, Ha & NH2); 6.83 (br d, 4H, $^{3}J_{Ha-Hd}$ = 7.9 Hz, Ha); 6.21 (d, 4H, $^{4}J_{β2-NH2}$ = 2.5 Hz, β2); 5.41 (d, 4H, $^{4}J_{β1-NH1}$ = 2.3 Hz, β1); 4.16-4.04 (m, 8H, Hl); 2.53-2.43 (m, 4H, Hh), 2.33-2.20 (m, 12H, Hh & Hj); 2.07 (dq, 4H, $^{2}J_{HCH2PO-P}$ = 19.3 Hz, $^{3}J_{HCH2PO-HCH3PO}$ = 7.7 Hz, $POCH_2$); 1.82-1.62 (m, 8H, Hi); 1.33 (dt, 6H, $^{3}J_{HCH3PO-P}$ = 21.7 Hz, $^{3}J_{HCH3PO-HCH2PO}$ = 7.7 Hz, $POCH_3$), 1.23 (app t, 12H, $^{3}J_{Hm-Hl}$ = 7.2 Hz, Hm); $^{13}C\{^{1}H\}$NMR (100.6 MHz, $CDCl_3$, 298 K): δ (ppm) = 173.84 (Ck); 151.76 (d, $^{2}J_{Cb-P}$ = 10.5 Hz, Cb); 147.78 (Cf); 136.16 (Cα2); 135.63 (Cα1); 127.95 (Cd); 125.35 (Ce); 120.61 (Cc); 117.61 (d, $^{3}J_{Ca-P}$ = 7.7 Hz, Ca); 108.02 (Cβ1); 105.54 (Cβ2); 60.40(Cl); 49.47 (Cg); 37.56 (Ch); 33.93 (Cj); 20.73 (d, $^{1}J_{CCH2PO-P}$ = 150.9 Hz, CCH2PO); 20.43 (Ci); 14.38 (Cm); 6.52 ($^{2}J_{CCH3PO-P}$ = 7.4 Hz, CCH3PO); $^{31}P\{^{1}H\}$NMR (162.0 MHz, $CDCl_3$, 298K): δ (ppm) = 29.05.HRMS (ESI-TOF): m/z Calcd for $C_{72}H_{82}N_4NaO_{14}P_2$ $[M+Na]^+$ =1311.5195; found = 1311.5195.

4a$_{ii}$: ^{1}H NMR (400 MHz, $CDCl_3$, 298 K): δ (ppm) = 8.62 (br s, 2H, NH); 8.31 (br s, 2H, NH); 7.25 (app t; 4H, $^{3}J_{Hd-Ha}$ = $^{3}J_{Hd-He}$ = 7.9 Hz, Hd); 7.06 (br d, 4H, ^{3}J = 7.9 Hz); 6.98 (br s, 4H, Hc); 6.90 (br s, 4H, ^{3}J = 7.9 Hz); 5.98 (d, 4H, $^{4}J_{Hβ-NH}$ = 2.6 Hz, β); 5.87 (d, 4H, $^{4}J_{Hβ-NH}$ = 2.3 Hz, β); 4.12 (q, 8H, $^{3}J_{Hl-Hm}$ = 7.4 Hz, Hl); 2.52 (br t, 4H, $^{3}J_{Hh-Hi}$ = 13Hz, Hh), 2.32-2.0 (m, 12H, Hh and Hj), 2.13 (dq, 4H, $^{2}J_{HCH2PO-P}$ = 19.0 Hz, $^{3}J_{HCH2PO-HCH3PO}$ = 7.6 Hz, CH2PO); 1.64-1.50 (m, 4H, Hi); 1.41 (dt, $^{3}J_{HCH3PO-P}$ = 22.0 Hz, $^{3}J_{HCH3PO-HCH2PO}$ = 7.6 Hz, CH3PO), 1.3-1.22 (m, 4H, Hi); 1.26 (t, 9H, $^{3}J_{Hm-Hl}$ = 7.0 Hz, Hm). $^{31}P\{^{1}H\}$NMR (162.0 MHz, $CDCl_3$, 298K): δ (ppm) = 30.57.

Synthesis of **4c**: Ethyl phosphonic dichloride (51 µL, 0.478 mmol) was slowly added to a stirred solution of **3c** (0.2g, 0.191 mmol) and anhydrous triethyl amine (530 µL, 3.8 mmol) in 11 mL of anhydrous THF at r.t. and under Ar atmosphere. The reaction mixture was left under the same conditions for 3h and 30minutes (a suspension is formed). Then, 15 mL of water and

10% aqueous HCl were added (until pH 1) and the organics were extracted (3 x 30 mL) with EtOAc. The EtOAc extracts were combined and washed (3 x 20 mL) with water. The EtOAc phase was separated, dried (Na_2SO_4), filtered and concentrated under reduced pressure. The three isomers were separated by two columns chromatography on SiO_2; column 1 DCM:THF 9:1 two fractions were collected, the first fraction is a mixture of **4c$_{oo}$** and **4c$_{io}$**, the second fraction is impure **4c$_{ii}$** which was purify by crystallization with MeOH. The first fraction was columned using 6g of SiO_2 and DCM:EtOAc 95:5 until the first product completely eluted (**4c$_{io}$**) then the polarity was increased at 9:1 to eluted second product (**4c$_{oo}$**). The products were isolated as white powders **4c$_{ii}$** (9 mg, 7.53 µmol, 4%), **4c$_{io}$** (47.9 mg, 40 µmol, 21%), **4c$_{oo}$** (35.9 mg, 30 µmol, 16%).

4c$_{io}$: ^{1}H NMR (400 MHz, $CDCl_3$, 298 K): δ (ppm) = 8.63 (br s, 1H, NH2); 8.14 (br s, 2H, NH1); 7.99 (br s, 1H, NH2); 7.20 (app t, 2H, $^3J_{Hd\text{-}Ha}$ = $^3J_{Hd\text{-}He}$ = 8.1 Hz, Hd); 7.13-7.06 (m, 4H); 7.03-6.96 (m, 4H); 6.94-6.88 (m, 4H); 6.86-6.81 (br d, 2H, $^3J_{Ha\text{-}Hd}$ = 7.9 Hz, Ha); 5.99 (d, 2H, $^4J_{Hβ2\text{-}NH2}$ = 2.6 Hz, β2); 5.97 (d, 2H, $^4J_{Hβ2\text{-}NH2}$ = 2.6 Hz, Hβ2); 5.8 (app br t, 2H, $^3J_{Hβ\text{-}Hβ'}$ = $^4J_{Hβ\text{-}NH1}$ = 2.8 Hz, Hβ1); 5.79 (app br t, 2H, Hβ1); 3.48-3.42 (m, 8H, Hk); 2.51-2.24 (m, 8H, Hh); 2.20-2.04 (m, 4H, $POCH_2$); 1.79-1.66 (m, 8H, Hj); 1.47-1.01 (m, 14H, $POCH_3$ and Hi). $^{13}C\{^1H\}$NMR (100.6 MHz, $CDCl_3$, 298 K): δ (ppm) = 151.14 (d, $^2J_{Cb\text{-}P}$ = 10.0 Hz, Cb); 149.98 (Cf); 149.88 (Cf); 148.05 (d, $^2J_{Cb\text{-}P}$ = 14.5 Hz, Cb); 136.84 (Cα); 136.48 (Cα); 136.12 (Cα); 135.71 (Cα); 129.02; 128.75; 124.72; 123.95; 121.61; 120.96; 119.56; 118.29; 107.02 (Cβ1); 106.83 (Cβ1); 105.89 (Cβ2); 105.69 (Cβ2); 48.71(Cg); 48.69 (Cg); 44.85 (Ck); 44.80 (Ck); 38.75 (Ch); 38.57 (Ch); 33.13 (Cj); 33.10 (Cj); 22.56 (Hi); 22.49 (Hi); 20.62 (d, $^1J_{CCH2PO\text{-}P}$ = 148.9 Hz, CCH2PO); 20.33 (d, $^1J_{CCH2PO\text{-}P}$ = 148.36 Hz, CCH2PO); 6.49 (d, $^2J_{CCH2PO\text{-}P}$ = 5.2 Hz, CCH3PO); 6.42 (d, $^2J_{CCH2PO\text{-}P}$ = 5.2 Hz, CCH3PO). $^{31}P\{^1H\}$NMR (162.0 MHz, $CDCl_3$, 298K): δ (ppm) = 31.6; 29.1. HRMS (ESI-TOF): m/z Calcd for $C_{64}H_{71}Cl_4N_4O_6P_2$ $[M+H]^+$ = 1193.3597; found = 1193.3599.

4c$_{oo}$: ^{1}H NMR (500 MHz, $CDCl_3$, 298 K): δ (ppm) = 7.67 (br s, 2H, NH); 7.25-7.20 (m, 6H, NH and He); 7.17 (app t; 4H, $^3J_{Hd\text{-}Ha}$ = $^3J_{Hd\text{-}He}$ = 8.0 Hz, Hd); 7.09 (br s, 4H, Hc); 6.93 (d, 4H, $^3J_{Ha\text{-}Hd}$ = 8.0 Hz, Ha); 6.15 (d, 4H, $^4J_{Hβ\text{-}NH}$ = 2.8 Hz, β2); 5.64 (d, 4H, $^4J_{Hβ\text{-}NH}$ = 2.1 Hz, β1); 3.55-3.44 (m, 8H, Hk); 3.38-2.23 (m, 8H, Hh), 2.09 (dq, 4H, $^2J_{HCH2PO\text{-}P}$ = 19.0 Hz, $^3J_{HCH2PO\text{-}HCH3PO}$ = 7.6 Hz, CH2PO); 1.81-1.68 (m, 8H, Hj); 1.47-1.40 (m, 8H, Hi); 1.36 (dt, 6H, $^3J_{HCH3PO\text{-}P}$ = 21.5 Hz, $^3J_{HCH3PO\text{-}HCH2PO}$ = 7.7 Hz, CH3PO). $^{13}C\{^1H\}$NMR (125.8 MHz, $CDCl_3$, 298 K): δ (ppm) = 151.38 (d, $^2J_{Cb\text{-}P}$ = 11.2 Hz, Cb); 147.09 (Cf); 136.15 (Cα2); 134.68 (Cα1);

128.73 (Cd); 124.31 (Ce); 120.73 (d; $^{3}J_{Cc\text{-}P}$ = 3.2 Hz, Cc); 118.42 (d, $^{3}J_{Ca\text{-}P}$ = 6.0 Hz, Ca); 107.80 (Cβ1); 105.84 (Cβ2); 49.10 (Cg); 44.87 (Ck); 38.97 (Ch); 33.01 (Cj); 22.66 (Ci); 20.50 (d, $^{1}J_{CCH2PO\text{-}P}$ = 151.2 Hz, CCH2PO); 6.45 (d, $^{2}J_{CCH3PO\text{-}P}$ = 6.5 Hz, CCH3PO). $^{31}P\{^{1}H\}$NMR (162.0 MHz, $CDCl_3$, 298K): δ (ppm) = 29.8. HRMS (ESI-TOF): m/z Calcd for $C_{64}H_{70}Cl_4N_4Na_2O_6P_2$ $[M+Na_2]^{2+}$ = 619.1655; found = 619.1678.

4c$_{ii}$: ^{1}H NMR (400 MHz, $CDCl_3$, 298 K): δ (ppm) = 8.69 (br s, 2H, NH); 8.22 (br s, 2H, NH); 7.24 (app t, 4H, $^{3}J_{Hd\text{-}Ha}$ = $^{3}J_{Hd\text{-}He}$ = 7.7 Hz, Hd); 7.05-7.95 (m; 8H, Hc and He); 6.92 (d, 4H, $^{3}J_{Ha\text{-}Hd}$ = 7.7 Hz, Ha); 5.96 (br s, 4H, β2); 5.89 (br s, 4H, β1); 3.46 (app t, 8H, $^{3}J_{Hk\text{-}Hj}$ = 6.7 Hz, Hk); 2.51 (br t, 4H, Hh), 2.26 (br t, 4H, Hh); 2.21-2.08 (m, 4H, CH2PO); 1.83-1.66 (m, 8H, Hj); 1.48-1.30 (m, 10H, Hi and CH3PO); 1.19-1.02 (m, 4H, Hi). $^{13}C\{^{1}H\}$NMR (100.6 MHz, $CDCl_3$, 298 K): δ (ppm) = 149.83 (d, $^{2}J_{Cb\text{-}P}$ = 10.4 Hz, Cb); 147.65 (Cf); 136.41 (Cα2); 135.99 (Cα1); 129.09 (Cd); 124.11 (Ce); 121.33 (Cc); 119.05 (Ca); 106.93 (Cβ1); 105.39 (Cβ2); 48.58 (Cg); 44.66 (Ck); 38.31 (Ch); 33.06 (Cj); 22.41 (Ci); 20.55 (d, $^{1}J_{CCH2PO\text{-}P}$ = 147.5 Hz, CCH2PO); 7.15 (d, $^{2}J_{CCH3PO\text{-}P}$ = 7.5 Hz, CCH3PO).

Synthesis of **4d$_{io}$**: **4c$_{io}$** (36.6 mg, 31 μmol) were dissolved in 5.2 mL of anhydrous pyridine under Ar atmosphere. The mixture was heated under stirring at 110 ºC overnight. Then, the reaction was cooled at r.t. and the pyridine was removed under reduced pressure. The resulting solid was suspended in DCM filtered and washed with acetone (2mL) and hexane (2mL). **4d$_{io}$** was isolated as a pale yellow solid (39 mg, 26μmol, 84%). ^{1}H NMR (400 MHz, D_2O, 298 K): δ (ppm) = 8.57-8.48 (m, 8H, Py^+); 8.42-8.35 (m, 4H, Py^+); 7.89-7.82 (m, 8H, Py^+); 7.34-7.23 (m, 4H), 7.02-6.95 (m, 4H); 6.93-6.81 (m, 4H); 6.73 (s, 2H); 6.63 (br s, 2H); 5.90 (s, 2H, Hβ); 5.82 (s, 2H, Hβ); 5.79 (br s, 2H, Hβ); 5.76 (br s, 2H, Hβ); 4.46-4.33 (m, 8H, Hk); 2.46-2.33 (m, 4H, Hh); 2.33-2.11 (m, 8H, Hh and CH2PO); 1.88-1.62 (m, 8H, Hj); 1.39-1.24 (m, 6H, CH3PO); 1.06-0.84 (m, 8H, Hi). HRMS (ESI-TOF): m/z Calcd for $C_{84}H_{90}ClN_8O_6P_2$ $[M-3Cl]^{3+}$ = 467.8710; found = 467.8710.

Synthesis of **4d$_{oo}$**: **4c$_{oo}$** (20 mg, 16 μmol) were dissolved in 2.8 mL of anhydrous pyridine under Ar atmosphere. The mixture was heated under stirring at 110 ºC overnight. Then, the reaction was cooled at r.t. and the pyridine was removed under reduced pressure. The resulting solid was suspended in DCM filtered and washed with acetone (2mL) and hexane (2mL). **4d$_{oo}$** was isolated as a pale yellow solid (20.5 mg, 14μmol, 81%). ^{1}H NMR (400 MHz, D_2O, 298 K): δ (ppm) = 8.61 (br d, 8H, ^{3}J = 5.0 Hz, Py^+); 8.46 (br t, 4H, ^{3}J = 8Hz, Py^+); 7.92 (app t, 8H, ^{3}J = 6.8Hz, Py^+); 7.37 (br t, 4H, Hd); 7.07 (br d, ^{3}J = 7.0 Hz, 2H); 6.95 (br d, 4H); 6.82 (s, 4H,

Hc); 5.91 (br s, 4H, Hβ); 5.82 (br s, 4H, Hβ); 4.47 (br t, 8H, Hk); 2.51-2.38 (m, 4H, Hh); 2.37-2.19 (m, 8H, Hh and CH2PO); 1.99-1.72 (m, 8H, Hj); 1.37 (dt, 6H, $^{3}J_{CH3\text{-}P}$ = 22.6 Hz, $^{3}J_{CH2\text{-}CH3}$ = 7.5 Hz, CH3PO); 1.16-0.90 (m, 8H, Hi). HRMS (ESI-TOF): m/z Calcd for $C_{84}H_{90}ClN_8O_6P_2$ $[M\text{-}3Cl]^{3+}$ = 467.8710; found = 467.8708.

Synthesis of ketone **6**:

Step1: A dried 250 mL round bottom flak equipped with a stir bar and an addition funnel, was charged with Mg turning (1.73g, 70.9 mmol) suspended in 5 mL of anhydrous THF under Ar atmosphere. A solution of 1-bromo-4-chloro butane (8.17 mL, 70.9 mmol) in 55 mL of anhydrous THF was slowly added with the addition funnel; first 2-3 mL of the solution was added without stirring, once the reaction started (the temperature increases), the mixture was stirred and the rest of the solution was dropwise added (40 minutes) taking care that the temperature was always below the 50 ºC (aprox) using a water bath if it is necessary. After the addition, 10 mL more of THF were used to the recover the rest of bromo-alkane that remained in the addition funnel and the mixture was stirred 20 minutes at r.t. The freshly prepared Grignard reagent was dropwise added via cannula (40 min) over a solution of 3-methoxybenzoil chloride (10 mL, 70.9 mmol) and Fe (III) Acetylacetonate (0.75g, 2.13 mmol) in 60 mL of anhydrous THF at -74 ºC (dry ice/acetone). After the addition, the reaction was stirred at the same temperature for 30 minutes. After that time, was left to slowly rich r.t. and was stirred overnight. Next day, the reaction was carefully quenched with water (300ml) and extracted with DCM (3 x 200mL); the DCM extracts were combined dried (Na_2SO_4), filtered and concentrated under reduced pressure. The crude was passed through a plot of SiO_2 using Et_2O as eluent. After evaporation of the solvent 16.1 g of a red oil was obtained which was used in the next step without additional purification.

Step2: The red oil obtained in the step 1, was dissolved in 95 mL of glacial acetic acid and 95 mL of HBr (48% aq solution) and the reaction was refluxed for 3h and 30 minutes. After that, the reaction was cooled down to r.t. and the crude was extracted with DCM (3 x 200 mL). The DCM extracts were combined, dried (Na_2SO_4), filtered and concentrated under reduced pressure yielding 12.08 g of a brown solid which was used in the next step without any additional purification (in this step the alkyl-chloride group is changed by Br).

Step3: The 12.08 g obtained in step 2 and MTBACl (3.32g, 14.04 mmol) were dissolved in 372 mL of 1,2-dichloroethane (DCE) and the reaction was refluxed overnight. Next day, the

reaction was cooled down to r.t. and 300 mL of water were added, the DCE phase was separated and the aqueous phase was twice extracted with DCM (2 x 100mL). The organics extracts were combined dried (Na_2SO_4), filtered and concentrated under reduced pressure yielding a black caramel. Et_2O (200 mL aprox) were added and the mixture was sonicated for 30 minutes. A black solid precipitated which was filtered. The filtrate was concentrated under reduced pressure yielding pure **6** as a light yellow solid (7.48g, 35.2 mmol, 50% calculated from 3-methoxybenzoyl chloride). ^{1}H NMR (400 MHz, $CDCl_3$, 298 K): δ (ppm) = 7.53-7.49 (m, 2H); 7.34 (app t, 1H, ^3J = 8.0 Hz); 7.08 (ddd, 1H, ^3J = 8.1, ^4J = 2.5 and 1.0 Hz); 5.99 (br s, 1H); 3.58 (t, 2H, ^3J = 6.3 Hz); 3.00 (t, 2H, ^3J = 6.9 Hz); 1.94-1.81 (m, 4H). ^{13}C{^{1}H}NMR (100.6 MHz, $CDCl_3$, 298 K): δ (ppm) = 200.2, 156.3, 138.2, 130.0, 120.7, 120.6, 114.5, 44.7, 37.8, 32.0, 21.5. HRMS (ESI-TOF): m/z Calcd for $C_{11}H_{12}ClO_2$ $[M-H]^-$ = 211.0531; found = 211.0537.

4.4.3 Figures

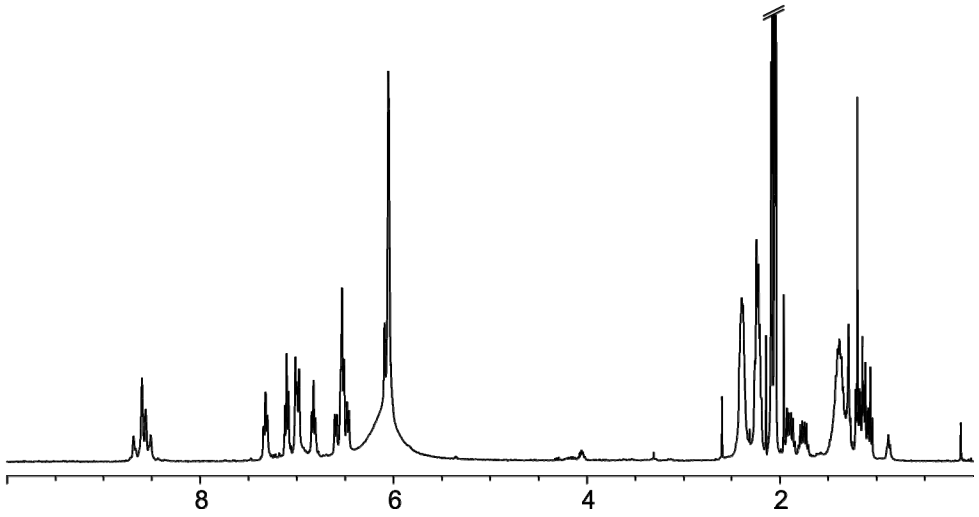

Figure 4. 7: ^{1}H NMR (acetone d6) spectrum of the crude reaction mixture after treatment of **4a$_{oo}$** with NaOH.

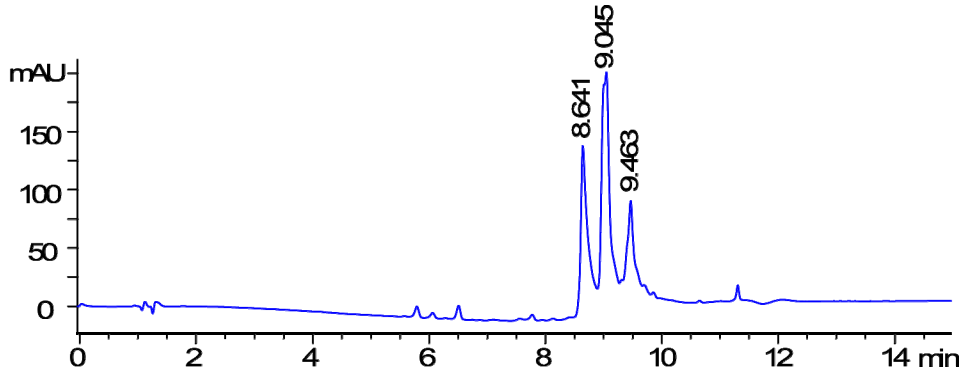

Figure 4. 8: Chromatogram of the crude reaction mixture after treatment of **4a$_{oo}$** with NaOH. PFP 100 x 4.6 mm, 5µm, H_2O:MeOH:HCOOH 90:10:0.1 to 0:100:0.1 in 10 minutes.

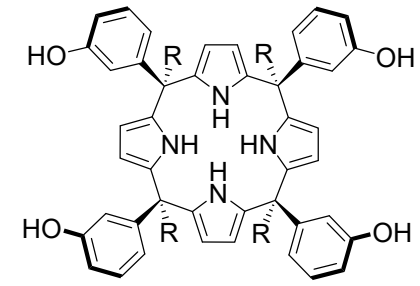

R= $(CH_2)_3CO_2H$

found: 1029.3 (M+H)
calculated (M): 1028.4

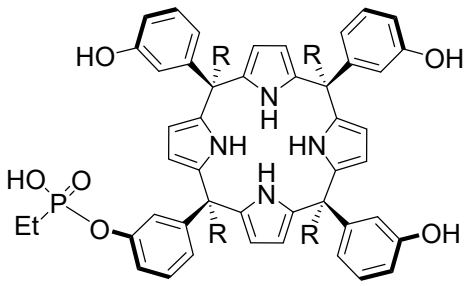

R= $(CH_2)_3CO_2H$

found: 1121.3 (M+H)
calculated (M): 1120.4

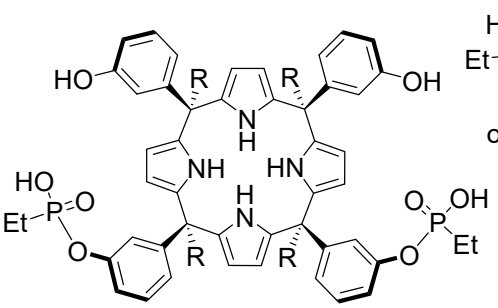

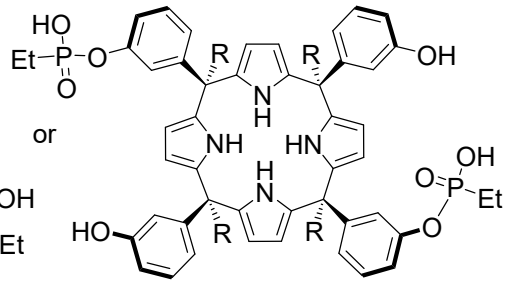

R= $(CH_2)_3CO_2H$

found: 1213.3 (M+H)
calculated (M): 1212.4

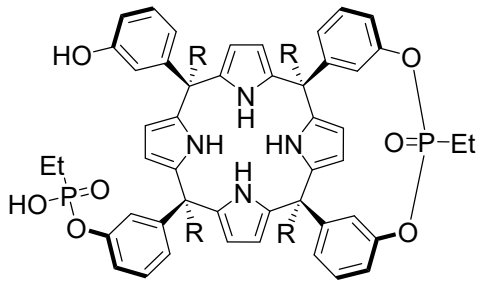

Found: 1239.2 $(M+HCOO)^-$
Calculated (M):1194.42

Figure 4. 9: Line-drawing of the proposed structures for some ions found in chromatogram Figure 4. 8.

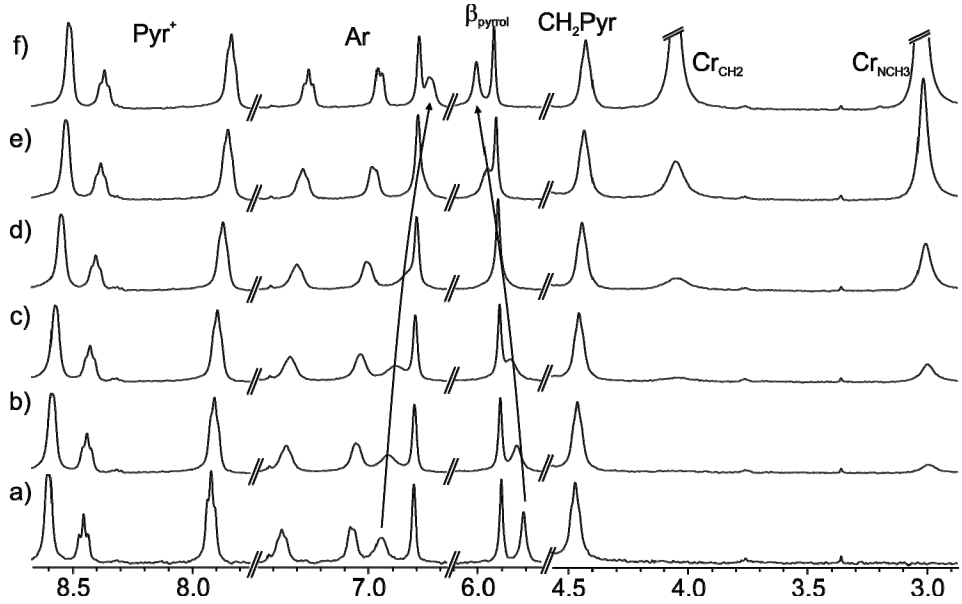

Figure 4. 10: Selected regions of the ^{1}H NMR spectra recorded during the titration of **4d$_{oo}$** in D_2O with incremental amounts of **Cr**. a) 0 eq.; b) 0.5 eq.; c) 1.0 eq.; d) 2.3 eq.; e) 4.6 eq.; f) 10.5 eq.

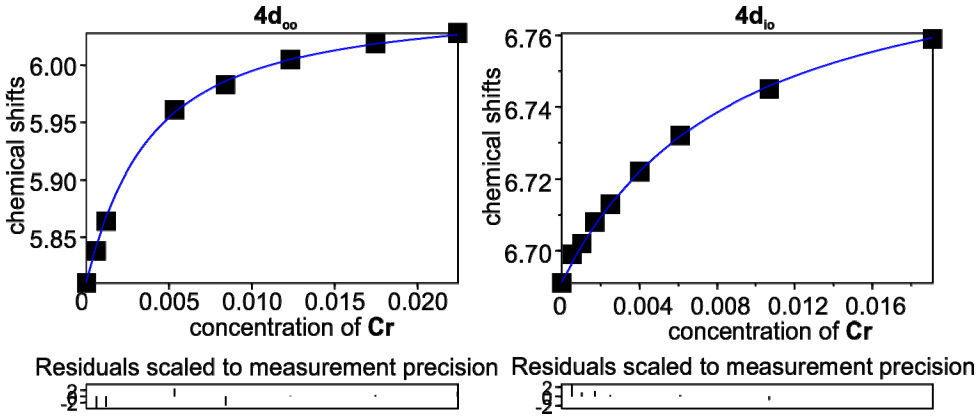

Figure 4. 11: Fit of the chemical shift changes, experienced by the receptor ^{1}H of **4d$_{io}$** and **4d$_{oo}$** during the titration with **Cr**, using a 1:1 binding model (blue line) implemented in the HypNMR2008 software.

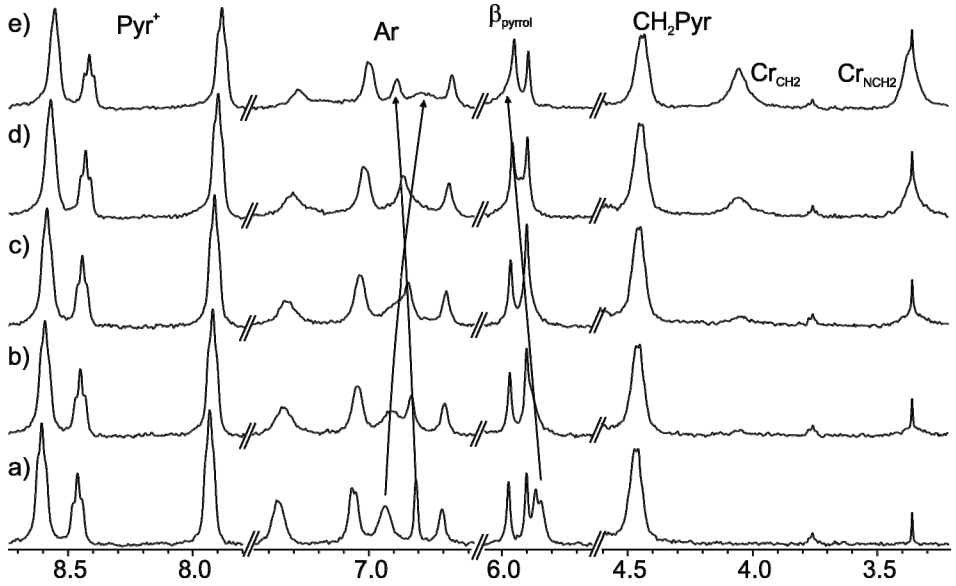

Figure 4. 12: Selected regions of the ^{1}H NMR spectra recorded during the titration of **4d$_{io}$** in D_2O with incremental amounts of **HxCr**. a) 0 eq.; b) 0.6 eq.; c) 1.0 eq.; d) 2.0 eq.; e) 3.6 eq.

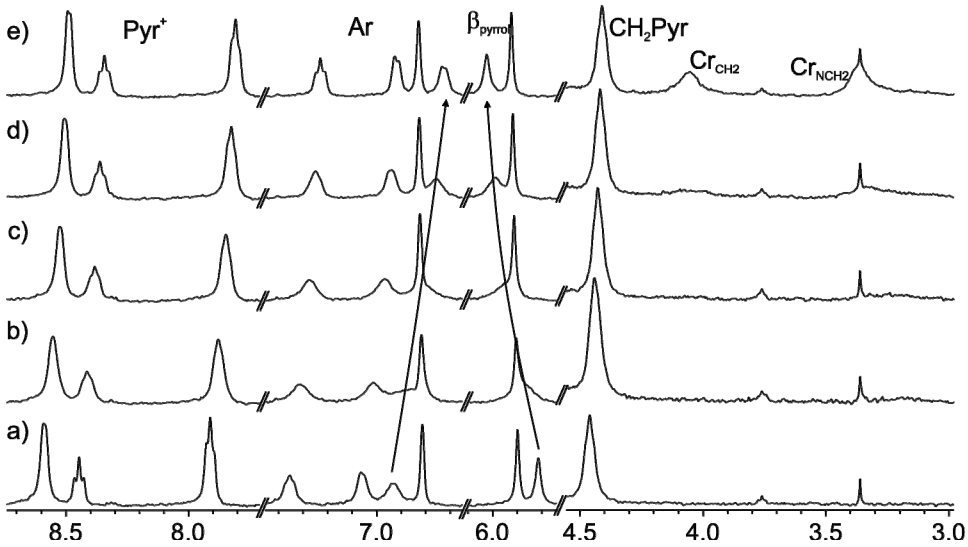

Figure 4. 13: Selected regions of the ^{1}H NMR spectra recorded during the titration of **4d$_{oo}$** in D_2O with incremental amounts of **HxCr**. a) 0 eq.; b) 0.4 eq.; c) 1.0 eq.; d) 1.7 eq.; e) 3.2 eq.

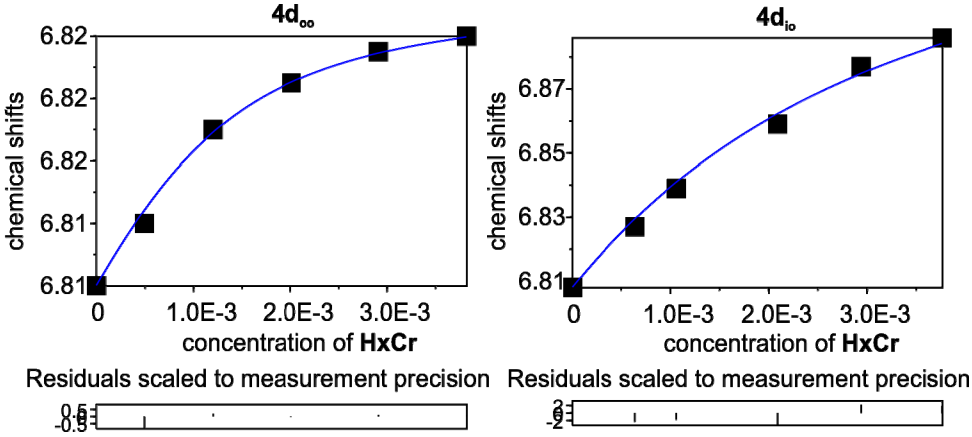

Figure 4. 14: Fit of the chemical shift changes, experienced by the receptor ^{1}H of **4d$_{io}$** and **4d$_{oo}$** during the titration with **HxCr**, using a 1:1 binding model (blue line) implemented in the HypNMR2008 software.

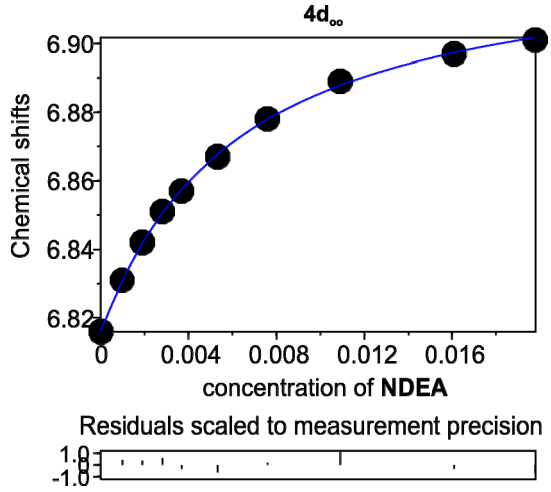

Figure 4. 15: Fit of the chemical shift changes, experienced by the receptor ^{1}H of **4d$_{oo}$** during the titration with **NDEA**, using a 1:1 binding model (blue line) implemented in the HypNMR2008 software

4.5 References and notes

[1] Biros, S. M.; Rebek, J. J. *Chem. Soc. Rev.* **2007**, *36*, 93-104.
[2] Shi, Q.; Mower, M. P.; Blackmond, D. G.; Rebek, J. *Proc. Natl. Acad. Sci.* **2016**, *113*, 9199-9203.
[3] Mosca, S.; Yu, Y.; Gavette, J. V.; Zhang, K.-D.; Rebek, J. *J. Am. Chem. Soc.* **2015**, *137*, 14582-14585.
[4] Masseroni, D.; Mosca, S.; Mower, M. P.; Blackmond, D. G.; Rebek, J. *Angew. Chem. Int. Ed.* **2016**, *55*, 8290-8293.
[5] Galan, A.; Ballester, P. *Chem. Soc. Rev.* **2016**, *45*, 1720-1737.
[6] Hooley, R. J.; Restorp, P.; Iwasawa, T.; Rebek, J. *J. Am. Chem. Soc.* **2007**, *129*, 15639-15643.
[7] Hooley, R. J.; Iwasawa, T.; Rebek, J. *J. Am. Chem. Soc.* **2007**, *129*, 15330-15339.
[8] Parthasarathy, A.; Ramamurthy, V. *J. Photochem. Photobiol., A* **2016**, *317*, 132-139.
[9] Ramamurthy, V. *Acc. Chem. Res.* **2015**, *48*, 2904-2917.
[10] Parthasarathy, A.; Samanta, S. R.; Ramamurthy, V. *Res. Chem. Intermed.* **2013**, *39*, 73-87.
[11] Gupta, S.; Choudhury, R.; Krois, D.; Wagner, G.; Brinker, U. H.; Ramamurthy, V. *Org. Lett.* **2011**, *13*, 6074-6077.
[12] Kulasekharan, R.; Choudhury, R.; Prabhakar, R.; Ramamurthy, V. *Chem. Commun.* **2011**, *47*, 2841-2843.
[13] Kaanumalle, L. S.; Gibb, C. L. D.; Gibb, B. C.; Ramamurthy, V. *Org. Biomol. Chem.* **2007**, *5*, 236-238.
[14] Podkoscielny, D.; Hooley, R. J.; Rebek, J.; Kaifer, A. E. *Org. Lett.* **2008**, *10*, 2865-2868.
[15] Dalcanale, E.; Costantini, G.; Soncini, P. *J. Inclusion Phenom.* **1992**, *13*, 87-92.
[16] Biros, S. M.; Ullrich, E. C.; Hof, F.; Trembleau, L.; Rebek, J. *J. Am. Chem. Soc.* **2004**, *126*, 2870-2876.
[17] Butterfield, S. M.; Rebek, J. *J. Am. Chem. Soc.* **2006**, *128*, 15366-15367.
[18] Hooley, R. J.; Van Anda, H. J.; Rebek, J. *J. Am. Chem. Soc.* **2007**, *129*, 13464-13473.
[19] Lledo, A.; Rebek, J. *Chem. Commun.* **2010**, *46*, 8630-8632.
[20] Zhang, K.-D.; Ajami, D.; Gavette, J. V.; Rebek, J. *Chem. Commun.* **2014**, *50*, 4895-4897.
[21] Masseroni, D.; Biavardi, E.; Genovese, D.; Rampazzo, E.; Prodi, L.; Dalcanale, E. *Chem. Commun.* **2015**, *51*, 12799-12802.
[22] Mosca, S.; Ajami, D.; Rebek, J. *Proc. Natl. Acad. Sci.* **2015**, *112*, 11181-11186.
[23] Pinalli, R.; Brancatelli, G.; Pedrini, A.; Menozzi, D.; Hernández, D.; Ballester, P.; Geremia, S.; Dalcanale, E. *J. Am. Chem. Soc.* **2016**, *138*, 8569-8580.
[24] Ciardi, M.; Tancini, F.; Gil-Ramírez, G.; Escudero Adán, E. C.; Massera, C.; Dalcanale, E.; Ballester, P. *J. Am. Chem. Soc.* **2012**, *134*, 13121-13132.
[25] Ciardi, M.; Galán, A.; Ballester, P. *J. Am. Chem. Soc.* **2015**, *137*, 2047-2055.
[26] Guinovart, T.; Hernández-Alonso, D.; Adriaenssens, L.; Blondeau, P.; Martínez-Belmonte, M.; Rius, F. X.; Andrade, F. J.; Ballester, P. *Angew. Chem. Int. Ed.* **2016**, *55*, 2435-2440.
[27] Verdejo, B.; Gil-Ramírez, G.; Ballester, P. *J. Am. Chem. Soc.* **2009**, *131*, 3178-3179.
[28] Hernandez-Alonso, D.; Zankowski, S.; Adriaenssens, L.; Ballester, P. *Org. Biomol. Chem.* **2015**, *13*, 1022-1029.
[29] Ahn, D.-R.; Kim, T. W.; Hong, J.-I. *Tetrahedron Lett.* **1999**, *40*, 6045-6048.
[30] Park, S. J.; Hong, J.-I. *Tetrahedron Lett.* **2000**, *41*, 8311-8315.
[31] Wyss, D. F.; Arasappan, A.; Senior, M. M.; Wang, Y.-S.; Beyer, B. M.; Njoroge, F. G.; McCoy, M. A. *J. Med. Chem.* **2004**, *47*, 2486-2498.
[32] Díaz-Moscoso, A.; Hernández-Alonso, D.; Escobar, L.; Arroyave, F. A.; Ballester, P. *Org. Lett.* **2017**, *19*, 226-229.
[33] Dal Molin, M.; Gasparini, G.; Scrimin, P.; Rastrelli, F.; Prins, L. J. *Chem. Commun.* **2011**, *47*, 12476-12478.
[34] Perumal, S. K.; Pratt, R. F. *J. Org. Chem.* **2006**, *71*, 4778-4785.
[35] Zhang, K.-D.; Ajami, D.; Gavette, J. V.; Rebek, J. *J. Am. Chem. Soc.* **2014**, *136*, 5264-5266.
[36] Zhang, K.-D.; Ajami, D.; Rebek, J. *J. Am. Chem. Soc.* **2013**, *135*, 18064-18066.

[37] Winiwarter, S.; Bonham, N. M.; Ax, F.; Hallberg, A.; Lennernäs, H.; Karlén, A. *J. Med. Chem.* **1998**, *41*, 4939-4949.
[38] Loeppky, R. N. In *Nitrosamines and Related N-Nitroso Compounds*; American Chemical Society: 1994; Vol. 553, p 1-18.
[39] Nair, J.; Ohshima, H.; Nair, U. J.; Bartsch, H. *Crit. Rev. Toxicol.* **1996**, *26*, 149-161.
[40] Hoffmann, D.; Rivenson, A.; Wynder, E. L.; Hecht, S. S. In *Nitrosamines and Related N-Nitroso Compounds*; American Chemical Society: 1994; Vol. 553, p 267-278.
[41] Balbo, S.; James-Yi, S.; Johnson, C. S.; O'Sullivan, M. G.; Stepanov, I.; Wang, M.; Bandyopadhyay, D.; Kassie, F.; Carmella, S.; Upadhyaya, P.; Hecht, S. S. *Carcinogenesis* **2013**, *34*, 2178-2183.
[42] Loeppky, R. N.; Michejda, C. J. *Nitrosamines and Related N-Nitroso Compounds*; American Chemical Society, 1994; Vol. 553.
[43] Tricker, A. R.; Preussmann, R. *Mutat. Res., Genet. Toxicol. Environ. Mutagen.* **1991**, *259*, 277-289.
[44] Minami, T.; Esipenko, N. A.; Zhang, B.; Kozelkova, M. E.; Isaacs, L.; Nishiyabu, R.; Kubo, Y.; Anzenbacher, P. *J. Am. Chem. Soc.* **2012**, *134*, 20021-20024.
[45] Verna, L.; Whysner, J.; Williams, G. M. *Pharmacol. Ther.* **1996**, *71*, 57-81.
[46] The assignment was done by comparison with previously reported nitrosamines. Brown, H. W.; Hollis, D. P. *J. Mol. Spectrosc.* **1964**, *13*, 305-312.; Glidewell, S. M. *Spectrochim. Acta, Part A* **1977**, *33*, 361-368.

UNIVERSITAT ROVIRA I VIRGILI
CALIX[4]PYRROLE-BASED RECEPTORS FOR BIOLOGICALLY RELEVANT POLAR MOLECULES: FROM ORGANIC TO AQUEOUS MEDIA
Daniel Hernández Alonso

Chapter 5

A fluorescent monophosphonate calix[4]pyrrole biscavitand for creatinine sensing

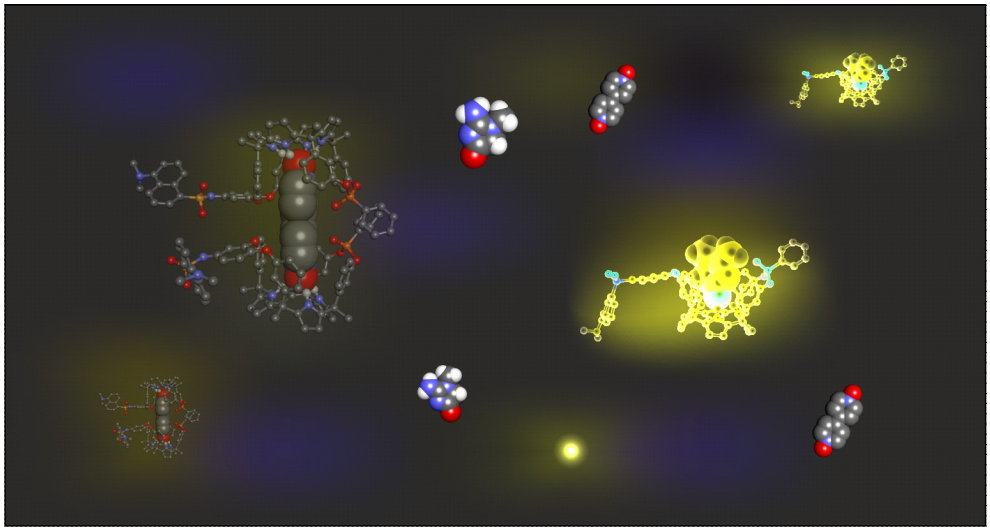

Unpublished results

UNIVERSITAT ROVIRA I VIRGILI
CALIX[4]PYRROLE-BASED RECEPTORS FOR BIOLOGICALLY RELEVANT POLAR MOLECULES: FROM ORGANIC TO AQUEOUS MEDIA
Daniel Hernández Alonso

5.1 Introduction

The detection of analytes of interest for human and environmental health (e.g. anions, cations, biologically relevant molecules) via fluorescent techniques has been a topic of interesting reviews. To achieve this goal different strategies have been designed.[1,2,3] A well-known strategy consist in the use of molecular chemosensors built by covalent connection of a binding unit specific for the analyte to a fluorescent tag through a spacer. Ideally, the establishment of non-covalent interactions between the analyte and the binding site of the molecular chemosensor will produce a conspicuous change in the emission properties of the covalently attached fluorescent tag (Figure 5. 1). The selection of the proper receptor able to selectively recognize the analyte at the desired concentrations (i.e. high binding constant), a fluorophore able to "feel" the presence of the analyte once is bound into the binding unit, or the spacer used to communicate the binding and signaling units are key points in the chemosensor design and must be carefully considered and evaluated. Therefore, the design of an efficient molecular chemosensor for a specific analyte is certainly challenging, especially when both the receptor and analyte are neutral species.

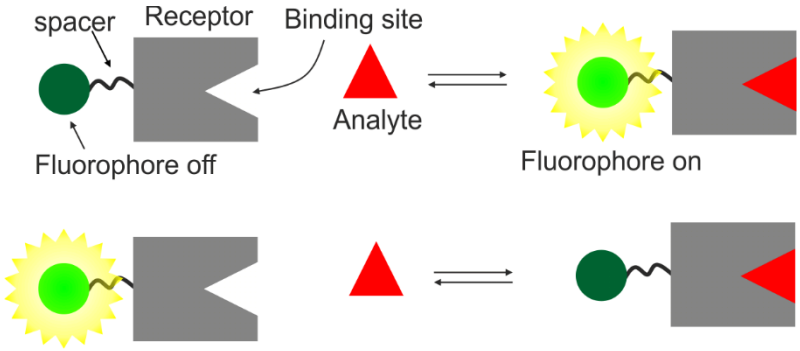

Figure 5. 1: Schematic representation of a fluorescent chemosensor in equilibria with an analyte. Top: The binding of the analyte produces an increase in the emission; bottom: the binding of the analyte produces a quenching of the emission.

Owing to the importance of creatinine detection from a biomedical point of view, several strategies for the sensing and quantification of creatinine using fluorescence spectroscopy and using synthetic receptors have been reported.[4,5,6,7,8]Among all of them, only the fluorescent receptors described by Minghua and Shikang;[8] and Tang[5] employ hydrogen bonds to complex creatinine Figure 5. 2.

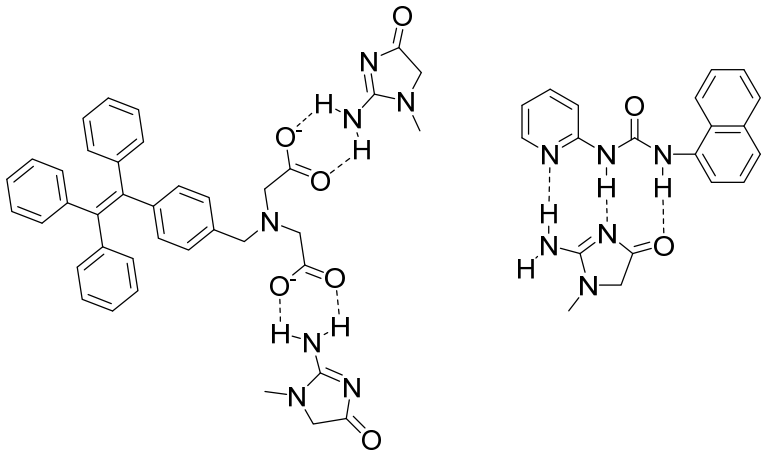

Figure 5. 2: Line drawing structure of the fluorescent receptor⊃creatinine complexes reported by Tang (left); Minghua and Shikang (right).

Calix[4]pyrrole scaffolds containing fluorescent groups covalently attached to their structure have shown to be excellent molecular chemosensors for the recognition of anions (mainly fluoride)[9,10,11,12,13,14,15,16,17,18] or cations.[19,20,21] Considering the very promising results obtained for the detection of creatinine in bodily fluids by incorporating monophosphonate aryl-extended calix[4]pyrrole cavitands as ionophore in ISE's membrane together with the molecular recognition properties of the former in organic solvents (Chapter 3),[22] we envisioned that the attachment of a fluorescent tag to a monophosphonate calix[4]pyrrole cavitand could be a good strategy for the development of a fluorescent chemosensor for the sensing of this important analyte in organic solution.[23]

The monophosphonate-methylene bridged biscavitand receptor **1** complexed both neutral creatinine (**Cr**) and the creatininium cation (**CrH**$^+$) Figure 5. 3. The neutral **Cr** exclusively produced a complex with 1:1 stoichiometry, while the **CrH**$^+$ cation was involved in the formation of complexes with **1** having 1:1 and 1:2 stoichiometry. Receptor **1** is fully complementary in terms of shape, size and functionality to the creatinine's structure. The formation of the **Cr⊂1** complex is driven by the establishment of multiple non-covalent interactions between receptor **1** and the bound **Cr**. Specifically, four convergent hydrogen bonds between the calix[4]pyrrole NHs and the creatinine oxygen atom. In addition, the methylene protons (CH_2) of **Cr** are involved in CH-π interactions with the aromatic walls of the receptor's cavity. Simultaneously, the acyclic NH group of the complexed **Cr** is hydrogen bonded to the oxygen atom of the inwardly directed PO group of the bridging phosphonate.

We demonstrated the key role played by this latter hydrogen-bonding interaction in the complexation of **Cr** and **CrH**$^+$ in non-polar organic solvents by using the parent bisCH_2 cavitand as reference.

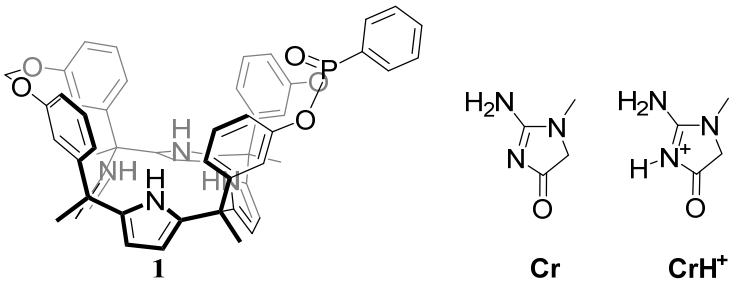

Figure 5. 3: Line-drawing structures of receptor **1**, creatinine (**Cr**), and creatininium cation (**CrH**$^+$).

In this work, we propose the synthesis of a fluorescent receptor **2** based on a monophosphonate aryl-extended calix[4]pyrrole scaffold (Figure 5. 4). Our final aim is the development of a fluorescence chemosensor for the sensing of **Cr** and the **CrH**$^+$ cation in non-polar organic solutions. We expect that the use of a monophosphonate calix[4]pyrrole biscavitand as binding site would improve the selectivity and sensibility of the resulting chemosensor in comparison to the previously described fluorescent creatinine receptors. The selection of the dansyl amide as the fluorescent tag was done after several unsuccessful synthetic attempts to obtain a calix[4]pyrrole based receptor bearing a bridging mono-phosphonate 2-anilino-napthalene fluorescent unit at its upper rim. This fluorophore was previously used by Dalcanale et al. to prepare a fluorescent mono-phosphonate cavitand derived from resorcin[4]arene.[24] We expected that the incorporation of the dansyl group would result in efficient fluorescent properties for the final molecular chemosensor (high emission quantum yields, large Stokes shifts and high sensitivity to changes in its environment, as well as easy derivatization). The dansyl group has been applied previously as fluorescent tag for the covalent construction of a wide range of synthetic chemosensors, which incorporated calix[4]arenes,[25,26,27,28] cyclodextrins,[29,30,31] and crown ethers[32,33,34] scaffolds as binding units.

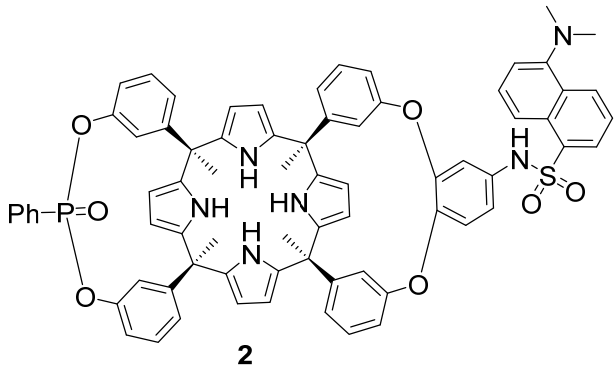

Figure 5. 4: Line-drawing structure of the designed fluorescent receptor **2** bearing a dansyl amide group as fluorescent tag.

5.2 Results and discussion

5.2.1 Design and synthesis

As mention above, our first synthetic attempt to obtain a fluorescent calix[4]pyrrole cavitand receptor bearing a monophosphonate bridging unit was based on the incorporation of 2-anilino-naptahlene-6-phosphonate. The use of this fluorophore was previously described by Dalcanale et al. in the synthesis of a fluorescent monophosphonate cavitands derived of resorcin[4]arene.[24]

Our synthetic strategy started from the already known tetra-hydroxy aryl-extended calix[4]pyrrole **3** (Scheme 5. 1). The reaction of calix[4]pyrrole **3** with 1 eq. of bromochloromethane produced the mono-methylene bridged cavitand **4** in 40 % yield after column chromatography purification of the crude reaction mixture. Addition of fluorophore **5** (which was synthetized accordingly to a previously described methodology,[24] to a pyridine solution of **4** produced a very complex reaction mixture. After several purification attempts, we were not able to identify the presence of the desired mono-phosphonate biscavitand in the crude reaction mixtures. Consequently, we decided to abandon this synthetic route.

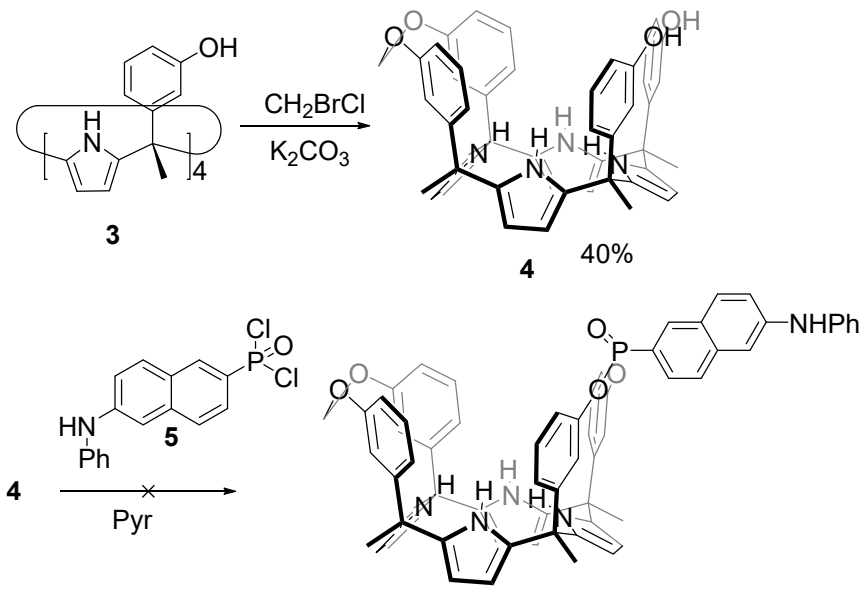

Scheme 5. 1: Reaction scheme for the preparation of fluorescent cavitand bearing the 2-anilino-naphthalene unit in the phosphonate bridging group.

We modified the initial synthetic strategy not only selecting a different fluorophore (i.e. dansyl amide) but also changing the location of its attachment from the phosphonate bridging group to a diametrically opposed bridging aromatic spacer that replaced the methylene-bridging unit of the original design (Scheme 5. 2). Simple molecular modeling studies of the inclusion complex of **Cr** with the newly designed chemonsersor **2** showed, that in complete analogy to the previously described mono-phosphonate methylene-bridged receptor **1**, the aromatic cavity of **2** nicely complements in terms of size, shape and function the hydrogen bonded guest (b, Figure 5. 5).

The synthetic strategy employed for the preparation of **2** involved four sequential steps. (Scheme 5. 2). Firstly, the mono-bridged intermediate **6** was prepared using similar reaction conditions reported by Rebek et al.[35] for the preparation of a structurally related mono-bridged resorcin[4]arene derived cavitand. The reaction of tetrahydroxi calix[4]pyrrole **3** with 3,4 difluoronitrobenzene (1.1 eq.) using excess of Cs_2CO_3 as base yielded the mono-bridged intermediate **6** in a 32 % yield as a racemic mixture. Next, **6** was reacted with phenylphosphonic dichloride in THF solution to produce the mono-phosphonate bis-cavitand **7** as a mixture of two diastereoisomers.

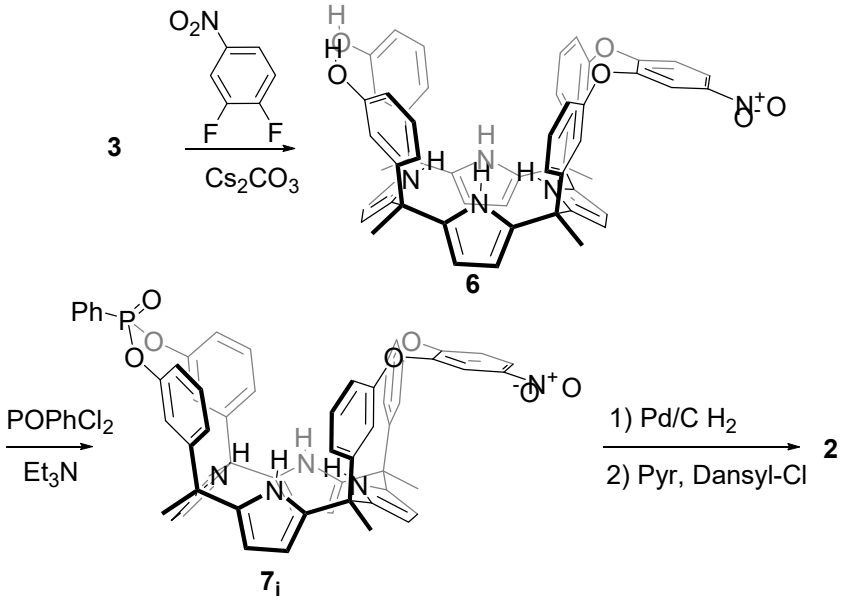

Scheme 5. 2: Synthetic scheme for the preparation of fluorescent monophosphonate cavitand chemosensor **2**. For simplicity, the cavitands are represented as single enantiomers, but were obtained as racemic mixtures and **7** was represented as isomer **7**$_i$.

The two diastereoisomers differ in the spatial orientation of the PO group installed at the upper rim. One has the PO group inwardly directed with respect to its aromatic cavity (**7**$_i$), and the other present the PO group outwardly directed (**7**$_o$). The two diastereoisomers were conveniently separated by flash column chromatography. Luckily, we were able to obtain single crystals that were suitable for X-ray diffraction analysis of the PO_{in} isomer (**7i**). The solid state structure of **7**$_i$ showed the calix[4]pyrrole core in the cone conformation with the four pyrrole NHs hydrogen bonded to the oxygen atom of an acetone molecule that was deeply included into its aromatic cavity (Figure 5. 5). Not surprisingly, the aromatic bridging panel adopted a pseudo-equatorial conformation.[36] Catalytic hydrogenation of the nitro group using 10% Pd/C produced the amino-derivative, which was coupled with dansyl chloride in pyridine solution affording the corresponding dansyl amide receptor **2**. It is worth noting that when the same reaction was performed in DCM solution using Et_3N as base, the isolated product contained two dansyl units covalently attached to the amine group. The ^{1}H NMR spectrum of **2** in CD_2Cl_2 solution is in agreement with a C_1 symmetry. As mentioned above, the mono-bridging of the tetrahydroxi calix[4]pyrrole **3** with 3,4 difluoronitrobenzene produced the nitro-derivative **6** as a racemic mixture of two possible enantiomers dictated by its inherently

chiral structure (lack of symmetry originates from the directional connection imposed by the NO_2 substituent). We did not attempt the separation of the enantiomers of **6** or **7**. Thus, the mono-phosphonate bis-cavitand **2** was also obtained as racemic mixture.

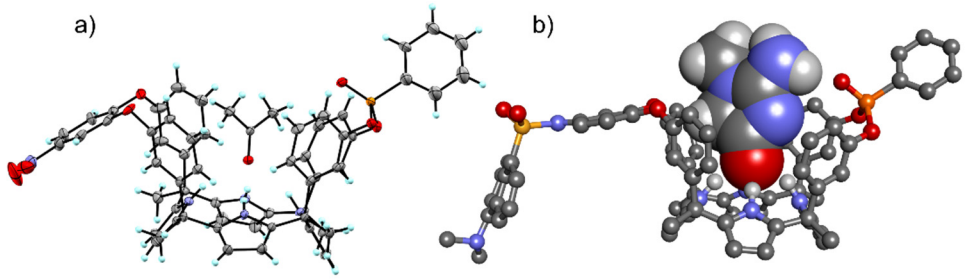

Figure 5. 5: a) X-ray structure of **7i**, thermal ellipsoids set at 50%probability; H atoms are shown as spheres of 0.15 Å. b) Energy-minimized (MM3) structure of **2⊃Cr** complex (non-polar protons from the host were removed for clarity reasons, **Cr** molecule is represented in CPK).

5.2.2 Binding studies

Having molecular chemosensor **2** in our hands, we decided to evaluate its ability to complex **Cr** in solution. Considering the low solubility of **Cr** in non-polar organic solvents [37] we performed a solid-liquid extraction. An excess of solid **Cr** was added to a millimolar solution of receptor **2** in $CDCl_3$ placed in a NMR tube. The NMR tube was hand-shacked for several minutes and a ^{1}H NMR spectrum of the solution phase was immediately registered (Figure 5. 6). The ^{1}H NMR spectrum of the solution showed sharp and well-defined proton signals. Remarkably, the comparison of the latter ^{1}H NMR spectrum with the one registered for **2** in the same solvent evidenced significant changes in the chemical shift values of the protons signals. For example, the singlets of the pyrrole NHs in **2** split into four different singlets with a 1:1:1:1 ratio of integral values. This result was consistent with the expected C_1 symmetry. Moreover, the four singlets assigned to the NHs experienced an intense downfield shift (from 8.63 and 7.95 ppm to 9.6-10.1 ppm) compared to the NHs of **2** dissolved in $CDCl_3$. This observation indicated that the pyrrole NHs were involved in hydrogen-bonding interactions after the solid-liquid extraction experiment with **Cr**. We also observed two new proton signals appearing at 2.64 ppm and 1.09 ppm of the $CDCl_3$ solution after the extraction. We assigned the new signals to the CH_3 and CH_2 protons of extracted **Cr**, respectively. When compared to the chemical shifts of neutral **Cr** in DMSO-d6 solution, these protons resonate significantly

upfield shifted (δ = 2.9 ppm for CH_3, $\Delta\delta$ = - 0.26 ppm; δ = 3.6 ppm for CH_2, $\Delta\delta$ = - 2.51 ppm). The large upfield shifts experienced for these proton signals and in particular for the CH_2, were in agreement with the deep inclusion of **Cr** in the aromatic cavity of **2** (Figure 5. 5). A closer look to the signal assigned to the CH_2 group revealed that they resonate as a germinal couplet doublet. This observation can be explained by the chiral nature of the container **2** that renders the methylene protons of the bound **Cr** diastereotopic.

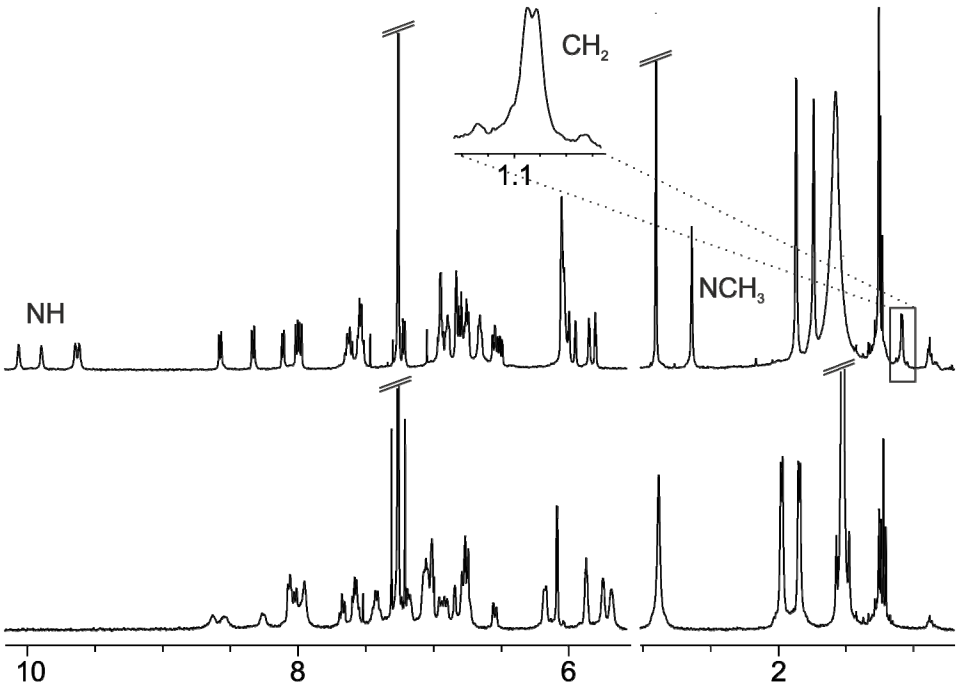

Figure 5. 6: Selected regions of ^{1}H NMR ($CDCl_3$) spectra recorded before (bottom) and after (top) solid-liquid extraction of **Cr** with a solution of **2**.

The extraction experiments performed using DCM-d_2 solutions showed completely analogous level of **Cr** extraction. We used DCM-d_2 for the **Cr** extraction experiments using the non-fluorescent counterpart **1** for which we have estimated a binding constant value for **Cr** of the order of 10^6 M^{-1}. We concluded that the structural modifications implemented in the design of the chemosensor **2** did not significantly modify its binding affinity for **Cr** compared to the non-fluorescent counterpart **1**. The large binding constants assigned to the inclusion complex of **Cr** with chemosensor **2** augured well for the application of the latter in the sensing of **Cr** using fluorescence experiments.

The UV-Vis spectrum of **2** (21.2 µM) in DCM solution showed two absorption bands (Figure 5. 7 a). The first band appeared below 300 nm and it is characteristic from aryl-extended calix[4]pyrrole macrocycles.[38] The second band centered at 350 nm, was attributed to the dansyl group.[39]

The emission spectrum of **2** (21.2 µM) in DCM solution (λ_{exc} = 350 nm) showed a strong band centered at 501 nm characteristic of the dansyl group (Figure 5. 7 a)). The excitation spectrum registered at the fixed wavelength of 501 nm verified that indeed the dansyl group was responsible for the strong emission band (Figure 5. 7 b)).

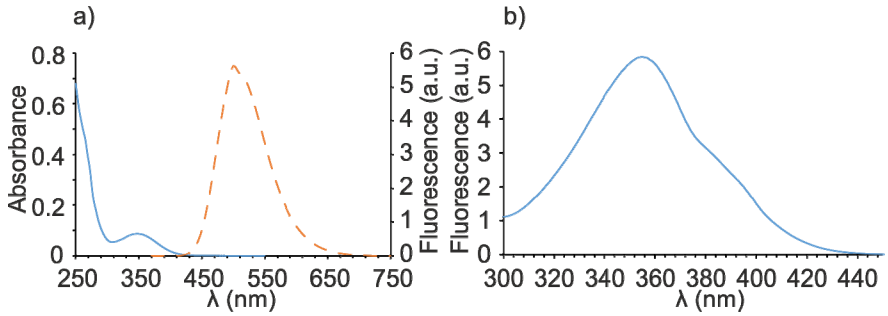

Figure 5. 7: a) Absorption (blue) and fluorescent (λexc = 350 nm, orange dash line) spectra of **2** in DCM; b) Excitation spectrum (501 nm) of free **2** in DCM.

Because of solubility reasons, all titration experiments of **2** were performed employing the synthetic version of **Cr** described in the previous chapters in which the CH_3 group was replaced by an *n*-hexyl chain (**HxCr** Scheme 5. 3). A DCM solution of receptor **2** (24.8 µM) was titrated with a solution of **HxCr** in the same solvent (0.54 Mm) using UV-vis spectroscopy. The concentration of **2** was kept constant throughout the titration. After each addition of **HxCr**, both the emission and UV-Vis absorption spectra of the resulting mixtures were recorded (Figure 5. 8). The incremental additions of **HxCr** did not produce any detectable change in the absorption band corresponding to the dansyl group. In contrast, they produced an increase in the absorption band at 250 nm, most likely due to the increase in concentration of **HxCr** in solution, which also absorbs at this wavelength. Likewise, the addition of incremental amounts of **HxCr** to the solution of **2** did not produce detectable changes in the emission spectra (λ_{exc} = 350 nm). Assuming that the estimated binding constants for **HxCr** and natural **Cr** with receptor **2** are similar to those observed for the non-fluorescent counterpart (Ka > 10^6 M^{-1}). The calculated speciation profiles for the working

conditions of the performed titration experiments, indicated that in presence of 1.3 eq. of **HxCr**, approximately 90% of receptor **2** should be bound (Figure 5. 14). Consequently, the observed lack of changes in the absorption and emission spectra of receptor **2** in the presence of incremental amounts of **HxCr** are not due to the absence of complex. Most likely, the long distance that exists between the recognition site and the signaling dansyl unit of the chemosensor, as well as the reduced conformational changes experiences by receptor **2** upon complex formation are responsible of the absence of spectral changes in both emission and absorption spectra. In short, the molecular recognition event is not transduced in spectral changes of the signaling unit of **2**.

In view of the results obtained, we decided to change the sensing strategy. It is well known that fluorophores at high concentration may experience self-quenching process. On the contrary, previous reports described the use of non-emitting high order fluorophore aggregates as sensing ensembles. The addition of suitable analytes to the solution containing the non-emitting aggregates induced their dissociation, producing an increase of the fluorescence associated with the mixture.[40,41]

We hypothesized that the formation of a dimeric complex by the addition of a ditopic guest (e.g. bis *N*-oxide) that could approach two calix[4]pyrroles units and more concretely two dansyl groups, could lead to a self-quenching of the fluorescence emission of the fluorophore.[42,43] The disruption of this capsule by the addition of a competitive monotopic guest (i.e. **HxCr**) could bring a recovery of the fluorescence and consequently a signal of the binding event of the latter guest.

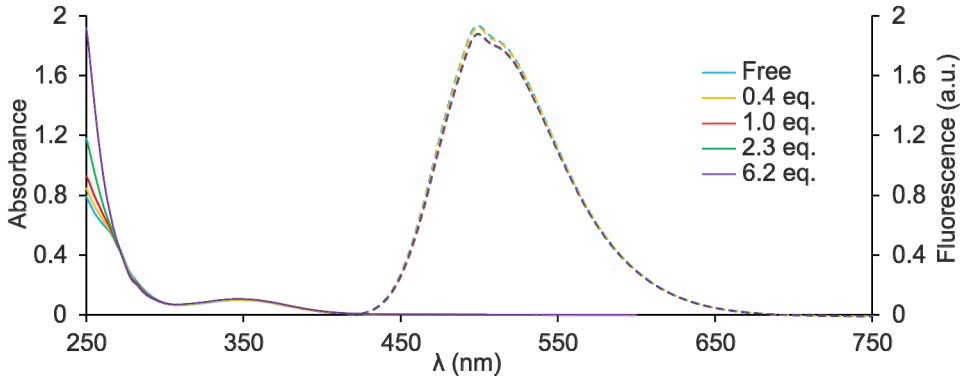

Figure 5. 8: Absorption (continuous line) and emission (dash line) spectra recorded during the titration of receptor **2** with **HxCr** in DCM solution.

Calix[4]pyrrole receptors bind *N*-oxides in polar and non-polar organic solvents with association constant values that are in the range of 10^4-10^7 M^{-1},[44,45] We considered using 4,4'-dipyridyl *N*,*N*'-dioxide (**DPNO**, Figure 5. 9) as template for the assembly of a complex with a 1:2 (**DPNO⊂2₂**) stoichiometry. Upon binding to the fluorescent calix[4]pyrrole **2**, the resulting termolecular 1:2 aggregate features a molecular structure that resembles a dimeric molecular capsule. Figure 5. 9 shows the energy minimized structure (MM3) of the putative **DPNO⊂2₂** complex. In the shown conformer, the pending dansyl units of the two calix[4]pyrroles involved in the assembly are located in very close spatial proximity. We foresee that the close proximity arrangement of the two fluorophores would induce the quenching of its emission. In the previous section, we estimated that the binding constant value for the association of **Cr** with the calix[4]pyrrole **2** was in the order of 10^6 M^{-1}. Consequently, we reasoned that the incremental addition of **Cr** to a solution containing the preassembled **DPNO⊂1₂** complex should produce the gradual disassembly of the termolecular aggregate and the concomitant formation of the 1:1 complex **2⊃Cr**.

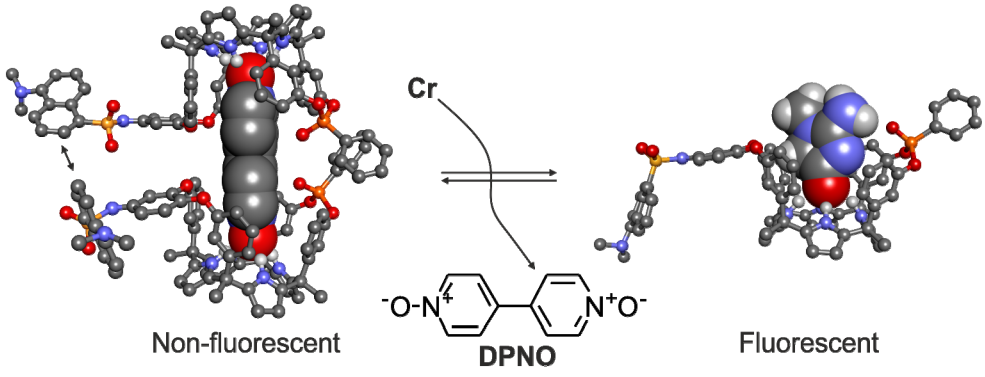

Figure 5. 9: Energy minimized structures (MM3) of **2⊃DPNO** 2:1 complex (left) and **2⊃Cr** complex (right). **DPNO** and **Cr** are represented in CPK model. Non-polar hydrogens of **2** are removed for clarity.

To test our hypothesis, first, we performed a ^{1}H NMR titration experiment by adding incremental amounts of **DPNO** to a DCM-d_2 solution of the calix[4]pyrrole receptor **2**. The addition of ~ 0.3 eq. of **DPNO** to the millimolar solution of **2** produced the appearance of a new set of signals that we attributed to the protons of the bound receptor (Figure 5. 10). This set of signals grew at expenses of the signals' intensity assigned to free **2**. These observations indicated that the exchange's kinetic of the binding equilibrium was slow on the chemical

shift ^{1}H NMR time scale. When 0.5 eq. of **DPNO** were added, only the new set of signals assigned to bound **2** was observed. The ^{1}H NMR spectrum of the formed species showed four separated signals for the pyrrole NHs resonating in the range of 10 to 9.6 ppm. These signals experienced a significant downfield shift compared to free **2**, suggesting its involvement in hydrogen-bonding interactions with the added *N*-oxide. We also detected a new doublet resonating at 4.64 ppm, which was assigned to the aromatic CH protons *α* to the *N*-atom of the bound *N*-oxide. These *α*-CH protons resonate at 8.2 ppm in the free guest. Thus, they experienced a complexation induced shift value of $\Delta\delta$ = - 3.56 ppm, which was indicative of a deep inclusion into the aromatic cavity of the calix[4]pyrrole **2**. The number of proton signals and their chemical shift values were fully consistent with the quantitative assembly in solution of the 1:2 complex (**DPNO⊂2$_2$)** under these working conditions (1 mM solution of **2** and 0.5 eq. of **DPNO** added).

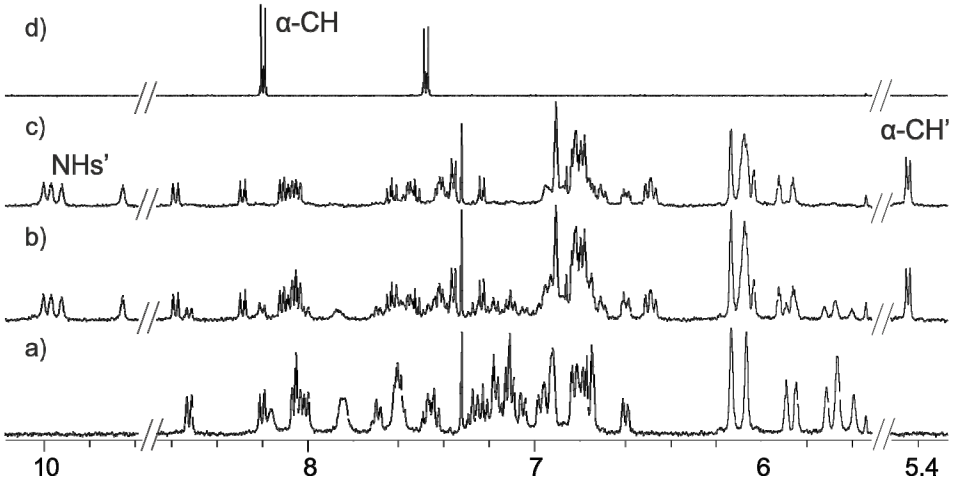

Figure 5. 10: Selected regions of ^{1}H NMR (DCM-d2) spectra recorded during the titration of **2** with **DPNO**. a) 0 eq; b) 0.37 eq; c) 0.51 eq; d) Free **DPNO**. Primed letters correspond to the 2:1 complex and double primed letters to the 1:1 complex.

As described in the previous section, we obtained receptor **2** as a racemic mixture. Consequently, the assembly of receptor **2** with **DPNO** in the 2:1 complex should produce a mixture of two diastereomeric aggregates, one as racemic mixture (R,R and S,S) and the other as a *meso*-aggregate. Assuming that the homochiral and the heterochiral assemblies were isoenergetic, they should assemble in accordance to the statistical distribution 25:25:50. Thus, one might expect to observe two separate set of signals of equal intensity in the ^{1}H NMR

spectrum of the mixture of assembled **DPNO⊂2₂** complexes, owing that the homochiral aggregates have an identical NMR spectrum. The observation of only one set of two doublets for the included **DPNO** suggested that the assembly of the termolecular **DPNO⊂2₂** complex occurred trough an efficient self-discrimination process that exclusive yielded the *meso*-aggregate.

When more than 0.5 eq. of **DPNO** were added to the solution a second set of proton signals for the calix[4]pyrrole receptor emerged (Figure 5. 11). The new set of proton signals grow in intensity as the concentration of **DPNO** is increased. The chemical shift values of the NHs in the species were indicative of their participation in hydrogen-bonding interactions. Taken together, these observations indicated the disassembly of the 2:1 complex and the concomitant formation of a 1:1 complex, **DPNO⊂2₂** when not working under strict stoichiometric control.

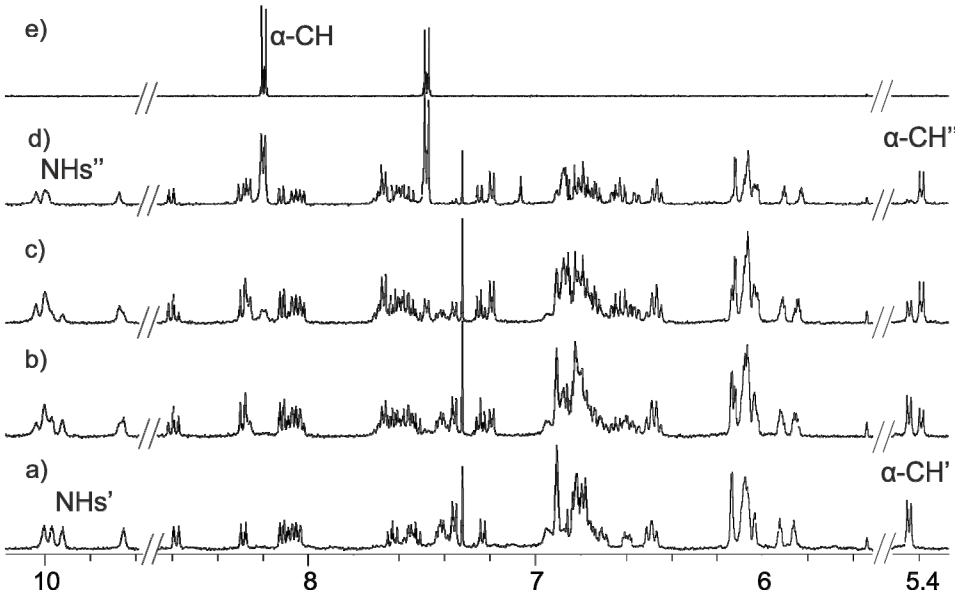

Figure 5. 11: Selected regions of ^{1}H NMR (DCM-d_2) spectra recorded during the titration of **2** with incremental addition of **DPNO**. a) 0.51 eq; b) 0.85 eq; c) 1.18 eq, d) 2.68 eq; e) Free **DPNO**. Primed letters correspond to the 2:1 complex and double primed letters to the 1:1 complex.

We were able to calculate the cooperativity coefficient (α) for the formation of the **DPNO⊂2₂** complex from the ratio of the integral values of protons α-CH' and α-CH'' observed during the dissociation process.

$$\mathbf{DPNO}\subset\mathbf{2_2} + \mathbf{DPNO} \rightleftharpoons 2\ \mathbf{DPNO}\subset\mathbf{2} \quad K_D$$

Considering the two equilibria:

$$\mathbf{2} + \mathbf{DPNO} \rightleftharpoons \mathbf{DPNO}\subset\mathbf{2} \quad K_1$$
$$\mathbf{DPNO}\subset\mathbf{2} + \mathbf{DPNO} \rightleftharpoons \mathbf{DPNO}\subset\mathbf{2_2} \quad K_2$$

K_1 and K_2 are the macroscopic constants for the formation of the 1:1 and 2:1 complexes. Considering that **2** can interact with **DPNO** for two equivalent sites the microscopic constant for the formation of the **DPNO⊂2** complex is $K_{m1} = K_1/2$. For the second binding event, **2** can bind to the **DPNO⊂2** complex in one way to form the termolecular complex **DPNO⊂2₂**. However, there are two possibilities for the disassembly of **DPNO⊂2₂**, thus the microscopic constant for the second binding event is $K_{m2} = 2 \times K_2$. We can define $\alpha = K_{m2}/K_{m1} = (K_2/K_1) \times 4 = 4/K_D$.

Considering that the concentration of receptor **2** free in solution is negligible, the calculated value for the cooperativity coefficient is $\alpha = 0.9 \pm 0.14$. This result indicates that there is no cooperativity for the binding of the second unit of **2**.

The interaction of **DPNO** with the calix[4]pyrrole receptor **2** was also probed using UV-vis absorption and emission spectroscopy. We titrated a solution of **2** in DCM (23.7 μM) with incremental amounts of **DPNO**. The concentration of **2** was maintained constant throughout the titration and we registered both emission and absorption spectra after each addition.

The addition of 0.17 eq. of **DPNO** to a solution of **2** produced the appearance of a new band centered at 322 nm in the UV-vis absorption spectrum (Figure 5. 12 a). We attributed this band to bound **DPNO**. Increasing the amount of **DPNO** produced an intensification of this band together with a concomitant red-shift of its maximum. The bathochromic shift of the band coincides with the absorption maximum of free **DPNO**. We were able to fit the titration data to a binding model that considered the formation of 2:1 and 1:1 complexes (Figure 5. 15). The returned binding constant values were in accordance with the estimated values based on the ^{1}H NMR titration experiment, $K_1 = 1.2 \times 10^6\ M^{-1}$ ($K_{m1} = 6.0 \times 10^5\ M^{-1}$), $K_2 = 6.3 \times 10^5\ M^{-1}$ ($K_{m2} = 1.3 \times 10^6\ M^{-1}$; $\alpha = 2.16$)[46] and $K_{2:1} = 7.5 \times 10^{11}\ M^{-2}$ for the 2:1 complex. The simulated speciation profile (Figure 5. 15 left) showed that at the working concentration of **2**

(23.7 µM), the addition of 0.5 eq. of **DPNO** approximately induced the assembly of 70% of receptor **2** in the 2:1 complex. The remaining 30% is free or involved in the 1:1 complex.

We performed fluorescence measurements in the same range of concentrations. We selected an excitation wavelength of 400 nm because the absorbance value at this wavelength remained constant throughout the titration. The emission spectrum of receptor **2** in DCM showed a broad band with the maximum centered at 501 nm. Addition of incremental amounts of **DPNO** produced a quenching of this band (Figure 5. 16). The largest fluorescence quenching (40% decrease from the original fluorescence intensity) was observed when 0.5 eq. of **DPNO** were added (Figure 5. 12). This corresponded to the maximum concentration of the self-assembled 2:1 complex present in solution.

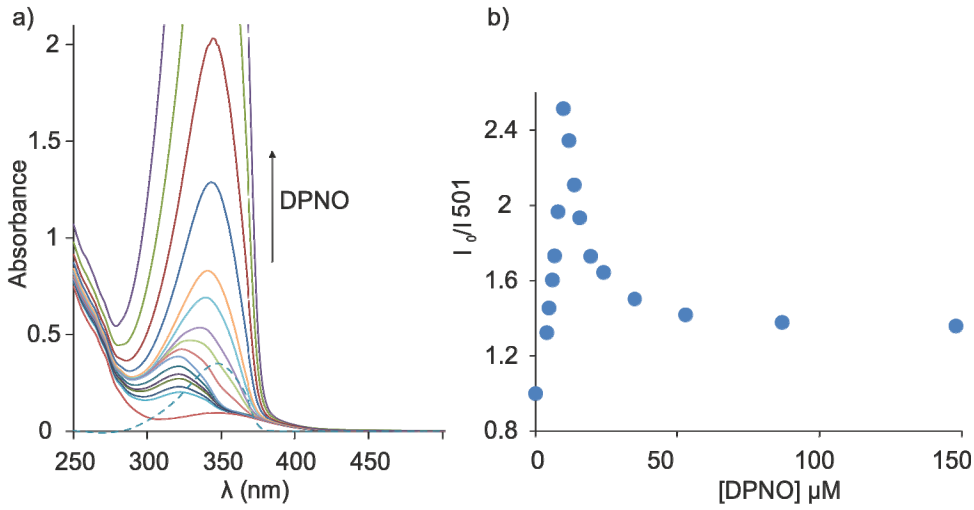

Figure 5. 12: a) Absorption spectra recorded during the titration of **2** (23.7 µM) with incremental amounts of **DPNO** (dot lines represent absorption spectrum of free **DPNO** at 9.69 µM). b) Fluorescent changes registered during the titration of **2** (23.7 µM) with incremental amounts of **DPNO** at 501nm.

Addition of more than 0.5 eq. of **DPNO** produced a gradual recovery of the fluorescence intensity. At the end of the titration, 6.2 eq. of **DPNO** were added and 73% of the original intensity value was recovered. We attributed the fluorescence intensity recovery to the disassembly of 2:1 complex that led to the formation of the 1:1 complex.

In order to evaluate the capability of the 1:2 assemble of **DPNO** and **2** for creatinine sensing, we prepared a new DCM solution containing a 23.7 µM concentration of receptor **2** and approximately 0.5 eq. of **DPNO** and the prepared solution was titrated by adding incremental

amounts of a 0.67 mM solution of **HxCr** in the same solvent. The concentrations of **2** and **DPNO** were maintained constant throughout the titration. After each addition, the absorption and fluorescence spectra of the mixtures were recorded.

The incremental additions of the **HxCr** to the solution mixture containing the **2**$_2$:**DNPO** assembly induced a red-shift of the UV-vis absorption band associated to the bound **DPNO** (Figure 5. 13). This observation supported the disassembly of the 2:1 termolecular complex probably due to the competitive formation of the 1:1 **2**⊃**HxCr** complex. More importantly, the incremental additions of **HxCr** to the solution containing the preassembled complex **DPNO**⊂**2**$_2$, produced a significant increase in the band of the emission spectrum of the mixture. When the concentration of added **HxCr** was 0.19 mM, the intensity at the emission maxima (501 nm) was increased almost two-fold (190%) compared to the initial fluorescence intensity of the solution mixture containing the **DPNO**⊂**2**$_2$ complex as the major component.

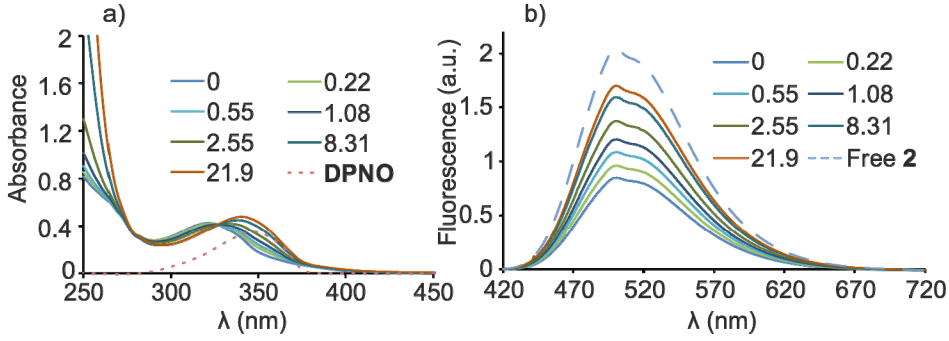

Figure 5. 13: Absorption a) and emission b) spectra recorded during the titration of **2** in the presence of 0.5 eq. of **DPNO** with **HxCr**. Inset shows eq. of **HxCr** added.

The plot of emission intensity against **HxCr** concentration (Figure 5. 17) shows a clear linear relationship in the range of 2.65 to 18.14 μM. The estimated detection limit (LOD)[47] of the ensemble mixture for **HxCr** is 1.6 μM.

These preliminary results augured well for the use of this system for the sensing of creatinine using fluorescence spectroscopy. However, creatinine is usually found in aqueous solution and thus, more experiments (i.e. liquid-liquid extractions) should be performed to demonstrate the viability of the system for its sensing. Additionally, the described termolecular **DPNO**⊂**2**$_2$ complex, differed from our initial purpose. Ideally, the signaling should take place upon

binding of the target analyte without the displacement a bound molecule. To overcome this problem receptor **2** should be redesigned again in such a way that the fluorescent tag can "feel" the presence of the bound analyte. For example, incorporating a different fluorophore, shortening the spacer or increasing the flexibility of the receptor (e.g. monocavitand) placing the fluorophore closer in space to the binding site.

5.3 Conclusions

We have prepared an unprecedented fluorescent receptor based on a aryl-extended calix[4]pyrrole cavitand. Our receptor possess a single phosphonate group, which not only acts as a bridging unit rigidifying the cavity, but also participates in the recognition process of creatinine through the establishment of hydrogen bond interactions with the guest. The new described receptor possess a strong emission band with a maxima at 501 nm attributed to the presence of a dansyl group that it is covalently linked to the calix[4]pyrrole cavitand. We have designed a preassembled system formed by two units of receptor **2** linked by **DPNO** to be further used for creatinine sensing. The supramolecular assembly was studied by ^{1}H NMR, absorption and emission spectroscopy. This preassembled system experimented a self-quenching process due to the close proximity of the dansyl units. Addition of a creatinine derivative **HxCr** provoked the disassembly of the termolecular complex with the consequent recovery of fluorescence emission. In all processes the fluorescence emission had a good linear fit with the concentration of **HxCr** and the estimated LOD result to be as low as 1.6 μM. However, additional experiments are required to prove its feasibility for the sensing of creatinine. In addition, the direct sensing of creatinine by complex formation with a chemosensor based on monophosphonate calix[4]pyrrole requires a careful redesign of receptor **2**.

5.4 Experimental Section

5.4.1 General information and instrumentation

All solvents and reagents used in the synthesis of the described compounds were obtained from commercial sources and were used without further purification except where noted. Pyrrole was distilled (50 mbar, 58–59 °C) and stored in the freezer (-20ºC) for further use. THF was distilled from sodium/benzophenone under argon atmosphere. Dried DMF was

purchased from Across Organics. Triethyl amine was distilled from CaH_2 under argon atmosphere. Pyridine was distilled from CaO under argon atmosphere. Flash column chromatography was performed with silica gel, technical grade, pore size 60 Å, and 230–400 mesh particle size. The $CHCl_3$ used in column chromatography was passed through basic alumina before use it. Calix[4]pyrrole **3** was synthetized according to previously described synthetic procedure.[22]

Routine ^{1}H-NMR and ^{13}C-NMR spectra were recorded on a Bruker Avance 400 (400 MHz for ^{1}H-NMR), Bruker Avance 500 (500 MHz for ^{1}H-NMR) ultrashield spectrometer, or on a Bruker Avance III 500 (500 MHz for ^{1}H-NMR) with a QNP cryoprobe. Deuterated solvents were purchase from Aldrich. Chemical shifts are given in ppm. The peaks were referenced relative to the solvent residual peak. All NMR J values are given in Hz. High resolution mass spectra were obtained on a MicroTOF II (Bruker Daltonics) ESI as ionization mode Mass Spectrometer. UV-Vis measurements were carried out on a Shimadzu UV-2401PC spectrophotometer equipped with a photomultiplier detector, double beam optics and D2 and W light sources or on a Shimadzu UV-1800 spectrophotometer. Fluorescence measurements were carried out on an Aminco-Bowman Series 2 Luminescence spectrofluorimeter equipped with a high voltage PMT detector and continuum Xe light source.

5.4.2 Synthetic procedures

Synthesis of **6**: **3** (1.5 g, 2.03 mmol) and Cs_2CO_3 (5.28 g, 16.2 mmol) were placed in a previously dried Ace pressure tube (100mL) equipped with a plunger valve and three cycles of vacuum/Ar were applied. Then, 67.5 mL of anhydrous DMF were added, and the mixture was vigorously stirred. 3,4-difluoronitrobenzene (0.25 mL, 2.26 mmol) were added and the mixture was heated at 60ºC for 1h and at 90ºC overnight in an oil bath. Next day, the reaction was cooled down at RT, diluted with EtOAc (90mL), and 10% HCl_{aq} was added until pH 1. A white solid precipitated which was filtered and washed with EtOAc. The two phases of the filtrated were separated, and the organic layer was washed with water (2 × 40mL) to remove the DMF. The EtOAc layer was collected, dried over Na_2SO_4, filtered and concentrated to dryness. **6** was isolated by flash column chromatography un SiO_2, absorbing the crude on a minimal amount of SiO_2 and eluting with a slow gradient of DCM:EtOAc from 100% DCM to 70:30. The fraction containing **6** was concentrated until have an oil which was rapidly redissolved in DCM and left it to slowly evaporate yielding yellow crystals of pure **5** (0.56 g,

32 %). ^{1}H-NMR (500 MHz, DMSO-d6, 298 K): δ = 9.39-9.32 (m, 3H, NH), 9.29 (s, 1H, OH), 9.27 (s, 1H, OH), 9.24 (bs, 1H, NH), 9.15 (dd, *J* = 9.1, 2.8 Hz, 1H, 2), 8.05 (d, *J* = 2.8 Hz, 1H, 3), 7.44 (d, *J* = 9.1 Hz, 1H, 1), 7.274 (t, 1H, *J* = 7.9 Hz, CH_{Ar}), 7.271 (t, 1H, *J* = 8.0 Hz, CH_{Ar}), 7.07-7.00 (m, 4H, CH_{Ar}), 6.79 (d, 1H, *J* = 7.9 Hz, CH_{AR}), 6.76 (d, 1H, *J* = 7.9Hz, CH_{Ar}), 6.50-6.48 (m, 1H, CH_{Ar}), 6.48-6.46 (m, 1H, CH_{Ar}), 6.39-6.36 (m, 2H, CH_{Ar}), 6.36-6.31 (m, 2H, CH_{Ar}), 6.00-5.96 (m, 6H, *β*-pyr), 5.95 (dd, 1H, *J* = 2.5, 1.8 Hz, CH_{Ar}), 5.92 (dd, 1H, *J* = 2.5, 1.8 Hz, CH_{Ar}), 5.82-5.79 (m, 2H, *β*-pyr), 1.75 (bs, 6H, CH_3), 1.70 (s, 3H, CH_3), 1.67 (s, 3H, CH_3). ^{13}C-NMR (125 MHz, DMSO-d6, 298 K): δ = 159.1, 158.5, 158.1 (x2), 153.9, 153.3, 153.2, 152.3, 152.2, 147.4, 145.2, 138.0 (x2), 137.6, 137.5, 137.4, 137.3, 136.8 (x2), 130.7 (x2), 129.6 (x2), 125.2, 122.7, 122.4, 122.1, 120.5, 118.1 (x2), 116.6, 116.4, 114.5 (x2), 113.8 (x3), 112.5, 105.1-104.9 (x8 *β*-pyr), 44.7, 44.6, 44.5 (x2), 31.89 (x2), 31.35 (x2)

Synthesis of **7**: To a four previously dried schlenk tubes we added in each of them **6** (100 mg, 0.116 mmol), and three cycles of vacuum Ar were applied. Then, anhydrous THF (6.8 mL) and dried triethyl amine (158 µL, 1.13 mmol) were added. Under vigorous stirring, Phenylphosphonic dichloride (20 µL, 0.14 mmol) was slowly added over a period of 10 to 15 minutes) and the reaction was left to stir at RT for 4 hours. After that time the reaction was quenched by adding water (5 mL) and 10% HCl_{aq} until pH 1. The content of the four flasks were combined and extracted with EtOAc (3 × 20mL). The EtOAC extracts were combined dried over Na_2SO_4, filtered and concentrated under reduced pressure yielding a light yellow solid (0.41 g). **7** was isolated by column chromatography on SiO_2 using DCM as eluent until the first product eluted (in isomer), then the polarity was increased until 95:5 DCM:EtOAc recovering out isomer. The two isomer were cristalized by using DCM:Hx with few drops of acetone. $\mathbf{7_{in}}$ (212 mg, 46%), $\mathbf{7_{out}}$ (98 mg, 22%). NOTE: In our hands and under the same conditions the scale up of the reaction produced **7** in lower yields. $\mathbf{7_{in}}$ ^{1}H-NMR (500 MHz, $CDCl_3$, 298 K): δ = 8.13 (bs, 1H, NH), 8.03-7.91 (m, 4H, 2xNH & 2xAr_{PO}), 8.89-7.74 (m, 3H, NH, 2xAr_{NO2}), 7.71-7.66 (m, 1H, Ar_{PO}), 7.62-7.56 (m, 2H, Ar_{PO}), 7.17 (d, *J* = 9.6Hz, 1H, Ar_{NO2}) 7.13-7.02 (m, 4H, CH_{Ar}), 7.00-6.87 (m, 7H, CH_{Ar}), 6.83 (d, *J* = 6.6 Hz, 1H, CH_{Ar}),6.81-6.75 (app. t, 2H, CH_{Ar}), 6.15 (app. d, 2H, *β*-pyr), 6.12-6.10 (m, 1H, CH_{Ar}), 6.10-6.08 (m, 1H, CH_{Ar}), 5.97-5.91 (m, 4H, *β*-pyr), 5.90-5.84 (m, 2H, *β*-pyr), 1.96 (s, 6H, CH_3), 1.86 (s, 6H, CH_3). ^{13}C{^{1}H}-NMR (125 MHz, $CDCl_3$, 298 K): δ = 158.5, 157.8, 154.7, 151.5, 151.4, 151.3, 150.0, 149.9, 147.7, 144.1, 137-136 (x8, *α*-pyr), 133.2 (Ar_{PO}), 131.2 (d, $^{2}J_{PC}$ = 10.6 Hz, Ar_{PO}), 129.2-128.6 (x4$CH_{Ar,}$ Ar_{PO}), 127.6 (d, $^{1}J_{PC}$ = 205.7, Ar_{PO}), 124.0 (x2, CH_{Ar}), 123.6 (CH_{NO2}), 122.2 (CH_{Ar}), 122.0 (x2, CH_{Ar},CH_{NO2}), 120.9 (x2, CH_{Ar}), 120.3 (Ar_{NO2}), 120.0 (x2, CH_{Ar}),

116.5 (CH_{Ar}), 116.4 (CH_{Ar}), 115.4 (CH_{Ar}), 113.8(CH_{Ar}), 106.3-105.9 (x8, *β*-pyr), 44.8 (**C**CH_3), 44.7 (**C**CH_3), 44.6 (x2, **C**CH_3), 29.4 (CH_3), 29.1 (CH_3), 28.8 (CH_3), 28.7 (CH_3). $^{31}P\{^1H\}$-NMR (202 MHz, $CDCl_3$, 298 K): δ = 15.4. **7_{out}** ^1H-NMR (500 MHz, THF -d6, 298 K): δ = 9.28 (bs, 1H, NH), 9.22 (bs, 1H, NH), 8.02 (dd, *J* = 9.6, 2.6 Hz, 1H, Ar_{NO2}) 7.99-7.89 (m, 3H, Ar_{NO2}, Ar_{PO}), 7.66-7.59 (m, 2H, NH Ar_{PO}), 7.59-7.50 (m, 3H, NH, Ar_{PO}), 7.30-7.21 (m, 4H, CH_{Ar}), 7.20-7.00 (m, 9H, Ar_{NO2}, 8xCH_{Ar}), 6.80-6.73 (m, 2H, CH_{Ar}), 6.12-6.06 (m, 3H, CH_{Ar}, 2x *β*-pyr), 5.99 (bs, 1H, CH_{Ar}), 5.84-5.79 (m, 2H, *β*-pyr), 5.44 (bs, 1H, *β*-pyr), 5.39 (bs, 1H, *β*-pyr), 5.36-5.29 (m, 2H, *β*-pyr), 1.98 (app s, 6H, 2xCH_3), 1.86 (s, 3H, CH_3), 1.84 (s, 3H, CH_3). $^{13}C\{^1H\}$-NMR (125 MHz, THF-d6, 298 K): δ = 159.7, 159.1, 156.3, 152.6 (d, $^2J_{PC}$ = 12.6 Hz), 152.2 (d, $^2J_{PC}$ = 6.6 Hz), 152.1, 151.9, 149.3, 145.4, 138.6, 138.4, 138.0, 137.9, 136.8 (*α*-pyr), 133.32 (Ar_{PO}), 131.9 (d, $^2J_{PC}$ = 10.2 Hz, Ar_{PO}), 129.5, 129.4, 129.2 (d, $^3J_{PC}$ = 20 Hz), 129.1 (x2), 124.5 (CH_{Ar}), 124.4 (CH_{Ar}), 124.3 (CH_{Ar}), 123.7 (CH_{Ar}), 123.3 (CH_{Ar}), 121.8 (CH_{NO2}), 121.1 (CH_{Ar}), 120.9 (CH_{Ar}), 120.3 (CH_{NO2}), 118.0 (CH_{Ar}), 117.9 (CH_{Ar}), 117.6 (CH_{Ar}), 117.2 (CH_{Ar}), 116.7 (CH_{Ar}), 115.6 (CH_{Ar}), 107.3-106.9 (x4 *β*-pyr), 106.1 (*β*-pyr), 106.0 (*β*-pyr), 105.6 (*β*-pyr), 105.5 (*β*-pyr), 46.0 (**C**CH_3), 45.9 (**C**CH_3), 45.8 (x2, **C**CH_3), 28.1 (CH_3), 27.6 (CH_3), 27.1 (CH_3), 27.0 (CH_3).[48] $^{31}P\{^1H\}$-NMR (202 MHz, THF-d6, 298 K): δ = 10.3

Synthesis of **2**:

Step1: **7_{in}** (50mg, 0.051 mmol) was dissolved in EtOAc (25 ml, HPLC gradient) and the solution was placed in an Ace pressure flask (75mL). 10% Pd/C (27 mg) was suspended in 3 mL of EtOAc in a vial, and the suspension was sonicated for 5 minutes. Then the catalyst was added to the reaction flask and the remaining catalyst was recovered by washing the vial with more EtOAc (total volume of EtOAc in reaction flask 33 mL). The flask was placed in a parr hydrogenator apparatus and was purged three times with H_2. The flask was pressurized with 4 bar of H_2 and shacked overnight. Next day, the flask was depressurized and the catalyst removed by filtration over zeolite. The zeolite was gently washed with EtOAc, and the filtrated concentrated under reduced pressure yielding a light-pink solid. The solid was purify by column chromatography on SiO_2 using DCM:EtOAc (98:2 to 95:5) yielding 29.2 mg 60% of pure reduced product as a white solid which was immediately used in the next step. ^1H-NMR (400 MHz, $CDCl_3$, 298 K): δ = 8.08-7.95 (m, 2H, 2xAr_{PO}, NH), 7.87 (bs, 2H, NH), 7.75-7.61 (m, 2H, ArPO, NH), 7.61-7.51 (m, 2H, Ar_{PO}), 7.18 (app. t, 2H, CH_{Ar}), 7.1-6.93 (m, 5H), 6.75 (d, *J* = 7.6 Hz, 1H, CH_{Ar}), 6.68 (d, *J* = 7.1 Hz, 1H, CH_{Ar}), 6.46 (dd, *J* = 8.8, 2.6 Hz,

1H, Ar_{NH2}), 6.34 (d, *J* = 2.6 Hz, 1H, Ar_{NH2}), 6.21 (bs, 2H), 6.12 (bs, 2H), 5.93 (app. d, 2H), 5.88(bs, 1H), 5.85 (bs, 1H), 5.82 (bs, 1H), 5.78 (bs, 1H), 1.97 (bs, 6H, CH_3), 1.87 (s, 3H, CH_3), 1.85 (s, 3H, CH_3).

Step 2: reduction product of $\mathbf{7_{in}}$ (20 mg, 0.021 mmol) and dansyl chloride (5.38 mg, 0.020 mmol) were dissolved in 1.1 mL of anhydrous pyridine under Ar atmosphere and the reaction was stirred at RT for 3 h. Then, the reaction was diluted with 2 mL of DCM and 2mL of water. The DCM extract was separated and the aqueous phase was extracted two additional times with the same amount of DCM. The DCM extracts were combined dried over Na2SO4, filtered and concentrated under reduced pressure, yielding a yellow solid. The solid was purify by column chromatography on SiO_2 using $CHCl_3$:EtOAc 97:3 yielding pure **2** (24.3 mg, 98%) as a yellow solid. ^{1}H-NMR (500 MHz, $CDCl_3$, 298 K): δ = 8.61 (bs, 1H, NH), 8.51 (bd, *J* = 6.5 Hz, 1H), 8.25 (bd, *J* = 7.2 Hz, 1Hz), 8.10-8.00 (m, 3H), 7.96 (bs, 3H, NH), 7.67 (t, *J* = 7.5 Hz, 1H, Ar_{PO}), 7.61-7.54 (m, 2H, Ar_{PO}), 7.42 (m, 2H), 7.25-7.13 (m, 4H), 7.09-6.97 (m, 6H), 6.95 (d, *J* = 7.7 Hz, 1H), 6.91 (d, *J* = 7.9 Hz, 1H), 6.83 (s, 1H), 6.81-6.70 (m, 5H), 6.55 (d, *J* = 9.5 Hz, 1H), 6.17 (s, 1H), 6.16 (s, 1H), 6.08 (app. d, 2H), 5.89-5.84 (m, 2H), 5.76 (bs, 2H), 5.70 (bs, 2H), 2.87 (s, 6H), 1.98 (s, 3H), 1.97 (s, 3H), 1.85 (s,3H), 1.84 (s,3H).[49] 137.8-136.8 (x8 *α*-pyr) , HRMS(ESI-TOF)m/z: $[M - H]^-$ Calcd for $C_{72}H_{60}N_6O_7PS$ = 1183.3987; Found = 113.3986.

5.4.3 Figures

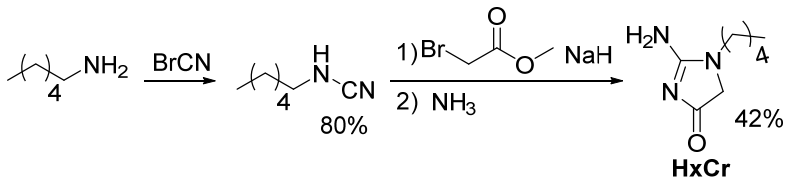

Scheme 5. 3: Synthetic scheme for the preparation of **HxCr**.

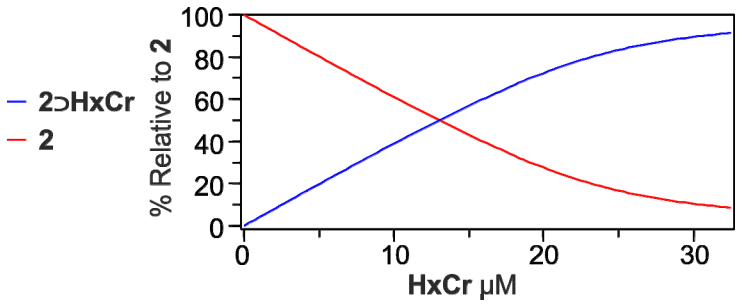

Figure 5. 14: Calculated speciation profile for the titration of **2** (24.8 μM) with **HxCr** considering a binding constant of 10^6 M^{-1}.

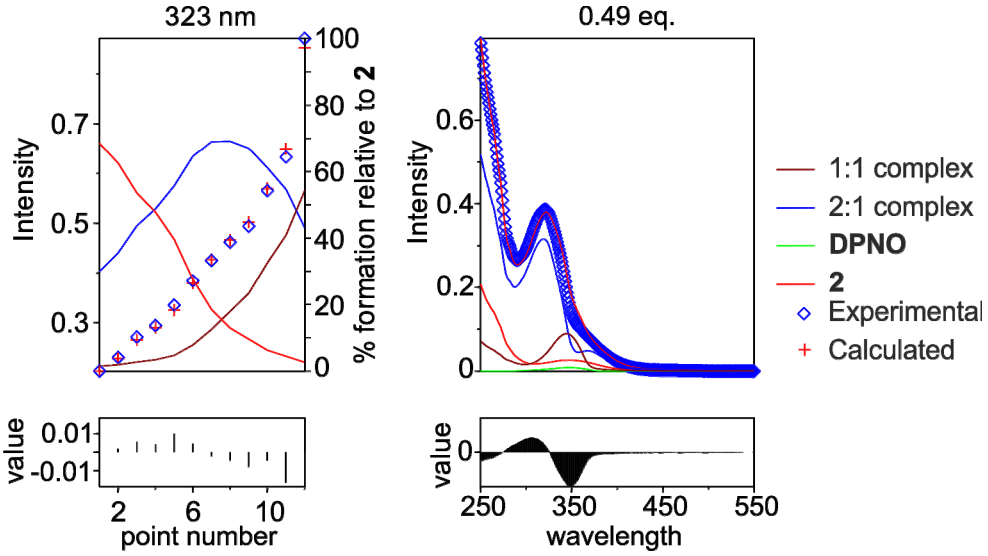

Figure 5. 15: Fitting of the absorption spectra recorded during the titration of receptor **2** with **DPNO** using HypSpec version 1.1.16.

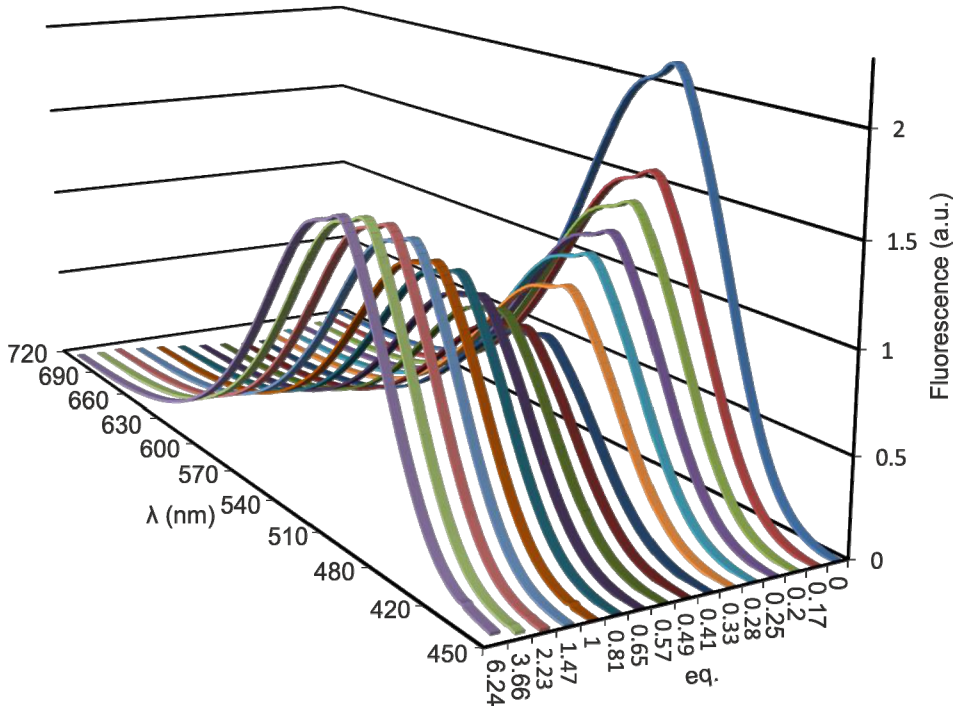

Figure 5. 16: Fluorescence spectra recorded during the titration of **2** with incremental amounts of **DPNO**.

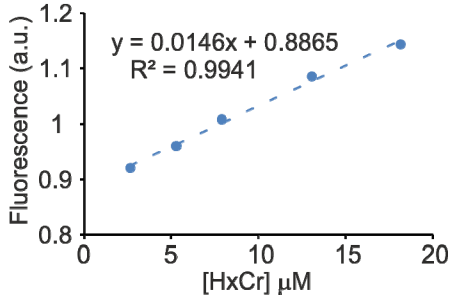

Figure 5. 17: Fluorescence emission of the preassemble system containing **2** and **DPNO** in a 2:1 molar ration versus creatinine concentration from 2.7 to 18.1 µM concentration. Inset shows the returned linear equation.

5.5 References and notes

[1] Bissell, R. A.; de Silva, A. P.; Gunaratne, H. Q. N.; Lynch, P. L. M.; Maguire, G. E. M.; Sandanayake, K. R. A. S. *Chem. Soc. Rev.* **1992**, *21*, 187-195.
[2] de Silva, A. P.; Fox, D. B.; Moody, T. S.; Weir, S. M. *Trends Biotechnol.* **2001**, *19*, 29-34.
[3] Wu, J.; Kwon, B.; Liu, W.; Anslyn, E. V.; Wang, P.; Kim, J. S. *Chem. Rev. (Washington, DC, U. S.)* **2015**, *115*, 7893-7943.
[4] Pal, S.; Lohar, S.; Mukherjee, M.; Chattopadhyay, P.; Dhara, K. *Chem. Commun.* **2016**, *52*, 13706-13709.
[5] Chen, T.; Xie, N.; Viglianti, L.; Zhou, Y.; Tan, H.; Tang, B. Z.; Tang, Y. *Faraday Discuss.* **2017**, *196*, 351-362.
[6] Tajarrod, N.; Rofouei, M. K.; Masteri-Farahani, M.; Zadmard, R. *Anal. Methods* **2016**, *8*, 5911-5920.
[7] Ellairaja, S.; Shenbagavalli, K.; Vasantha, V. S. *ChemistrySelect* **2017**, *2*, 1025-1031.
[8] Minghua, M.; Shikang, W. *Acta Chim. Sinica* **2002**, *60*, 866-869.
[9] Gotor, R.; Costero, A. M.; Gavina, P.; Gil, S.; Parra, M. *Eur. J. Org. Chem.* **2013**, 1515-1520.
[10] Taner, B.; Kursunlu, A. N.; Güler, E. *Spectrochim Acta A Mol Biomol Spectrosc* **2014**, *118*, 903-907.
[11] Ghorpade, T. K.; Patri, M.; Mishra, S. P. *Sensor Actuat B-Chem* **2016**, *225*, 428-435.
[12] Sareen, D.; Lee, J. H.; Hwang, H.; Yoo, S.; Lee, C. H. *Chem. Commun.* **2016**, *52*, 5852-5855.
[13] Anzenbacher, P.; Liu, Y. L.; Palacios, M. A.; Minami, T.; Wang, Z.; Nishiyabu, R. *Chem. Eur. J.* **2013**, *19*, 8497-8506.
[14] Samanta, R.; Mahanta, S. P.; Ghanta, S.; Panda, P. K. *Rsc Advances* **2012**, *2*, 7974-7977.
[15] Miyaji, H.; Sato, W.; An, D. Q.; Sessler, J. L. *Collect. Czech. Chem. Commun.* **2004**, *69*, 1027-1049.
[16] Saha, I.; Lee, J. H.; Hwang, H.; Kim, T. S.; Lee, C. H. *Chem. Commun.* **2015**, *51*, 5679-5682.
[17] Lv, Y. J.; Xu, J.; Guo, Y.; Shao, S. J. *Chem. Pap.* **2011**, *65*, 553-558.
[18] Anzenbacher, P.; Jursíková, K.; Sessler, J. L. *J. Am. Chem. Soc.* **2000**, *122*, 9350-9351.
[19] Bhatt, K. D.; Makwana, B. A.; Vyas, D. J.; Mishra, D. R.; Jain, V. K. *J. Lumin.* **2014**, *146*, 450-457.
[20] Miyaji, H.; Kim, H. K.; Sim, E. K.; Lee, C. K.; Cho, W. S.; Sessler, J. L.; Lee, C. H. *J. Am. Chem. Soc.* **2005**, *127*, 12510-12512.
[21] Yoo, J. D.; Jeoung, E. H.; Lee, C. H. *Supramol. Chem.* **2009**, *21*, 164-172.
[22] Guinovart, T.; Hernández-Alonso, D.; Adriaenssens, L.; Blondeau, P.; Martínez-Belmonte, M.; Rius, F. X.; Andrade, F. J.; Ballester, P. *Angew. Chem. Int. Ed.* **2016**, *55*, 2435-2440.
[23] The same strategy for the fluorescent detection of creatinine in water cannot be applied due to the low stability of the complex.
[24] Maffei, F.; Betti, P.; Genovese, D.; Montalti, M.; Prodi, L.; De Zorzi, R.; Geremia, S.; Dalcanale, E. *Angew. Chem. Int. Ed.* **2011**, *50*, 4654-4657.
[25] Ocak, Ü.; Ocak, M.; Bartsch, R. A. *Inorg. Chim. Acta* **2012**, *381*, 44-57.
[26] Dhir, A.; Bhalla, V.; Kumar, M. *Org. Lett.* **2008**, *10*, 4891-4894.
[27] Chen, Q.-Y.; Chen, C.-F. *Tetrahedron Lett.* **2005**, *46*, 165-168.
[28] Métivier, R.; Leray, I.; Valeur, B. *Chem. Eur. J.* **2004**, *10*, 4480-4490.
[29] Corradini, R.; Dossena, A.; Galaverna, G.; Marchelli, R.; Panagia, A.; Sartor, G. *J. Org. Chem.* **1997**, *62*, 6283-6289.
[30] Pagliari, S.; Corradini, R.; Galaverna, G.; Sforza, S.; Dossena, A.; Montalti, M.; Prodi, L.; Zaccheroni, N.; Marchelli, R. *Chem. Eur. J.* **2004**, *10*, 2749-2758.
[31] F. M. Nelissen, H.; Venema, F.; M. Uittenbogaard, R.; C. Feiters, M.; J. M. Nolte, R. *J. Chem. Soc., Perkin Trans. 2* **1997**, 2045-2053.
[32] Sulowska, H.; Wiczk, W.; Młodzianowski, J.; Przyborowska, M.; Ossowski, T. *J. Photochem. Photobiol., A* **2002**, *150*, 249-255.
[33] Hossain, M. A.; Schneider, H.-J. *J. Am. Chem. Soc.* **1998**, *120*, 11208-11209.
[34] Pearson, A. J.; Xiao, W. *J. Org. Chem.* **2003**, *68*, 5361-5368.
[35] Lledo, A.; Rebek Jr, J. *Chem. Commun.* **2010**, *46*, 1637-1639.
[36] Galán, A.; Escudero-Adán, E. C.; Frontera, A.; Ballester, P. *J. Org. Chem.* **2014**, *79*, 5545-5557.

[37] Beckles, D. L.; Maioriello, J.; Santora, V. J.; Bell, T. W.; Chapoteau, E.; Czech, B. P.; Kumar, A. *Tetrahedron* **1995**, *51*, 363-376.
[38] Verdejo, B.; Gil-Ramírez, G.; Ballester, P. *J. Am. Chem. Soc.* **2009**, *131*, 3178-3179.
[39] Tewari, N.; Joshi, N. K.; Rautela, R.; Gahlaut, R.; Joshi, H. C.; Pant, S. *J. Mol. Liq.* **2011**, *160*, 150-153.
[40] Kim, S. K.; Lim, J. M.; Pradhan, T.; Jung, H. S.; Lynch, V. M.; Kim, J. S.; Kim, D.; Sessler, J. L. *J. Am. Chem. Soc.* **2014**, *136*, 495-505.
[41] Liu, Y.; Perez, L.; Mettry, M.; Easley, C. J.; Hooley, R. J.; Zhong, W. *J. Am. Chem. Soc.* **2016**, *138*, 10746-10749.
[42] Lakowicz, J. R. *Principles of Fluorescence Spectroscopy*; third ed.; Springier Science+Business Media: New York, 2006.
[43] Chadha, G.; Yang, Q.-Z.; Zhao, Y. *Chem. Commun.* **2015**, *51*, 12939-12942.
[44] Aragay, G.; Hernández, D.; Verdejo, B.; Escudero-Adán, E.; Martínez, M.; Ballester, P. *Molecules* **2015**, *20*, 16672.
[45] Escobar, L.; Aragay, G.; Ballester, P. *Chem. Eur. J.* **2016**, *22*, 13682-13689.
[46] The discrepancy observed for α when compared to NMR experiments may be due to the use of different concentrations, or errors during the fit of the UV-vis data, since all the species in equilibria (**2**, **DPNO**, 2:1 and 1:1 complexes) absorb in the region of 310-380nm.
[47] LOD = (standard error at the intercept x 3.3)/slope
[48] C bound to phosphorous is not observed at the used concentration.
[49] We do not report the $^{13}C\{^{1}H\}$ NMR because of overlapping of signals.

UNIVERSITAT ROVIRA I VIRGILI
CALIX[4]PYRROLE-BASED RECEPTORS FOR BIOLOGICALLY RELEVANT POLAR MOLECULES: FROM ORGANIC TO AQUEOUS MEDIA
Daniel Hernández Alonso

General conclusions

In summary, the work presented in this thesis describes the synthesis and binding studies of novel receptors based on aryl-extended calix[4]pyrrole macrocycles towards biologically relevant molecules.

In particular, in chapter 2 we have described the synthesis of a novel water-soluble tetraphenyl-extended calix[4]pyrrole. In contrast to previous examples, the carboxylic water-solubilizing groups in the described receptor are distal to the polar aromatic binding site. This leaves the aromatic binding site and the upper rim of the receptor pristine, making possible the future functionalization of the *meso*-aryl rings, thus, permitting the construction of more elaborated water soluble calix[4]pyrroles. We demonstrated that the receptor forms thermodynamically and kinetically stable complexes with a series of pyridine *N*-oxide guests in water. The binding geometry of these complexes was probed using ^{1}H NMR titrations and their thermodynamic characteristics were determined using ITC experiments. The obtained results also demonstrated that in water the receptor preferentially engages in hydrogen bonding interactions of its four pyrrole NHs with a *N*-oxide moiety than with a carboxylate group. Nevertheless, the tetraanionic receptor binds negatively charged pyridine *N*-oxides with high affinity. Our results highlight the ability of the receptor's aromatic pocket to protect the pyrrole *N*-H groups and ensure selective hydrogen-bonding interactions even in water solution.

We have also described in chapter 3 the synthesis an unprecedented monophosphonate bridged receptor capable of establishing a three-dimensional array of intermolecular interactions with neutral creatinine (**Cr**) and the creatininium cation (**CrH**$^{+}$). This receptor forms thermodynamically stable inclusion complexes with a 1:1 stoichiometry in the case of neutral **Cr**. On the other hand, titration experiments with **CrH**$^{+}$ showed the formation of two different aggregates having 1:1 and 2:1 stoichiometry. The use of a reference receptor, bis(methylene)-bridged derivative allowed us to assess the importance and the magnitude of the additional hydrogen-bonding interaction that is stablished between the inwardly directed polar phosphonate group and the NH_2 unit of the included guest.

Combining our results described in chapter 2 and 3, in the chapter 4 we described the synthesis of two unprecedented diastereoisomeric water soluble bisphosphonate calix[4]pyrrole biscavitands **4d$_{io}$** and **4d$_{oo}$**. The water solubilizing groups were installed at the ends of the

meso-alkyl substituents far away from the deep polar aromatic binding pocket. This approach aims to minimize possible perturbations of the binding site. During the optimization of the reaction conditions employed for the synthesis of the parent tetahydroxy calix[4]pyrrole we discovered a significant templating effect. Thus, the addition of methyltrialkyl ammonium chloride salts as reaction additive provoked a significant improvement in the isolated yield of the tetra-α isomers bearing functionalized alkyl chains at the *meso*-carbons. We assessed the binding constants of the two diastereoisomeric bis-phosphonate cavitands, **4d$_{io}$** and **4d$_{oo}$**, with natural creatinine and with a lipophilic synthetic version containing a hexyl chain (**HxCr**) in water. Both receptors formed thermodynamically stable complexes featuring 1:1 stoichiometry. Surprisingly to us, the **4d$_{oo}$** receptor displayed higher binding affinities towards both guests. Remarkably, the presence of a phosphonate group inwardly directed towards the aromatic cavity in the **4d$_{io}$** isomer that can be involved in an extra hydrogen bonding interaction with the included guest do not provide additional energetic stabilization to its complexes. We attributed this result to a more energetically demanding desolvation process for the cavity entrance in the **4d$_{io}$** compared to the **4d$_{oo}$** counterpart. This difference is mainly dictated by the presence of the inwardly directed PO group in the **4d$_{io}$** isomer. Finally, we reported that the **4d$_{oo}$** isomer is an effective receptor for diethyl nitrosamine (**NDEA**), a potent carcinogenic agent, in water. The complexation process is mainly driven by hydrogen bonding interactions established between the oxygen atom of the *N*-nitroso moiety and the pyrrole NHs of the receptor. To the best of our knowledge, this finding represent the first report of a synthetic receptor for **NDEA**

Fynally, in chapter 5 we have described the synthesis of a fluorescent receptor based on a aryl-extended calix[4]pyrrole cavitand. Our receptor possess a single phosphonate group, which not only acts as a bridging unit rigidifying the cavity, but also participates in the recognition process of creatinine through the establishment of hydrogen bonding interactions with the guest. The new described receptor possess a strong emission band with a maxima at 501 nm attributed to the presence of a dansyl group that it is covalently linked to the calix[4]pyrrole cavitand. We have designed a preassembled system formed by two units of the fluorescent receptor linked by 4,4' dipyridyl *N,N'*-dioxide (**DPNO)** to be further used for creatinine sensing. The supramolecular assembly was studied by ^{1}H NMR, absorption and emission spectroscopy. This preassembled system experimented a self-quenching process due to the close proximity of the dansyl units. Addition of a creatinine derivative **HxCr** provoked the disassembly of the aggregate with the consequent recovery of fluorescence emission. In

all processes, the fluorescence emission had a good linear fit with the concentration of **HxCr** and the estimated LOD result to be as low as 1.6 μM

UNIVERSITAT ROVIRA I VIRGILI
CALIX[4]PYRROLE-BASED RECEPTORS FOR BIOLOGICALLY RELEVANT POLAR MOLECULES: FROM ORGANIC TO AQUEOUS MEDIA
Daniel Hernández Alonso

List of abbreviations

ºC	–	Celsius
CIS	–	Complexation induced shift
COSY	–	Correlation spectroscopy
CPK	–	Corey-Pauling-Koltun model
Cr	–	Creatinine
DCM	–	Dichloromethane
DMF	–	Dimethyl formamide
DMSO	–	Dimethyl sulfoxide
DOSY	–	Diffusion Ordered Spectroscopy
ESI	–	Electrospray ionization
eq.	–	equivalent
HPLC	–	High performance liquid chromatography
HRMS	–	High resolution mass spectrometry
ITC	–	Isothermal titration calorimetry
K	–	Kelvin
Kcal	–	Kilocalorie
MeOH	–	Methanol
MHz	–	Megahertz
MM3	–	Molecular mechanics force field
MS	–	Mass spectroscopy
NMR	–	Nuclear magnetic resonance
PNO	–	Pyridine *N*-oxide
ROESY	–	Rotating frame Overhauser Effect SprectorscopY
TLC	–	Thin Layer Chromatography
UV	–	Ultraviolet

UNIVERSITAT ROVIRA I VIRGILI
CALIX[4]PYRROLE-BASED RECEPTORS FOR BIOLOGICALLY RELEVANT POLAR MOLECULES: FROM ORGANIC TO AQUEOUS MEDIA
Daniel Hernández Alonso

UNIVERSITAT ROVIRA I VIRGILI
CALIX[4]PYRROLE-BASED RECEPTORS FOR BIOLOGICALLY RELEVANT POLAR MOLECULES: FROM ORGANIC TO AQUEOUS MEDIA
Daniel Hernández Alonso

UNIVERSITAT ROVIRA I VIRGILI
CALIX[4]PYRROLE-BASED RECEPTORS FOR BIOLOGICALLY RELEVANT POLAR MOLECULES: FROM ORGANIC TO AQUEOUS MEDIA
Daniel Hernández Alonso